**Final Report**
**2009 UPPER GREEN RIVER WINTER OZONE STUDY**

Prepared for

Cara Keslar
Air Quality Division
Wyoming Department of Environmental Quality
122 West 25th Street
Herschler Building, 4-W
Cheyenne, WY 82002

Prepared by

ENVIRON International Corporation, Novato CA
Meteorological Solutions Incorporated, Salt Lake City UT
T&B Systems Incorporated, Santa Rosa CA
Dennis Fitz and Kurt Bumiller, Univ. of Calif. Riverside

March 2010

# TABLE OF CONTENTS

**Page**

**1. INTRODUCTION ..... 1-1**

**2. SUMMARY OF FIELD OPERATIONS ..... 2-1**

2.1. Continuous Measurements ..... 2-3
2.2. Intensive Operating Period Measurements ..... 2-10
2.3. Other Measurement Programs ..... 2-14
2.4. UGWOS Web-Site ..... 2-15
2.5. Intensive Operating Periods: Forecasting and Summary of Conditions ..... 2-17

**3. DATA QUALITY ASSURANCE, VALIDATION AND ARCHIVING ..... 3-1**

3.1. Data Management and Reporting ..... 3-1
3.2. Quality Assurance ..... 3-2
3.3. Data Validation ..... 3-7
3.4. Data Archiving ..... 3-30

**4. RESULTS ..... 4-1**

4.1. Summary of Meteorological and Air Quality Conditions ..... 4-1
4.2. Surface Wind Patterns ..... 4-9
4.3. Ozone Spatial and Temporal Distributions ..... 4-16
4.4. Conditions Aloft ..... 4-31
4.5. Analysis of Precursor Data ..... 4-47

**5. SUMMARY, CONCLUSIONS AND RECOMMENDATIONS ..... 5-1**

5.1. Summary and Conclusions ..... 5-1
5.2. Recommendations ..... 5-3

**REFERENCES ..... R-1**

## TABLES

Table 2-1. Summary of measurement methods used for 2009 field study ..... 2-1
Table 3-1. Data flags used in the UGWOS database ..... 3-1
Table 3-2. Ozone audit results ..... 3-5
Table 3-3. Boulder audit results – UGWOS measurements ..... 3-6
Table 3-4. VOC/carbonyl flow comparisons ..... 3-7
Table 3-5. Laboratory data qualifiers for VOC and carbonyl data ..... 3-7
Table 3-6. Field sampling data qualifiers for VOC and carbonyl data ..... 3-8

Table 3-7. Ratios of each 2B hourly ozone measurement to Boulder FEM measurement averaged over all hours with average wind speed greater than 7 m/s ..... 3-14
Table 3-8. Rawinsonde/Ozonesonde ground truth summary ..... 3-19
Table 3-9. VOC/carbonyl samples (times in MST) collected during each IOP ..... 3-26
Table 3-10. Sampler contamination check results (only compounds detected above three times the MDL are listed)..... 3-27
Table 4-1. Surface and 700 mb Temperatures for the February and March Period..... 4-1
Table 4-2. Scalar Wind Speeds at the Surface and Aloft for the February and March Period ..... 4-2
Table 4-3. Surface Pressure and Pressure Heights Aloft for the February and March Period ..... 4-2
Table 4-4. Monthly average and maximum 8-hour average ozone concentrations for February – March 2005 – 2009 at permanent monitoring sites..... 4-3
Table 4-5. Daily maximum 8-hour average ozone concentrations (ppb) on all IOP days [1] (values above 70 ppb in red; shaded cell indicates location of maximum on each day)..... 4-6
Table 4-6. Rawinsonde/ozonesonde Sky Conditions Summary (note: msg = missing value)..... 4-32
Table 4-7. Rawinsonde/ozonesonde Data Summary..... 4-33
Table 4-8. Significant Wind Layers ..... 4-36
Table 4-9. Summary of miniSodar data, Boulder UV measurements and maximum ozone concentrations at the Sodar site..... 4-44
Table 4-10. VOC/carbonyl samples (times in MST) collected during each IOP ..... 4-47
Table 4-11. Canister samples analyzed for CO and $CH_4$ (times in MST)..... 4-48
Table 4-12. Summary of VOC compound detections (ND indicates compounds was not detected in *any* of the samples analyzed; percentage values indicate fraction of samples above the method detection limit; shaded rows indicate compounds detected in at least one sample at all sites)..... 4-49
Table 4-13. Summary of carbonyl compound detections (ND indicates compounds was not detected in *any* of the samples analyzed; percentage values indicate fraction of samples above the method detection limit; shaded rows indicate compounds detected in at least one sample at all sites)..... 4-51
Table 4-14. Average NMHC method detection limits (ppbV)..... 4-52
Table 4-15. Average method detection limits (ppbV) for carbonyl species..... 4-54
Table 4-16. VOC summary statistics based on values above MDL for samples collected at Jonah ..... 4-55

Table 4-17. VOC summary statistics based on values above MDL for samples collected at Boulder ..... 4-56
Table 4-18. VOC summary statistics based on values above MDL for samples collected at the Sodar site ..... 4-57
Table 4-19. Summary of carbonyl data ..... 4-58
Table 5-1. Summary of operator responses to WDEQ Health Advisories during 2-3 February 2009 ..... 5-2

## FIGURES

Figure 2-1. UGWOS 2009 monitoring site locations. ..... 2-2
Figure 2-2. Solar powered tripod mesonet station used for wind and ozone measurements at Warbonnet (see map, Figure 2-1). Mast height is just under 3 m. Battery pack and 2B ozone analyzer are located in the cooler at base of tripod. ..... 2-4
Figure 2-3. Example UGWOS '09 website data display ..... 2-5
Figure 2-4: Boulder II (Left) Collocated with WDEQ Boulder Site(Right). Insulated cooler used to house 2B ozone analyzer is visible next to the Boulder II shelter ..... 2-6
Figure 2-5: Boulder II analyzers and data acquisition system ..... 2-7
Figure 2-6. Typical chromatogram from the NO2/PAN gas chromatograph ..... 2-8
Figure 2-7. Installation of the NOy and NO2/PAN analyzers in the Boulder shelter ..... 2-9
Figure 2-8: Boulder II: VOC canister and carbonyl cartridge sequential sampling system ..... 2-11
Figure 2-9: VOC/carbonyl sampling system at Jonah ..... 2-12
Figure 2-10. Photograph of the k1 measurement tube at the Boulder site ..... 2-14
Figure 2-11. 2009 UGWOS web site home page ..... 2-15
Figure 2-12. Single station data display ..... 2-15
Figure 2-13. Strip chart of pollutants from each monitoring station ..... 2-16
Figure 2-14. Equipment status matrix ..... 2-17
Figure 2-15. Example daily UGWOS forecast ..... 2-18
Figure 2-16. Example UGWOS operational mode form ..... 2-19
Figure 2-17. Constant pressure map for 700 mb, AM (1200 UTC), 02/03/09 (Source: http://www.spc.noaa.gov ..... 2-21
Figure 2-18. Constant pressure map for 700 mb, PM (2400 UTC), 02/04/09 (Source: http://www.spc.noaa.gov ..... 2-22
Figure 2-19. Constant pressure map for 700 mb, AM (1200 UTC), 02/28/09 (Source: http://www.spc.noaa.gov ..... 2-23
Figure 2-20. Constant pressure map for 700 mb, PM (2400 UTC), 03/02/09 (Source: http://www.spc.noaa.gov ..... 2-24
Figure 3-1. Comparison of FEM and 2B collocated ozone readings – February-March 2009 ..... 3-9
Figure 3-2. Time-series plot of FEM and 2B collocated ozone readings – February 2009 ..... 3-10
Figure 3-3. Plot of the difference between the 2B and FEM as a function of box temperature ..... 3-10
Figure 3-4. Comparison of FEM and 2B collocated ozone readings after pump replacement ..... 3-11

Figure 3-5. Comparison of FEM and 2B collocated ozone readings – hourly averages > 60 ppb ..... 3-12
Figure 3-7. Boulder UV vs. chemiluminescent ozone data: February 1-28, 2009 ..... 3-15
Figure 3-8. Boulder UV vs. chemiluminescent ozone data: March 1-31, 2009 ..... 3-16
Figure 3-9. Comparison of hourly ozone concentration ratio measured at Boulder using UV method (y-axis) and chemiluminescent method (x-axis) for the period 22 January-10 February ..... 3-16
Figure 3-10. Comparison of hourly ozone concentration ratio measured at Boulder using UV method (y-axis) and chemiluminescent method (x-axis) for the period 10 February-31 March ..... 3-17
Figure 3-11. Residuals from regression of UV against chemiluminescent ozone ..... 3-17
Figure 3-12. Calibration of the NOx analyzer on January 29, 2009 ..... 3-20
Figure 3-13. Calibration of the NOy analyzer on January 29, 2009 ..... 3-21
Figure 3-14. NOy analyzer NO span checks (400 ppb target) ..... 3-21
Figure 3-15. NOx analyzer NO span checks (400 ppb target). ..... 3-22
Figure 3-16. Time series of NO2 span checks (300 ppb target) for both the NOy and NOx analyzers ..... 3-22
Figure 3-17. Comparison of NOy and NOx on March 1, 2009 ..... 3-23
Figure 3-18. Time series of NO2 span checks (300 ppb target) for NO2 gas chromatograph ..... 3-24
Figure 3-19. VOC canister duplicate results sampled 2/21/09 ..... 3-28
Figure 3-20. VOC canister duplicate results sampled 3/4/09 ..... 3-29
Figure 3-21. Carbonyl duplicate results sampled 2/21/09 ..... 3-29
Figure 3-22. Carbonyl duplicate results sampled 3/4/09 ..... 3-30
Figure 4-1. MODIS satellite images on clear days during 2009 (left) and 2008 (right). ..... 4-4
Figure 4-2. Daily maximum 8-hour average ozone concentrations for all monitoring sites in the Upper Green River Basin operating between 20 January and 31 March 2008 ..... 4-7
Figure 4-3. Daily maximum 8-hour average ozone concentrations at monitoring sites in southwestern Wyoming (only maximum daily value shown for the group of Jonah-Pinedale area sites for which data were presented in Figure 4-2) ..... 4-8
Figure 4-4. IOP 1 Vector winds – February 4, 2009 ..... 4-11
Figure 4-5. IOP 1 Vector winds – February 5, 2009 ..... 4-12
Figure 4-6. IOP 2 Vector winds – February 22, 2009 ..... 4-13
Figure 4-7. IOP 2 Vector winds – February 23, 2009 ..... 4-14
Figure 4-8. IOP 3 Vector winds – March 1, 2009 ..... 4-15
Figure 4-9. IOP 3 Vector winds – March 2, 2009 ..... 4-16
Figure 4-10 IOP 1. ..... 4-21
Figure 4-11 IOP 1. ..... 4-21
Figure 4-12. IOP 1 ..... 4-22
Figure 4-13. IOP 1 ..... 4-22
Figure 4-14. IOP 1. ..... 4-23
Figure 4-15. IOP 1. ..... 4-23
Figure 4-16. IOP 2. ..... 4-24
Figure 4-17. IOP 2. ..... 4-24
Figure 4-18. IOP 2. ..... 4-25
Figure 4-19. IOP 2 ..... 4-25
Figure 4-20. IOP 2. ..... 4-26

Figure 4-21. IOP 2. ..... 4-26
Figure 4-22. IOP 3. ..... 4-27
Figure 4-23. IOP 3. ..... 4-27
Figure 4-24. IOP 3. ..... 4-28
Figure 4-25. IOP 3. ..... 4-28
Figure 4-26. IOP 3. ..... 4-29
Figure 4-27. IOP 3. ..... 4-29
Figure 4-28. IOP 3. ..... 4-30
Figure 4-29. Key structural elements of a typical rawinsonde/ozonesonde sounding ..... 4-33
Figure 4-30. Ozonesonde profiles – IOP 1 ..... 4-37
Figure 4-31. Ozonesonde profiles – IOP 3. ..... 4-37
Figure 4-32. February 28 sounding – 16 MST. ..... 4-38
Figure 4-33. March 1 sounding – 16 MST. ..... 4-38
Figure 4-34. Comparison of late afternoon ozonesondes from 11 March 2008 (left) with 2 March 2009 (right). Note the different horizontal ozone scales ..... 4-39
Figure 4-35. March 1, 2009 facsimile display ..... 4-43
Figure 4-36. Comparison of IOP 1 and IOP 3 upper level winds ..... 4-45
Figure 4-37. TNMHC concentrations (wide light blue bars) and average NMHC sample compositions by sampling location ..... 4-59
Figure 4-38. TNMHC concentrations (wide light blue bars) and average NMHC sample composition by sampling time (6:00 – 11:00 and 13:00 – 18:00 MST) based on data from all sampling locations ..... 4-60
Figure 4-39. Average contributions of individual NMHC species to species groups (only species contributing more than 0.5% to each lumped species group are listed) ..... 4-61
Figure 4-40. Average concentrations of most common NMOC species at each monitoring location (species listed are those detected in at least 75% of all samples collected at Jonah) ..... 4-62
Figure 4-41. Comparison of median NMHC percent composition at Jonah and Boulder from 2009 data (values from the SODAR site not shown due to limited sample size). ..... 4-63
Figure 4-42. Box plot comparison of TNMHC concentrations in 2008 and 2009 at Boulder and Jonah ..... 4-64
Figure 4-43. Key to box plot symbols used in Figure 4- 42. ..... 4-64
Figure 4-44. Average NMHC composition of most abundant species at Jonah (top) and Boulder (bottom) in 2008 as compared to 2009 ..... 4-66
Figure 4-45. Comparison of average maximum incremental reactivity (MIR) weighted concentrations average concentrations and of most common NMOC species at Jonah (species listed are those detected in at least 75% of all samples collected at Jonah) ..... 4-67
Figure 4-46. Comparison of average concentrations and average maximum incremental reactivity (MIR) weighted concentrations of most common NMOC species at Boulder (species listed are those detected in at least 50% of all samples collected at Boulder) ..... 4-68
Figure 4-47. Methane as a percent of TOG (top panel) and regressed against TOG (bottom panel ..... 4-69
Figure 4-48. Comparison of NO2 measured by chhemiluminescent NOx analyzer and NO2 gas chromatograph ..... 4-70
Figure 4-49. Chroamtogram from sample analyzed at 16:00 hours on 3/1/09 showing distinct PAN peak at 19 seconds ..... 4-71

Figure 4-50. Time series plot of PAN concentrations on February 23, 2009 ..... 4-71
Figure 4-51. Time serier plot of PAN concentrations on March 1, 2009 ..... 4-72
Figure 4-52. Time serier plot of PAN concentrations on March 2, 2009 ..... 4-72
Figure 4-53. Comparison of measured and modeled k1 ..... 4-74
Figure 4-54. Comparison of measured k1 with total solar radiation ..... 4-75
Figure 4-55. Comparisons of incoming and reflected UV measured at Boulder during January – March 2008 (top) and 2009 (bottom). Measurements during much of 2008 and, to a lesser extent during certain periods in 2009 were impacted by an apparent negative bias in the incoming UV measurement, possibly associated with dirt or frost buildup on the instrument (see ENVIRON, 2008b). These results should therefore only be interpreted in a qualitative sense ..... 4-76

# 1.0 INTRODUCTION

Ozone episodes observed in the Upper Green River Basin typically occur during the late winter and early spring (late January to April). Several episodes of elevated ozone concentrations have been observed in rural Sublette County, Wyoming since monitoring began in 2005. Concentrations in excess of the National Ambient Air Quality standard were recorded on several days during February of 2005 and 2006. An additional high ozone event occurred in April of 2006. Concentrations were generally lower in 2007, but one additional elevated ozone event occurred in late January. Several more such high ozone events were recorded during February and early March of 2008. The most severe event recorded to date occurred during 19 – 24 February 2008 when concentrations at either Jonah or Boulder (or both) exceeded the EPA 75 ppb 8-hour standard on each day, with a 122 ppb 8-hour average concentration observed at Boulder on 21 February.

Such high concentrations of ozone are unusual in a rural environment, especially during the winter months when low temperatures and low sun angles normally act to limit ozone formation. This is in marked contrast to ozone episodes in other areas, which occur during the warm summer months when abundant solar radiation and high temperatures act to increase precursor emissions and enhance many of the atmospheric reactions that result in ozone formation near the earth's surface (i.e., within the planetary boundary layer). In addition, the Upper Green River Basin is a rural area lacking the extensive conglomeration of ozone precursor sources found in urban areas, thus leading to questions about the availability of sufficient amounts of reactive volatile organic compounds and nitrogen oxides (NOx) needed for ozone production.

The recent high ozone readings occur at a time when economic growth in the area is rapid, primarily driven by an increase in oil & gas production. Air quality impacts from this growth have been a key concern of local citizens, environmental groups, the State of Wyoming and the U.S. Environmental Protection Agency. Impacts of concern in the Upper Green River Basin have historically focused on visibility and acid deposition, particularly in the nearby protected Bridger and Fitzpatrick Wilderness Areas, but the recent monitoring data have resulted in a new interest in ozone impacts.

Due to the pressing need to manage air quality in the Upper Green River Basin and the limited amount of information which was available about the nature and causes of the unusual wintertime high ozone events first observed during February and March of 2005 and 2006, the WDEQ funded a major field study known as the Upper Green Winter Ozone Study (UGWOS). UGWOS operations first took place during the 2007 late winter – early spring season; results from the 2007 UGWOS study were summarized in a previous report (ENVIRON, 2008a). Unfortunately, weather conditions during the February – March 2007 study period were generally not conducive to formation of high ozone levels. As a result, field study operations were curtailed in 2007 and the remaining project resources, together with additional funding provided by the WDEQ, were used to conduct a similar field study carried out from mid-January to March, 2008. As was the case in the 2007 study, the UGWOS '08 study was designed to meet the following objectives:

- Provide information needed to develop a conceptual understanding of processes leading to the occurrence of high ozone events in the Upper Green River Basin.

- Provide data needed to develop accurate meteorological and air quality numerical simulations of high ozone events in the region. These numerical models will be needed to evaluate the benefits of alternative emission reduction strategies.

Conditions during the UGWOS 2008 study period were more conducive to ozone formation than was the case in 2007 and several high ozone events were captured during February and March. A report summarizing results from the 2008 study is available (ENVIRON, 2008b).

Results from the 2008 study revealed several key features of the Upper Green River Basin winter ozone episodes:

- A stable vertical atmospheric structure resulting from high pressure and relatively warm air aloft with colder air trapped near the surface;
- Clear skies and light surface winds;
- A diurnal wind reversal at the surface from northwest winds during the night and morning hours to southeast during the afternoon which recirculates pollutants within the basin;
- Extensive snow cover which significantly limits daytime solar heating and resulting vertical convection and nearly doubles the total (actinic) flux of UV radiation which drives photochemical reactions;
- Ozone and ozone precursor pollutants trapped in a shallow surface layer throughout all or most of the day.

In addition to identifying these key features, analysis of results from the 2008 study identified several key issues which were targeted for further study, including:

- A need to better understand the principal NOx chemistry pathways operating during these cold winter ozone episodes;
- Evaluation of the full southern spatial extent of the high ozone concentrations;
- Examination and evaluation of high concentrations of unidentified organic compounds in air samples collected at Boulder (and to a lesser extent at Jonah);
- Direct measurements of $NO_2$ photolysis rates to confirm the effect of high UV albedos over snow and to support future modeling.

To address these questions, WDEQ sponsored a third field study during mid-January – March, 2009. Planning for UGWOS ’09 began in late October, 2008 and continued through early January, 2009. Routine field operations took place between mid-January and the end of March, 2009. As in the two previous years, the field study design included a set of routine measurements conducted throughout the two and a half month study period and a set of intensive measurements conducted during selected Intensive Operating Periods (IOPs) when conditions similar to those associated with previous high ozone episodes were forecast to occur. Daily weather forecasts were issued by a team of meteorologists assigned to the project for purposes of identifying upcoming periods potentially suitable for conducting IOP operations. Routine operations during UGWOS ’09 included an expanded network of temporary, “mesonet” monitoring sites of the type used in UGWOS ’08. In addition, an expanded continuous instrumentation suite was operated out of a second instrument shelter temporarily placed next to

the WYDEQ Boulder monitoring site. This allowed for the collection of continuous trace level $SO_2$, CO, and nitrogen species (NO, $NO_2$, NOy, PAN) data. Due to funding limitations, no aircraft data were collected in 2009 as was done in 2008 and the number of daily balloon-borne soundings launched and number of daily organic compound samples collected was reduced from 2008.

This report presents a summary of UGWOS '09 field operations and results of the measurement programs. An overview of the routine and supplemental measurements carried out as part of UGWOS '09 is presented in Section 2 together with a description of the forecast procedures and methodologies used to identify the IOPs. Data quality assurance, validation and archiving procedures are described in Section 3. Procedures and results of the routine and intensive monitoring are presented in Section 4; a summary of results and our conclusions are presented in Section 5. A complete set of study data are available in an ACCESS database at http://deq.state.wy.us/AQD/Monitoring%20Data.asp.

## 2. SUMMARY OF FIELD OPERATIONS

Planning for the UGWOS 2009 field operations began in late October, 2008 and continued through early January, 2009. Forecasting for IOP conditions began January 15, 2009 and remained operational through March 31, 2009. A map showing the monitoring sites is shown on Figure 2-1. This map shows several monitoring sites which were not officially part of the UGWOS study but were established as part of the Sublette County Human Health Risk Study (shown in green). A summary of the measurement methods used via the various instrument platforms is provided in Table 2-1. Field operations consisted of two tiers of measurements: routine measurements conducted throughout the study period and intensive operating period (IOP) measurements conducted on selected days with high ozone formation potential as forecast by the study team. Routine and IOP measurements are discussed in more detail below.

Most monitoring network components were fully operational by 20 January except the Jonah monitoring site which started operation 29 January. Collection of ozone data at the SODAR site started in mid-January but collection of NOx data did not start at this site until the end of February as this was not part of the original study design.

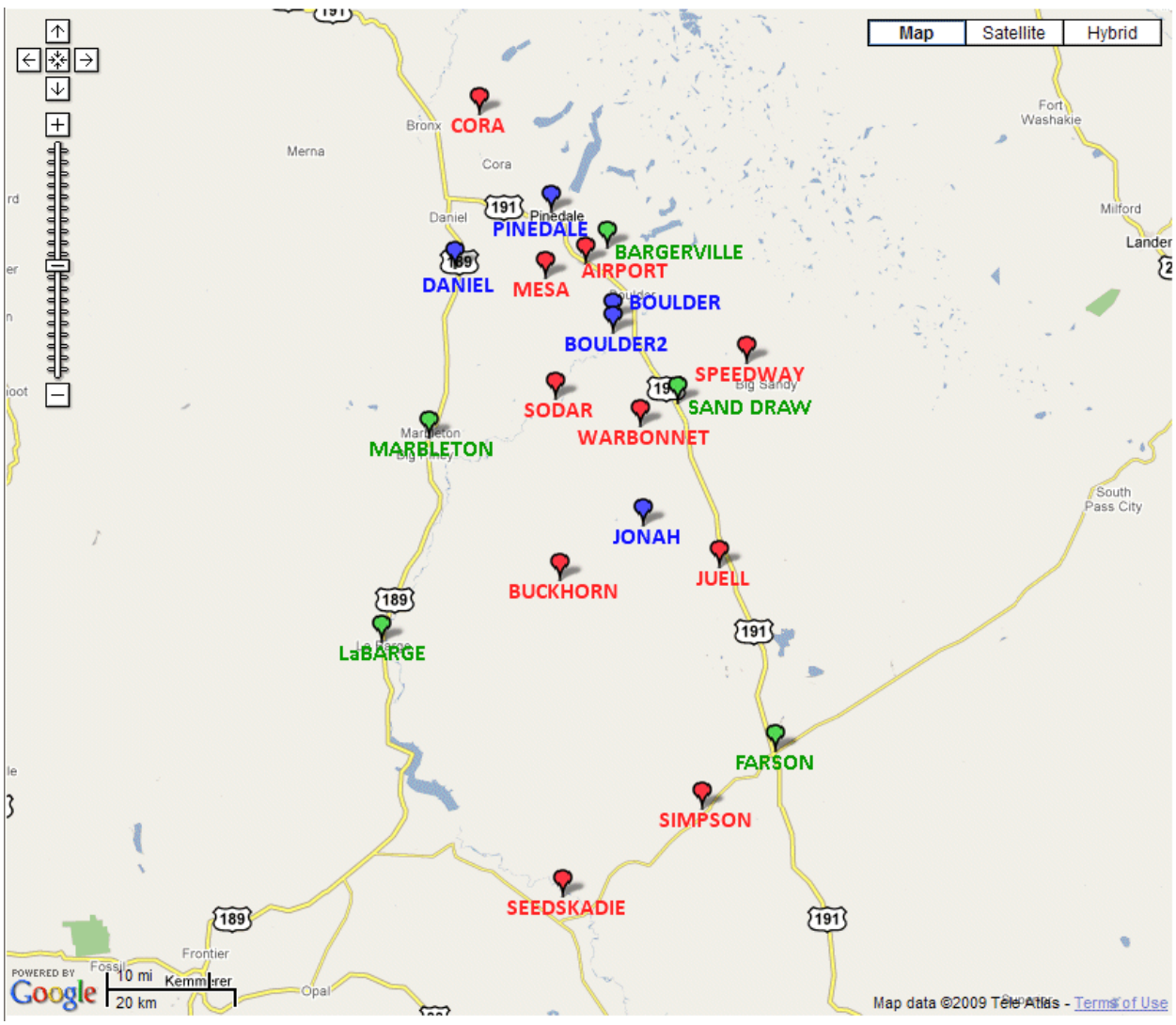


**Figure 2-1.** UGWOS 2009 monitoring site locations.

**Table 2-1.** Summary of measurement methods used for 2009 field study.

| Platform | Mode | Measurement | Instrumentation | |
|---|---|---|---|---|
| | | | **Method** | **Model** |
| Mesonet sites | Continuous | Wind speed | Propeller anemometer | RM Young 05305 |
| | | Wind direction | Vane | RM Young 05305 |
| | | Temperature | Thermistor Probe | CSI 109 |
| | | Ozone | UV photometric | 2B Technologies 202 |
| Sodar | Continuous | Upper level winds | Doppler sodar | ASC 4000 miniSodar |
| | | Mixing height | Doppler sodar | ASC 4000 miniSodar |
| | | Surface wind speed, wind direction, temperature, relative humidity, pressure and precipitation detection | Integrated sonic anemometer, thermistor probe, RH and pressure sensors with separate precipitation detection sensor | Vaisala WXT-510 |
| | | Ozone | UV photometric | 2B Technologies 202 |
| | | NOx | Chemiluminescence | T-API 200E |
| | IOP #3 | VOCs | SUMMA canisters; TO-14 | Canisters provided by EAS, Inc. |
| Boulder II | Continuous | Ozone | Chemiluminescent | 265A |
| | | Carbon Monoxide (CO) | IR absorption | 300EU |
| | | Sulphur Dioxide ($SO_2$) | UV fluorescence | 100EU |
| | | $NO_X$ | | UC Riverside |
| | | $NO_2$ | | UC Riverside |
| | | $NO_Y$ | | UC Riverside |
| | **Intensive (IOPs)** | VOCs | SUMMA canisters; TO-14 | Canisters provided by EAS, Inc. |
| | | Carbonyls<br><br>$NO_2$ Photolysis | Pump, flowmeter, and DNPH-coated cartridges; TO-11<br>Actinometer | MSI sampler design, cartridges provided by EAS, Inc.<br>UC Riverside |
| Pinedale Airport | Continuous | Surface wind speed | Propeller anemometer | RM Young 05305 |
| | | Surface wind direction | Vane | RM Young 05305 |
| | | Temperature | Thermistor Probe | CSI 109 |
| | | Ozone | UV Photometric | Dasibi 1003 AH |
| Rawinsonde | Intensive (IOPs) | Upper level winds, temperature, RH | GPS-based balloon soundings | SIPPICAN Mark II Microsondes |
| Ozonesonde | Intensive (IOPs) | Upper level ozone | GPS-based balloon soundings, KI method | EN-SCI Corporation KZ-ECC Ozonesondes |
| WDEQ monitoring sites | Continuous | Ozone | UV photometric | T-API 400E/400A |
| | | $NO_X$ | Chemiluminescent | T-API 200E/200A |
| | | $PM_{10}$ | Tapered element oscillating micro-balance | TEOM 1400a |
| | | $PM_{2.5}$ (Pinedale only) | Beta attenuation gauge | BAM 1020 |
| | Intensive (IOPs) Jonah site only | VOCs | SUMMA canisters; TO-14 Pumped and Negative Pressure Flow Controller | Canisters provided by EAS, Inc. |
| | | Carbonyls | Pump, flowmeter, and DNPH-coated cartridges; TO-11 | MSI sampler design, cartridges provided by EAS, Inc. |

## 2.1 Continuous Measurements

### 2.1.1 Overview

Project-specific measurements from the continuous monitoring sites shown in Figure 2-1 were obtained for the mid January –March 2009 field study period. These measurements included surface and boundary layer meteorological data and surface air quality data.

Routine aerometric monitoring was conducted at the permanent WDEQ monitoring sites: Boulder, Pinedale (downtown), Jonah, and Daniel. Meteorological measurements included wind speed and direction, temperature, solar radiation, relative humidity, precipitation and barometric pressure. Aerometric measurements included $O_3$, $NO_x$, and continuous $PM_{10}$. $PM_{2.5}$ measurements were recorded at the Pinedale site. Ozone was measured at the airport (Wenz Field) using a Federal Equivalent Method UV analyzer (Dasibi 1003-AH). Ozone, $NO_x$ and boundary layer acoustic sounding (sodar) meteorological measurements were performed at the Sodar site.

Continuous ozone and meteorological measurements were conducted over a network of eight tripod mounted stations (mesonet sites) similar to those used in the 2008 study. A typical station is shown in Figure 2-2. Data from the mesonet is available starting at various periods in mid-January through late March or early April:

- Cora January 14 through April 1
- Mesa January 16 through March 22
- Speedway Pit January 15 through March 31
- Juell Springs January 14 through April 1
- Buckhorn Draw January 13 through April 2
- Simpson January 14 through April 1
- Warbonnet January 13 through April 1
- Seedskadee January 15 through April 1

**Figure 2-2.** Solar powered tripod mesonet station used for wind and ozone measurements at Warbonnet (*see map, Figure 2-1*). Mast height is just under 3 m. Battery pack and 2B ozone analyzer are located in the cooler at base of tripod.

Each of the mesonet stations continuously recorded ozone concentrations, wind direction, wind speed, and temperature. Stations collected 5-minute average data, were solar powered and were polled every 15 minutes through a cellular modem. Data were posted automatically to a project website as illustrated by the example in Figure 2-3.

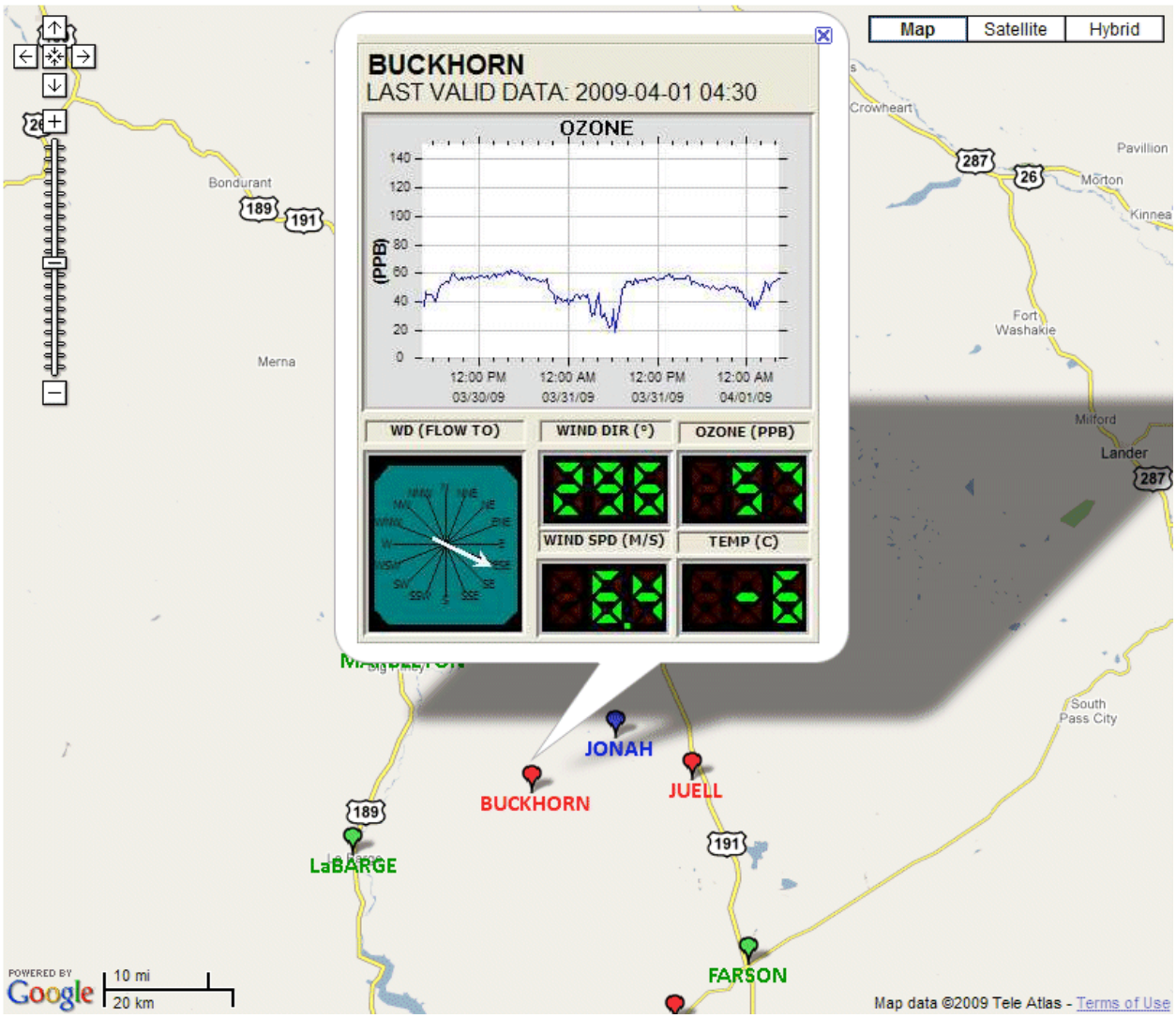


**Figure 2-3**. Example UGWOS '09 website data display.

## 2.1.2 Boulder II Monitoring Site

CO, $SO_2$, $O_3$, $NO_y$, $NO_2$, and PAN were monitored at a new temporary instrument shelter known as the Boulder II site which was collocated adjacent to the WDEQ Boulder site. Trace level CO and $SO_2$ were monitored from January 17 through April 1 (see Figures 2-4 and 2-5). Ozone was also monitored at the Boulder II site during the same period using a T-API chemiluminescent analyzer. In addition, a 2B ozone analyzer was located just outside of the shelter in an insulated box for measurement method comparison purposes with the two FEM analyzers – the UV photometric unit at Boulder and the "Chemi" unit at Boulder II.

**Figure 2-4:** Boulder II (Left) Collocated with WDEQ Boulder Site(Right). Insulated cooler used to house 2B ozone analyzer is visible next to the Boulder II shelter.

**Figure 2-5**: Boulder II analyzers and data acquisition system.

### 2.1.3 Boulder II $NO_2$, NOY and PAN Measurements

$NO_y$ was measured with a commercial chemiluminescent $NO_x$ analyzer (Thermo Environmental Instruments model 42C) that was modified by removing the converter from the instrument and placing it outside in its own shelter (Fitz et al. 2003). The reason for doing this is that some of the $NO_y$ species such as nitric acid ($HNO_3$) adhere to sample lines (even inert Teflon) so that quantitative measurement is not possible. The standard converter is used but by locating it outside an extremely short sampling line may be used. The shelter that houses the converter is

slightly warmed from the heat of the 350C converter, thus further minimizing loss of $NO_y$ species. Once these species pass through the converter they are all reduced to nitric oxide (NO) which easily passes through sample lines. Since the converter is outside some distance away from the analyzer itself (which needs to be maintained at constant temperature) a bypass flow was added to decrease the residence time in the sample line between the converter and the detector of the analyzer. The analyzer alternatively samples with and without the converter in line for ten seconds and measures the amount of $NO_y$ and NO. The instrument is calibrated with NO calibration gas using gas phase titration to produce $NO_2$ to test converter efficiency.

Nitrogen dioxide ($NO_2$) and peroxyacetyl nitrate (PAN) were measured using a gas chromatograph equipped with a luminol-based detector (Fitz et al. 2002). These detectors are sensitive to oxidizers such as ozone, PAN, and $NO_2$. The advantage of this instrument over a chemiluminescent NO-$NO_x$ analyzer is that $NO_2$ is measured without any interferences. With the NO-$NO_x$ analyzer, $NO_2$ is measured as the difference between $NO_x$ and NO and $NO_x$ in ambient air may contain other nitrogenous species (such as PAN and $HNO_3$) that therefore contribute to a positive interference when measuring $NO_2$. Samples were injected every two minutes and $NO_2$ was separated from the PAN; ozone is removed by the chromatographic column as it reacts on the walls of the column. A computer using LabView®-based data acquisition software controlled the injection sequence, calculated the area of the resulting chromatographic peaks, and displayed the results in engineering units. The PAN response is virtually the same as $NO_2$. The instrument is therefore calibrated using $NO_2$ produced by gas phase titration of NO. Figure 2-6 shows a typical chromatogram.

The diagram in Figure 2-7 shows how the instruments were installed in the shelter.

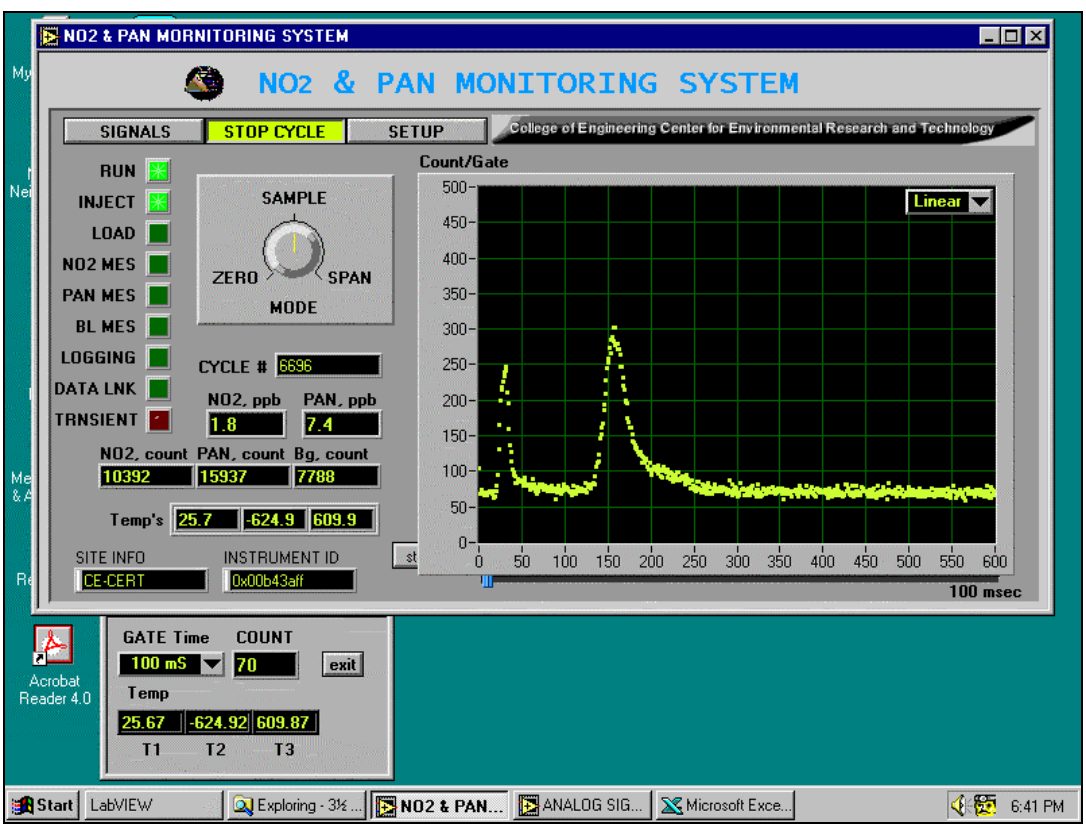


**Figure 2-6.** Typical chromatogram from the $NO_2$/PAN gas chromatograph.

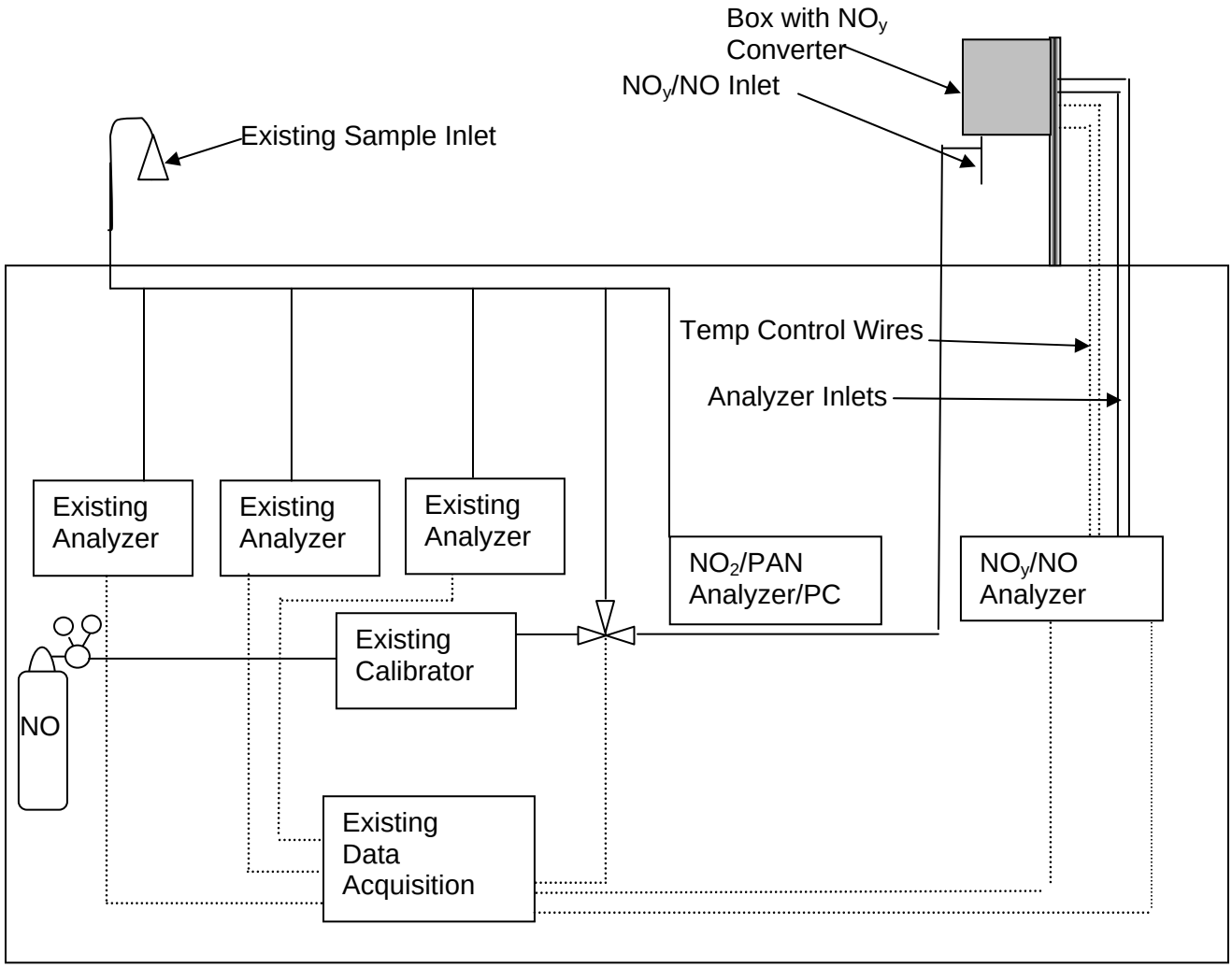


**Figure 2-7.** Installation of the $NO_y$ and $NO_2$/PAN analyzers in the Boulder shelter.

## 2.2 Intensive Operating Period Measurements

During periods when high ozone levels were forecast, a variety of supplemental measurements were initiated. The key components of these intensive operating periods (IOPs) were:

- VOC and carbonyl measurements at Boulder II and Jonah (During IOP#3, VOC measurements were added at the SODAR site)
- Ozone/rawinsonde operations

### 2.2.1 Ozone/Rawinsonde Operations

During IOP operations, standard high-resolution balloon borne rawinsondes were launched approximately 15 m from the UGWOS Airport meteorological site outside of the main hanger at Wenz Field. Typically, two morning launches measuring height above ground level (m agl), temperature (C), relative humidity (RH), wind speed (meters per second) and wind direction were made at around 0730 MST and 1030 MST during each IOP day. Rawinsonde measurements that included ozone (ozonesondes) as well as the meteorological parameters were made during the afternoons from the same location at the Wenz Field hanger: nominally at 1400 MST and 1630 MST. Ground truth surface ozone measurements were collocated at the airport approximately 10 meters from the balloon launch location.

### 2.2.2 Gaseous Organic Compound Sampling

NMHC and carbonyl samples were collected twice daily (6:00 – 10:00 and 13:00 – 17:00 MST) at the Boulder II and Jonah sites during each IOP. VOC samples were also taken at the miniSodar site during IOP #3. Two four-hour samples were taken daily on IOP days: one from 0600-1000 MST and one from 1300-1700 MST. Sampling systems are shown in Figures 2-8 and 2-9.

**Figure 2-8:** Boulder II: VOC canister and carbonyl cartridge sequential sampling system.

**Figure 2-9:** VOC/carbonyl sampling system at Jonah.

### 2.2.3 Boulder II $NO_2$ Photolysis ($k_1$)

An actinometer for measurement of the $NO_2$ photolysis rate was deployed at the Boulder II site. A stream of nitrogen dioxide (in $O_2$-free $N_2$ at approximately 1 ppm) was flowed through a quartz tube. The tube is approximately 2.2 cm ID with an active (uncovered) length of 70 cm. The last 10 cm of both ends of the tube were covered with black tape to prevent irradiation while plug flow is established. The tube was set up on an open area approximately 2m above the ground. A length of 1/8 in OD stainless tubing was used to input the $NO_2$ and ¼ in OD PFA Teflon tubing (covered with black plastic to prevent additional photolysis) was used to sample the effluent from the tube with the NO-$NO_x$ analyzer. Figure 2-10 is a photograph of the tube installed at the Boulder monitoring site.

The amount of $NO_2$ photolyzed was measured with a ThermoAnalytical Instruments model 42 chemiluminescent oxides of nitrogen analyzer sampling at the outlet. The photolysis rate was calculated from the $NO_2$ concentration, the inlet/outlet NO concentrations, the tube geometry, the flow rate, and the effective quantum yield (Zafonte et al., 1977). The equation below was used:

$$k_1 = [(NO-NO_d)/(NO_2 + 0.5(NO-NO_d))] * F/V* (1/\Phi)$$

where:
NO = measured NO in ppm
$NO_d$ = measured NO in ppm while operated in dark
$NO_2$ = measured $NO_2$ in ppm while operated in the dark
F = flow rate in L/min (nominally 1alpm)

V = volume of illuminated tube in L (0.2665 L)
Φ = Quantum yield factor (1.653)

The NO-$NO_x$ analyzer was calibrated at the site and operated whether NO was flowing through the tube or not. When NO was not flowing, the NO and $NO_x$ measured was compared with the other site analyzers to evaluate the accuracy of the measurements. At times the inlet to the analyzer was also attached to the site's sampling manifold and subjected to daily span checks. All span checks showed less than 10% difference from the calibration standard and no span corrections were made. It should be noted that calibration has no effect on the $k_1$ measurements since a ratio of concentrations is used. Zero checks were used to correct for zero drift.

The $k_1$ measurement device was generally operated by starting the flow of $NO_2$ in $N_2$ during intensive operating days and for several other days during which the snow cover was representative of IOP days. The cylinder of $NO_2$ in $N_2$ was exhausted on March 1, 2009 and replaced with another cylinder of similar composition from the same vendor several days later.

The flow rate of the NO was measured with a mass flow meter and recorded on the site's data logger. The flow rate was corrected for temperature to 298°K using the temperature data collected from the site's sensor. It was corrected to the pressure of the CE-CERT facility (elevation 1200 feet, 730 mm Hg) using the 7000 foot elevation of the site (587 mm Hg).

The $NO_d$ and $NO_2$ values were chosen from periods operated in darkness either on that day or a nearby measurement day.

The $k_1$ tube used for the Boulder site was compared to that used at the CE-CERT environmental chamber facility prior to installation. The array of black light used to illuminate the chamber was used as the light source. The dedicated $k_1$ tube gave a $k_1$ of 0.218 $min^{-1}$ while the tube for Wyoming gave a value of 0.222 $min^{-1}$. These values are consistent with prior measurements for this light source. The chamber's NO-$NO_x$ analyzer, $NO_2$ in $N_2$ tank, and mass flow meter were installed at the Boulder site. After the equipment was removed, the $k_1$ was again measured using the black light panel in the CE-CERT as the light source. The measured $k_1$ dropped to 0.201 $min^{-1}$, but this was likely due to the ageing of the light source.

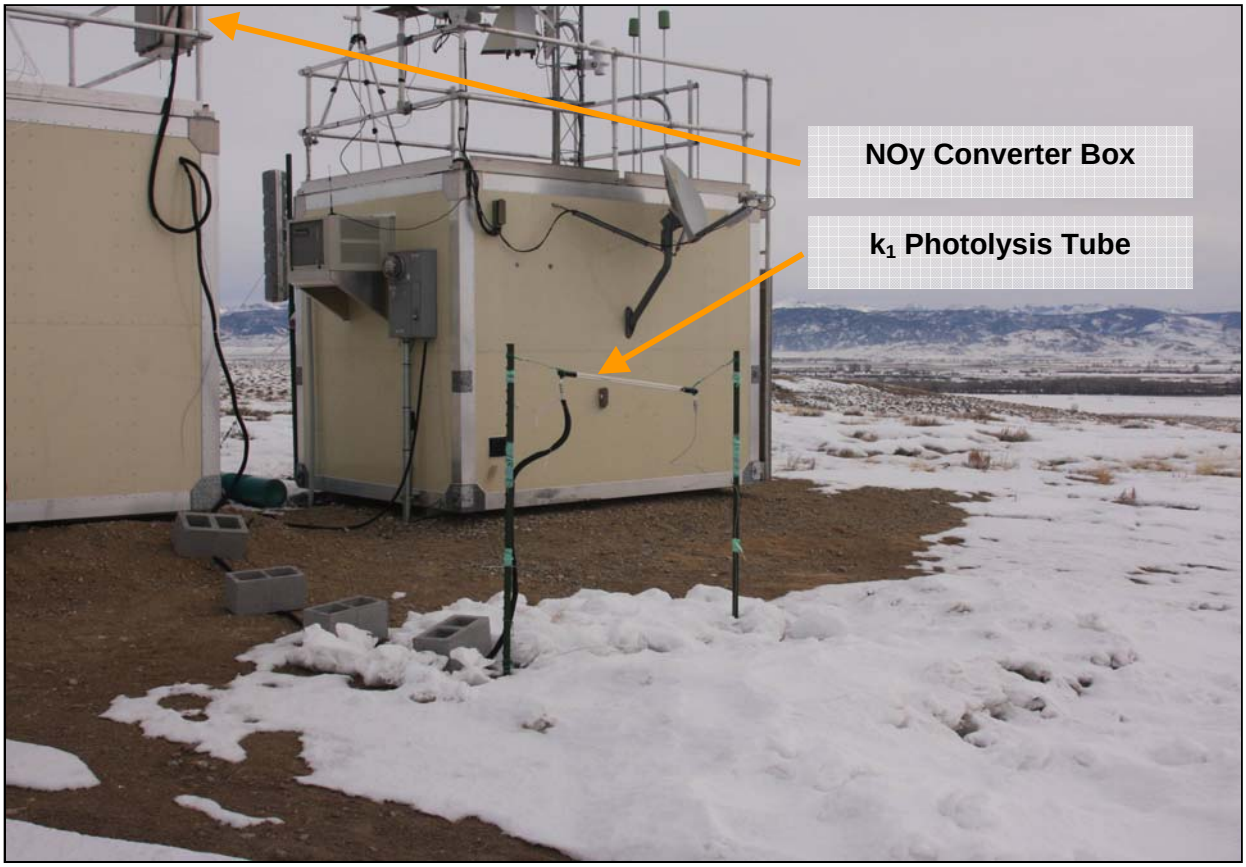


**Figure 2-10**. Photograph of the $k_1$ measurement tube at the Boulder site.

## 2.3 Other Measurement Programs

In addition to measurements that were part of the UGWOS '09 study as summarized above, a number of other ancillary measurements were collected during the study period by other organizations. These included:

- A pair of upward and downward facing UV radiometers as originally described by ENVIRON (2008a) was operated by ARS at the Boulder site.
- An extensive air toxics measurement program undertaken at the direction of the Sublette County Commissioners, the Wyoming Department of Health and the WDEQ began operations during February 2009. This study consisted of a network of five ozone, air toxics and meteorological monitoring sites, and nine air toxics sites located in Sublette and Sweetwater Counties.
- Continuous VOC measurements at Boulder via pneumatic focusing gas chromatography carried out by ARS.

## 2.4 UGWOS Web-Site

In 2009, a new UGWOS web-site was developed that allowed access to station data for all UGWOS participants. This included sites from WDEQ's monitoring stations (labeled in blue in Figure 2-11), and sites specifically installed for the study (labeled in red in Figure 2-11). The information from these sites was updated as often as every 15 minutes, and included text as well as graphic presentations. A network of monitoring stations was set up for the Human Health Risk Assessment Air Toxics Inhalation Project sponsored by Sublette County, the Wyoming DEQ, and the Wyoming DOH; five of these stations with ozone data were accessible to the UGWOS study and were included on the web site late in the study period (stations labeled in green in Figure 2-11). This near real-time information was useful to the participants in making decisions as quickly as possible when elevated ozone events were possible. It was also important in allowing repairs of equipment quickly, assuring minimal data loss.

The home page, seen in Figure 2-11, contained two scrollable frames. The frame on the left listed information that was available and could be viewed or plotted in the frame on the right. This included individual weather and air quality parameters from each location (see Figure 2-12), or shown as a group; strip charts of these parameters (see Figure 2-13); links to the UGWOS forecast and operational mode forms; access to the equipment status matrix (see Figure 2-14), which was an important addition to the web-site in that it allowed all participants to see what issues required attention; and links to the State of Wyoming's WyVisNet.

The latest data in text format from the individual monitoring stations was arranged by network and included in the left frame. This particular listing contained links to pictures taken at the chosen site and to live camera images from the WDEQ sites.

A second web-site was also developed which was open to the public. This second web site contained a large subset of information from the main web site, including 8-hour rolling average ozone data.

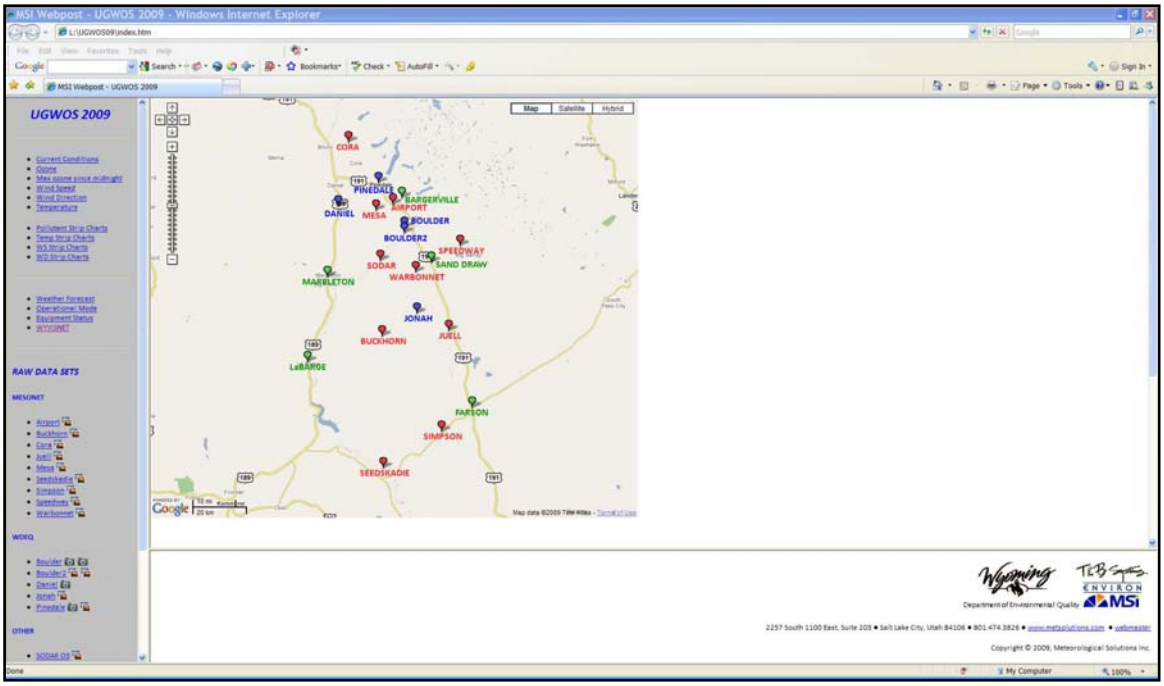


**Figure 2-11.** 2009 UGWOS web site home page.

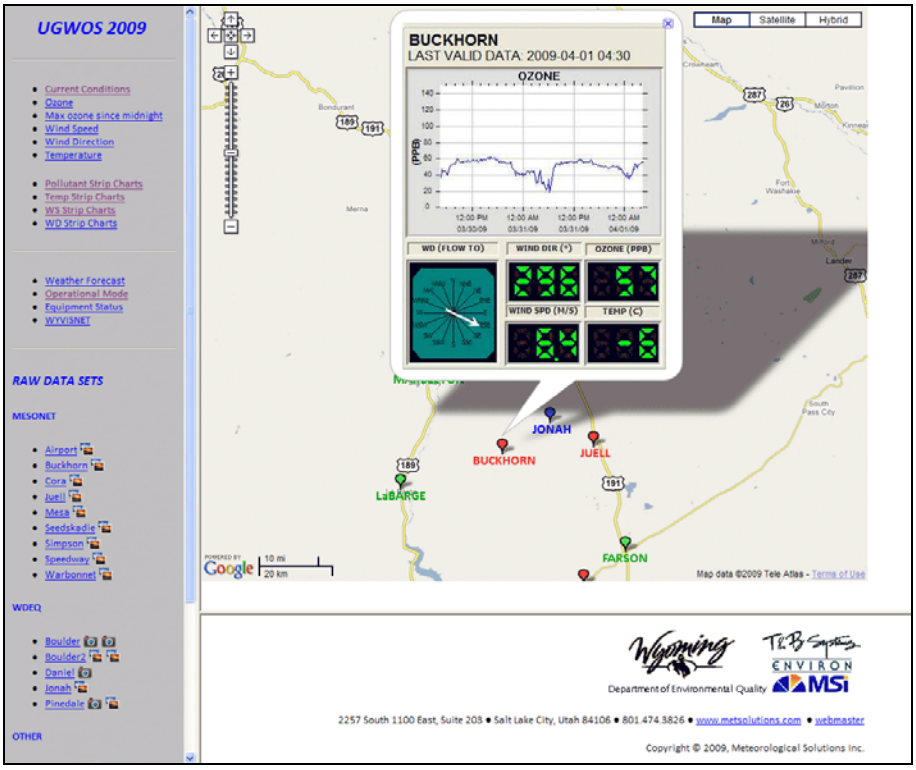


**Figure 2-12.** Single station data display.

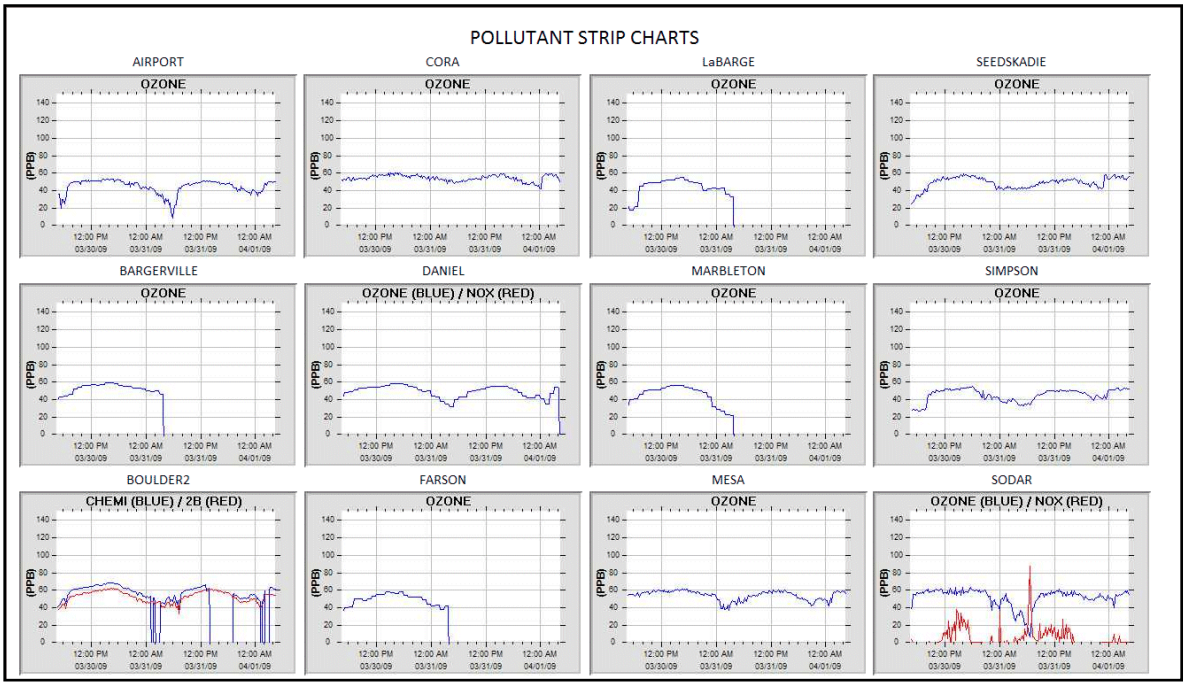


**Figure 2-13.** Strip chart of pollutants from each monitoring station.

UGWOS 2009 Equipment Matrix and Current Status - Last Modified on 04/03/2009 11:56:31

| No. | Site Name | Latitude/Longitude | Site Operator | Telemetry | WS | WD | TEMP | O3 (2B) | O3 (UV) | Trace SO2 | Trace CO | NOX | NO | NOY | NO2 | O3 (Chemi) |
|---|---|---|---|---|---|---|---|---|---|---|---|---|---|---|---|---|
| 1 | Airport | 42.7982, 109.8049 | T&B/MSI | X | X | X | X | X | | | | | | | | |
| 2 | Buckhorn | 42.3523, 109.8543 | MSI | X | X | X | X | X | | | | | | | | |
| 3 | Cora | 43.0067, 110.0083 | MSI | X | X | X | X | X | | | | | | | | |
| 4 | Juell | 42.5716, 109.5503 | MSI | X | X | X | X | X | | | | | | | | |
| 5 | Mesa | 42.7774, 109.8829 | MSI | X | X | X | X | X | | | | | | | | |
| 6 | Seedskadee | 41.9050, 109.8502 | MSI | X | X | X | X | X | | | | | | | | |
| 7 | Simpson | 42.0284, 109.5812 | MSI | X | X | X | X | X | | | | | | | | |
| 8 | Speedway | 42.6572, 109.4982 | MSI | X | X | X | X | X | | | | | | | | |
| 9 | Warbonnet | 42.5703, 109.7014 | MSI | X | X | X | X | X | | | | | | | | |
| 10 | Boulder | 42.7190, 109.7540 | ARS | X | X | X | X | | X | | | X | | | | |
| 11 | Boulder2 | 42.7190, 109.7540 | MSI | X | | | | X | | X | X | | X | X | X | X |
| 12 | Daniel | 42.7910, 110.0650 | IML | X | X | X | X | | X | | | X | | | | |
| 13 | Jonah | 42.4360, 109.6960 | MSI | X | X | X | X | | X | | | X | | | | |
| 14 | Pinedale | 42.8698, 109.8707 | MSI | X | X | X | X | | X | | | X | | | | |
| 15 | SODAR | 42.6070, 109.8646 | T&B | X | X | X | X | X | | | | | | | | |
| 16 | LaBarge | 42.2642, 110.1947 | ARS | X | | | | X | | | | | | | | |
| 17 | Marbleton | 42.5528, 110.1050 | ARS | X | | | | X | | | | | | | | |
| 18 | Bargerville | 42.8200, 109.7653 | ARS | X | | | | X | | | | | | | | |
| 19 | Farson | 42.1100, 109.4428 | ARS | X | | | | X | | | | | | | | |
| 20 | Sand Draw | 42.6019, 109.6294 | ARS | X | | | | X | | | | | | | | |

| | |
|---|---|
| X | Operational |
| X | Suspect |
| X | Delayed Connectivity |
| X | Inoperative |
| X | Not installed yet |

**Figure 2-14.** Equipment status matrix.

## 2.5 Intensive Operating Periods: Forecasting and Summary of Conditions

### 2.5.1 Forecasts and Operational Readiness

Given the intermittent nature of elevated ozone episodes in the study area and the need for a 48 hour lead time to allow for deployment of the IOP supplemental measurement program described in Section 2.3, an IOP forecasting protocol was developed and implemented. Daily forecasts were a key part of the decision making process for operations during the 2009 UGWOS study. New forms were developed for the 2009 study to provide information on forecast conditions, the readiness of the project for operations and to inform participants on the current and future operational mode. The structure of the forecast was essentially the same as in prior years, with the main change being the formalization of the appearance and content. The operational readiness portion, which in the past had been embedded with the forecast, was moved to its own form. Both the forecast and the operational readiness forms were converted to PDF files and submitted to the official UGWOS web site by 10:00 MST / 9:00 PST each morning, seven days a week. These PDF files were also archived. The forms were viewable to participants in the project, and beginning February 10th following a request from the WDEQ, both the forecast and readiness forms were made available to the general public on the public web-site.

The forecast or "Weather Outlook" form consisted of three sections. The first of these was a synopsis of the current weather features that would be affecting the study area over at least the next 48 hours; the second section was a detailed short-term forecast out through day three. This forecast contained the usual discussion of temperatures, winds, precipitation and sky conditions, but would also emphasize parameters that were of specific interest to the study such as inversion development. At the end of this section there was a discussion on ozone development; the third section was an outlook that covered the time period from day four through day seven. This outlook was similar in content to the second section with only the time frame being different. Also similar to the second section, a brief discussion on any expected ozone development was included. An example of the forecast form can be found in Figure 2-15.

**Upper Green Winter Ozone Study**

Weather Outlook

**PLEASE NOTE: This product is not a public weather forecast and is solely intended to be used as a guide by UGWOS study participants to determine if and when conditions potentially favorable for field operations might occur. This product is independent of the Wyoming Department of Environmental Quality's (WDEQ) Ozone Advisory forecasting process and is not intended for assessing the potential for unhealthy air quality. The WDEQ Ozone Advisory can be accessed at: http://deq.state.wy.us**

Issued: Saturday, February 28, 2009 at 1000 MST/0900 PST

SYNOPSIS

The high pressure ridge is just to the west of western Wyoming this morning and will move over-head today and Sunday before it is pushed east and flattened by an incoming storm late Monday and Tuesday. Another storm is likely towards next weekend. There continues to be a chance for a longer period of high pressure which may develop between the 10th and 15th of March.

SHORT TERM FORECAST (THRU DAY 3)

Cold this morning with light winds and sunshine through the day, high temperatures should be a little below to near freezing. Tonight will be 10 to 12° F warmer with light winds and clear skies. Sunday should see increasing clouds and it will be warmer with most locations in the mid 30's to around 40° F with winds likely remaining light. Inversions will be in place for most if not all of the day today and will strengthen tonight. With warmer temperatures Sunday this inversion should weaken considerably and possible mix out entirely in the southern portion of the study area.

OZONE: Today will see elevated ozone at some monitoring locations this afternoon, and Sunday will likely see the same despite increasing clouds, as winds are expected to be light. It now looks like elevated ozone could occur on Monday as well if increasing winds aloft do not mix to the surface.

LONG RANGE OUTLOOK (DAY 4 TO 7)

Longer range outlook for Tuesday (3rd) through Friday (6th): A brisk southwest flow is expected to develop over the study area and there will be clouds and possibly some light snow at times over the area as systems travel across Wyoming.

OZONE: Increased mixing is expected to keep ozone readings near background levels.

**Figure 2-15.** Example daily UGWOS forecast.

The operational readiness or "Operational Mode" form contained five sections: The first showed what the current operational mode was for the day. There were three categories for operational mode. "STAND DOWN" was the first of these categories and was used when no IOP's were planned over the next 48 hours. The second was "ALERT', and was used when operations were possible within 48 hours. Participants were expected to watch the situation closely and be ready to go into an operational mode quickly. The third category was" IOP", which meant that the study was currently in an Intensive Operational Period, and that the participants were either preparing for operations or already engaged with operations. The current operational mode was highlighted in large lettering in this section of the form; the second section of the form was a brief discussion or summary of the current weather conditions; the third section was a summary of equipment readiness indicating what, if any, issues were currently being addressed or needed correction; the fourth section was a summary of personnel and whether there were any problems or issues with availability; and the fifth section was a brief discussion of the decision that was made on the current mode of operation. An example of the operational mode form can be found in Figure 2-16.

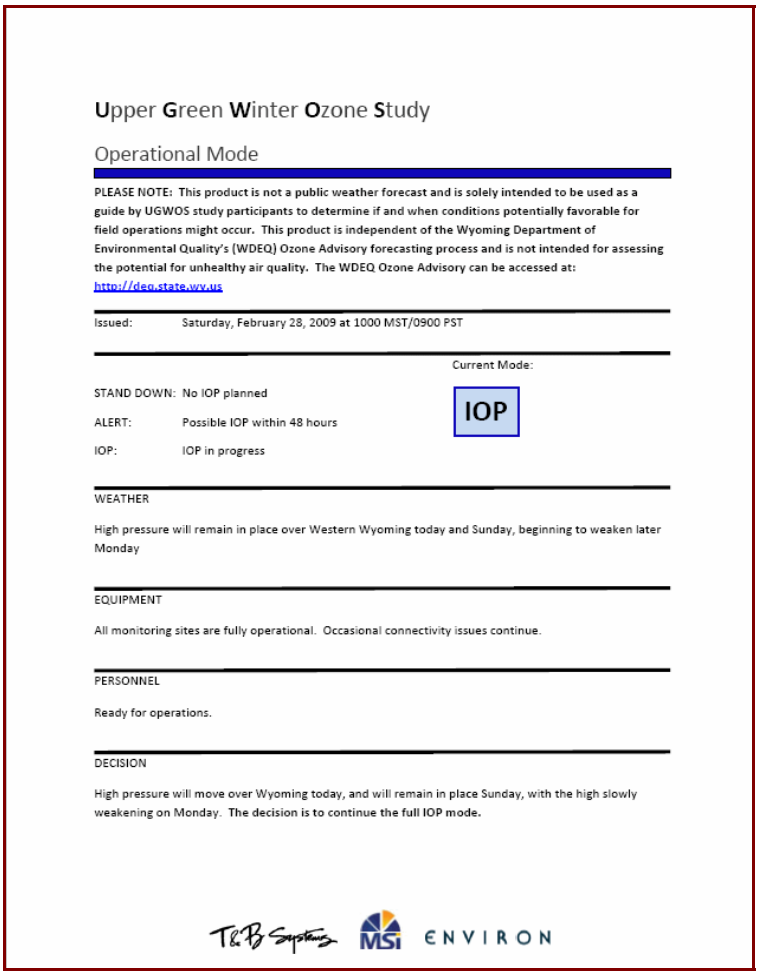

Upper Green Winter Ozone Study

Operational Mode

PLEASE NOTE: This product is not a public weather forecast and is solely intended to be used as a guide by UGWOS study participants to determine if and when conditions potentially favorable for field operations might occur. This product is independent of the Wyoming Department of Environmental Quality's (WDEQ) Ozone Advisory forecasting process and is not intended for assessing the potential for unhealthy air quality. The WDEQ Ozone Advisory can be accessed at: http://deq.state.wy.us

Issued: Saturday, February 28, 2009 at 1000 MST/0900 PST

Current Mode:

STAND DOWN: No IOP planned

ALERT: Possible IOP within 48 hours

IOP: IOP in progress

IOP

WEATHER

High pressure will remain in place over Western Wyoming today and Sunday, beginning to weaken later Monday

EQUIPMENT

All monitoring sites are fully operational. Occasional connectivity issues continue.

PERSONNEL

Ready for operations.

DECISION

High pressure will move over Wyoming today, and will remain in place Sunday, with the high slowly weakening on Monday. The decision is to continue the full IOP mode.

**Figure 2-16.** Example UGWOS operational mode form.

## Forecast Techniques

The forecasting methodology from prior years was used in the 2009 UGWOS study. The analysis of critical points for several meteorological parameters in the development of high ozone levels were constructed prior to the 2007 study and continue to hold true. These criteria points are listed below.

- Mean sea level pressure 1020 mb or higher;
- Surface wind speeds less than 4 meters per second (m/s);
- 700 mb pressure level higher than 3060 meters (m);
- 700 mb pressure level temperatures 0 to -8 °C;
- 700 mb pressure level wind speeds less than 10 m/s;
- 500 mb pressure level higher than 5700 m;
- 500 mb pressure level winds less than 15 m/s;
- Surface snow cover present.

Forecasts issued over the 2009 season were based on these criteria and other observations made during the 2007 and 2008 ozone studies by the project meteorologists. Some of these observations were that:

- The end of elevated ozone events is frequently due to atmospheric mixing and increased wind speeds and not on the development of overcast skies and precipitation in cases where a storm moves across the study area. Where storms are weak, the erosion of the surface inversion and the mixing-out of the trapped pollutants can take a long time.
- The development of elevated ozone levels is more likely to occur when the ridge axis aloft has moved east of the study area and the flow turns southwesterly.

Three IOP events were forecast during the 2009 study: IOP #1 (3-5 February), IOP #2 (21-22 February) and IOP #3 (28 February – 3 March ). IOP #2 was forecast to be a marginal event with only limited pollutant build-up and therefore not all IOP measurements were conducted during this event.

### 2.5.2 Synoptic Weather Summaries of IOP Events

The forecasting protocol that has been established for the determination of the commencement of IOP operations calls for a synoptic scale high pressure ridge to be located over or just to the east of the UGWOS project area. This type of feature typically produces the stable stagnant local weather conditions conducive to winter ozone development in the Upper Green River Basin. During the three month period of January through March of 2009, this desired synoptic weather scenario only occurred twice, while during the rest of the period the weather pattern was characterized by persistent northwesterly flow and a seemingly endless stream of Pacific short wave troughs and strong windy cold air advection. The short were ridges that were interspersed between the troughs never developed to any great extent, and the few times that they did, the ridge axis's never reached the project area. The two exceptions to that pattern were the large high pressure ridges that migrated across the western US during the first few days of February, and at the beginning of March. The two full-scale IOP operations of the UGWOS 2009 monitoring project took place during those two ridging episodes. In addition, a reduced set of measurements were conducted during 21 and 22 February when marginal IOP conditions were forecast.

In the remainder of this section, the synoptic scale weather features affecting the project area during the two full IOP's are summarized using a few example weather charts for each IOP period. The 700 mb constant pressure synoptic weather maps, generated and archived twice daily by the NOAA Storm Prediction Center (SPC), were chosen as the best weather depiction products to illustrate the large-scale weather patterns.

#### Feb 3 – 5

The first opportunity to initiate a full-scale IOP field monitoring operation during UGWOS 2009 appeared to be taking shape in the first week of February. A large omega-type high pressure ridge had built in the Eastern Pacific and had moved into the interior west by February 3$^{rd}$. Figure 2-17 clearly shows the location and configuration of the ridge as it appeared on the 700 mb constant pressure map during the morning of February 3, 2009. The axis of the ridge extended from southwestern Canada southward through the western Great Basin all the way down to northwestern Mexico. Pressure gradients within the interior of the ridge were very weak and wind flow was somewhat variable, but around the northern and eastern parameters of the ridge, pressure gradients were quite strong. As a result of the gradient, strong northwesterly flow

and cold air advection aloft predominated in the Rocky Mountain States east of the high pressure ridge. This included all of Wyoming, and the project area.

Synoptic scale weather forecasts preceding the initiation of the IOP, and during the early stages as well, called for the western high pressure ridge to slowly weaken but continue to drift eastward during February 4th and 5th, with the ridge axis passing over southwestern Wyoming during the afternoon of the 4th. Figure 2-18 presents the 700 mb constant pressure chart for that afternoon. By that time, the ridge axis was just slipping into the southwestern Wyoming, but the northern perimeter of the ridge had pushed farther south than expected and had also flattened out. As a result, the light gradient flow and increasing subsidence associated with a high pressure ridge did not materialize to as full an extent as originally expected. Wind speeds were lighter, mixing layer wind directions became southerly to southeasterly and relatively strong inversions persisted in the area, but the mixing layers were relatively deep and the resulting dilution limited pollutant buildup. The high pressure ridge continued to flatten and stall during February 5th, slowly bringing an end to the relatively weak ozone episode by February 6th.

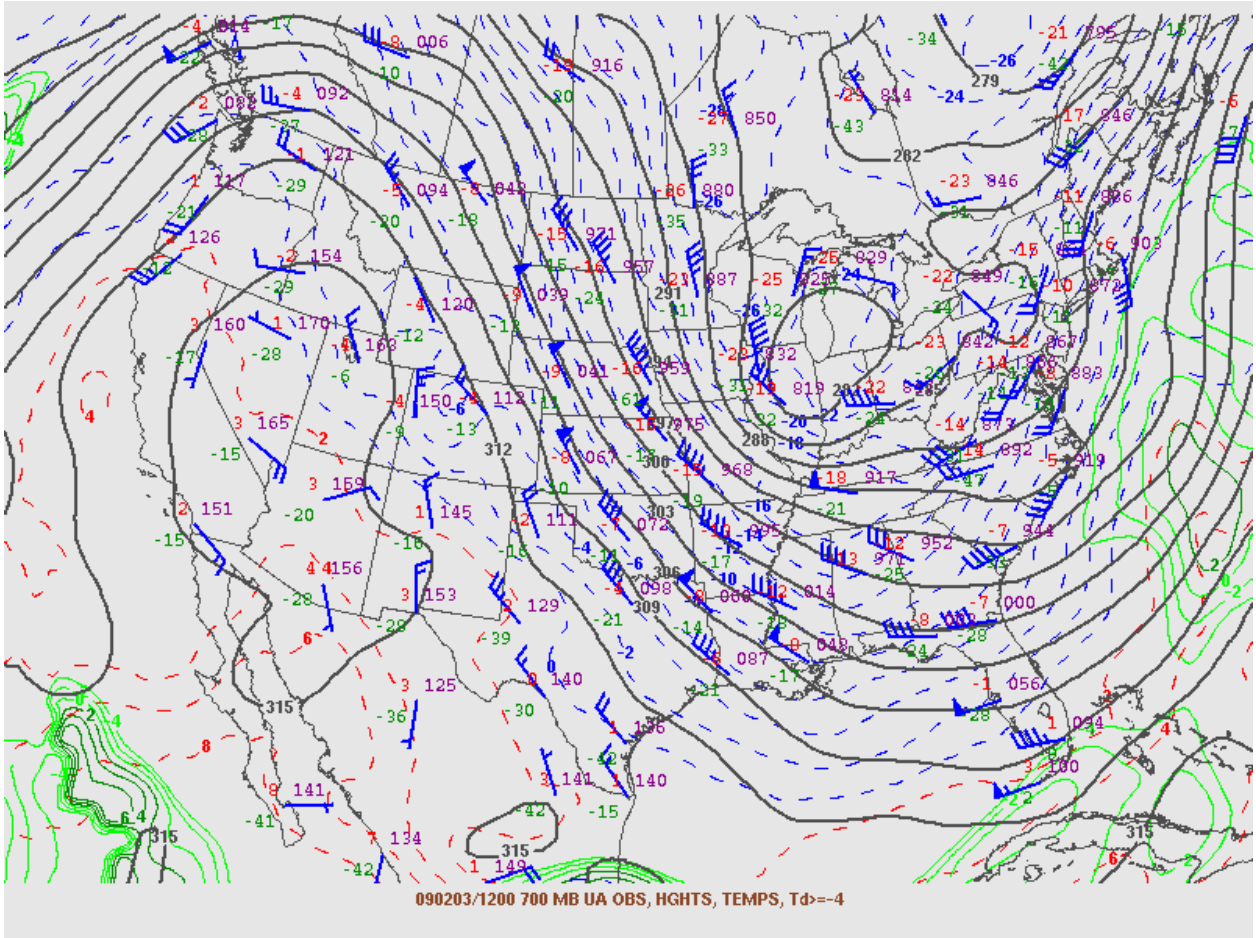


**Figure 2-17.** Constant pressure map for 700 mb, AM (1200 UTC), 02/03/09 (Source: http://www.spc.noaa.gov).

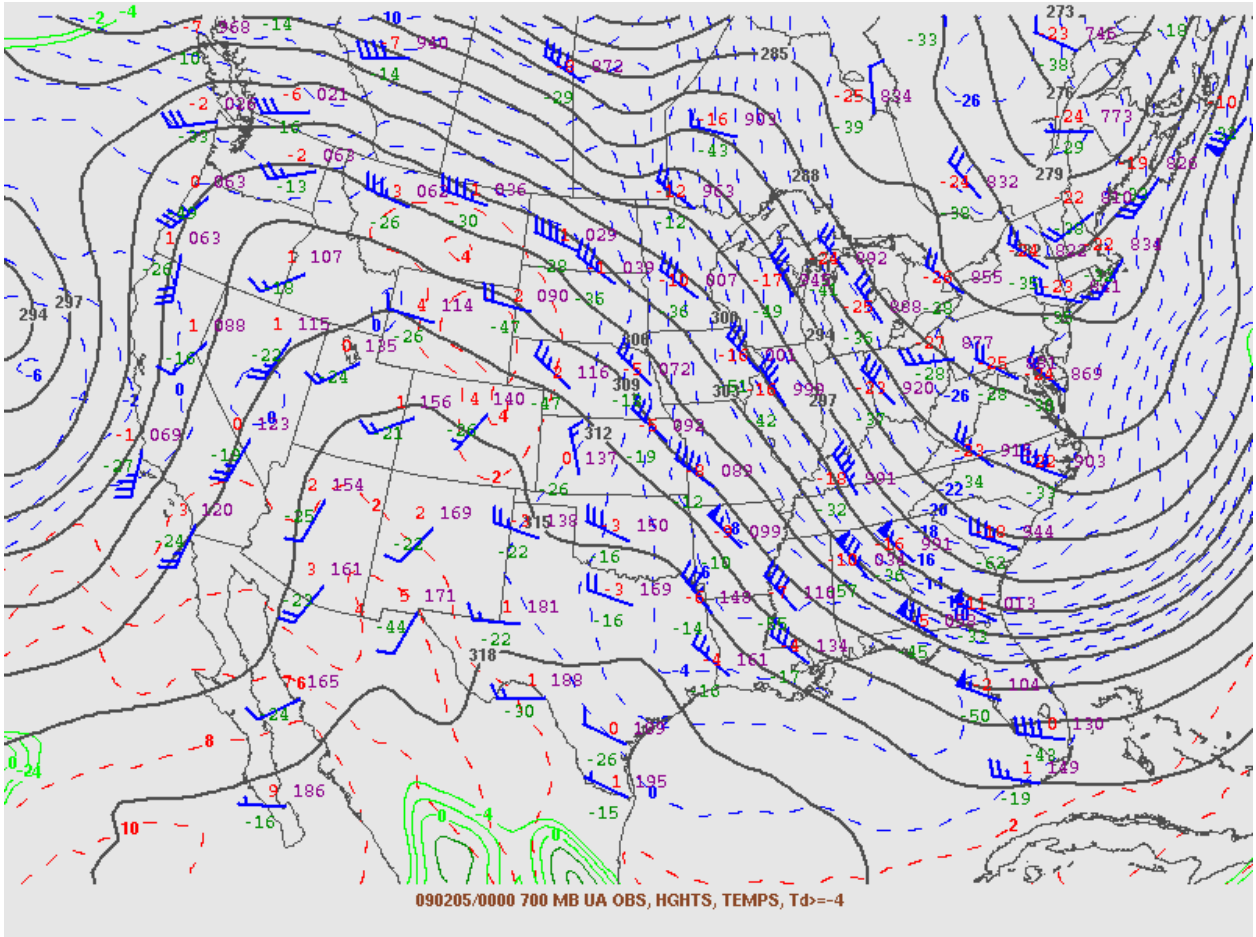


**Figure 2-18.** Constant pressure map for 700 mb, PM (2400 UTC), 02/04/09 (Source: http://www.spc.noaa.gov).

Feb 28 – Mar 03

The second full-scale IOP operation during the UGWOS 2009 project was characterized by the passage of a large long wave high pressure ridge during March 1st and 2nd, 2009. Figure 2-19 presents the 700 mb constant pressure chart for the morning of February 28, 2009. A large omega-type ridge, which had moved into the western interior from the eastern Pacific, can be seen over the Great Basin west of southwestern Wyoming on the chart. Like the high pressure ridge that moved through the same area during the first IOP in early February, this ridge was extensive in size, and was forecast to remain intact as it moved through the Rocky Mountain states during March 1st and 2nd. Unlike the ridge associated with the early February IOP, this ridge extended much farther north into western Canada and therefore the northern perimeter was not as close to southern Wyoming as was the case with the ridge that approached on February 3th. Also, the pressure gradient around the northern and eastern perimeter of this high pressure area was not as strong as in the first IOP, and therefore, gradient winds in the project area were lighter and cool air advection was much less a factor as the ridge approached on the 28th.

Figure 2-20 shows the ridge configuration and location on the 700 mb constant level chart by the afternoon of March 2, 2009. By that time, the axis of the ridge had drifted to just east of the project area, and was still intact over the Intermountain area. Under this configuration, it had produced stagnant, low wind, stable conditions in southwestern Wyoming during March 1st and

2nd. With the light gradient winds and significant subsidence conditions, light localized flow patterns developed during this two day period and low boundary layer capping inversions persisted through both afternoons. A vigorous Pacific trough moving across California on the 2nd induced slowly increasing southwesterly gradient flow that finally lead to the abrupt end of the ozone episode by March 3rd. Increasing baroclinicity ahead of the trough resulted in the total obliteration of the low-level temperature inversions of the previous two days. This, combined with the strong southwesterly winds, produced excellent ventilation in the project area and put an end to the IOP on March 3, 2009.

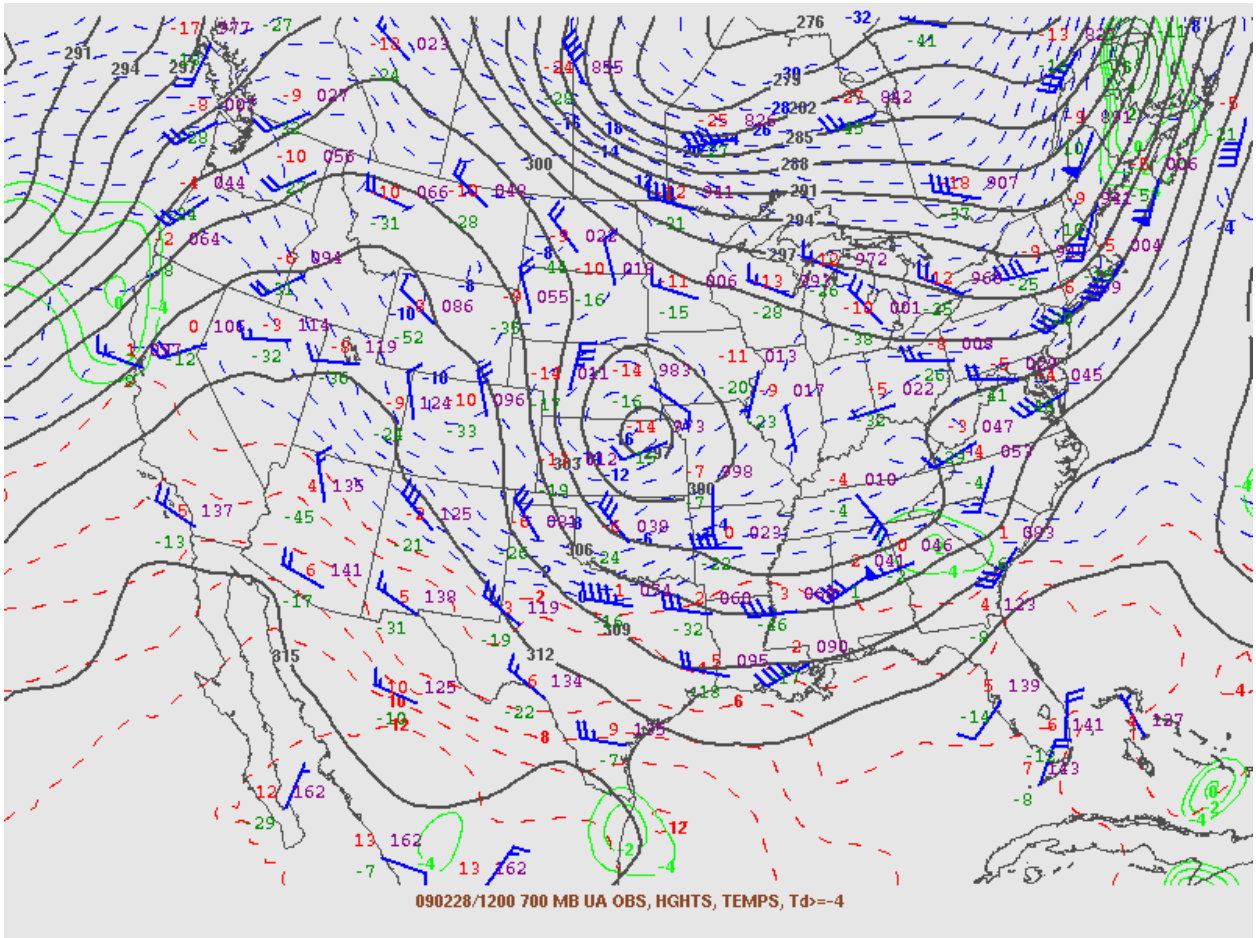


**Figure 2-19.** Constant pressure map for 700 mb, AM (1200 UTC), 02/28/09 (Source: http://www.spc.noaa.gov).

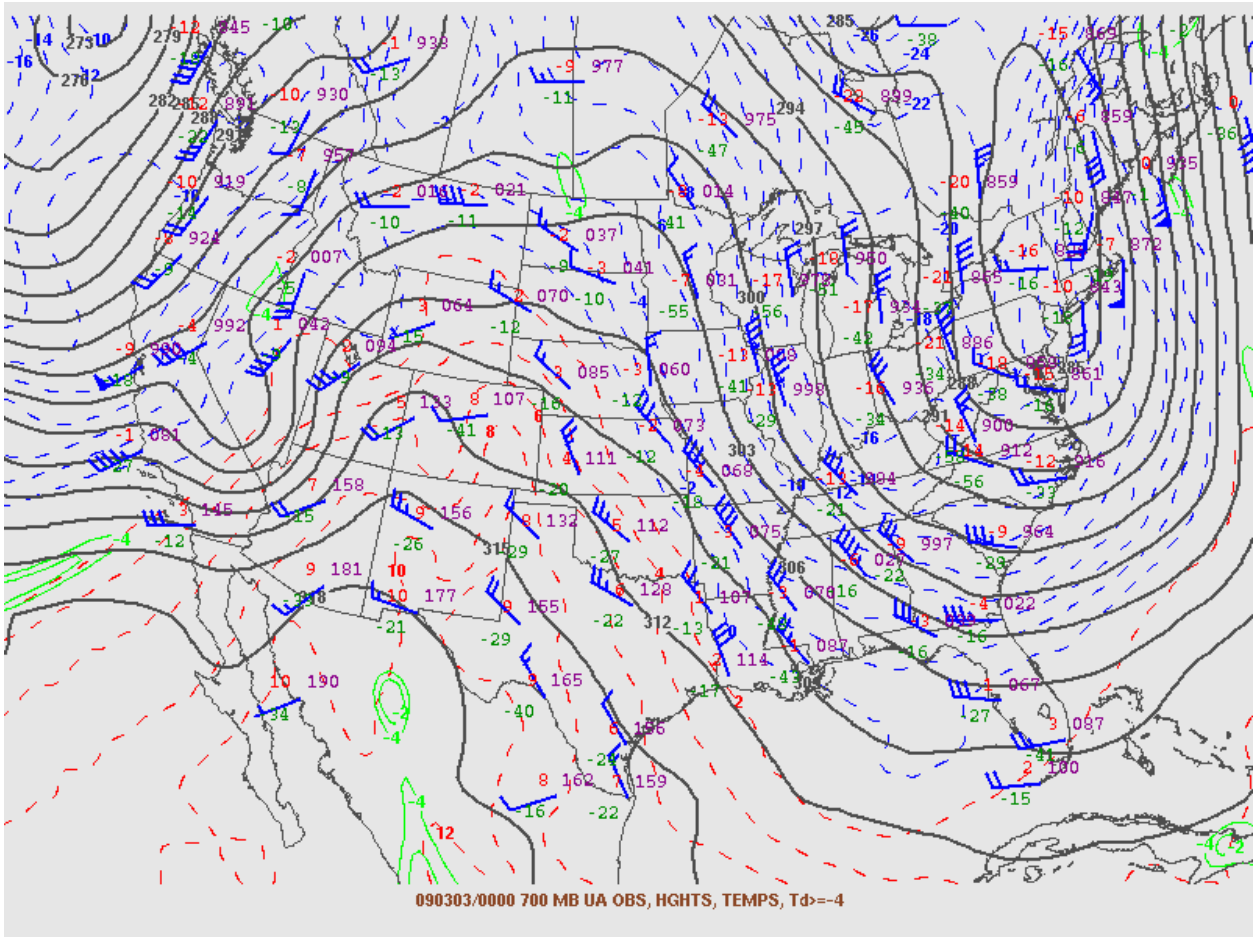


**Figure 2-20.** Constant pressure map for 700 mb, PM (2400 UTC), 03/02/09 (Source: http://www.spc.noaa.gov).

# 3. DATA QUALITY ASSURANCE, VALIDATION AND ARCHIVING

A primary study objective was to produce an adequately validated data set from the field measurements that is well defined and documented. The data management system utilized was designed to be straightforward and easy to maintain. Each study participant was responsible for reviewing and validating their collected data, and submitting the data to the Data Manager in a prescribed format. A brief summary of procedures used is provided in this section. A complete description of data collection, quality assurance, validation, and data reporting procedures is available in Appendix A.

## 3.1 Data Management and Reporting

The overall goal of the data management effort was to create a well documented system such that data could be readily input and easily accessed. A Monitoring and Quality Assurance document was prepared and approved by all the project participants (see Appendix A). Each of the participants that provided data was responsible for reviewing and validating their respective data. This included flagging values for instrument downtime and performance tests, applying any adjustments for calibration deviation, investigating extreme values and applying appropriate flags.

Flags used for the UGWOS data set are presented in Table 3-1. Each data provider was also responsible for documenting their validation process so that it could be provided to the Data Manager and other analysts if needed.

**Table 3-1.** Data flags used in the UGWOS database.

| Flag | Description |
|---|---|
| V | Valid |
| S | Suspect: data appears to be a data spike or outside normal data range |
| I | Data invalid |
| M | Missing – measurement not taken |
| U | Invalidated data – user is responsible for validation |
| N | Instrument noise detected in sub-hourly data used to create hourly average |

In addition, each data provider was responsible for furnishing information regarding the monitoring equipment used in the field study and any additional information to the Data Manager requested to enhance the overall documentation of the study. In particular, participants provided the Monitoring Quality Objectives (MQOs) defining the quality of all data submitted as "valid." These MQOs contained the accuracy, precision, lower quantifiable limit, resolution and completeness of each measurable. This information is available in metafiles that accompany the data base.

Standards for time reference, averaging period, parameter names and units were all defined beforehand and are consistent throughout the database. Data fields have a second column for each measured value for the accompanying QC code as needed. Data flagged as invalid or missing were given a value of -9999. Suspect data were flagged as such but the data was included.

## 3.2 Quality Assurance

As part of the quality assurance program, quality control procedures were implemented to assess and maintain control of the quality of the data collected. A Monitoring and Quality Assurance Plan was submitted to the WDEQ and approved prior to the start of monitoring (See Appendix A). This document provides a detailed discussion of the quality assurance program implemented in this study. A summary of key elements of the QC program for each measurement is presented in the remainder of this section.

All equipment underwent a complete checkout and acceptance prior to the start of monitoring. This included a dry run of all measurement methods, during which operating procedures were refined and fully documented. Standard operating procedures (SOPs) for measurements were completed prior to the start of monitoring.

All ozone analyzers and samplers were routinely checked using a traceable transfer standard following operating procedures consistent with EPA guidelines. Calibrations were conducted on the mesonet ozone analyzers before and after each IOP. Linear regressions were calculated for each calibration. The averages of the linear regression slopes and intercepts from all of the calibrations performed on each analyzer during the course of the study were used to adjust the raw data. More discussion on the adjustment of the ozone data is presented in Section 3.3.2.

The status of the miniSodar was checked daily via remote access of the data. When problems were noted, WDEQ field staff was called upon to assist in correcting them. In addition, the miniSodar data were available in real time so that team members were able to use the data to assist in special monitoring and forecasting. Additional information on quality assurance procedures for these data is provided in Appendix A.

VOC canister samplers were checked for contamination prior to the IOP by filling a clean canister using each individual sampler and submitting it for analysis. VOC and carbonyl sampling field blanks totaling approximately 5 percent of the collected field samples were collected and analyzed. In addition, during sampling periods immediately following IOP#2 and IOP#3, two VOC and carbonyl samplers were collocated to collect duplicate samples as a precision check. On-going laboratory QA was performed on each batch of samples as they were received and analyzed including method blanks, QC duplicates, laboratory control spikes and laboratory control duplicates.

### 3.2.1 Calibrations

The purpose of a calibration is to establish a relationship between the ambient conditions and an instrument's response by challenging the instrument with known values and adjusting the instrument to respond properly to those values. The calibration method for each of the air quality and meteorological variables is detailed in the Monitoring and Quality Assurance Plan (Appendix A).

Calibrations of the ozone instruments were performed upon initial installation and at the end of the study period. Additional calibrations were performed on an as-needed basis in the event of equipment repair or replacement. All calibrations were performed in accordance with the manufacturer’s recommendations and were consistent with USEPA guidelines. Calibrations and zero/span checks of all mesonet ozone monitoring equipment were conducted before and after each IOP using an ozone calibrator verified against a transfer standard certified quarterly by

MSI. USEPA FEM analyzers at Boulder II and the airport were checked using this transfer standard. This transfer standard in turn had been certified against MSI's primary standard maintained following EPA's guidelines at their office in Salt Lake City, Utah. This standard has also been certified in July, 2008 against the US EPA Region 8 primary standard maintained at Boulder, CO.

All meteorological sensors were calibrated at the beginning and ending of the study. Wind speed sensors were calibrated using an RM Young constant rpm motor simulating wind speeds at several points across the sensor's operating range. Wind direction sensors were calibrated by checking responses at standard increments with an RM Young vane angle fixture. Temperature sensors were calibrated using a certified reference temperature sensor.

### 3.2.2 QA Audits

As part of the UGWOS quality assurance program, an independent audit program was implemented to verify the site operations and data accuracy. The auditor and the equipment used for the audit were independent of the measurement program. Audits were performed in accordance with the principles set forth by the US EPA.

Ozone analyzers were audited using a Dasibi Model 1008 PC transfer standard that is certified against T&B System's primary standard maintained following EPA's guidelines at their office in Valencia, CA. The Model 1008 PC is an ozone photometer equipped with self-contained zero air and ozone generation. For the mesonet audits, the transfer standard was operated within the SUV used during the audit. The transfer standard was powered using a true sine wave inverter, and was allowed to warm up prior to the audit to a point where the temperature within standard's photometer cell was relatively stable. Ozone concentrations were fed to the mesonet site's sample inlet with an 8-foot ¼" Teflon line, with a venting tee placed at the inlet. The airflow to the tee was approximately 2.5 lpm, minimizing residence time within the line. For ozone analyzers sited within buildings, introduction of the audit concentrations through the sample inlet was not possible, though the setup was configured to go through as much as the sample train as possible.

At the mesonet sites, wind speed sensors were audited using an RM Young constant rpm motor simulating wind speeds at several points across the sensor's operating range. Wind direction sensors were audited by checking the sensor orientation and responses in 30° or 45° increments using the marks on the wind direction sensor. The wind speed starting threshold was checked using and RM Young torque disc. Wind sensors were left in place during the audit to minimize the audit effort and prevent any accidental damage to the monitoring system. This setup likely resulted in a decrease in the precision of the wind direction checks, particularly under windy or extremely cold conditions. In addition, wind direction starting thresholds could not be directly checked, thought the bearings were inspected by feel.

Temperature sensors were audited using a water bath and a certified audit sensor. Two points were checked using an ice bath and an upscale water bath between $10^{o}$ and $20^{o}$C. For the Cora site, ambient temperatures were cold enough during the audit to provide an additional check at a sub-zero level using a collocated temperature sensor.

The nitrogen species, CO, $SO_2$, and non-methane measurements at Boulder 2 and the University of Wyoming Trailer were audited using a certified dilution system and a certified span gas

cylinder. For the CECERT measurements, audit concentrations were introduced through the sample inlet, which was critical due to the location of the NOy converter.
Comparisons were made of the operator's ability to measure VOC and carbonyl flows by conducting flow measurements of one sampler using both the study flow meter and an audit Gilibrator II bubble flow meter.

The following summarizes the audit results, including any noted recommendations.

**Mesonet**

- Ozone audit results are summarized in Table 3-2. The table is divided into three sections, with the first section summarizing the mesonet stations calibrated using the 2B ozone standard, the second summarizing special study analyzers calibrated using traditional transfer standards, and the third summarizing the first quarter 2009 results from the routine quarterly audits conducted by T&B Systems of the WDEQ network analyzers. Two sets of values are shown: initial results using the reported data from the data logger, and results after adjusting data using calibration MSI-provided adjustment factors for each of the UGWOS mesonet ozone analyzers which were based on routine calibrations conducted during the study. With the exception of the 2B monitor at Boulder, results for the initial, unadjusted data show all monitors meeting the network monitoring quality objective of ±10% (audit slope of 0.9 to 1.10). However, while doing a good job of standardizing responses (as evidenced by the improved zeros and standard deviations), use of the MSI adjustment factors in general lowers the monitors' responses. The table reveals a noticeable bias between the 2B calibrator and the audit transfer standard, with adjusted results averaging almost 10% lower than anticipated. This, in essence, would imply that the ozone concentrations generated by the 2B calibrator are on the order of 10% higher than anticipated. In contrast, audit results for the conventionally calibrated analyzers show very good agreement with the audit input concentrations, with the audit slopes typically within about 2% of 1.000. These results are discussed further in Section 3.3.2 below.

- Audits of the mesonet meteorological systems revealed that all wind and temperature sensors were operating correctly. Audit results for some wind direction points fell slightly outside of the $\pm 5^{o}$ audit criteria, but this was likely due to the difficulty in conducting the audits, with the discrepancies occurring primarily during periods of high wind speed or extreme cold.

**Boulder 2**

- All special study gaseous analyzers at the Boulder II trailer easily met the audit criteria. Chemiluminescent ozone data were first adjusted using factors supplied by MSI to account for differences between the ozone calibrator and the transfer standard. Results of the audit are summarized in Table 3-3. It should be noted that the higher intercepts for the NOx and NOy analyzers are due to programmed offsets in the data logger, which will be subtracted during processing of the data. Review of the analyzer displays during the audit showed both analyzers to be reading essentially 0.000 when sampling zero air.

- The measurement of VOC and carbonyl flow rates were confirmed by a comparison between audit and operator flow measurements during maintenance of one of the samplers. Results are presented in Table 3-5. All results easily met the audit criteria of ±10%.
- It was noted that the upward facing UV sensor had a thin coating of ice crystals on it. It is unclear if data were affected by this, but it was recommended that the sensor be cleaned periodically, particularly before IOPs.

**Table 3-2.** Ozone audit results.

| Site | Audit Results - Initial | | Results after data adjustment | | MSI Adjustment Factors | |
|---|---|---|---|---|---|---|
| | Slope | Int (ppm) | Slope | Int (ppm) | Slope | Int (ppb) |
| Cora | 0.950 | 0.002 | 0.907 | 0.002 | 0.955 | 0 |
| Boulder 2 | 0.838 | 0.009 | 0.925 | 0.000 | 1.104 | -8.6 |
| Mesa | 0.945 | 0.004 | 0.894 | 0.001 | 0.946 | -2.6 |
| Sodar | 1.023 | 0.003 | 0.901 | 0.001 | 0.881 | -1.8 |
| Warbonnet | 0.950 | 0.000 | 0.905 | 0.002 | 0.953 | 2.4 |
| Buckhorn | 0.978 | 0.007 | 0.928 | 0.003 | 0.949 | -3.6 |
| Speedway | 0.941 | 0.005 | 0.902 | 0.000 | 0.959 | -5.1 |
| Juell Springs | 0.930 | -0.003 | 0.903 | 0.003 | 0.971 | 6.2 |
| Seedskadie | 0.950 | 0.000 | 0.921 | 0.000 | 0.969 | 0 |
| Simpson Gulch | 0.931 | 0.001 | 0.893 | 0.003 | 0.959 | 2.8 |
| Average | 0.944 | 0.003 | 0.908 | 0.002 | | |
| Std Dev | 0.046 | 0.004 | 0.012 | 0.001 | | |
| Airport | 0.951 | 0.003 | 0.999 | 0.001 | 1.050 | -2 |
| Boulder Chem | 1.143 | -0.003 | 0.962 | -0.004 | 0.840 | -2 |
| Sand Draw | 0.998 | 0.000 | 0.998 | 0.000 | | |
| Bargerville | 1.012 | 0.000 | 1.012 | 0.000 | | |
| Marbleton | 0.962 | -0.002 | 0.962 | -0.002 | | |
| Boulder | 1.000 | 0.000 | 1.000 | 0.000 | | |
| Daniel | 1.016 | -0.002 | 1.016 | -0.002 | | |
| Jonah | 0.944 | 0.000 | 0.944 | 0.000 | | |
| Pinedale | 1.009 | -0.003 | 1.009 | -0.003 | | |
| Average for FEMs | | | | | | |
| Average | | | 0.992 | -0.001 | | |
| Std Dev | | | 0.026 | 0.001 | | |

**Table 3-3.** Boulder audit results – UGWOS measurements.

| Analyzer | | Slope | Intercept (ppm) |
|---|---|---|---|
| NOy | NO | 0.968 | 0.008 |
| (Nitric Acid) | NOy | 0.979 | 0.006 |
| | NA | 0.979 | -0.001 |
| NOx | NO | 1.041 | 0.010 |
| (K1) | NOx | 1.043 | 0.011 |
| | $NO_2$ | 1.045 | 0.001 |
| $O_3$ (Chemiluminescent) | | 1.143 | -0.003 |
| $SO_2$ | | 0.942 | 0.000 |
| CO | | 1.010 | 0.04 ppm |

**Table 3-4.** VOC/carbonyl flow comparisons.

| | Audit (ccpm) | Site (ccpm) | % Difference |
|---|---|---|---|
| VOC 1 | 47.9 | 50.0 | 4.4% |
| VOC 2 | 47.3 | 49.2 | 4.0% |
| Carbonyl | 1760 | 1707 | -3.0% |

**Sodar**

A system audit was conducted of the sodar site. This included a check of the antenna alignment and level, and a review of the data being collected. No problems were noted.

*Air Toxic Ozone Monitoring Sites*

While not directly part of UGWOS, ozone data from the recently installed Sublette County air toxics network represent a valuable source of data on conditions in the Upper Green River Basin. Three of the network analyzers were operational at the time of the UGWOS audits, and were subsequently audited. Results for the air toxic ozone analyzers audits are include in Table 3-1. Three air toxic sites were operational and providing routine ozone monitoring at the time of the audits: Bargerville, Sand Draw, and Marbleton. Audit results were good for all three sites, easily meeting the audit criteria. The Bargerville and Sand Draw analyzers showed nearly perfect agreement with the audit standard. The Marbleton analyzer was responding about 4% low relative to the audit standard, which, while easily meeting audit criteria, was lower than expected, particularly given the excellent results from the other two sites. It was recommended that the audit results be verified to determine if any potential operational issues exist.

## 3.3 Data Validation

### 3.3.1 Procedures

Each study participant was responsible for reviewing and validating their collected data. The data were validated to *Level 1* as described by Watson, et al. (2001) before being submitted to the database. This included flagging values for instrument downtime and performance tests,

applying any adjustments for calibration deviation, investigating extreme values and applying appropriate flags.

Mesonet data from all sites (including the data from the Pinedale Airport) were plotted together and reviewed for inconsistencies. In addition, the 5-minute average data for each site were reviewed for any unusual spikes that may have affected the 1-hour averages. Data from each mesonet ozone analyzer were adjusted for calibration results as described in Sections 3.2 and 3.3.2.

Each VOC canister was accompanied by a field data sheet which included the following information: Sample date and start and stop time, canister number, sample number, canister pressure at the start and canister pressure at the end of the sampling period. Sample date and start time were checked against the date and start time embedded in the sample number. All canister documentation was checked to confirm that samples were taken during the 3-hour period specified for the IOP measurement. All canisters were checked to confirm that they had reasonable positive pressure at the end of sampling. Analytical results were checked to confirm the proper canister number and sample number.

Carbonyl DNPH cartridges were accompanied by a field data sheet which included the following information: sample date, start and stop times, sample number and sample flow rate. Sample date and start time were checked against the date and start time embedded in the sample number. All carbonyl documentation was checked to assure that samples were taken during the 3-hour period specified for the IOP measurement. After sampling, DNPH cartridges were inserted into the aluminized envelopes provided and sealed with stickers containing the sample number. Sample flow rates were verified periodically during the IOP and if the rates changed an average flow rate was assigned to the appropriate period.

Analytical results for both VOC and Carbonyl samples contain fields for data qualifiers assigned by the laboratory (LAB QUALS) and by the field sampling technicians (SAM QUALS). Laboratory and field sampling data qualifiers are presented in Table 3-5 and Table 3-6, respectively.

**Table 3-5.** Laboratory data qualifiers for VOC and carbonyl data.

| LAB QUALS Data Qualifiers | Description |
|---|---|
| B | This compound was detected in the blank above the Reporting Limit (RL) |
| D | This report was calculated from a secondary dilution factor |
| E | Compound exceeds the calibration range and is an estimated value |
| J | The amount reported is an estimated value because it is between the Reporting Limit (RL) and the Method Detection Limit (MDL) |
| F | Higher detection limit due to sample matrix |
| G | Higher detection limit due to limited sample size |
| Q | Compound secondary ion ratio qualifiers are outside the standard acceptance criteria |
| R | Compound secondary retention time (RT) is outside the acceptance criteria for the method |
| U | Compound is less than the Method Detection Limit (MDL) |

**Table 3-6.** Field sampling data qualifiers for VOC and carbonyl data.

| SAM QUALS Data Qualifiers | Description |
|---|---|
| Z | Zero air sample to check for sampler contamination |
| FB | Field Blank |
| NP | Negative pressure sampling method using a flow controller |
| D | Duplicate sample taken with a collocated sampler |

The UGWOS database for both VOC and Carbonyl data was spot checked against the original analytical results to confirm content.

Daily reviews of the SODAR data included a general scan of the data to identify any potential instrument problems but did not include data editing.

Rawinsonde and ozonesondes quality checking began with ground truth readings prior to instrument releases. Temperature, relative humidity, and ozone readings from independent sensors were recorded and compared with the sonde readings prior to releasing. Some differences between the sonde and ground-based sensors are expected due to a variety of reasons such as local exposure and owing to the lack of flow over sonde sensors when not in motion (ascending). If any sensor deviated significantly from the ground readings, in the judgment of the technician, the sonde was rejected. Post processing procedures included reviews of the data by an experienced meteorologist. Successive soundings were compared for reasonableness.

### 3.3.2 Review of 2B Technologies Ozone Analyzer Performance

When analyzing ozone data collected during UGWOS 2009, it is important to discuss the different equipment used to measure ozone during the study. The WDEQ sites (Boulder, Jonah, Daniel) and the Pinedale CASTNET site all employ EPA "equivalent" designated (i.e., Federal Equivalent Method or FEM) analyzers approved for regulator air quality monitoring. These analyzers operate using a UV photometric method for analyzing ozone, based on the known degree of absorption of UV light by ozone. Similarly, an FEM designated analyzer was also installed for the study at the Airport site, where power was readily available. Analyzers used for the HAPs Network (Bargerville, Sand Draw, Marbleton, La Barge, Farson) were also FEMs. A Teledyne API Model 265A chemiluminescent ozone analyzer was operated continuously at Boulder II adjacent to the existing WDEQ Boulder monitoring station. This analyzer operates on a different principle than the more prevalent UV photometric analyzers and is not subject to the same potential interferences (e.g. from mercury and certain hydrocarbons) which can affect the UV photometric data.

The mesonet sites (Cora, Mesa, Warbonnet, Juell Springs, Simpson Gulch, Speedway, Buckhorn and Seedskadie) monitored ozone using a 2B Technologies Model 202 ozone analyzer. The 2B also operates using the UV photometric method, but is designed to be compact and to operate using a 12 V DC power source. Due to its simplified construction, the sampler does not have an EPA FEM designation. However, the analyzer was subjected to the same calibrations as those used for the conventional EPA FEM analyzers, using ozone concentrations traceable to a certified ozone standard. (See the QA plan in Appendix A). The mesonet 2B analyzers were checked at the beginning and end of each IOP period. Average slopes and intercepts generated from the results of these calibration verification checks were used to adjust data from the 2B analyzers. In addition, a factor of 1.05 was applied to all 2B mesonet data to normalize results to

the FEM analyzer at Boulder based on the intercomparison conducted at that site and supported by audit results of the entire project ozone monitoring network (see discussion below).

To specifically address the comparability of the 2B analyzers with the conventional FEM analyzers, a 2B analyzer was collocated with the FEM analyzer at the Boulder site, and collocated data were collected throughout the study period. Figure 3-1 is a scatter plot showing the results of the comparison of the collocated 2B Technologies ozone analyzer and the routine FEM analyzer at Boulder. In this plot, all available hourly averages collected over the study period were compared. The 2B data for this plot were adjusted by MSI based on the routine calibrations conducted during the study. The FEM data are the finalized data supplied by ARS. As can be seen in the plot, there is considerable disagreement between the two analyzers, mainly for concentrations below 50 ppb. There are numerous instances where the 2B analyzer is reading over 20 ppb lower than the FEM.

Figure 3-2 is a time series plot of the two analyzers for the month of February. Both analyzers agree on the mid-day peaks, though the 2B readings appear to be biased low. However, the plot shows that during the nighttime hours, there can be considerable disagreement between the two analyzers. This is particularly apparent during periods of approximately constant ozone concentrations reported by the FEM (February 1-3 and 26-27), where the 2B response steadily drops during the nighttime hours. This implies a potential dependency on temperature for the 2B analyzer. Figure 3-3 plots the relationship between the difference between the 2B and FEM as a function of box temperature. The plot clearly shows a strong dependency on temperature, with significant difference becoming more notable when the box temperature dropped below 0°C during the nighttime.

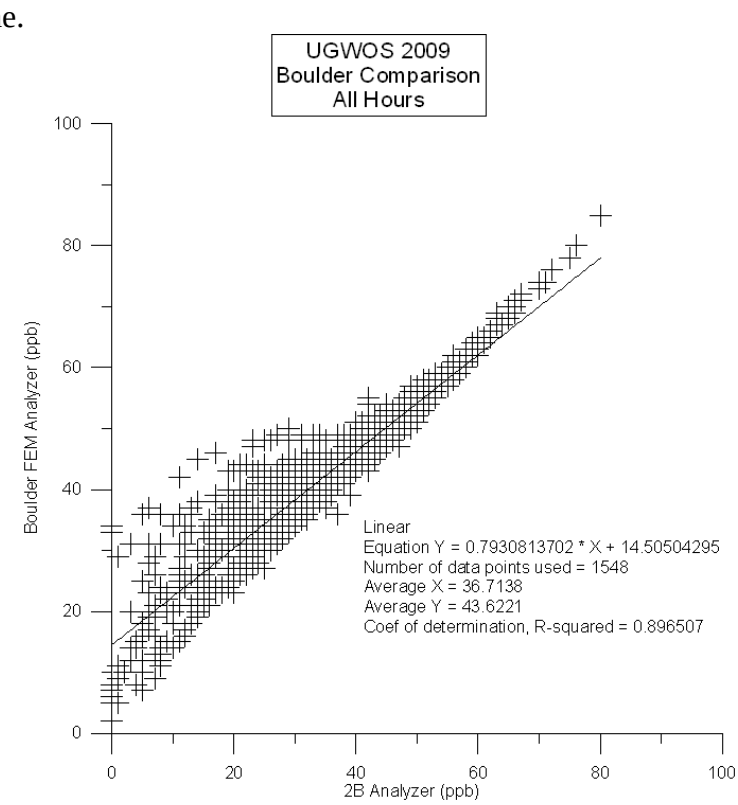


**Figure 3-1**. Comparison of FEM and 2B collocated ozone readings – February-March 2009.

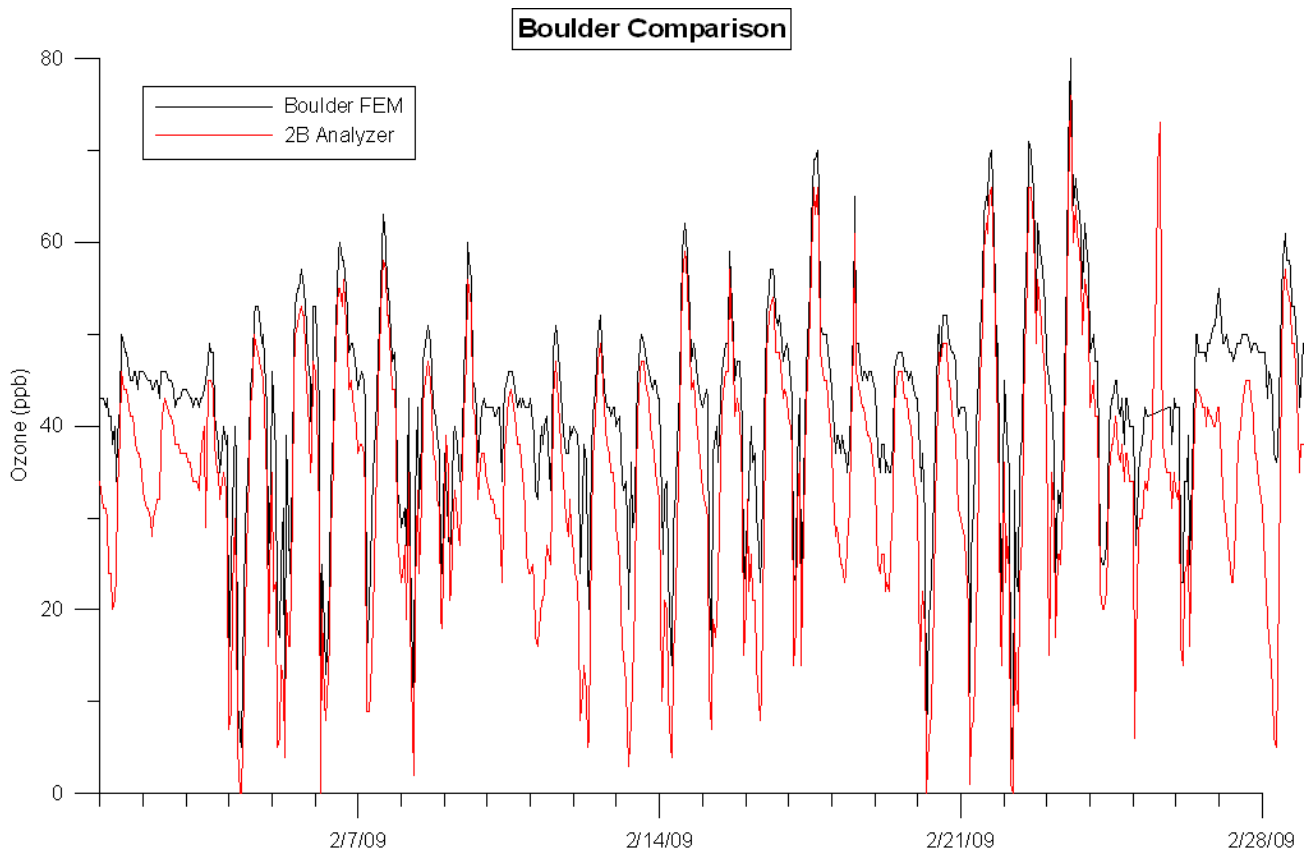


**Figure 3-2.** Time-series plot of FEM and 2B collocated ozone readings – February 2009.

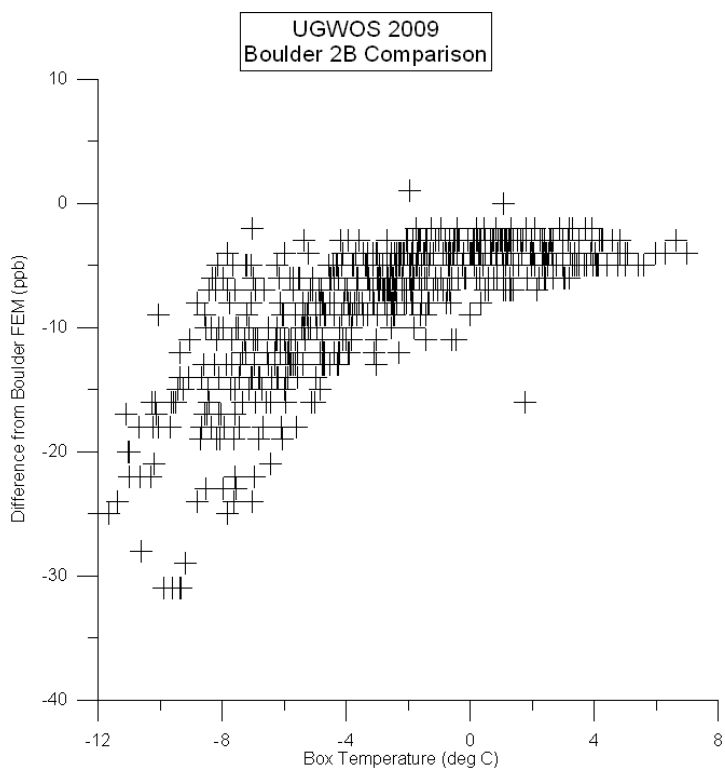


**Figure 3-3.** Plot of the difference between the 2B and FEM as a function of box temperature.

The collocated 2B analyzer at the Boulder site was unique during the study in that it was necessary to change the sample pump midway through the study (in early March). This introduced the possibility that poorer flow had earlier an influence on the temperature dependency. Figure 3-4 was generated using only data obtained after the 2B pump replacement, demonstrating much better agreement with the collocated FEM. The improved correlation is readily apparent, though the regression line is still skewed somewhat toward a slope of less than 1.0 and an intercept that significantly deviates from zero, indicating some lingering effects of temperature on the lower (colder) concentrations. Routine calibrations of the 2B analyzer showed a linear relationship between input and reported concentrations, and thus there is no apparent reason for the zero offset. Thus, for comparison, a second regression equation is presented in red that allows for the forcing of the line through zero.

A second approach to comparing the collocated data is to restrict concentrations to those of most concern, such as those above 60 ppb as presented in Figure 3-5. At these concentrations there is very good correlation between the two analyzers (likely due to the warmer conditions under which they were obtained), though the 2B concentrations are still biased low by about 6% relative to the FEM. Forcing the regression equation through zero doesn't affect the overall agreement, and the resulting slope shows a 6% bias.

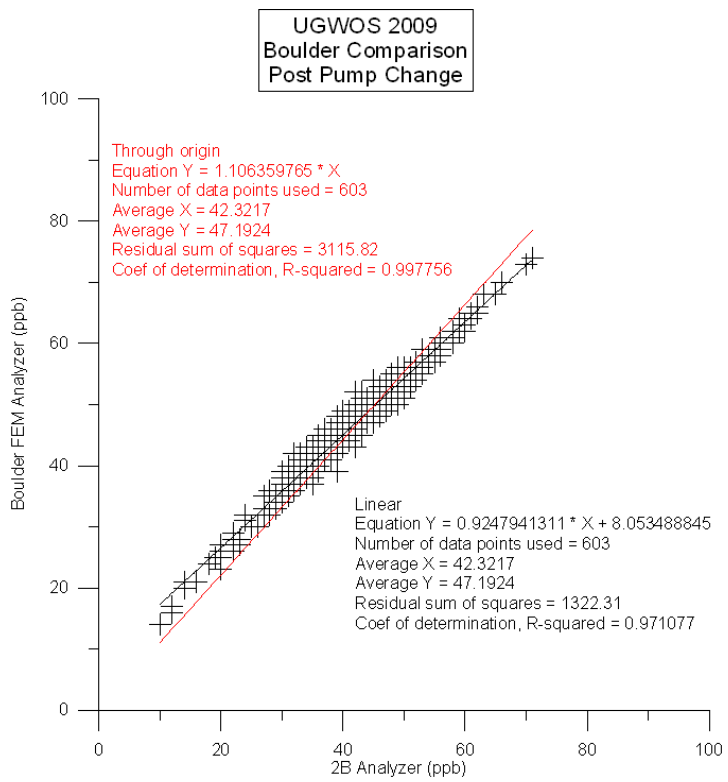


**Figure 3-4.** Comparison of FEM and 2B collocated ozone readings after pump replacement.

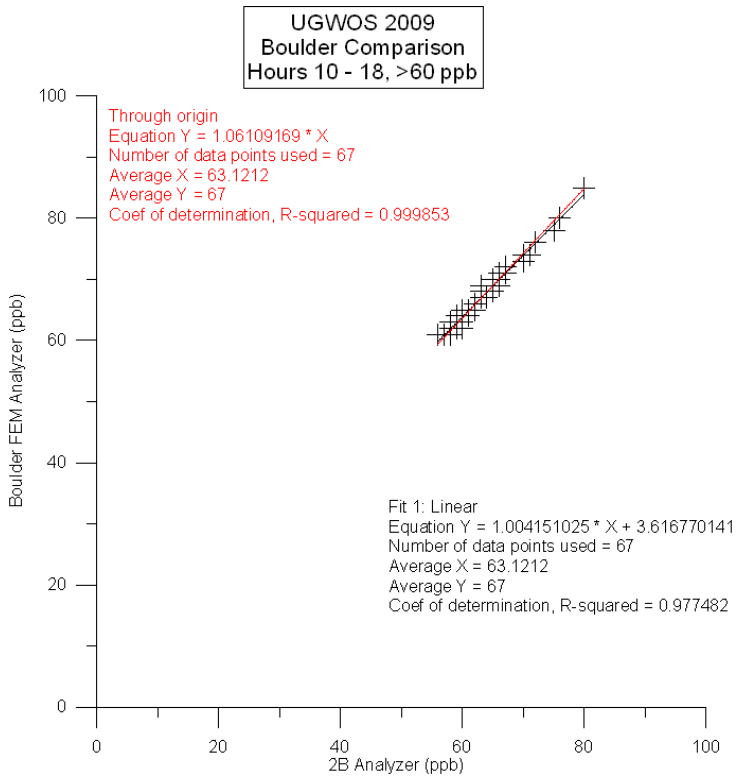


**Figure 3-5.** Comparison of FEM and 2B collocated ozone readings – hourly averages > 60 ppb.

While the above results imply that the major cause of the temperature dependency was a faulty pump, further investigation was conducted to see if other 2B analyzers showed obvious temperature-related issues.

Table 3-1 is a slightly revised version of a table included in the audit report using the finalized data adjustment factors supplied by MSI. As discussed earlier, the audit results are presented in three groups, starting with the 2B analyzer sites, followed by special monitoring sites employing FEMs (with the exception of the chemiluminescence analyzer at Boulder), and lastly the WDEQ FEM sites. The adjusted 2B data is about 9 % low relative to the audit standard (see column labeled "Audit results – adjusted). The apparent bias is remarkably consistent throughout the network. In contrast, results for audits of FEM analyzers using the same audit standard typically show agreement to within 2%. Traceability calculations for both the MSI and T&B transfer standards have all been investigated exhaustively, and no issues were found. However, the at least 6% bias noted in the collocated measurements supports the audit observations, and points to a systematic bias between the mesonet 2B data and the FEM data. There are additional major systematic differences between the calibration and auditing of the mesonet sites. Calibrations were performed using the 2B Model 400 calibrator, and not the usual UV photometer type transfer standard. Also, the audit methodology for the mesonet sites was also somewhat atypical, as the technician had to operate from of a utility vehicle using an inverter power source, and not an ideal controlled environment.

The 9% bias noted during the audit is very close to the 10% data quality objective set for the study. Furthermore, given the interest in concentrations only slightly above the 75 ppb standard, a 10% bias, if it is real, can have a notable impact on results relative to the standard. Based on the results of the collocated comparison, the decision was made to normalize the mesonet data

against the FEMs (specifically the Boulder FEM) by multiplying the MSI-processed data by 1.05. This is a compromise between ignoring the bias and applying a full 9% correction based on the audit, and acknowledges that we do not know exactly the source of the discrepancy. Regardless, this would insure that mesonet values are within ±5%.

This concept of normalizing the sites to the FEM provides another means of investigating whether or not other mesonet sites were susceptible to temperature. To investigate this, hourly averages from all sites were compared against the Boulder FEM averages during periods of regionally good atmospheric mixing – for this case it was assumed to be those hours when the hourly average wind speed at Boulder was greater than 7 m/s. Under these conditions it was assumed that ozone would be spatially consistent, at least in a relative sense. Table 3-7 presents the results of the comparison, which consists of the average of the ratios of each site's ozone concentrations relative to the Boulder FEM measurements for days meeting the above criteria. February was significantly colder than March, and nighttime hours were of course colder than daytime hours. The relative differences between these categories hopefully would reveal possible changes in responses due to temperature. The following observations were made:

- La Barge appears to be in a different meteorological domain, as evidenced by notably lower ratios in all categories.
- Some of the comparisons for the other FEM sites likely are influenced by a different meteorological domain or by local emissions regularly scavenging ozone. For example, the lower ratios for Jonah may be due to local emissions, and the Farson and Marbleton sites may be in notably different meteorological domains. However, for the sake of this comparison, these sites were left in when determining an overall average for the FEM sites, since the same may also be true for some of the mesonet sites.
- Based on the above assumptions, the comparison shows the mesonet sites biased low by about 5%, supporting observations above.
- The improvement in the Boulder II 2B analyzer performance (in terms of temperature dependency) is apparent in the improvement in the nighttime ratios between February and March (the pump was changed in early March).
- With the exception of the Boulder II site mentioned above, there is little change in the mesonet ratios from February to March. Furthermore, while there is a drop in the average ratios between daytime and nighttime, the drop is very similar to that for the FEM average. This would imply that lower nighttime ratios are more likely due to siting than to a temperature affect.
- Looking closer at specific sites, a notable difference between daytime and nighttime ratios is noted at Seedskadie and Simpson Gulch. However, these changes are consistent with an even greater difference for the FEM analyzer at Farson. Similarly, the ratio differences for Warbonnet and Buckhorn are higher than others, but not inconsistent with similar differences noted at the nearby Jonah site. Again, this implies that siting is the likely cause for the differences.

Base on all of the above, it can be concluded that the temperature dependency noted during February for the Boulder II 2B analyzer was likely limited to that analyzer, and was due to a faulty pump.

### 3.3.3 Comparisons of UV and Chemiluminescent Ozone Monitoring Methods

Figure 3-6 through Figure 3-8 present UV photometric ozone data collected at the WDEQ Boulder site plotted with chemiluminescent ozone data from the adjacent Boulder II station. Both analyzers show good general agreement and track well together especially after February 10, 2009. On this date, the chemiluminescent unit was reset with a factory calibration and the span check target was changed from 400 ppb to 200 ppb. Data from this analyzer were adjusted based on the average slope and intercept generated from automated zero/span/precision checks. Prior to February 10, 2009, there were three periodic checks between February 2 and February 10. After this date, automated checks were performed daily.

**Table 3-7.** Ratios of each 2B hourly ozone measurement to Boulder FEM measurement averaged over all hours with average wind speed greater than 7 m/s.

| Site | Daytime | | Nighttime | | Difference | |
|---|---|---|---|---|---|---|
| | February | March | February | March | February | March |
| Cora | 0.95 | 0.94 | 0.94 | 0.96 | 0.01 | -0.02 |
| Boulder 2 | 0.87 | 0.92 | 0.76 | 0.89 | 0.11 | 0.03 |
| Mesa | 0.94 | 0.91 | 0.94 | 0.91 | 0.00 | 0.00 |
| Sodar | 0.86 | 0.86 | 0.84 | 0.81 | 0.02 | 0.05 |
| Warbonnet | 0.89 | 0.89 | 0.83 | 0.81 | 0.06 | 0.08 |
| Buckhorn | 0.91 | 0.88 | 0.85 | 0.79 | 0.06 | 0.09 |
| Speedway | 0.92 | 0.92 | 0.90 | 0.86 | 0.02 | 0.06 |
| Juell Springs | 0.89 | 0.90 | 0.84 | 0.84 | 0.05 | 0.06 |
| Seedskadie | 0.88 | 0.89 | 0.84 | 0.76 | 0.04 | 0.13 |
| Simpson Gulch | 0.88 | 0.89 | 0.79 | 0.79 | 0.09 | 0.10 |
| Average | 0.899 | 0.900 | 0.853 | 0.842 | | |
| Std Dev | 0.030 | 0.023 | 0.059 | 0.063 | | |
| Airport | 0.96 | 0.90 | 0.98 | 0.88 | -0.02 | 0.02 |
| Boulder Chem | 0.84 | 0.89 | 0.81 | 0.87 | 0.03 | 0.02 |
| Sand Draw | 0.94 | 0.96 | 0.86 | 0.88 | 0.08 | 0.08 |
| Bargerville | 1.00 | 0.99 | 0.96 | 1.00 | 0.04 | -0.01 |
| Marbleton | 0.88 | 0.91 | 0.78 | 0.84 | 0.10 | 0.07 |
| Farson | | 0.97 | | 0.79 | 0.00 | 0.18 |
| La Barge | 0.77 | 0.86 | 0.68 | 0.68 | 0.09 | 0.18 |
| Boulder | 1.00 | 1.00 | 1.00 | 1.00 | 0.00 | 0.00 |
| Daniel | 0.98 | 0.95 | 0.97 | 0.92 | 0.01 | 0.03 |
| Jonah | 0.84 | 0.90 | 0.76 | 0.81 | 0.08 | 0.09 |
| Pinedale | 0.90 | 0.88 | 0.94 | 0.92 | -0.04 | -0.04 |
| Average of FEMs (w/o La Barge) | | | | | | |
| Average | 0.938 | 0.940 | 0.906 | 0.893 | | |
| Std Dev | 0.059 | 0.044 | 0.094 | 0.075 | | |

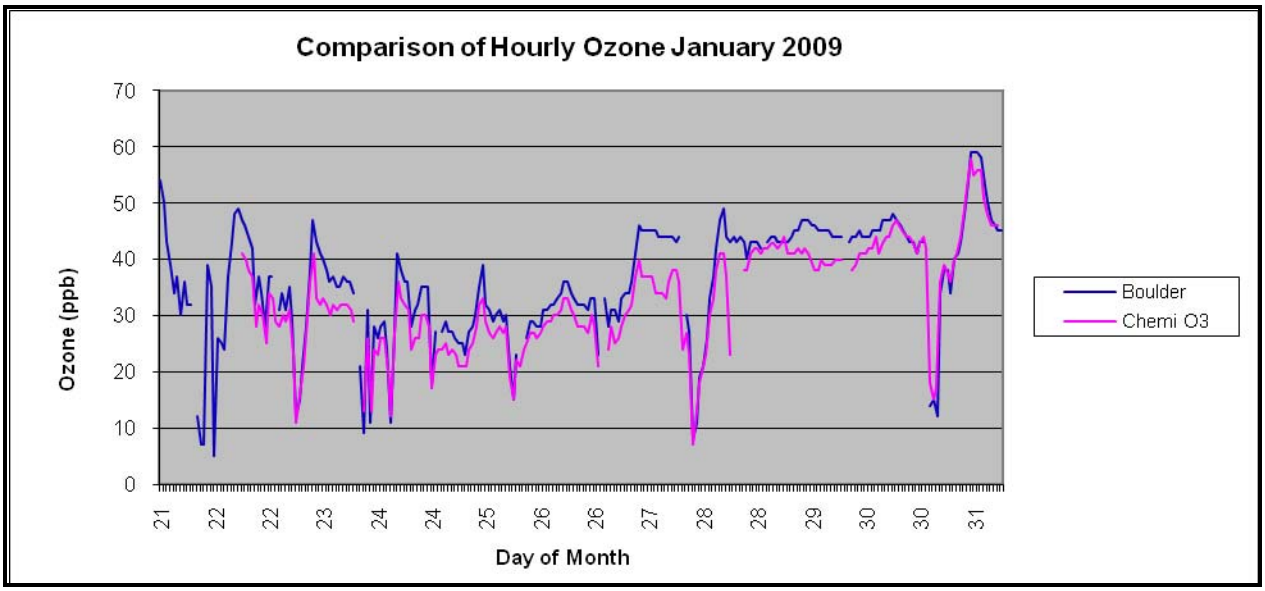


**Figure 3-6**. Boulder UV vs. chemiluminescent ozone data: January 21-31, 2009.

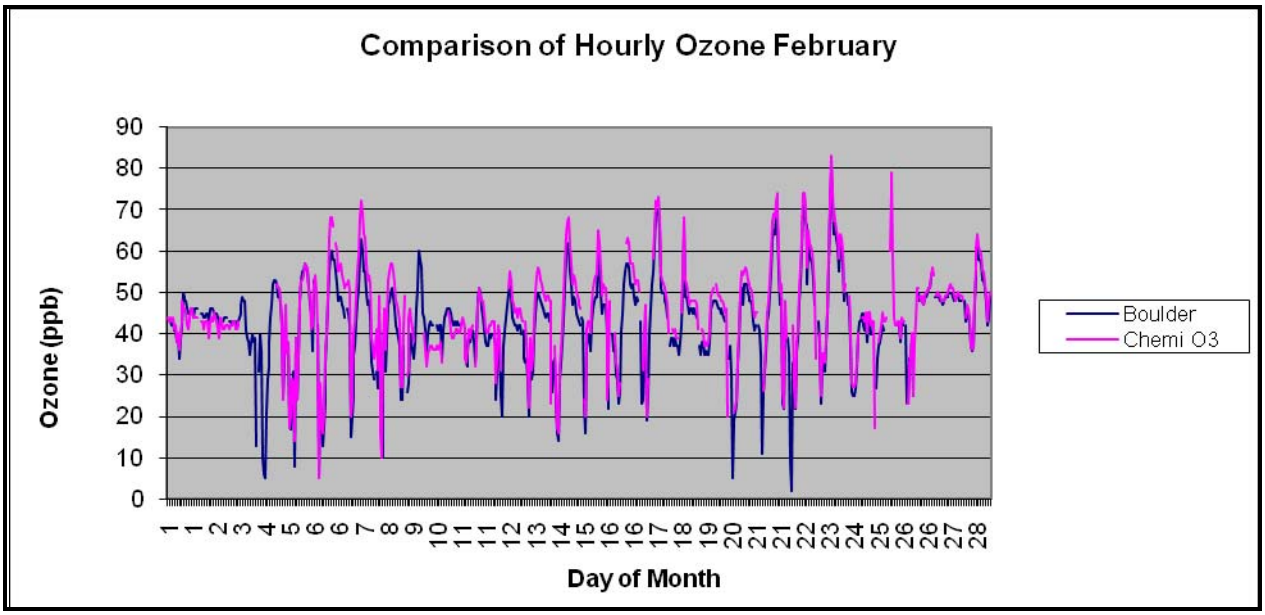


**Figure 3-7.** Boulder UV vs. chemiluminescent ozone data: February 1-28, 2009.

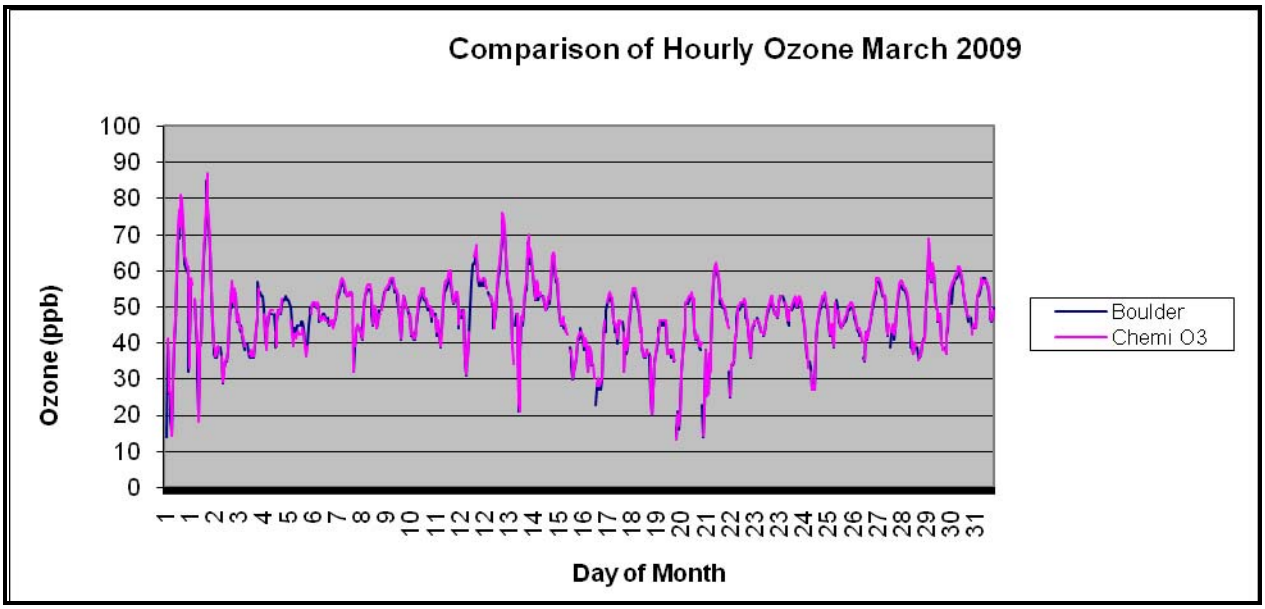


**Figure 3-8**. Boulder UV vs. chemiluminescent ozone data: March 1-31, 2009.

Correlations of data from the UV photometric and chemiluminescent analyzers show much better agreement after the February 10, 2009 reset of the chemi unit. Figure 3-9 shows a data comparison prior to the reset and Figure 3-10 shows a comparison afterwards.

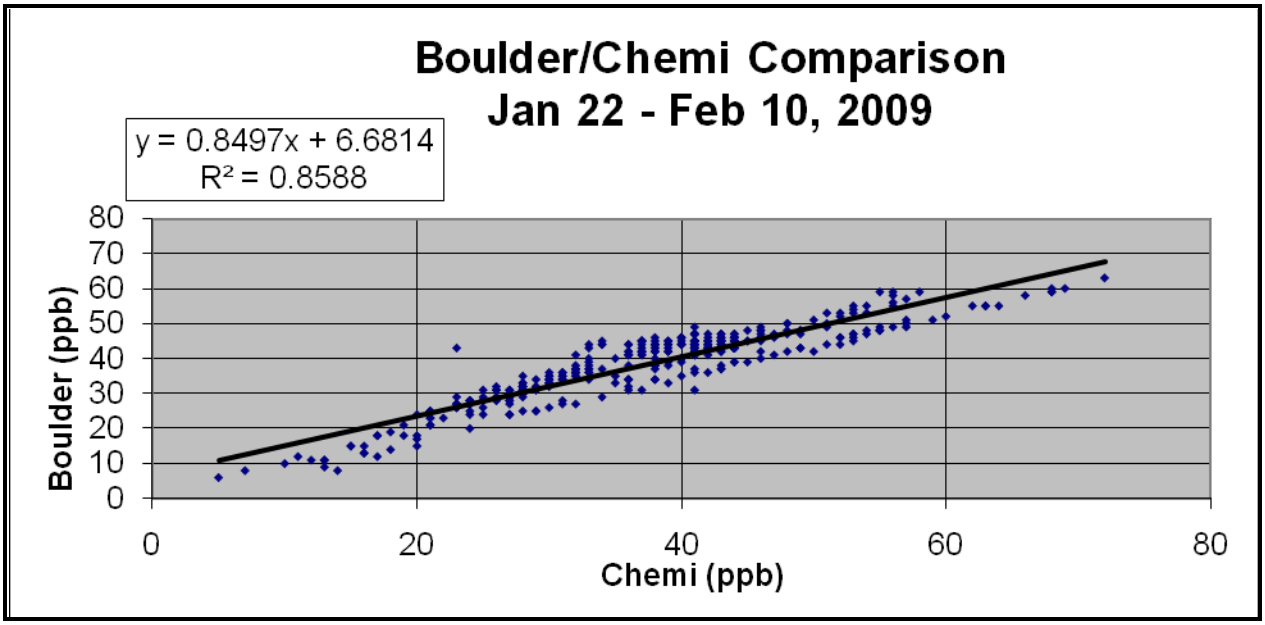


**Figure 3-9.** Comparison of hourly ozone concentration ratio measured at Boulder using UV method (y-axis) and chemiluminescent method (x-axis) for the period 22 January-10 February.

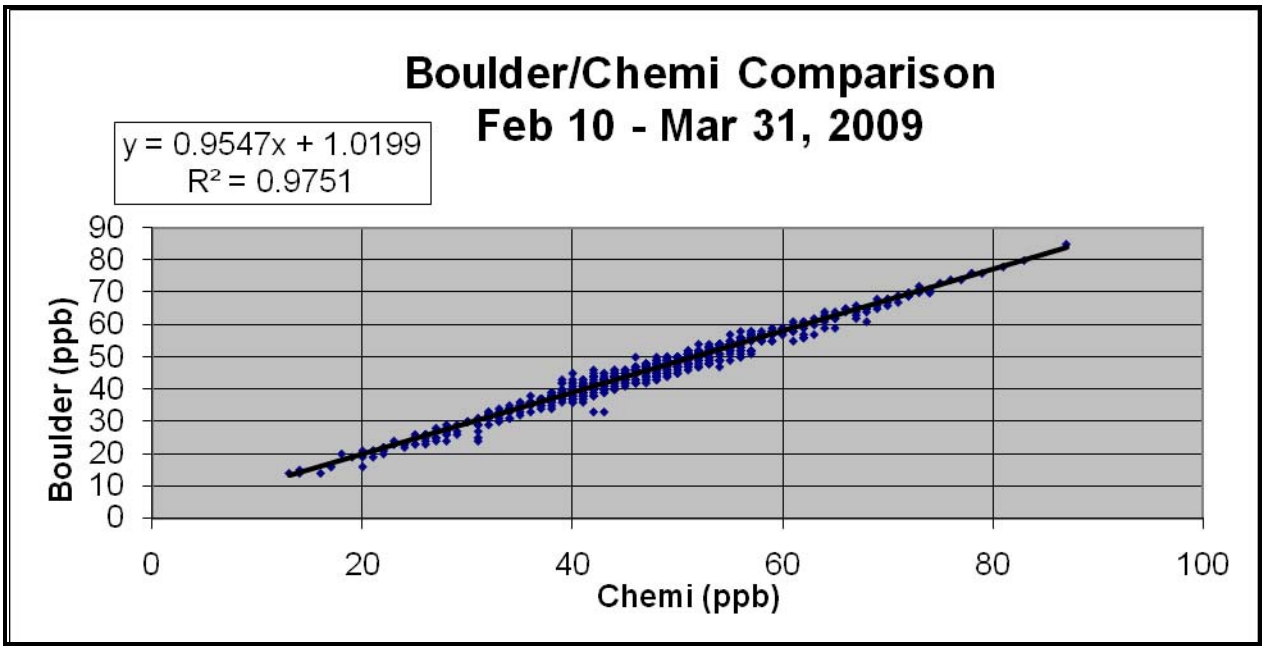


**Figure 3-10.** Comparison of hourly ozone concentration ratio measured at Boulder using UV method (y-axis) and chemiluminescent method (x-axis) for the period 10 February-31 March.

These results suggest that chemiluminescent data collected after the instrument reset on 10 February are more appropriate to use as the basis of comparison with the UV photometric data than the data collected prior to the reset. For the 10 February to 31 March period, UV data are in excellent agreement with the chemiluminescent data with a least squares slope estimate of 0.95 ± 0.01 and an intercept at 1.54 ± 0.47 ppb. Least squares regression errors exhibit no trend with concentration as illustrated in Figure 3-11 and over 99% of hourly values have errors of less than ± 5 ppb. There is no evidence of significant interference biases in the UV data.

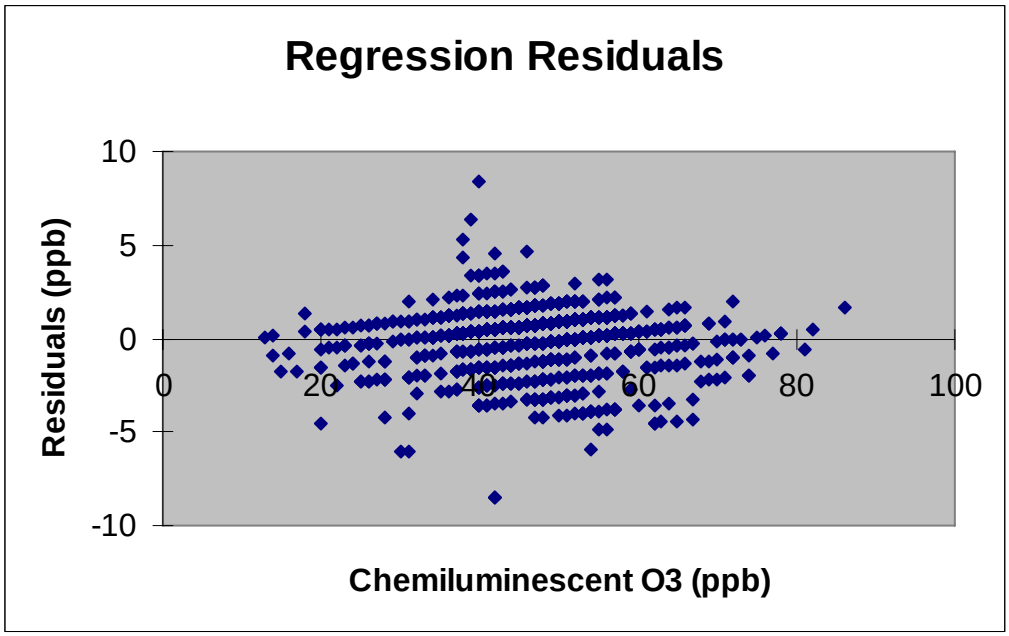


**Figure 3-11.** Residuals from regression of UV against chemiluminescent ozone.

### 3.3.4 Rawinsonde/Ozonesonde Data Validation and Adjustment

Table 3-8 presents a summary comparing surface sonde measurements immediately at release and independently measured "Launch Site Ground Readings" of temperature, humidity and ozone. The independent ground readings for relative humidity are from the Wenz Field measurements routinely taken under FAA guidelines at the airport and not a part of the UGWOS network. All other measurements were extracted from the UGWOS 2009 Data Base.

In general, the independent "ground truth" readings at the UGWOS Airport site indicated reasonable agreement with the initial rawinsonde readings. This was particularly true of the ambient temperature readings, which were typically within 0.5 (C) at launch. Initial wind speeds and directions measured by the sondes represent an integrated value in a layer about 15 meters above the ground (agl)—beginning at rest before slowly moving with the mean air flow. Hence, sonde winds do vary initially somewhat from the ground measurements, especially during very light winds. As a result, it is probably better to assume that the "ground truth" winds are more representative of possible transport drift in the lowest 20 meters of the atmosphere than are the initial rawinsonde values. Relative humidity values measured by the carbon hygristor used in the sondes employed in this project have typically been questionable at both the low and high ends of the scale. However, in the medium range they are usually within 10% of the manufacturer's specifications. It has been our experience when comparing rawinsonde humidity vertical profiles with other methods (e.g. aircraft and towers) that the sondes do accurately depict, for the most part, the relative changes with height. As previously mentioned, relative humidity at the surface are more accurately represented by site-based instrumentation than by sondes.

During data validation it was noted that "ground truth" ozone readings were consistently higher than the initial ozone values measured by the sondes during the first IOP. Comparisons were closer (within 10%) during the third IOP. The ozonesonde manufacturer suggested that the seemingly low ozone readings during the first IOP were the result of storing the prepared sondes under exceptionally cold ambient conditions (as experienced in the hanger facility). The problem was mitigated, as much as practical given the hanger facilities, during the period between IOP 1 and IOP 3 (no rawinsondes/ozonesondes were released during IOP 2), resulting in significantly improved results for IOP 3, with agreement similar to that experienced in other studies. Calibration records of both the airport ground monitor and the ozonesondes indicate that response times for both methods were not an issue.

As can be seen from Table 3-8, significant ozone concentration differences were observed between the ozonesonde and station analyzer during the February 3-5 episode. The manufacturer's recommendations were to assume a constant offset throughout the sounding based on the surface difference. (It should be noted that the principal at En-Sci, the manufacturer, is considered the principal developer of the ozonesonde.) The ozonesonde measurements in the UGWOS database have been corrected accordingly.

**Table 3-8**. Rawinsonde/Ozonesonde ground truth summary.

| Launch Date | Flight ID | Launch Time (mst) | Launch Site Ground Readings | | | | Initial Sonde Readings | | | |
|---|---|---|---|---|---|---|---|---|---|---|
| | | | Temp (C°) | RH (%) | WD/WS (mps) | $O_{3\ (ppb)}$ | Hgt.(m agl) | Temp (C°) | RH | $O_{3\ (ppb)}$ |
| 2/3/09 | wen20307 | 754 | -7.3 | 79 | 298/4.9 | 39 | 0 | -7.9 | 71 | NA |
| 2/3/09 | wen20311 | 1110 | -2.5 | 69 | 305/6.5 | 46 | 83 | -0.5 | 48 | NA |
| 2/3/09 | wen20314 | 1419 | 2.8 | 60 | 300/2.5 | 46 | 0 | 2.8 | 37 | NA |
| 2/3/09 | wen20316 | 1717 | 0.5 | 58 | 120/1.2 | 38 | 20 | 0.4 | 52 | 20 |
| 2/4/09 | wen20407 | 722 | -17.4 | 78 | 316/2.7 | 29 | 50 | -13.4 | 66 | NA |
| 2/4/09 | wen20410 | 1028 | -11.7 | 62 | 274/1.4 | 43 | 0 | -11.9 | 25 | NA |
| 2/4/09 | wen20413 | 1411 | -3.5 | 44 | 025/0.8 | 51 | 359 | -1.3 | 31 | 30 |
| 2/4/09 | wen20416 | 1656 | -1.4 | 56 | 315/1.0 | 49 | 0 | -3.1 | 34 | 34 |
| 2/5/09 | wen20507 | 730 | -18.9 | 78 | 302/1.6 | 28 | 0 | -19.8 | 62 | NA |
| 2/5/09 | wen20511 | 1124 | -8.3 | 56 | 285.9 | 49 | 0 | -7.9 | 32 | NA |
| 2/5/09 | wen20514 | 1430 | -2.2 | 41 | 132/0.7 | 58 | 9 | -3.8 | 31 | 50 |
| 2/5/09 | wen20516 | 1654 | -2.9 | 64 | 025/0.5 | 49 | 6 | -2.7 | 47 | 14 |
| 2/28/09 | wen22811 | 1107 | -12.1 | 57 | 295/0.9 | 54 | 0 | -12.3 | 28 | NA |
| 2/28/09 | wen22814 | 1418 | -6.7 | 54 | 269/1.8 | 60 | 0 | -7.1 | 26 | NA |
| 2/28/09 | wen22816 | 1629 | -4.0 | 50 | 325/1.1 | 53 | 13 | -5.0 | 30 | 51 |
| 3/1/09 | wen30107 | 736 | -11.4 | 73 | 286/1.0 | 41 | 9 | -11.5 | 51 | NA |
| 3/1/09 | wen30111 | 1058 | -3.9 | 58 | 072/0.7 | 59 | 0 | -4.4 | 16 | NA |
| 3/1/09 | wen30113 | 1329 | 1.3 | 48 | 330/1.2 | 68 | 67 | -2.2 | 23 | 65 |
| 3/1/09 | wen30116 | 1634 | 1.6 | 44 | 335/1.5 | 70 | 33 | 0.1 | 29 | 81 |
| 3/2/09 | wen30207 | 728 | -9.3 | 79 | 309/3.1 | 41 | 6 | -8.7 | 67 | NA |
| 3/2/09 | wen30211 | 1036 | -1.2 | 60 | 095/0.4 | 53 | 0 | -2.7 | 32 | NA |
| 3/2/09 | wen30213 | 1336 | 3.3 | 52 | 355/0.5 | 64 | 9 | 2.5 | 21 | 60 |
| 3/2/09 | wen30216 | 1623 | 3.4 | 63 | 241/0.6 | 77 | 0 | 3.4 | 33 | 82 |
| 3/3/09 | wen30307 | 732 | -3.5 | 86 | 150/1.8 | 22 | 0 | -2.1 | 69 | NA |
| 3/3/09 | wen30311 | 1037 | 3.5 | 73 | 119/2.5 | 46 | 0 | 3.0 | 39 | NA |
| 3/3/09 | wen30314 | 1404 | 7.9 | 46 | 209/3.0 | 49 | 0 | 7.4 | 14 | NA |
| 3/3/09 | wen30316 | 1600 | 7.5 | 50 | 239/2.5 | 54 | 0 | 7.1 | 28 | 49 |

### 3.3.5 Boulder II $NO_y$, NO, and NOx Data

Data collection started of January 28, 2009 and ended on March 31, 2009. Figures 3-12 and 3-13 show the initial calibration results for the $k_1$ $NO_x$ analyzer (referred to here as the $NO_x$ analyzer) and the $NO_y$ analyzer, respectively. The final calibrations conducted at the end of the study (not shown) were essentially the same as the initial calibrations. Figure 3-14 is a time series of NO span checks for the $NO_y$ analyzer and Figure 3-15 is the time series for the NOx analyzer. The target concentration was 400ppb. Span checks for both the $NO_y$ and $NO_x$ analyzers agreed with the initial and final calibrations. While these checks were conducted at the same time, there are fewer $NO_x$ checks since the sample line needed to be manually attached to the span source as this analyzer normally sampled from the $k_1$ tube. No corrections were made for this acceptable span drift. Figure 3-16 shows a time series of $NO_2$ span plots (300 ppb target) for both the $NO_x$ and $NO_y$ analyzers. This plot shows that the converters for the analyzers were working properly for the entire measurement period.

The NO channel of the $NO_y$ analyzer, while responding properly during zero/span checks produced data that tended to drift and was not consistent with either the NO channel of the $NO_x$ analyzer or the NOx analyzer located in the Boulder I instrument shelter. These data were therefore not reported and any mention in this report of Boulder II NO data is in reference to data from the $k_1$ $NO_x$ analyzer. The zero checks showed only a few ppb drift for the $NO_y$, NO, and $NO_x$ over the measurement period. The raw data were corrected for this minor drift. Other than zero/span checks and data logger failures, there were no gaps in these data.

While both analyzers operated within expected limits, a normalization factor derived from the span data should be applied to account for the small calibration differences if $NO_x$ and $NO_y$ are to be compared directly. Because the span data are tightly centered about the target concentration the use of means rather than a least squares correlation plot would be the best approach to determine this factor. Based on both the NO and $NO_2$ span mean data the $NO_y$ should be multiplied by 1.05. This is also in excellent agreement with the calibrations performed at installation and teardown. An alternative normalization approach would be to determine factors from measurements immediately before and after a photochemical event when $NO_y$ species are primarily NO and $NO_2$.

As an example Figure 3-17 shows a plot of NOx vs NOy for data collected on the IOP day of March 1, 2009 (a day with significant pollutant build-up and photochemical activity). The slope is 1.00 (when rounded to two decimal places) without correcting the NOy by the recommended factor of 1.05. With this correction made the slope would be 0.95, indicating that NOy is 5% higher than NOx for the day.

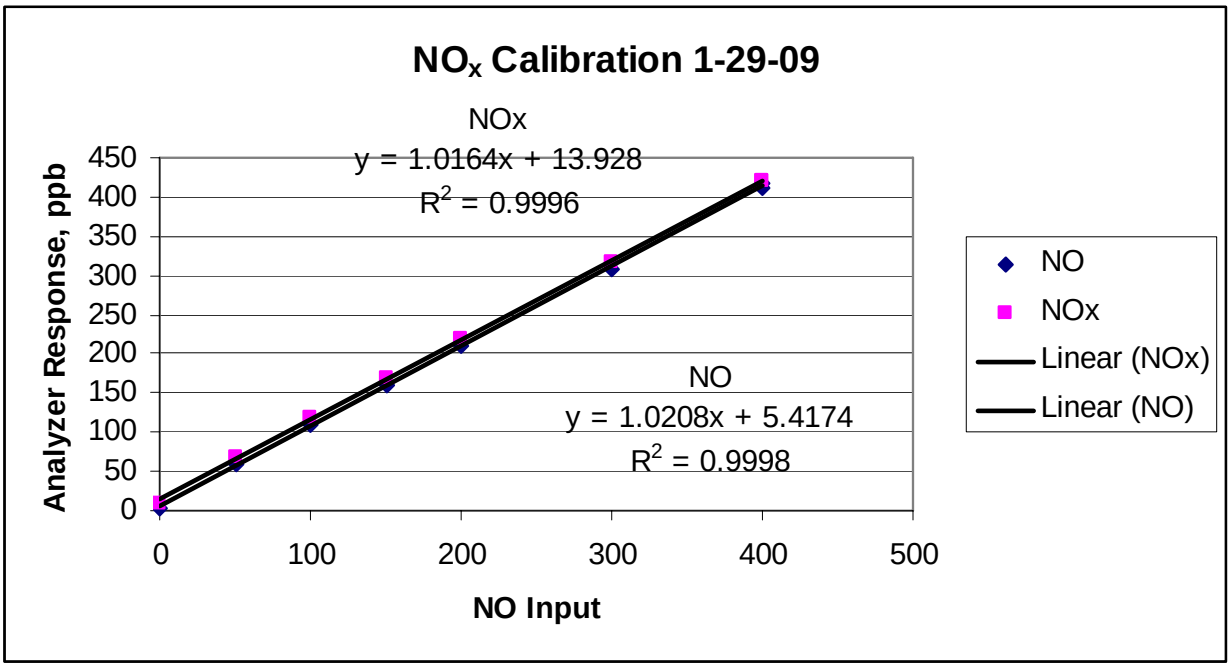


**Figure 3-12.** Calibration of the $NO_x$ analyzer on January 29, 2009.

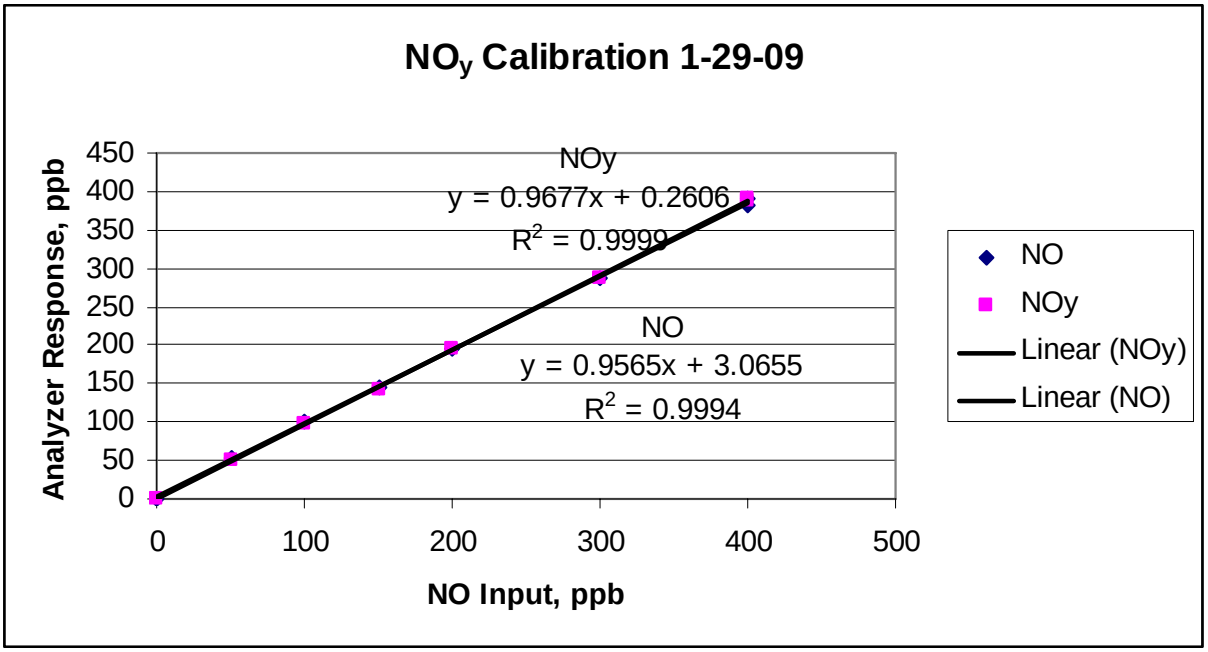


**Figure 3-13.** Calibration of the $NO_y$ analyzer on January 29, 2009.

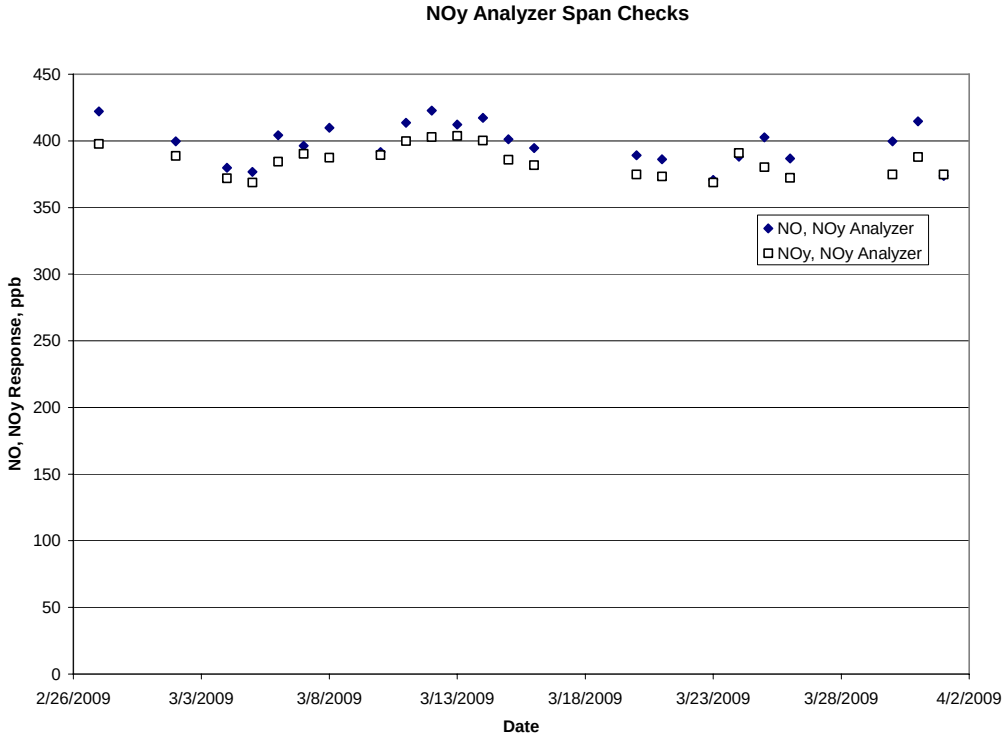


**Figure 3-14**. $NO_y$ analyzer NO span checks (400 ppb target).

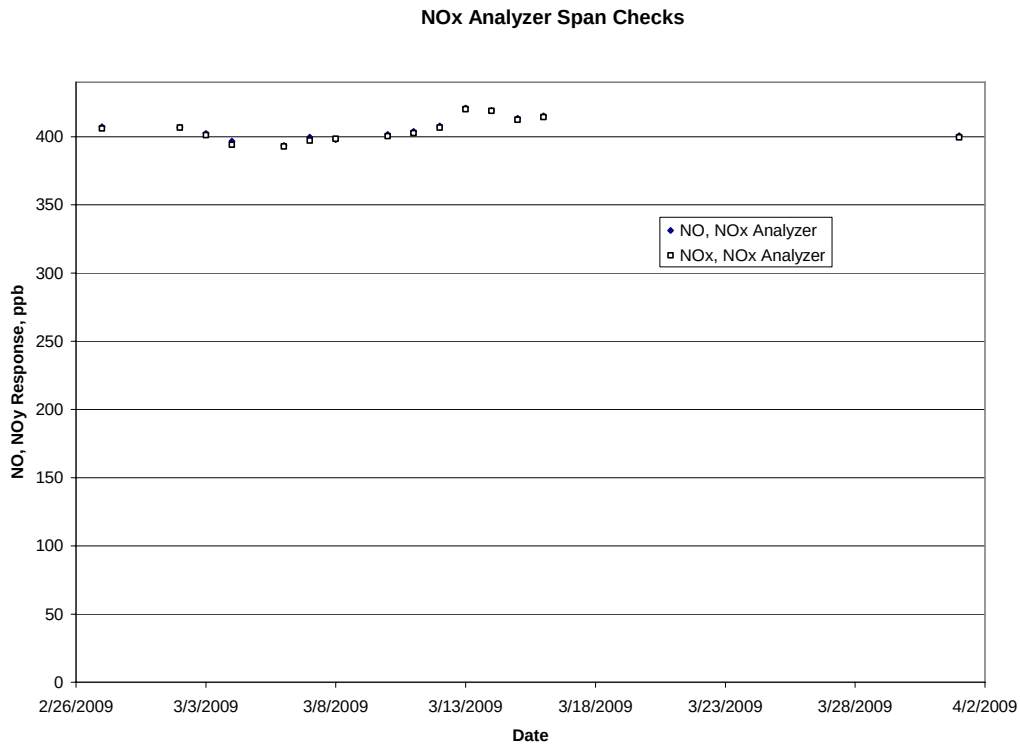


**Figure 3-15.** NOx analyzer NO span checks (400 ppb target).

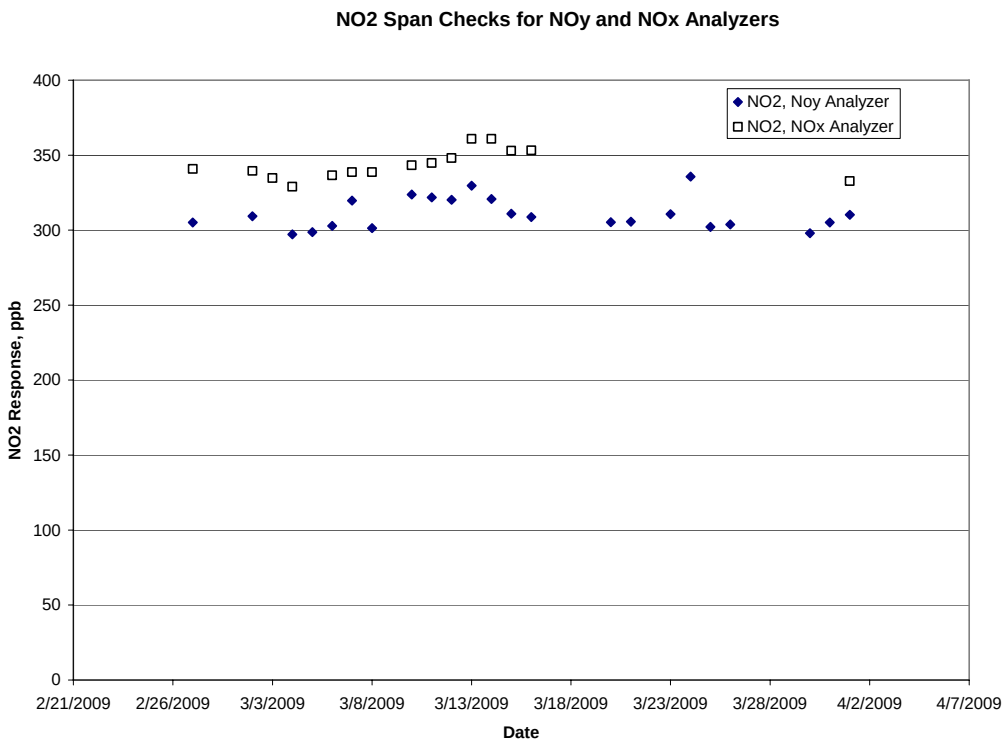


**Figure 3-16.** Time series of NO2 span checks (300 ppb target) for both the NOy and NOx analyzers.

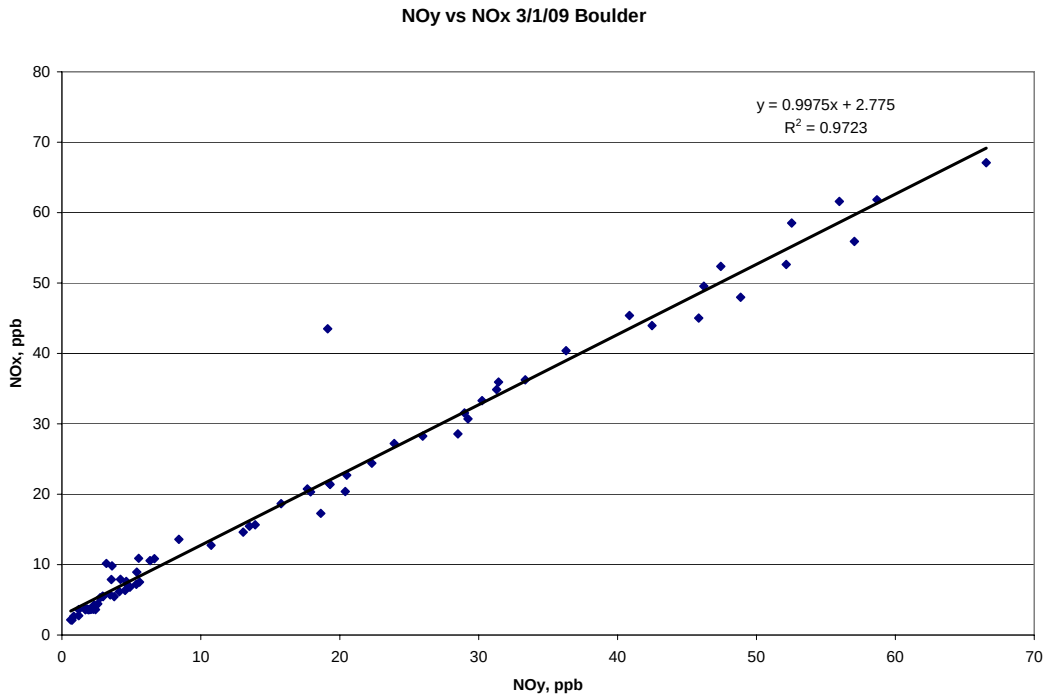


**Figure 3-17.** Comparison of NOy and NOx on March 1, 2009.

### 3.3.6 Boulder II $NO_2$ and PAN Data

Data collection started January 28, 2009 and ended on March 31, 2009. A full calibration at startup was not conducted since the analyzer was still stabilizing. A full calibration was completed during tear down, but a slight non-linearity was observed which may have been due to incomplete gas phase titration in the on-site calibrator generating the $NO_2$. This non-linearity was not observed using CE-CERT calibration equipment. Figure 3-18 shows a time series of the span checks. A slow downward drift in sensitivity was observed. This was corrected in the data by applying a drift of 0.00470588 per day to the span factor. The data were also corrected for a 37% response to ozone determined from the automated ozone span checks. This correction was made using ozone data from the chemiluminescent ozone analyzer located at the site. When these data were not available or suspect, the $NO_2$ data were reported as missing.

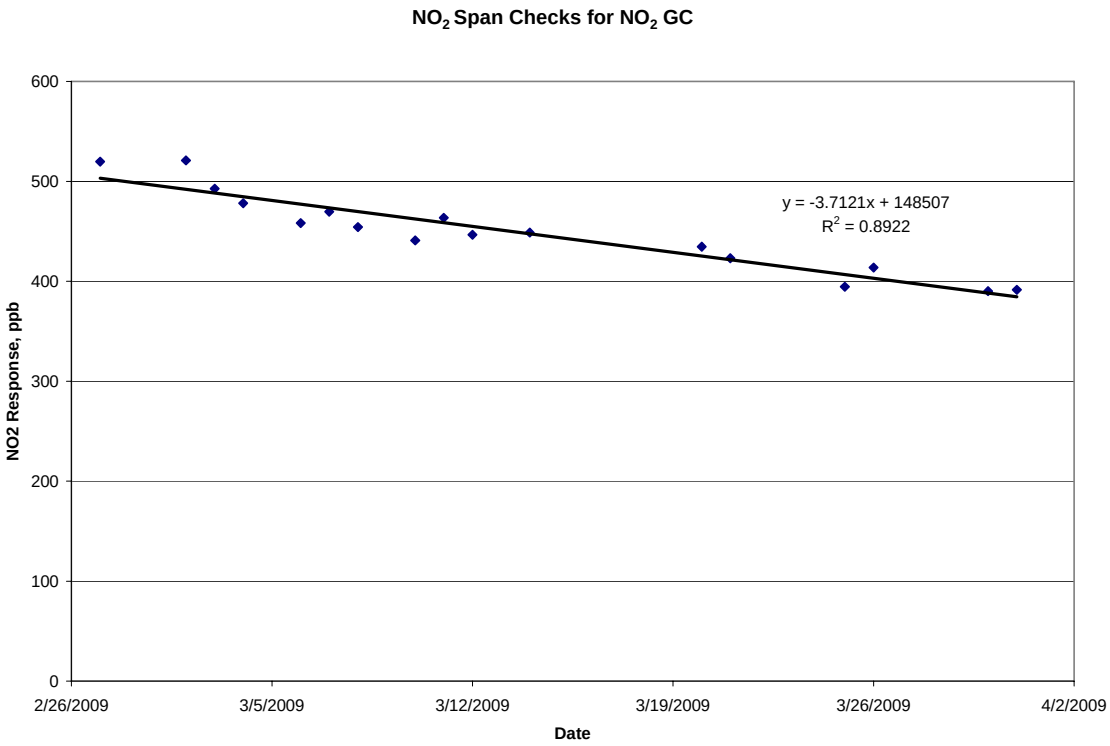


**Figure 3-18**. Time series of $NO_2$ span checks (300 ppb target) for $NO_2$ gas chromatograph.

### 3.3.7 Organic Compound Sampling and Analysis

**EPA TO-14 Hydrocarbon Speciation**

The EPA TO-14 Hydrocarbon Speciation method for the analysis of hydrocarbons was performed using a dedicated gas chromatograph (GC) equipped with a flame ionization detector (FID). The FID provides maximum sensitivity for hydrocarbons and has a selective response to carbon atoms. The method uses analysis and calibration guidelines in the EPA document "Technical Assistance Document For Sampling and Analysis of Ozone Precursors", October 1991, EPA/600-8-91/215.

For the single column approach, the $C_2$ to $C_{12}$ hydrocarbons and stable oxygenates are analyzed using a single fused silica capillary column on an HP 5890 GC with a FID detector. A 0.025 to 20 ml sample is loaded onto a 1/8" by 8" glass bead freeze out loop immersed in liquid oxygen using an 8 port valve and fixed volume sample loops. The components are desorbed onto a capillary cryofocussing loop by heating to 125ºC. They are then desorbed from the cryofocus loop, and separated using a 100-meter, 0.25-micron fused silica PetroCol capillary column with a 0.5-micron phase coating. The column is programmed from -10ºC to 225ºC at 4 C/min. Total analysis time is about 65 minutes. The compounds are detected on a FID set to operate at high sensitivity. The detector temperature is 275ºC. The chromatographs are integrated using the HP Chemstation computer and stored on the computer for further examination if required at a later date.

Hydrocarbon compounds are quantitatively calibrated using an NIST traceable C2 to C6 n-alkane standard. On the FID, hydrocarbons have a uniform response based on the number of

carbon atoms so the individual compounds are calibrated against the propane and hexane peak. The other hydrocarbons are used as a QC check to make sure the detector response is uniform. The calibrated response has been checked against the 57 component EPA PAMS sample and other reference samples provided by agencies or other participant labs.

Qualitative calibration of the hydrocarbon retention times is performed using an 82 compound hydrocarbon mix in an AL150 cylinder. The retention times are verified using a Kovats retention time index available for the PetroCol 100 m capillary column.

**EPA TO-11 Carbonyl Analyses**

Formaldehyde and carbonyl samples were collected onto DNPH (2,4-dinitrophenyl-hydrazine) cartridges purchased from Supelco Inc. The samples were collected at a flow rate of 1-2 L/min. A formaldehyde blank is run on each batch of cartridges to characterize the background formaldehyde (carbonyls) on the cartridges.

The carbonyl-DNPH derivatives are eluted with 4 mL of carbonyl-free methanol. The derivatives are analyzed by HPLC with UV detection at 360 nm. The Mobile phase is distilled water/acetonitrile: 40/60 v/v at 1.5 mL/min. A 100 ul sample of the methanol extract is injected onto two 25 cm Restek Pinnacle TO-11 columns that are connected in series. A Shimadzu Model LC-6A Pump and SPD-6AV UV detector is used for analysis. The output of the detector is connected to a computer with the HP Chemstation Software. The standards used are commercially available carbonyl-DNPH derivatives of the target compound list.

**VOC/Carbonyl Sampling**

During each IOP, VOC canister/ Carbonyl cartridge sample pairs were collected simultaneously at Boulder II and Jonah. Sampling was set to start at 0600 and 1300 MST during each IOP day. Sample duration was four (4) hours. During IOP#3, VOC canisters were collected at the SODAR site on the same schedule. Sample collection is summarized in Table 3-9. Sample numbers listed in the UGWOS database contain sampling site, date and start time embedded in the sample number identifier (e.g. JON0303091300 is the sample collected at Jonah between 13:00–17:00 MST on 3 March 2009).

**Table 3-9.** VOC/carbonyl samples (times in MST) collected during each IOP**.**

| Date | Jonah Site | Boulder II Site | SODAR Site |
|---|---|---|---|
| **IOP #1** | | | |
| 2-3-09 | 0600 (VOC/Carb) | 0600 (VOC/Carb) | |
| | 1300 (VOC/Carb) | 1300 (VOC/Carb) | |
| 2-4-09 | 0600 (VOC/Carb) | 0600 (VOC/Carb) | |
| | 1300 (VOC/Carb) | 1300 (VOC/Carb) | |
| 2-5-09 | 0600 (VOC/Carb) | 0600 (VOC/Carb) | |
| | 1300 (VOC/Carb) | 1300 (VOC/Carb) | |
| **IOP #2** | | | |
| 2-21-09 | | 0600(VOC/Carb) | |
| | | 1300(VOC/Carb) | |
| | | 1300(VOC/Carb Duplicate) | |
| | | 1255(VOC/Carb Blank) | |
| 2-22-09 | | 0600(VOC/Carb) | |
| | | 1300(VOC/Carb) | |
| **IOP #3** | | | |
| 2-28-09 | 0600 (VOC/Carb) | 0600 (VOC/Carb) | 0600 (VOC) |
| | 1300 (VOC/Carb) | 1300 (VOC/Carb) | 1300 (VOC) |
| 3-1-09 | 0600 (VOC/Carb) | 0600 (VOC/Carb) | 0600 (VOC) |
| | 1300 (VOC/Carb) | 1300 (VOC/Carb) | 1300 (VOC) |
| 3-2-09 | 0600 (VOC/Carb) | 0600 (Carb) | 0600 (VOC) |
| | 1300 (VOC/Carb) | 1300 (Carb) | 1300 (VOC) |
| 3-3-09 | 0600 (VOC/Carb) | 0600 (VOC/Carb) | 0600 (VOC) |
| | 1300 (VOC/Carb) | 1300 (VOC/Carb) | 1300 (VOC) |
| | | 1903 (VOC/Carb Blank) | |
| 3-4-09 | | 0600 (VOC/Carb Duplicate) | |
| 4-2-09 | | | 0830 (VOC Blank) |

## Sampler Contamination Checks

VOC canister samplers were checked for contamination on January 16, 2009 prior to IOP#1 and again on February 11, 2009 by filling a clean canister with ultra-pure air using each individual sequential sampler channel and submitting it for analysis. Since there were two samplers each with two channels, four canisters were submitted for each round of a contamination check. Two rounds of contamination checks were documented during UGWOS 2009. During IOP sampling, channel #1 was used for the 0600-1000 canister sample and channel #2 was used for the 1300-1700 sample. During the first round of checks, residual amounts of ethane, ethanol, propane and small amounts of i-butane and n-butane were detected in some of the channels. All other compounds in the modified TO-14 list were either not detected (ND) or were less than three times the MDL. Contamination checks are summarized in Table 3-10 which lists only compounds detected above three times the MDL.

After the first IOP, a second round of sampler contamination checks was collected on February 11, 2009. Sampler #2 was installed at the Boulder II site and sampler #3 was installed at Jonah.[1] Sampler #2, channel #1 showed some residual ethanol, i-butane and toluene. There were also small amounts of ethane and propane although these were detected in amounts considerably less than the first contamination check of this sampler channel in January. Sampler #2, channel #2

[1] Sampler #1 was only used during the preliminary study discussed in Section 4.5.1.

and Sampler #3, channel #1were fairly clean. The analytical results for Sampler #3, channel #2 show some contamination. The fact that the majority of the compounds detected there were not detected elsewhere may indicate a possible leak during sampling in this part of the sampling system.

**Table 3-10**. Sampler contamination check results (only compounds detected above three times the MDL are listed).

| Compound | Sampler #2 Channel #1 | | Sampler #2 Channel #2 | | Sampler #3 Channel #1 | | Sampler #3 Channel #2 | |
|---|---|---|---|---|---|---|---|---|
| | 1/16/2009 | 2/11/2009 | 1/16/2009 | 2/11/2009 | 1/16/2009 | 2/11/2009 | 1/16/2009 | 2/11/2009 |
| Ethane | 9.39 | 1.89 | 4.71 | ND | ND | 1.01 | ND | 2.73 |
| Ethanol | ND | 6.86 | ND | ND | ND | ND | ND | ND |
| i-Butane | 2.15 | 2.87 | 2.03 | ND | 1.19 | ND | 1.70 | 3.57 |
| n-Butane | 1.78 | ND | 1.69 | ND | ND | ND | 1.45 | 3.21 |
| Propane | 13.92 | 1.40 | 15.87 | ND | 1.98 | ND | 13.07 | 1.49 |
| Toluene | ND | 2.78 | ND | ND | ND | ND | ND | 5.42 |
| 2,2,4-Trimethylpentane | ND | ND | ND | ND | ND | ND | ND | 2.11 |
| 2,3-Dimethylpentane | ND | ND | ND | ND | ND | ND | ND | 1.53 |
| 2-Methylpentane | ND | ND | ND | ND | ND | ND | ND | 1.47 |
| Benzene | ND | ND | ND | ND | ND | ND | ND | 1.33 |
| Cyclopentane | ND | ND | ND | ND | ND | ND | ND | 1.06 |
| i-Pentane | ND | ND | ND | ND | ND | ND | ND | 8.22 |
| n-Hexane | ND | ND | ND | ND | ND | ND | ND | 1.30 |
| n-Pentane | ND | ND | ND | ND | ND | ND | ND | 3.81 |

**NMHC/Carbonyl Blanks and Duplicates**

During UGWOS 2009, three canister field blanks and two DNPH cartridge blanks were submitted for analysis. Blanks were transported to the site, mounted in the sampler without turning the sampler on and then removed immediately and transported back to the field headquarters at the Pinedale airport for shipment to the analytical laboratory. DNPH cartridges were always shipped and transported in a cooler with ice and stored in a refrigerator until use or shipment.

Analytical results generally showed either non-detects (ND) or concentrations that were less than three times the minimum detectable limit (MDL). One of the canister blanks showed a fairly significant concentration of ethanol which can only be explained as a possible lab or handling contaminant.

Two duplicate sample pairs were collected during the program, one during IOP#2 and one immediately following IOP#3. The sampler from the Jonah site including inlet tubing was removed to the Boulder II site for collocation with the Boulder II sampler. Teflon inlet tubes were positioned within several inches of one another and samplers were started and stopped on the same schedule.

VOC canister duplicates (Figures 3-19 and 3-20) showed fairly good agreement except for ethene in the 2/21/09 sample pair and ethanol in the 3/4/09 sample pair. Carbonyl duplicate results were mixed with poor agreement on 2/21/09 but better agreement in the samples collected

on 3/4/09 (Figures 3-21 and 3-22). Given these results and the quantification of ethanol in blanks noted above, ethanol results from this study should be treated as suspicious.

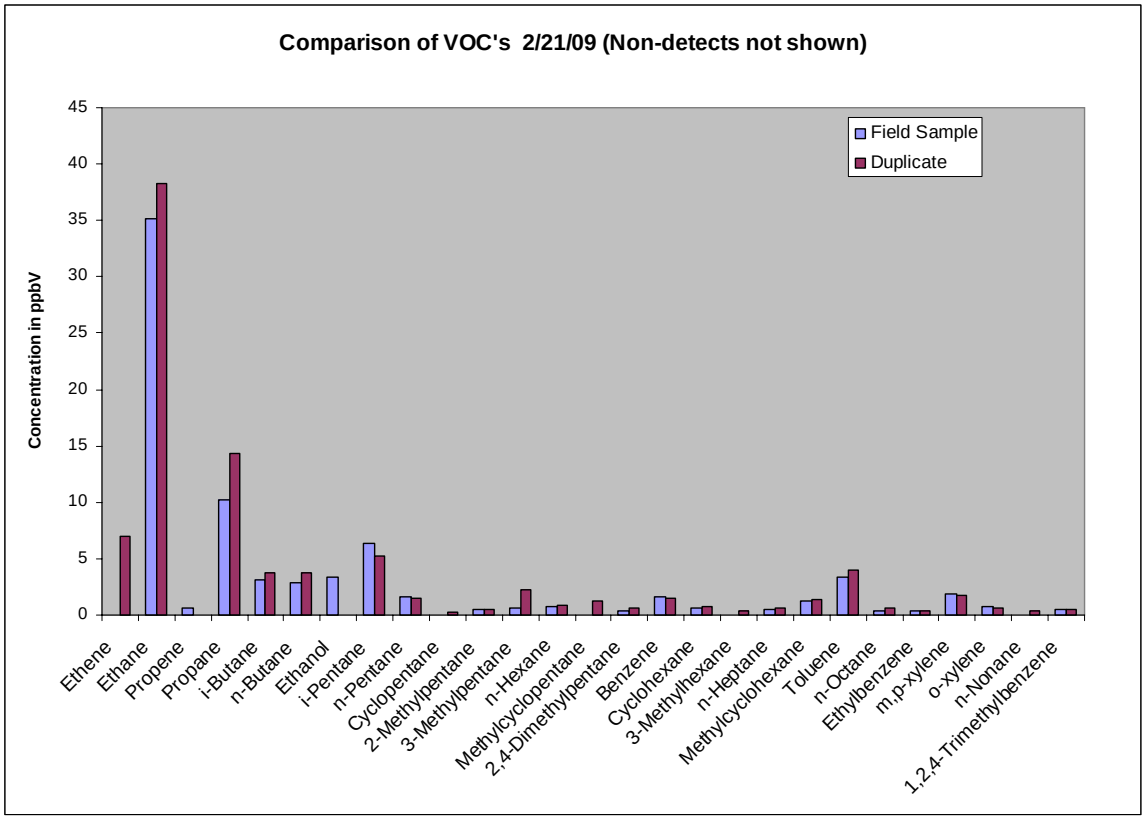


**Figure 3-19.** VOC canister duplicate results sampled 2/21/09.

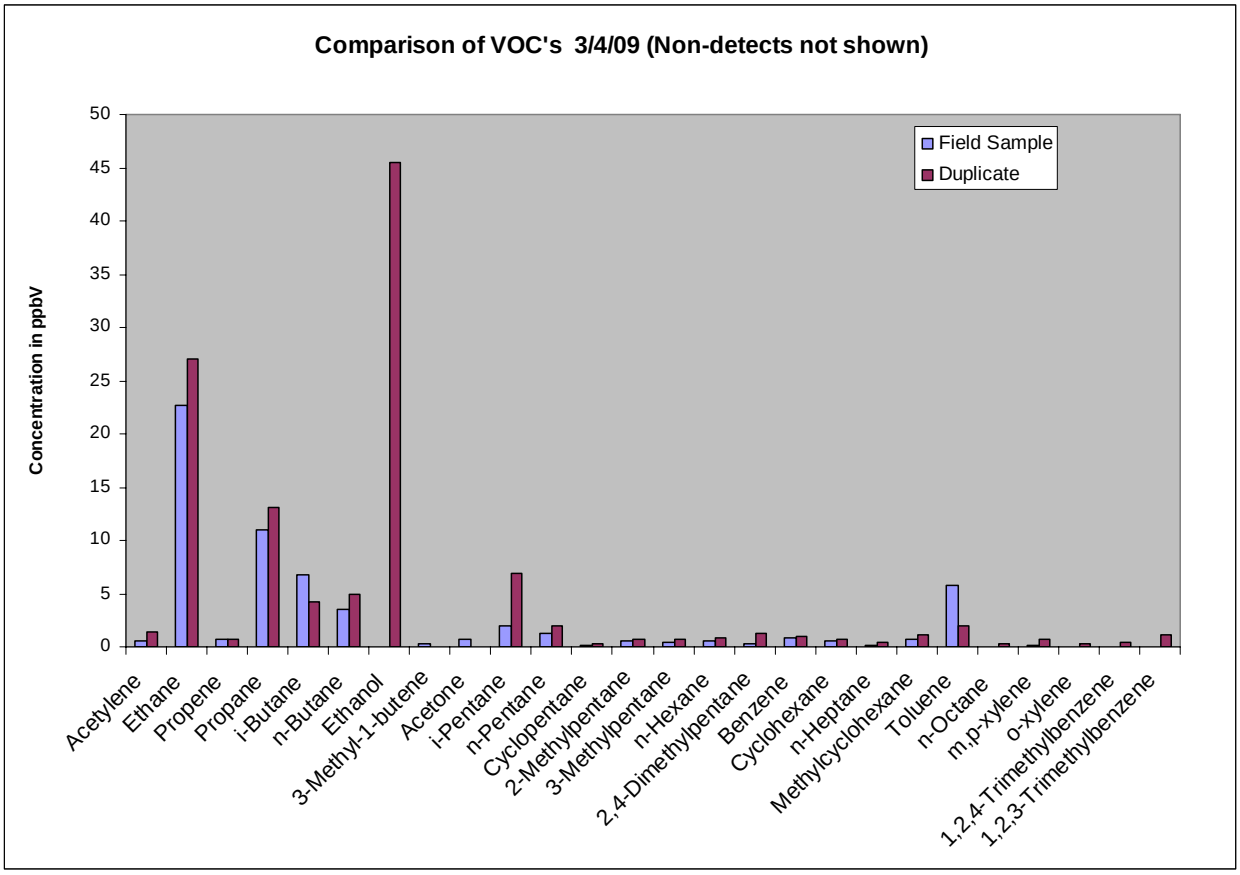


**Figure 3-20.** VOC canister duplicate results sampled 3/4/09.

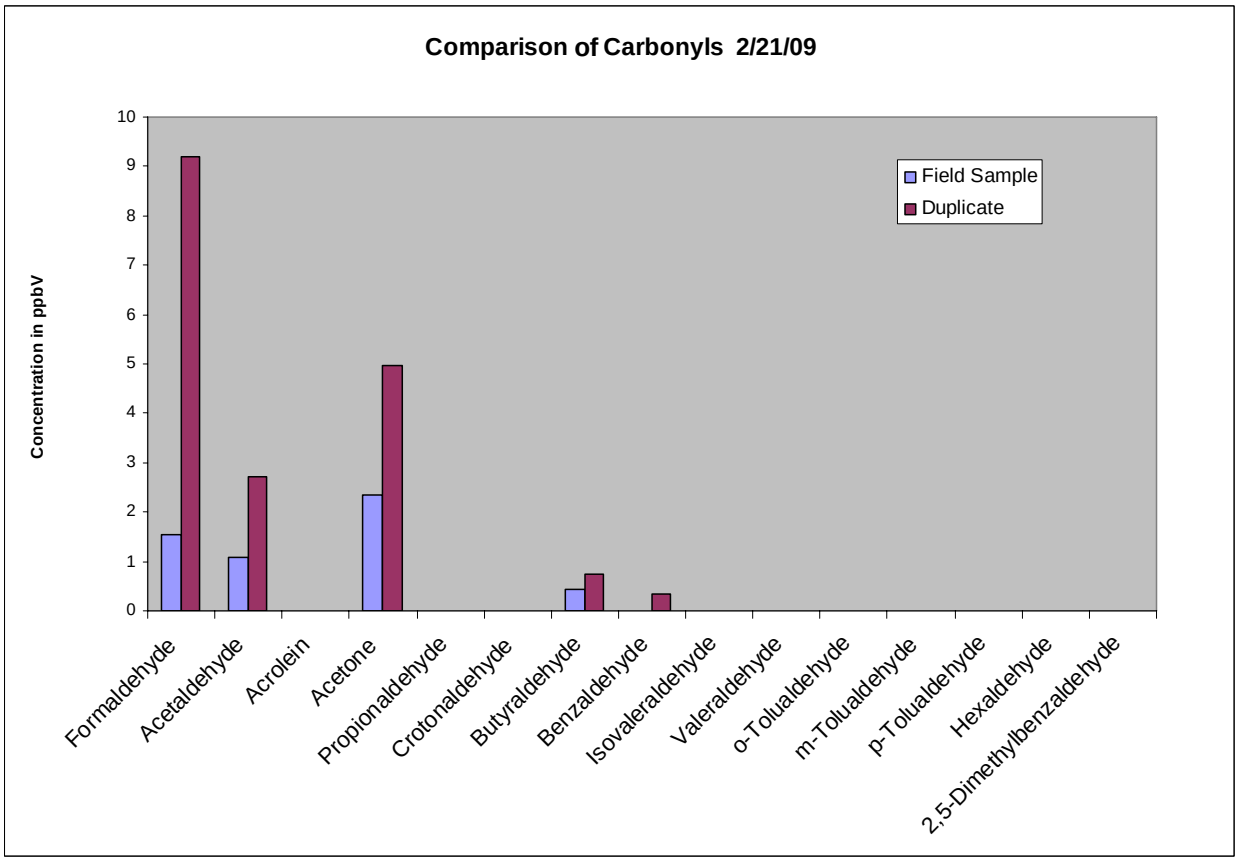


**Figure 3-21.** Carbonyl duplicate results sampled 2/21/09.

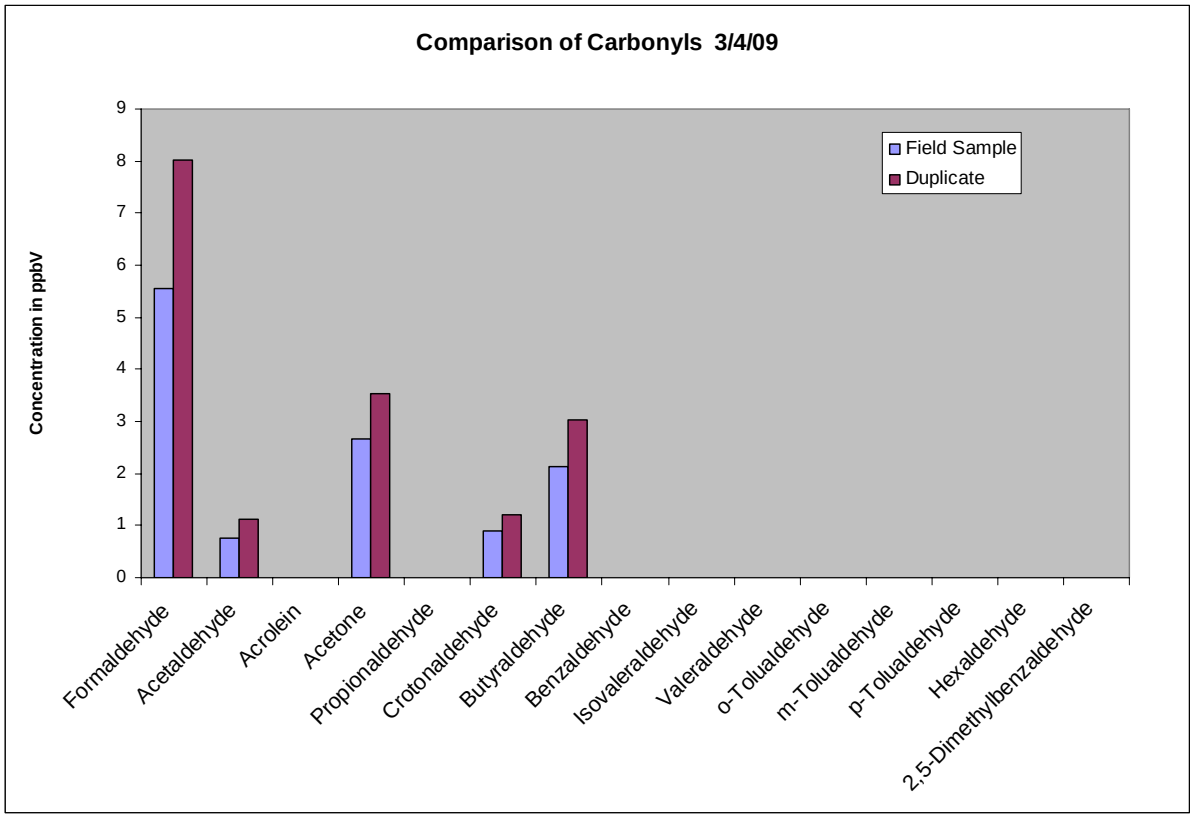


**Figure 3-22.** Carbonyl duplicate results sampled 3/4/09.

On-going laboratory QA was performed on each batch of samples as they were received and analyzed by the lab, including method blanks, QC duplicates, laboratory control spikes and laboratory control duplicates. All of these QA results are included in the UGWOS database.

## 3.4 Data Archiving

All validated data except the SODAR data were merged into an integrated relational Microsoft ACCESS database. The database contents and format are described in Appendix B. Data were formatted into the final database with the following unit configurations and naming conventions:

- Parts per million for $O_3$, NO, $NO_2$, NOx
- Micrograms per cubic meter for $PM_{10}$
- Meters per second for wind speed (as a general rule, metric units will be used)
- Degrees Celsius for ambient temperature
- Percent for relative humidity
- Parts per Billion Carbon for non-methanated hydrocarbon species
- Watts/$m^2$ for radiation
- SITE = Alpha-numeric site code identifier
- DATE = (MM/DD/YY)
- HOUR= Nearest whole begin hour (HH) (MST)
- TIME, START_TIME or END_TIME = Time stamp of data (HH:MM:SS) (MST)
- HEIGHT = Elevation in meters above MSL

- QC_CODE, WS_QC, WD_QC, O3_QC, etc =
  "V" (valid), "M" (missing), "I" (invalid), "S" (secondary MQOs)
- NOTES = any additional information

The ACCESS database along with documentation is available for download from the Wyoming Department of Environmental Quality website (http://deq.state.wy.us/AQD/Monitoring%20Data.asp).

# 4. RESULTS

## 4.1 Summary of Meteorological and Air Quality Conditions

### 4.1.1 Comparison of Meteorological Patterns: 2009 vs. 2007 and 2008

Winter weather patterns strongly influence the frequency and severity of ozone episodes in the Upper Green River Basin (UGRB) and these patterns have differed during each of the three UGWOS study years (2007, 2008 and 2009). Averaged[1] maps of surface pressure/pressure heights, temperature and wind speed at the surface and upper air levels over the February and March periods have been developed for the 2007 and 2008 study periods (ENVIRON 2008a,b), and these maps have been constructed again for the 2009 study. Conditions at the 700mb (approximately 10,000 ft) and at the surface are the most influential to weather and ozone development in the study area which is at an approximate altitude of 7,000 feet. These levels were also the primary levels evaluated by the project meteorologists in developing the daily forecasts for the UGWOS project. Therefore, the focus of this comparison is on these two levels and also includes a brief look at 500 mb heights. A complete set of the averaged maps developed is available from the authors upon request.

**Temperatures**

The averaged surface temperature maps show very similar patterns over the three years with the coldest readings centered over the ID/WY/MT border area. In 2009 the average temperature over the UGWOS area was around -4°C. This compared to a colder 2008 and a much warmer 2007. The 700 mb temperatures followed the trends seen with surface readings for all three years. In 2007 there were no IOP's and temperatures were the warmest of the study years. In 2008 there were three IOP's and readings for this year were the coldest of the three study years. In 2009 there were three IOP's.

The colder the average temperature during the study period the more likely there will be a substantial snowpack. As has been learned over the past three years, a snowpack will allow the formation of strong and shallow inversions which in turn allow for precursor concentrations to increase; this allows for higher ozone concentrations to occur. Table 4-1 shows averaged temperatures at the surface and 700 mb over the past three study periods.

**Table 4-1.** Surface and 700 mb Temperatures for the February and March Period.

| February/March Period | Surface Temperature (°C) | 700 mb Temperature (°C) |
|---|---|---|
| **2007** | -2.6 | -5.1 |
| **2008** | -5.2 | -8.2 |
| **2009** | -4.0 | -6.5 |

[1]Averaged data from ESRL web site using NCEP Reanalysis data, http://www.cdc.noaa.gov/cgi-bin/PublicData/getpage.pl

## Wind Speeds

Averaged wind speeds have fluctuated only slightly over the three study periods at both the surface and at 700 mb. Averaged surface speeds have varied by only 0.4 m/s and 700mb winds by 0.8 m/s. The stronger the wind speeds at the surface the more likely inversions will be weaker or not form at all. In agreement with this concept is the fact that the two years that had elevated ozone had the lowest averaged winds speeds.

The overall wind patterns remained fairly consistent. At the surface the maximum winds occurred in west central Montana each year, while the minimum was over western Colorado. At 700 mb the maximum occurred well to the northeast of the study area in the upper plains states while the lowest averages were over southern and central Utah. Table 4-2 presents the averaged surface and 700 mb wind speeds for each of the study years.

**Table 4-2.** Scalar Wind Speeds at the Surface and Aloft for the February and March Period.

| February/March Period | Surface Wind Speed (m/s) | 700 mb Wind Speed (m/s) |
|---|---|---|
| **2007** | 4.2 | 10.4 |
| **2008** | 3.8 | 10.1 |
| **2009** | 3.9 | 9.6 |

## Pressure and Pressure Heights

Pressure patterns see the most variance from year to year. At the surface the sea level pressure maximum occurred from Oregon to northeast Idaho/southwest Montana. Despite pattern differences the averaged surface sea level pressure over the study area has not varied by more than 1.8 mb. Aloft, at 700 and 500 mb, the averaged pressure height pattern was similar in 2007 and 2008 with higher pressure to the west and with heights dropping from west to east over Wyoming. In 2009 the 500 mb averaged pattern was fairly flat from west to east, and showed a substantial difference to previous years when a high pressure ridge was present over the western US. The 700 mb level pattern was also flatter, with a slight ridge axis from Utah north through Idaho. Averaged pressure heights over the study area have varied by as much as 24 meters at 700 mb and 39 meters at 500 mb over the three study years. Table 4-3 presents pressure and pressure heights at the surface, 700mb and 500 mb.

**Table 4-3**. Surface Pressure and Pressure Heights Aloft for the February and March Period.

| February/March Period | Surface Pressure (mb) | 700 mb Height (m) | 500 mb Height (m) |
|---|---|---|---|
| **2007** | 1019.7 | 3042 | 5604 |
| **2008** | 1020.8 | 3018 | 5552 |
| **2009** | 1019.0 | 3024 | 5565 |

**Snow Cover**

As pointed out by ENVIRON (2008), snow cover plays a significant role in the development of conditions conducive to ozone formation. Snow cover in the UGRB during the January – March period has been observed to vary significantly from week to week and the frequency and average amount of snow cover varies significantly from year to year.

Conditions during 2007 were very dry whereas snow cover in 2008 was quite extensive. Snow cover in 2009 was less extensive and persistent than in 2008 but not nearly as little as in 2007. This is illustrated by the MODIS satellite photos on clear sky days from 2008 and 2009 shown in Figure 4-1.

### 4.1.2 Air Quality Conditions

Average and maximum ozone levels during February – March 2009 were significantly lower than those experienced during the same period in 2008 but generally not as low as observed in 2007 (see Table 4-4). Maximum 8-hour ozone levels in 2009 were lower than maximum levels in 2005 and 2006 (except for the March 2005 maximum at Jonah). These results are consistent with overall lower ozone production during 2009; no exceedances of the ozone standard (75 ppb) were observed at these three permanent monitoring sites during the first three months of 2009.

**Table 4-4.** Monthly average and maximum 8-hour average ozone concentrations for February – March 2005 – 2009 at permanent monitoring sites.

| | Average | | | Maximum | | |
|---|---|---|---|---|---|---|
| **February** | **8-Hour Ozone (ppb)** | | | **8-Hour Ozone (ppb)** | | |
| **Year** | **Jonah** | **Boulder** | **Daniel** | **Jonah** | **Boulder** | **Daniel** |
| **2005** | 42.9 | 51.1 | NA | 98 | 89 | NA |
| **2006** | 39.5 | 48.1 | 49.5 | 93 | 71 | 82 |
| **2007** | 29.3 | 42.7 | 40.7 | 46 | 59 | 57 |
| **2008** | 40.6 | 54.1 | 50.7 | 102 | 122 | 76 |
| **2009** | 33.2 | 42.1 | 43.1 | 69 | 67 | 64 |
| | **Average** | | | **Maximum** | | |
| **March** | **8-Hour Ozone (ppb)** | | | **8-Hour Ozone (ppb)** | | |
| **Year** | **Jonah** | **Boulder** | **Daniel** | **Jonah** | **Boulder** | **Daniel** |
| **2005** | 40.0 | 48.3 | NA | 58 | 71 | NA |
| **2006** | 44.9 | 48.9 | 50.8 | 68 | 67 | 71 |
| **2007** | 32.7 | 44.3 | 40.7 | 44 | 65 | 55 |
| **2008** | 39.0 | 53.0 | 50.1 | 98 | 102 | 75 |
| **2009** | 39.0 | 46.2 | 43.0 | 63 | 70 | 67 |

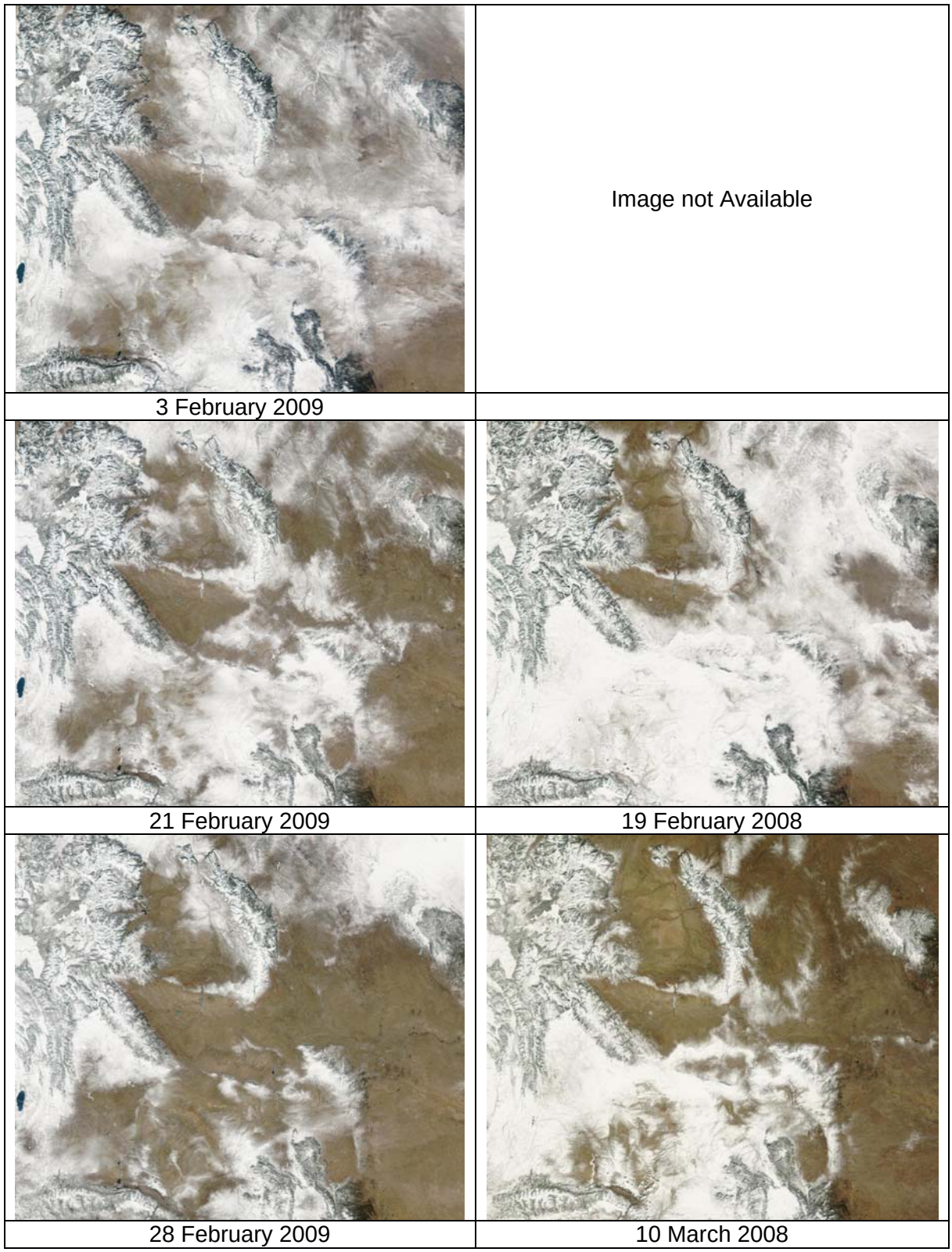


**Figure 4-1.** MODIS satellite images on clear days during 2009 (left) and 2008 (right).

In contrast to 2008, only a few days with elevated ozone occurred during the 2009 study period as illustrated by the time series of daily maximum 8-hour average values in Figure 4-2. Concentrations in the Upper Green River Basin (UGRB) exceeded 70 ppb on just 3 days between 20 January and 31 March: 23 February, 1 March and 2 March (see Table 4-5). Both the Mesa and Sodar sites recorded readings above 70 ppb on all three of these days whereas the only other site recording a value above 70 ppb was Warbonnet on 1 March. A value of 78 ppb was recorded at South Pass on 28 February but concentrations did not exceed 60 ppb on this date in the UGRB and the circumstances of the unusual high overnight ozone at South Pass on this day are not fully understood. No exceedances of EPA's 75 ppb ozone standard were recorded at any of the permanent monitoring sites in the UGRB (Jonah, Boulder, Pinedale or Daniel) during the study period. [1]

[1] Caution is required in comparing results from different monitoring sites shown in Table 4-5 and Figure 4-2: data at the Cora, Mesa, Warbonnet, Juell, Simpson, Speedway, Buckhorn, Seedskadie, and Sodar sites were collected using battery powered 2B ozone analyzers that do not meet Federal Equivalent Method (FEM) monitoring requirements for ozone. Only FEM data can be compared directly with EPA's ambient air quality standard to determine if an exceedance has occurred. Non-FEM instrumentation such as the 2B monitors provides approximate ozone concentrations that do not meet EPA's legal requirements for quantifying ozone in ambient air.

**Table 4-5.** Daily maximum 8-hour average ozone concentrations (ppb) on all IOP days [1] (values above 70 ppb in red; shaded cell indicates location of maximum on each day).

| Site/Date | 2/3/2009 | 2/4/2009 | 2/5/2009 | 2/21/2009 | 2/22/2009 | 2/23/2009 | 2/28/2009 | 3/1/2009 | 3/2/2009 | 3/3/2009 | 3/4/2009 |
|---|---|---|---|---|---|---|---|---|---|---|---|
| Cora | 45 | 47 | 58 | 52 | 53 | 66 | 51 | 59 | 70 | 53 | 52 |
| Mesa | 43 | 55 | 59 | 54 | 59 | 74 | 52 | 85 | 75 | 50 | 49 |
| Warbonnet | 44 | 61 | 60 | 53 | 68 | 60 | 54 | 72 | 67 | 47 | 48 |
| Juell | 44 | 51 | 53 | 58 | 59 | 62 | 60 | 59 | 58 | 47 | 50 |
| Simpson | 40 | 48 | 54 | 55 | 55 | 38 | 44 | 50 | 42 | 47 | 49 |
| Speedway | 43 | 44 | 48 | 52 | 55 | 51 | 54 | 59 | 60 | 50 | 51 |
| Buckhorn | 43 | 65 | 62 | 62 | 60 | 67 | 49 | 57 | 48 | 45 | 47 |
| Seedskadie | 37 | 44 | 50 | 46 | 48 | 36 | 43 | 44 | 41 | 46 | 48 |
| Sodar | 42 | 61 | 57 | 57 | 57 | 73 | 60 | 72 | 76 | 47 | 48 |
| Airport | 43 | 46 | 48 | 54 | 57 | 65 | 51 | 62 | 64 | 48 | 49 |
| Boulder | 45 | 50 | 53 | 63 | 63 | 67 | 56 | 70 | 70 | 51 | 51 |
| Jonah | 39 | 55 | 59 | 55 | 69 | 60 | 48 | 63 | 55 | 45 | 47 |
| Pinedale | 40 | 42 | 47 | 50 | 47 | 59 | 47 | 53 | 58 | 42 | 42 |
| Daniel | 42 | 50 | 57 | 53 | 50 | 64 | 48 | 54 | 67 | 48 | 49 |
| Pinedale-CASTNET | 46 | 51 | 55 | 51 | 55 | 57 | 56 | 59 | 66 | 52 | 50 |
| Bargerville | NA | NA | NA | 59 | 63 | 69 | 56 | 66 | 64 | 53 | 52 |
| Farson | NA | NA | NA | 47 | 49 | 41 | NA | NA | NA | NA | 51 |
| La Barge | NA | NA | NA | 37 | 36 | 38 | 38 | 48 | 35 | 43 | 45 |
| Marbleton | NA | NA | NA | 49 | 47 | 60 | 45 | 52 | 49 | 47 | 47 |
| Murphy Ridge | 40 | 39 | 35 | 44 | 42 | 35 | 42 | 46 | 37 | 42 | 45 |
| OCI Trona | 34 | 30 | 40 | 39 | 36 | 34 | 40 | 44 | 38 | 44 | 45 |
| Sand Draw | NA | NA | NA | NA | NA | NA | 53 | 63 | 67 | 48 | 49 |
| South Pass | 45 | 53 | 49 | 50 | 55 | NA | 78 | 56 | 46 | 47 | 53 |
| Wamsutter | 41 | 43 | 49 | 46 | 50 | 42 | 43 | 51 | 45 | 45 | 47 |
| Network Max | 46 | 65 | 62 | 63 | 69 | 74 | 78 | 85 | 76 | 53 | 53 |

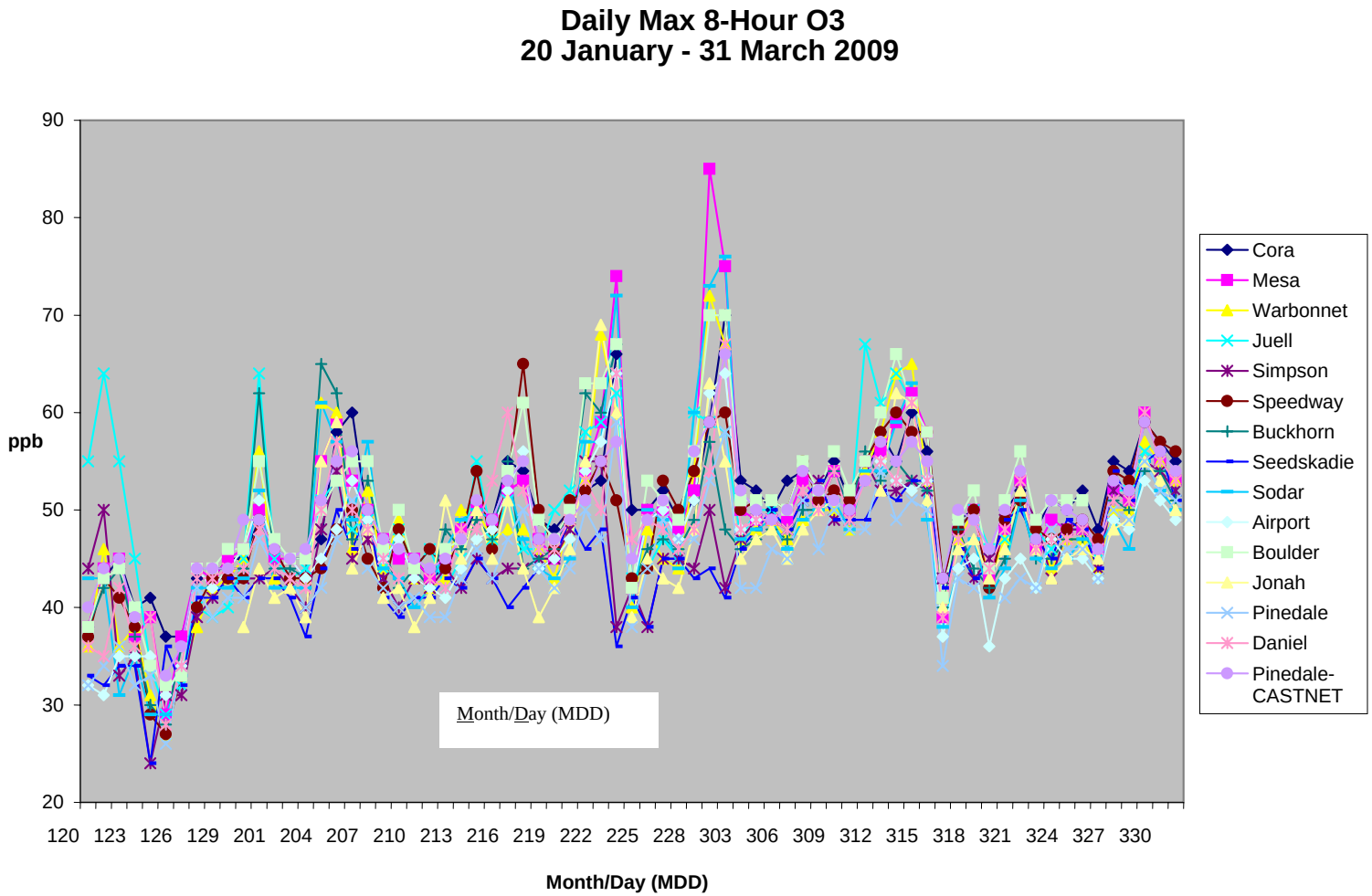


**Figure 4-2.** Daily maximum 8-hour average ozone concentrations for all monitoring sites in the Upper Green River Basin operating between 20 January and 31 March 2008.

A comparison of the maximum daily 8-hour ozone concentrations over all of monitoring sites in the UGWOS study area as listed in Table 4-5 with data from other southwestern Wyoming sites and at Yellowstone National Park is shown in Figures 4-3. Data from the EPA CASTNET Pinedale monitor, which is located 220 m above the town of Pinedale, are also included in this figure. With the exception of a few days on which unusual high ozone readings were recorded at South Pass, the UGWOS maximum concentration is always higher than concentrations recorded at any of the other southwestern Wyoming monitors on days when UGWOS ozone exceeds 50 ppb, consistent with the formation of significant amounts of ozone from precursor sources local to the Jonah – Pinedale area. The high South Pass ozone values occurred mostly during the hours between midnight and dawn and are not well correlated with the UGWOS ozone maximums, suggesting they are not associated with emissions from sources in the UGWOS study area. These unusual events are the subject of an on-going investigation by the WYDEQ. As was the case during previous winter episodes, ozone levels at the Pinedale CASTNET site, while correlated with the UGWOS maximum, were much lower and did not exceed 75 ppb. Overall, the high Jonah-Pinedale ozone events did not extend to other sites in southwestern Wyoming.

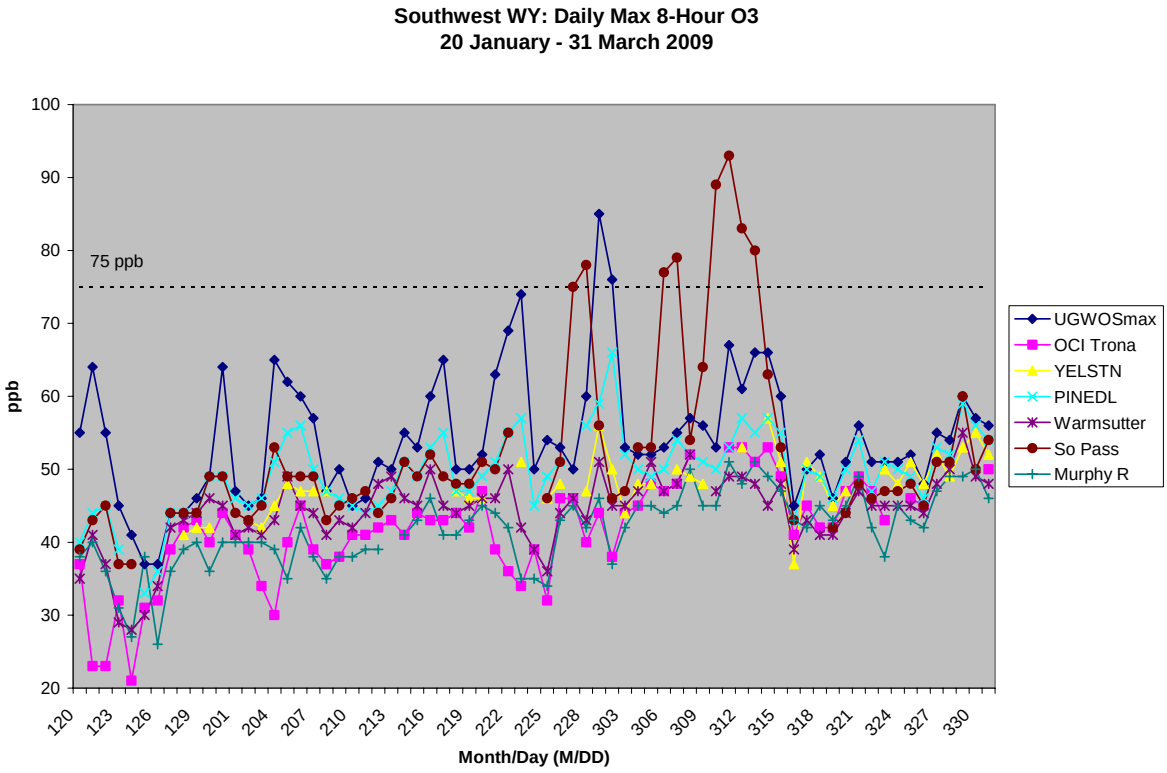


**Figure 4-3.** Daily maximum 8-hour average ozone concentrations at monitoring sites in southwestern Wyoming (only maximum daily value shown for the group of Jonah-Pinedale area sites for which data were presented in Figure 4-2).

## 4.2 Surface Wind Patterns

Northwest winds prevailed in the boundary layer during the winter. Wind patterns during periods of increased ozone levels were consistent with those observed during the 2008 study. In general, the measured daytime winds were light and variable throughout the study area. In the central area near Jonah, wind directions frequently reversed to a southeasterly flow or were variable, creating a situation where precursor-laden air is recirculated back into the well fields where additional emissions are added to the already polluted air. Each meteorological situation varied to some degree. Often, small variations in the wind field produced substantially different areal impacts.

Figures 4-4 through 4-9 present time-series representations of measured surface winds for key days during each of the IOPs. Site locations are shown in Figure 2-1. The plots are laid out such that winds at the northernmost site (Cora) are shown at the top of the figure and the southernmost site (Seedskadie) at the bottom with the sites in between listed in a roughly north to south order. Each successive site is south along roughly a north/south plane that extends through the heart of the Jonah and Pinedale anticline. The network of measurements in the area was designed specifically to document the meteorology, both spatially and quantitatively, that lead to the development of high ozone concentrations. In reviewing these data, it is necessary to keep in mind that wind measurements at the permanent monitoring sites (Jonah, Boulder, Daniel and Pinedale) are made at a standard height of 10 m agl (above ground level) whereas wind measurements at the tripod mounted mesonet sites (all other locations except at the airport) were made at a height of just under 3 m agl; airport wind measurements were also made at a height of approximately 3 m agl. A summary of the winds during each IOP is presented in the following subsections.

### IOP 1

Increased ozone concentrations were observed on February 4th and 5th. These days exhibited meteorological patterns consistent with the conceptual model and observed patterns that produce elevated ozone levels in the Pinedale and Jonah anticlines, as discussed above. The general characteristics of this wind pattern are seemingly a necessary component for episodic conditions, although not the only component. In this episode, morning winds are for the most part light and from the northwest, becoming light and variable during the middle of the day, allowing for recirculation of ozone and precursors. As can be seen from Figures 4-4 and 4-5, the winds at Buckhorn, Jonah, and Warbonnet show a reversal of wind direction during the afternoon hours, providing the mechanism for bringing already precursor-laden air back into the region where fresh emissions are added. Winds at the Sodar site show a drainage flow down the New Fork River, possibly transporting precursor emissions from gas production activity associated with the Riverside area.

During this IOP, the northwesterly winds that develop during the night of the 4$^{th}$ and morning of the 5th were strong enough to transport the polluted airmass which developed during the 4$^{th}$ out of the region, apparently eliminating any carryover contribution to concentrations on the 5$^{th}$. Afternoon winds at several sites had an easterly component, keeping developing plumes on both days towards the western portion of the study area.

**IOP 2**

Wind patterns on February 22 and 23 are similar to those for the first IOP, again with notable variations. Winds are uncharacteristically variable and not always light during the key afternoon period on the 22nd, which seems to have prevented ozone from accumulating significantly. However, nighttime winds between the two days are lighter than those during IOP 1, providing an opportunity for greater accumulation of precursors, or even the possibility of carryover from the previous day in some areas. A well defined southeasterly reversal of flow on the 23rd prior to 12:00 MST at Buckhorn, Jonah and Warbonnet. This was followed by light afternoon winds in the areas north of Jonah, resulting in moderately high, sustained ozone concentrations at the Sodar and Mesa sites, with 8-hour averages approaching 75 ppb.

**IOP 3**

Winds consistent with the conceptual model are again noted on March 1 and 2, during which the highest ozone concentrations for 2009 were recorded. Again, a reversal of flow was measured at Buckhorn and Jonah on the 1st, with light and variable afternoon winds reported at the other sites in the network. This allowed high ozone levels to develop throughout the region. Steady northwesterly winds again set up during the nighttime, limiting the chance for significant carryover contribution on the 2nd. However, similar daytime wind patterns developed early on the 2nd. Notably, wind speeds increased in the early afternoon, effectively ending the episode. Winds at Cora show a definitive reversal from northwesterly to southeasterly at 1400, providing a mechanism for the ozone-laden air to push to the northwest, outside the study area.

It is worth noting that during the episodes, the winds measured at the Pinedale AQ site, located in the populated area of Pinedale, closely match those recorded at Cora. At these two sites, winds are predominantly from the northwest, and while there are periods during midday when winds become light, no winds were observed that would have allowed for sustained transport of ozone to Pinedale from sources to the south.

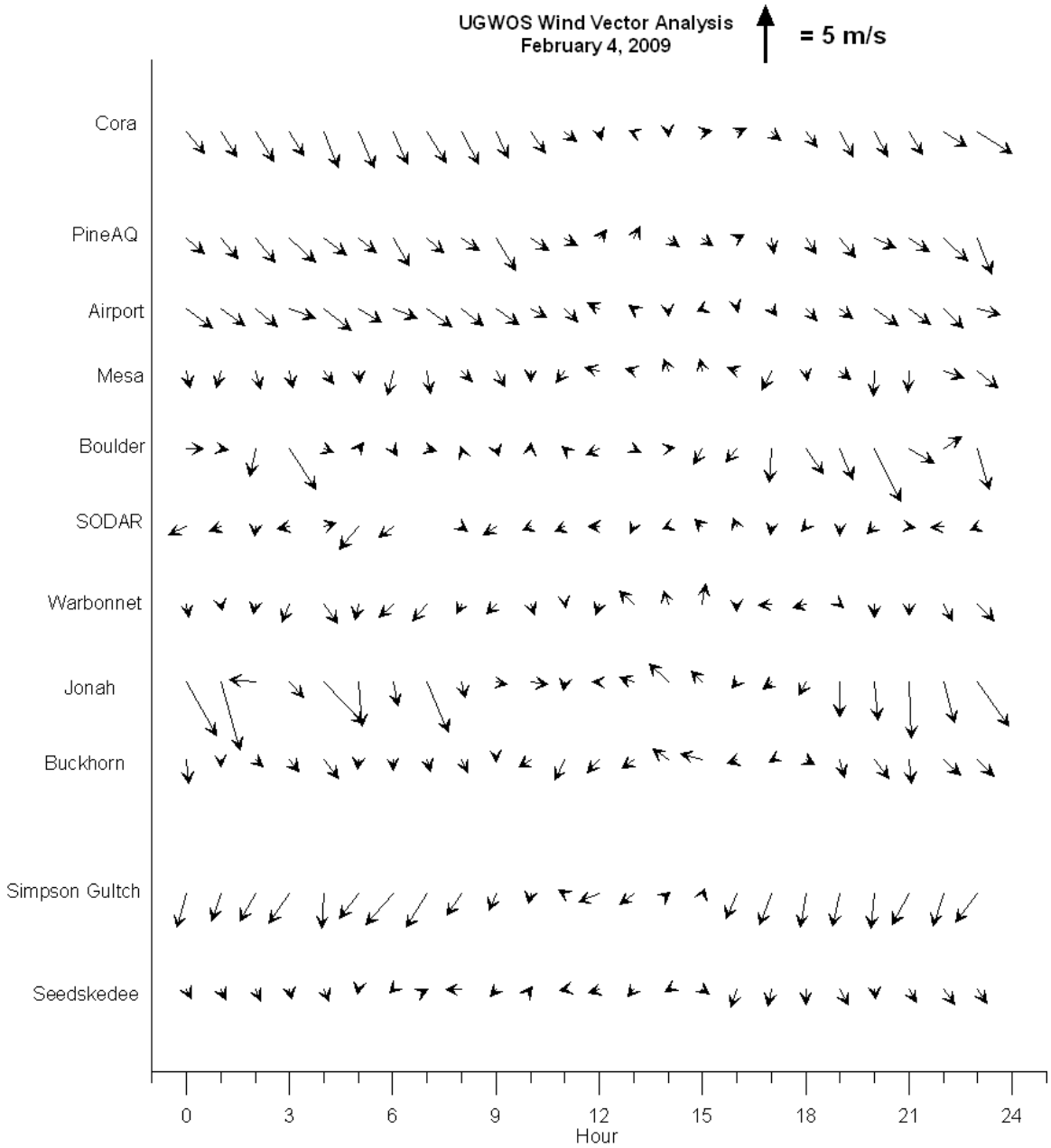


**Figure 4-4.** IOP 1 Vector winds – February 4, 2009.

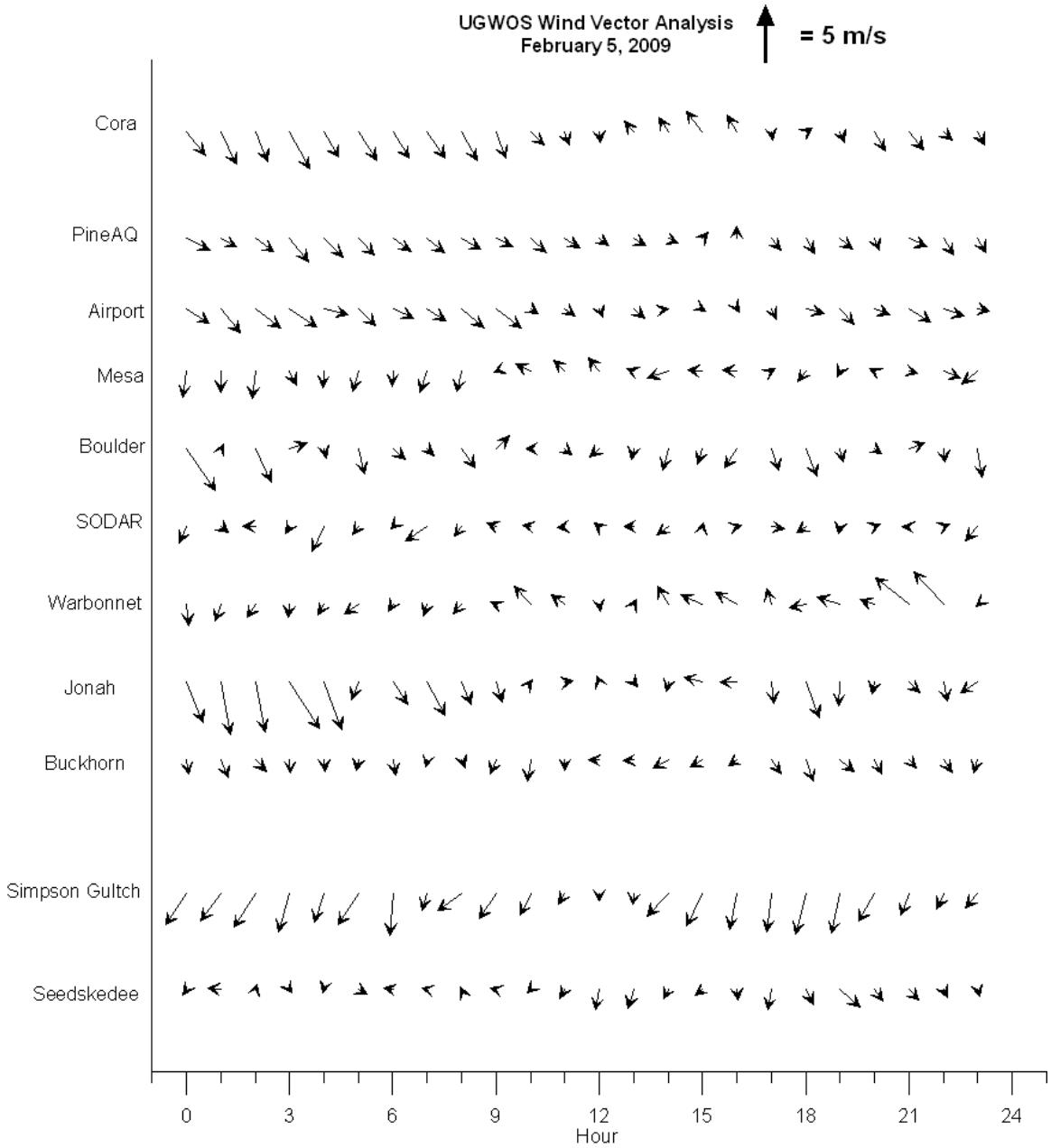


**Figure 4-5**. IOP 1 Vector winds – February 5, 2009.

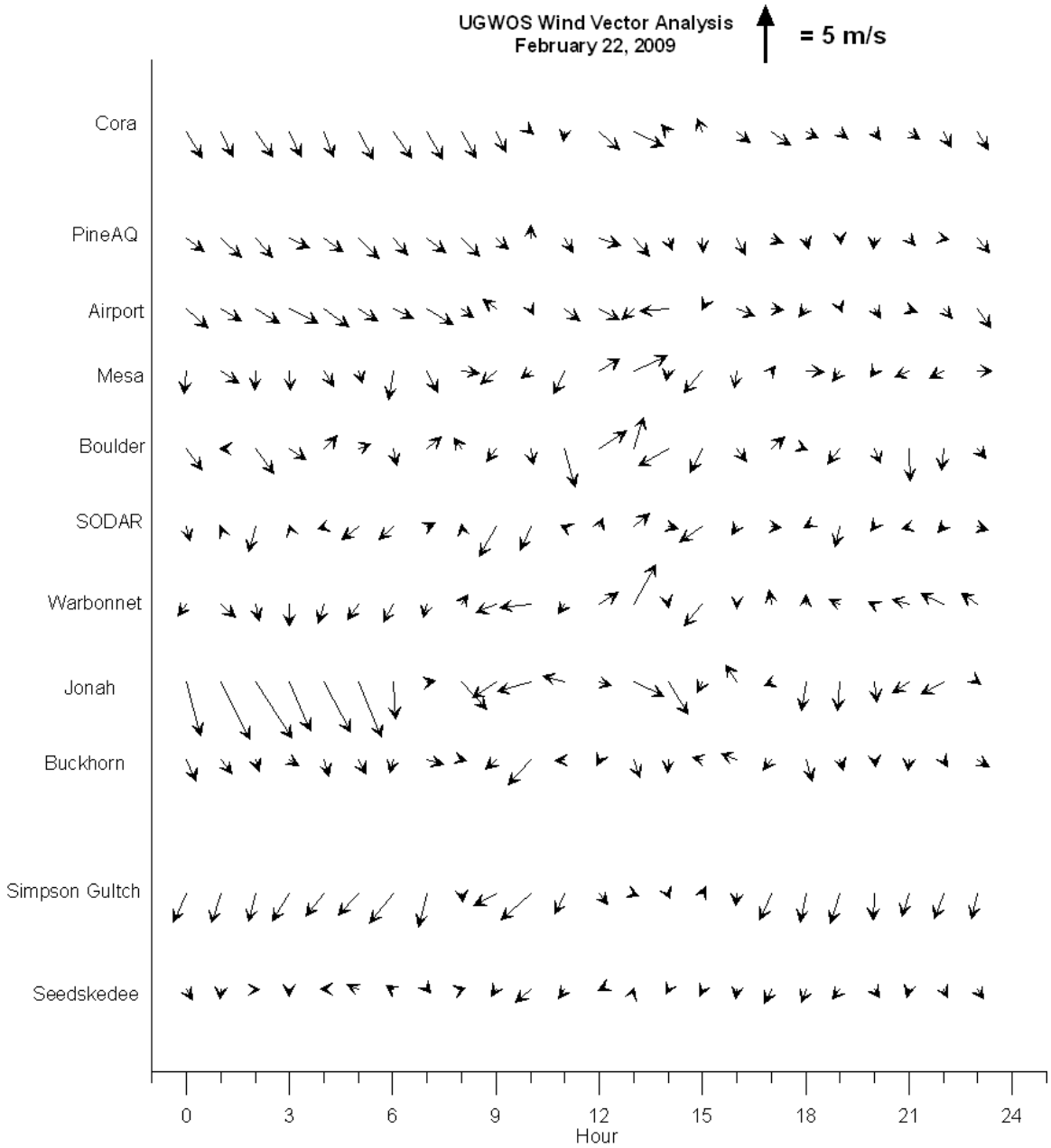


**Figure 4-6**. IOP 2 Vector winds – February 22, 2009.

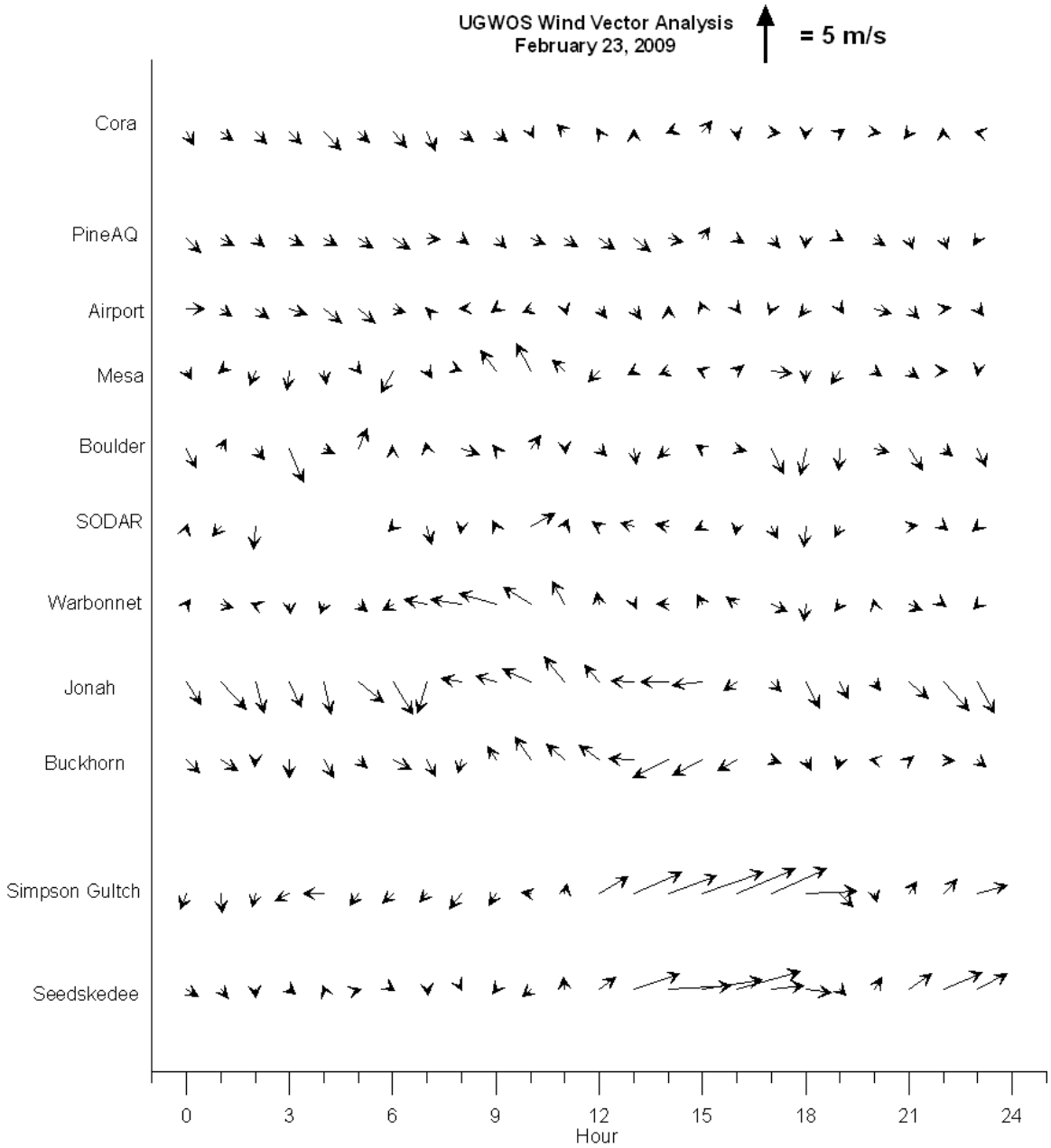


**Figure 4-7**. IOP 2 Vector winds – February 23, 2009.

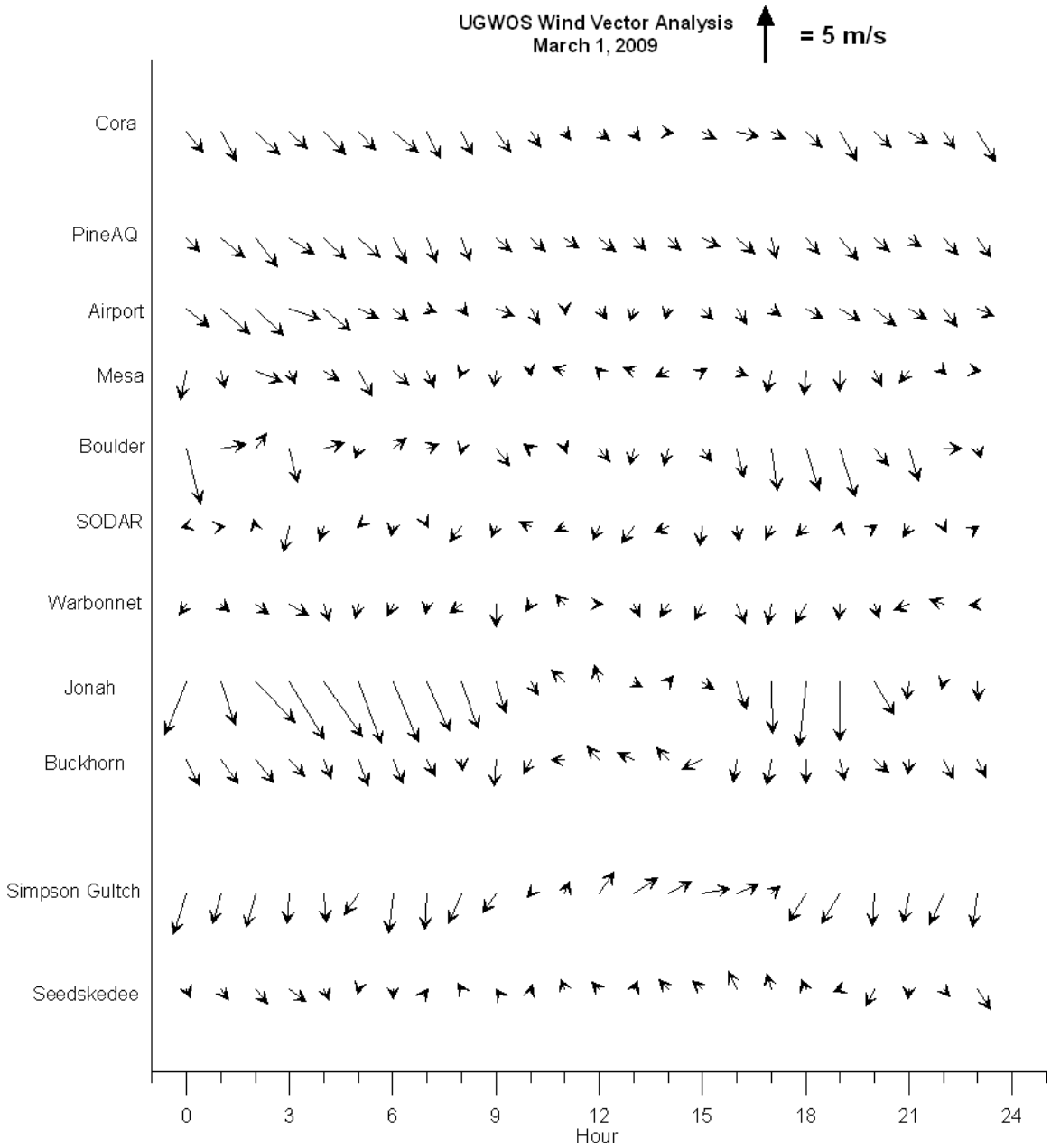


**Figure 4-8.** IOP 3 Vector winds – March 1, 2009.

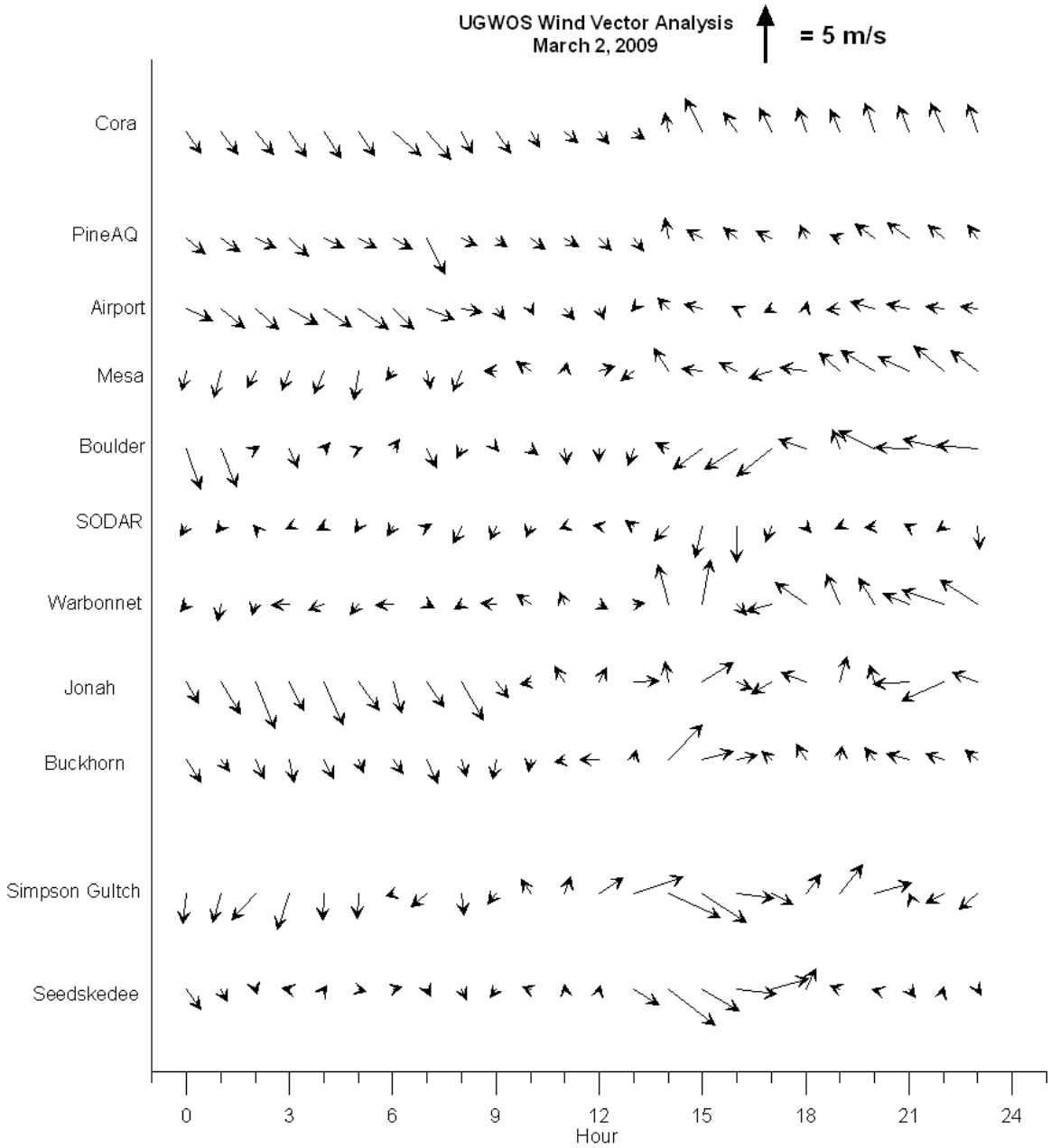


**Figure 4-9.** IOP 3 Vector winds – March 2, 2009.

## 4.3 Ozone Spatial and Temporal Distributions

The highly spatially and temporally resolved monitoring network operated in the 2008 study proved invaluable for characterizing ozone development and impacts in the Upper Green River basin. The network was refined for the 2009 study to eliminate redundancy noted in the 2008 analysis, and expanded the network farther south and west as recommended in the 2008 report. An independent study designed to assess health impacts owing to local emission sources established additional ozone monitoring sites that were incorporated into the 2009 field study design.

To illustrate the following discussion, the spatial and temporal distribution of ozone during the IOPs were visualized by creating ozone isopleth maps using all UGWOS, continuous, and special study monitoring sites within the study domain (refer to Figures 4-10 through 4-28). Isopleths (contours) of ozone concentrations are based on hourly averages, with concentrations displayed in ppb. Note that the interpolation algorithm used to create these contour maps does not always represent spatial concentration gradients in a realistic manner in that it has a tendency to draw contours at constant radii around monitoring sites, creating a "bulls eye" effect. Thus, the spatial interpolation patterns shown here should be interpreted with caution, keeping in mind that concentrations are only known at the actual monitoring site locations and are likely to be strongly influenced by terrain (which is not taken into account by the interpolation algorithm), especially under the low mixing height, low wind speed conditions associated with elevated ozone levels. In addition to the ozone data, wind vectors are displayed for each monitoring site to assist in the understanding of air parcel movement. Hours demonstrating noteworthy ozone development phases for each IOP were selected for the following discussion. The wind vector time-series plots presented above (Figures 4-4 through 4-9) provide information for additional hours referenced in the discussion.

### 4.3.1 IOP 1

- Figure 4-10 – February 4, 1300. By 1300 MST, ozone is building rapidly in the Jonah area where regional ozone development activity has historically been the greatest. Review of the wind data presented above shows that initially winds move the air mass southeast for several hours, then reverse direction, bringing the polluted air mass back over the Jonah fields. Hourly average concentrations at Jonah increase rapidly in concert with the flow reversal, jumping from 43 ppb at 11:00 MST to 86 ppb at 13:00 MST, implying ozone produced downwind of the Jonah field is being recirculated over the monitor. Note that the entire region surrounding the Jonah field is experiencing elevated ozone levels of approximately 60-65 ppb.

- Figure 4-11 – February 4, 1500. Light, easterly winds on the Pinedale anticline that developed at 13:00 push the area of elevated ozone that had been centered at Jonah toward Buckhorn. Peak ozone concentrations are observed from just south of Buckhorn to the Sodar site. While the contours as drawn show a separation between Buckhorn and Sodar, there are no sites available to directly support this view, and the area west of Jonah could have generally higher concentrations. On the other hand, the apparent terrain driven drainage winds at the Sodar site suggest that ozone plumes from emissions in the Mesa area may have a significant impact.

- Figure 4-12 – February 4, 1700. Elevated ozone concentrations remain in the general area, under continued light winds. Again, the low readings at Jonah are likely due to scavenging of ozone by fresh NO emissions in the area.

- Figure 4-13 – February 5, 1200. As during the previous day, the plume begins with an initial development over Jonah, a likely center of significant precursor emissions. Light winds during the three hours preceding 1300 have kept the emissions and subsequent ozone development focused in the area around Jonah.

- Figure 4-14 – February 5, 1400. Light and variable winds cause a general broadening of the plume, though, consistent with the wind vectors shown, a gradual movement west is noted.

- Figure 4-15 – February 5, 1600. The plume continues to move to the west under light easterly winds.

### 4.3.2 IOP 2

- Figure 4-16 – February 22, 1300. Consistent with the winds, dispersion in the major emissions source regions is strong enough to prevent ozone concentrations from developing to the extent as occurred by this time during the first IOP. Recorded winds would suggest that the plume is being pushed to the north and east of the major emissions, although the peak ozone is observed at Jonah and Warbonnet.

- Figure 4-17 – February 22, 1500. By 1500, the general flow has reversed, recirculating the polluted air into emission source areas and providing the opportunity to add additional precursors to the air mass. Owing to better dispersion conditions, peak hourly (and hence 8-hour average) ozone concentrations did not exceed 75 ppb with the notable exception of a 87 ppb 1-hour average at Warbonnet.

- Figure 4-18 – February 22, 1700. As apparent in the wind plots above, winds in the area remain light and variable during hours 1600 and 1700. The extent of air mass stagnation was a major factor for ozone concentrations exceeding 100 pbb. This stagnation also allowed ozone concentrations at all other sites to remain low, relatively speaking. A reversal of wind direction at Jonah at 1600 may have contributed to the high readings at this site.

- Figure 4-19 – February 23, 1200. Winds remain light and variable in the area throughout the night. While the developing plume is very similar in area and concentration to that depicted for the previous day (Figure 4-16), it is noteworthy that the plume has developed an hour earlier than the previous day, suggesting the possibility that carryover from the previous day has contributed to the rising ozone concentrations. The average concentration of the central monitoring sites (Mesa, Boulder; Bargerville, Sodar, Warbonnet, Jonah, Juell Springs, and Buckhorn) for hour 1200 is 64 ppb – 9 ppb higher than it was for the same hour on February 22.

- Figure 4-20 – February 23, 1400. Light easterly winds move the plume slightly westward. Moderate ozone concentrations are observed throughout the region.

- Figure 4-21 – February 23, 1600. Light northeast winds in the Jonah area are juxtaposed with southwest winds between Seedskedee and Farson with additional southerly component winds at most sites further north causing the high ozone to drift to the northwest. While hourly ozone concentrations never culminate in the >100 ppb values noted on February 22, they remaining moderately high throughout the region for an extended amount of time, resulting in 8-hour averages of 72 ppb at the Sodar site and 74 ppb at Mesa.

### 4.3.3. IOP 3

- Figure 4-22 – February 28, 1300. Some initial development of higher ozone concentrations is observed. Steady northwest winds push precursors and ozone southeast of the regions of emissions resulting in Juell Springs being the only site in the network measuring moderately high ozone concentrations.

- Figure 4-23 – March 1, 1100. Around 0900, winds at Jonah, Warbonnet, and Mesa shift from northwesterly to southeasterly, bringing "older" precursor-laden air back into the regions. A rapid and early increase in ozone concentrations is seen at the Jonah and Sodar sites, with hourly averages increasing by 25 ppb at Jonah and 17 ppb at Sodar between hours 1000 and 1100.

- Figure 4-24 – March 1, 1300. Winds remain light and variable, allowing the buildup of high ozone in the area. Network peak hourly averages of greater than 100 ppb are recorded at the Mesa and Warbonnet sites.

- Figure 4-25 – March 1, 1700. By 1500, many of the sites are showing a northerly component in their winds, and a portion of the plume has pushed south. Nevertheless, concentrations in the anticline remain moderately high. An 8-hour average of 85 ppb is recorded at Mesa.

- Figure 4-26 – March 2, 1200. Light winds allow pooling of precursors and accompanying high ozone concentrations in the Warbonnet area. Moderately high ozone concentrations are observed throughout the surrounding area.

- Figure 4-27 – March 2, 1400. By 1400, the winds at most of the sites have taken on a southerly component, and the plume begins moving in a northwesterly direction. Moderate southwest winds at Buckhorn are pushing cleaner air into the Jonah area and onward up into Warbonnet, causing ozone concentrations to drop rapidly at these sites. Light, drainage winds at the Sodar site, potentially bring in additional precursors from the Riverside area, allow ozone concentrations to continue to rise at this site.

- Figure 4-28 – March 2, 1600. Winds continue to push the plume in a northwesterly direction, decreasing concentrations in the southern sites. Correspondingly, notably higher concentrations are observed at the northern sites. Cora hourly averages peak at 91 ppb. While the advection of cleaner air from the south has prevented the occurrence of high 8-hour averages at the southern sites, concentrations at the Sodar and Mesa sites remained moderately high enough to result in 8-hour concentrations of 76 ppb and 75 ppb, respectively.

In summary, considering the weak synoptic-scale pressure gradients during periods when high ozone is experienced, it is not surprising that local winds play a decisive role in determining the development and spatial distribution of high ozone concentrations. The 2009 measurements also showed the significance of the air mass history (trajectory) to peak ozone. Although only three episodes were measured, there was evidence of day-to-day carryover of ozone and precursors, of recirculation of polluted air over the major sources, and direct transport of a plume from its origin to points within and likely beyond the network boundary. These three episodes

demonstrate the potential for high ozone concentrations to potentially occur anywhere in the region. As was the case in the 2008 study, though more conclusive now due to increased monitoring coverage, wind patterns at Pinedale and Bargerville for the most part cause areas of elevated ozone to move away from these populated areas. Similarly, neither La Barge or Marbleton exhibited any tendency for elevated readings, though monitoring at Marbleton has been limited. Neither site was operating during the first IOP, when contour plots showed the plume pushed to the west, potentially impacting the Big Piney / Marbleton area.

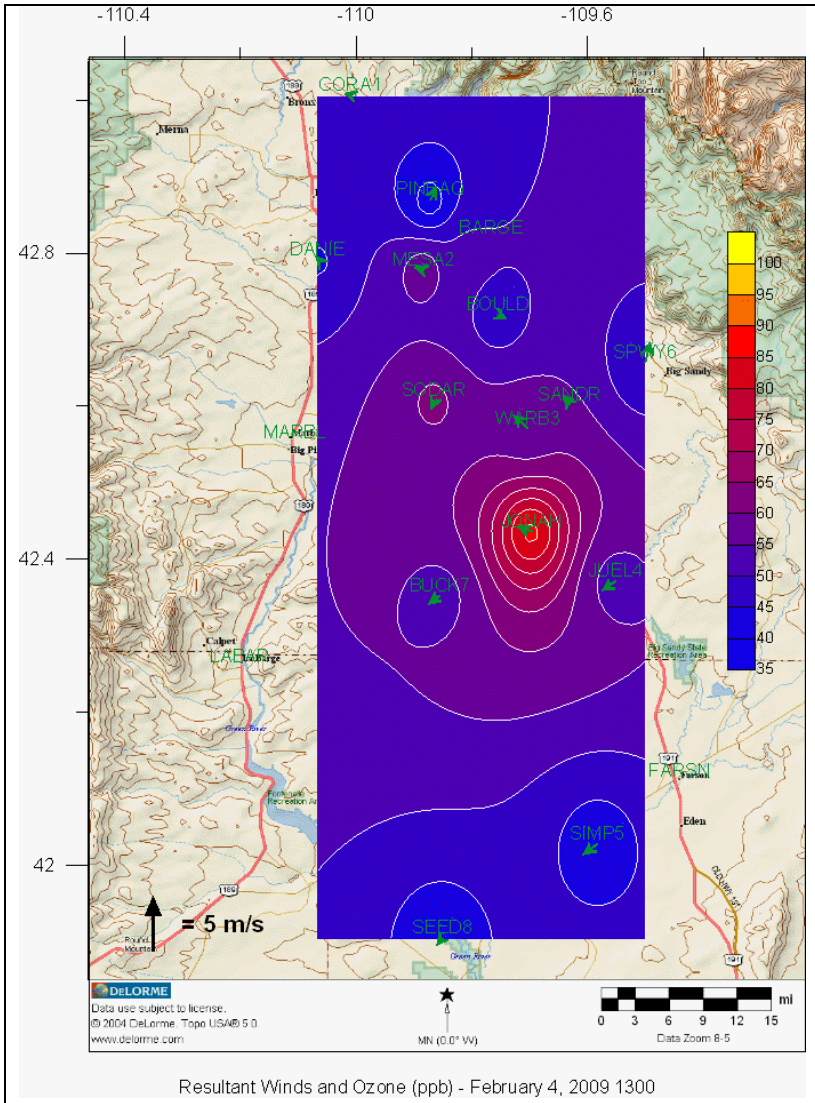


**Figure 4-10.** IOP 1.

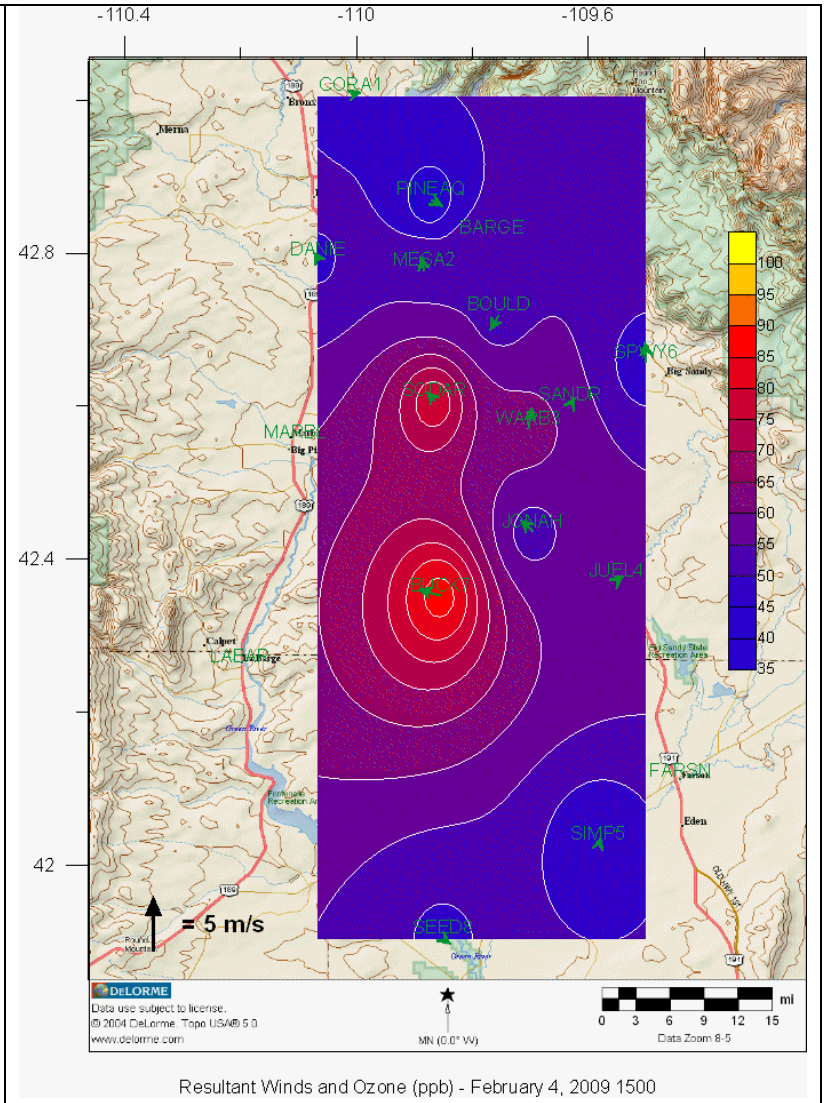


**Figure 4-11.** IOP 1.

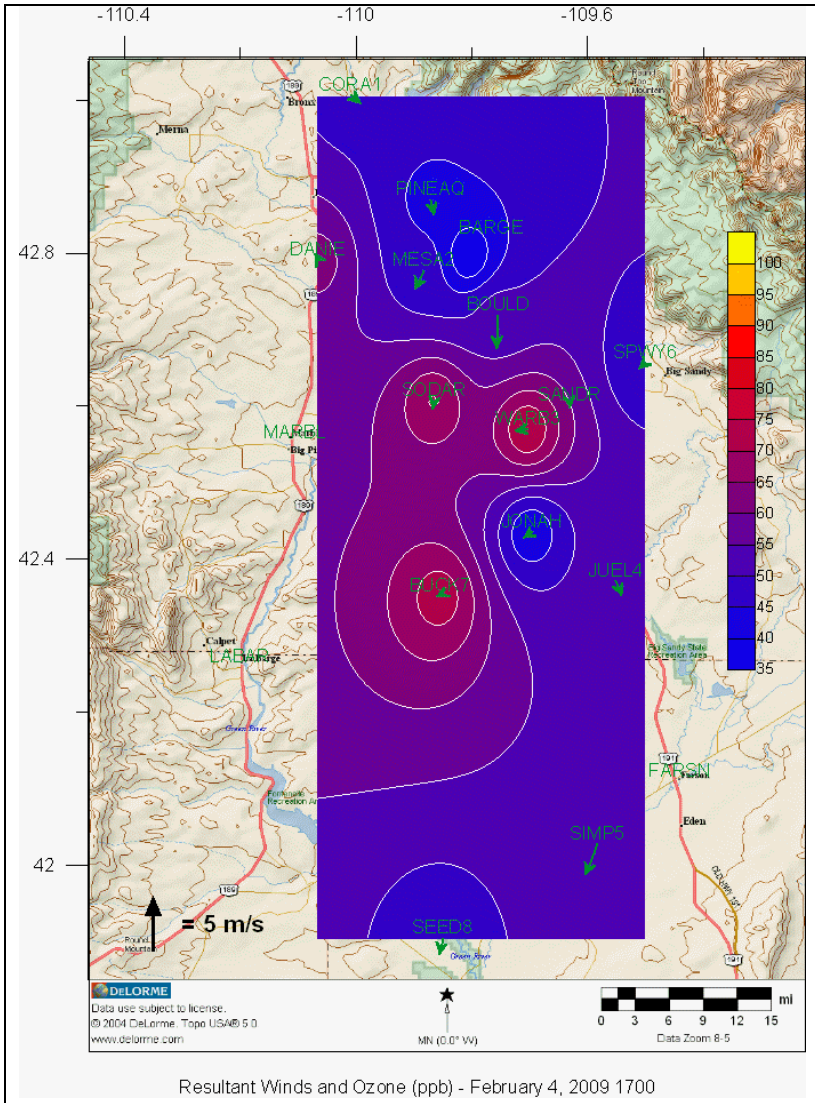


**Figure 4-12.** IOP 1.

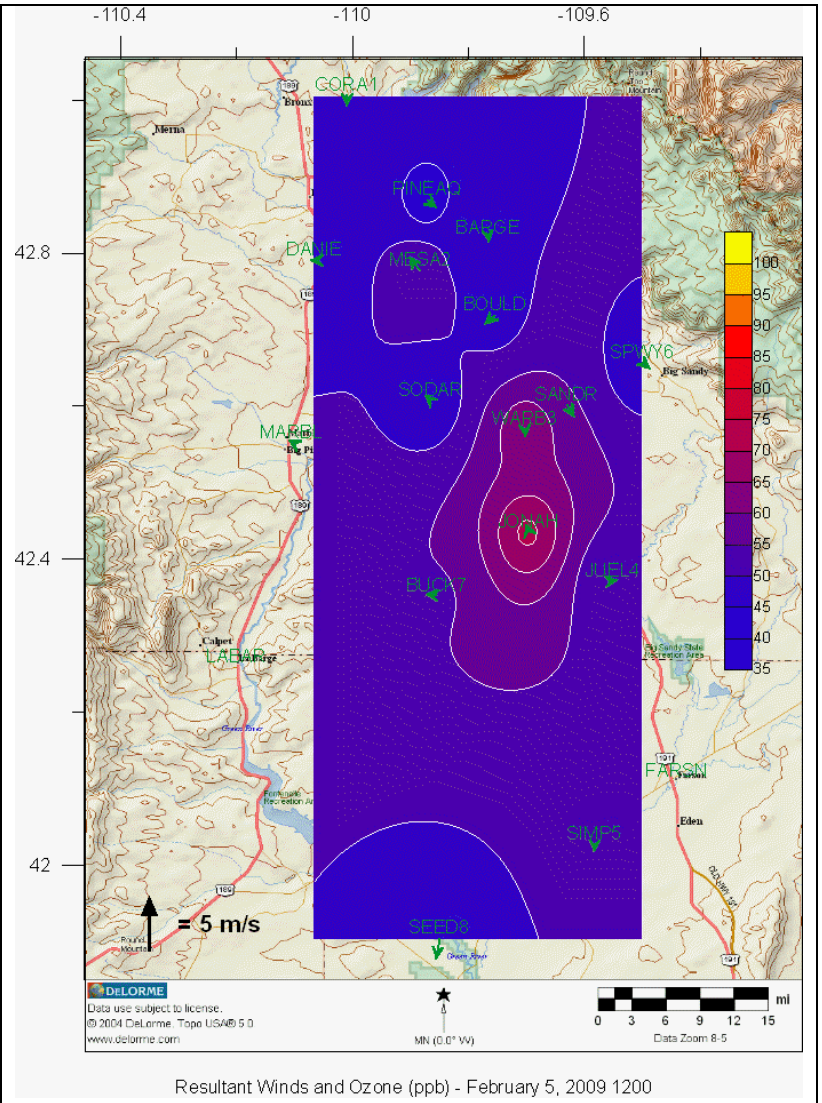


**Figure 4-13.** IOP 1.

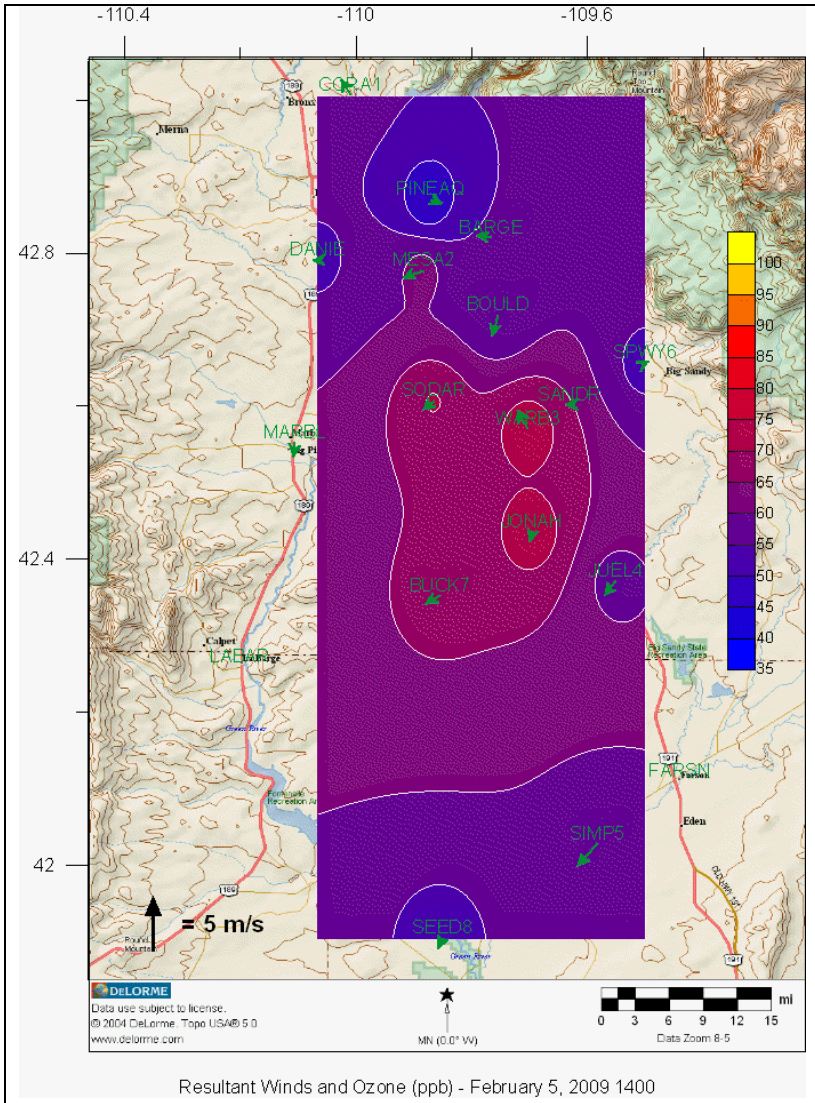


Resultant Winds and Ozone (ppb) - February 5, 2009 1400

**Figure 4-14.** IOP 1.

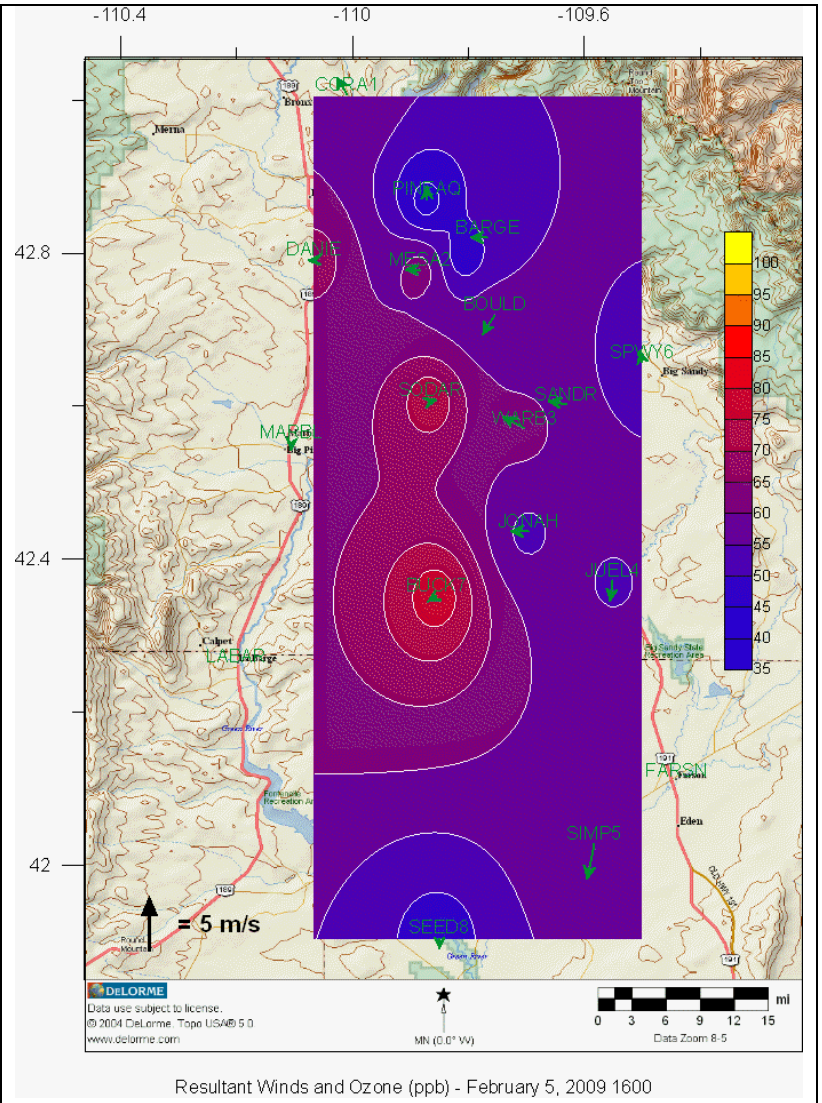


Resultant Winds and Ozone (ppb) - February 5, 2009 1600

**Figure 4-15**. IOP 1.

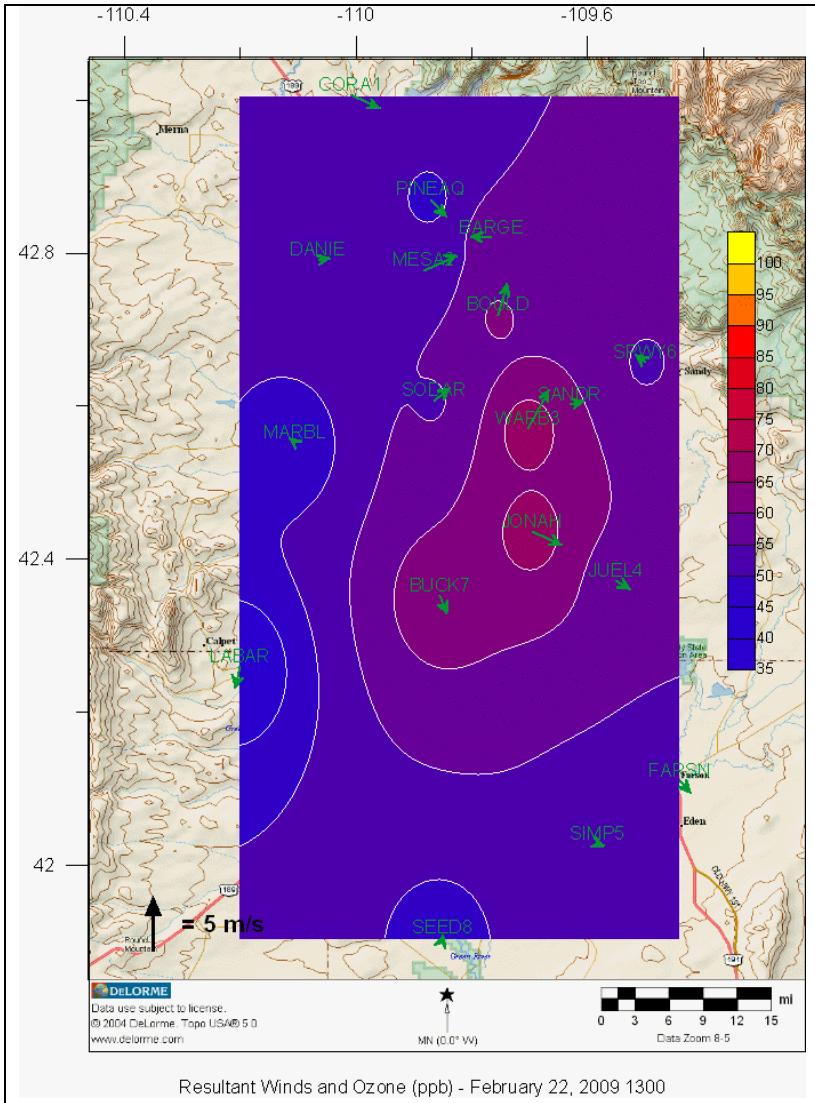


**Figure 4-16.** IOP 2.

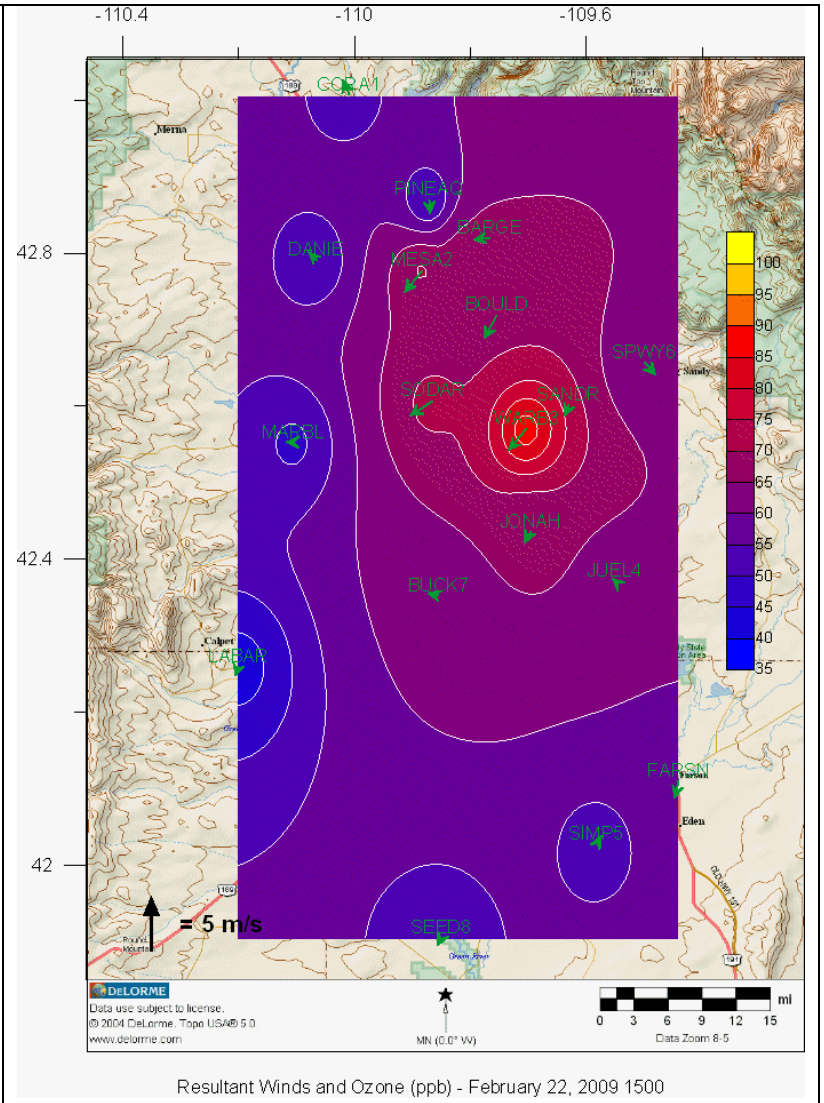


**Figure 4-17.** IOP 2.

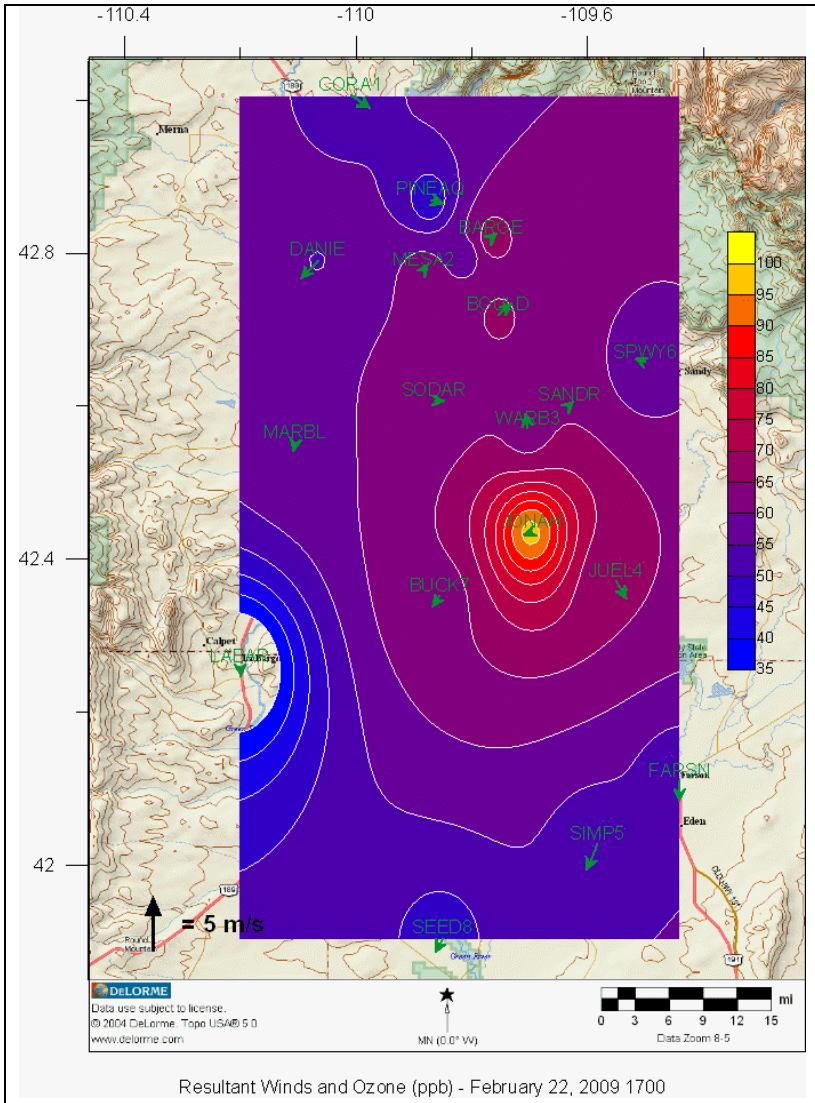


**Figure 4-18.** IOP 2.

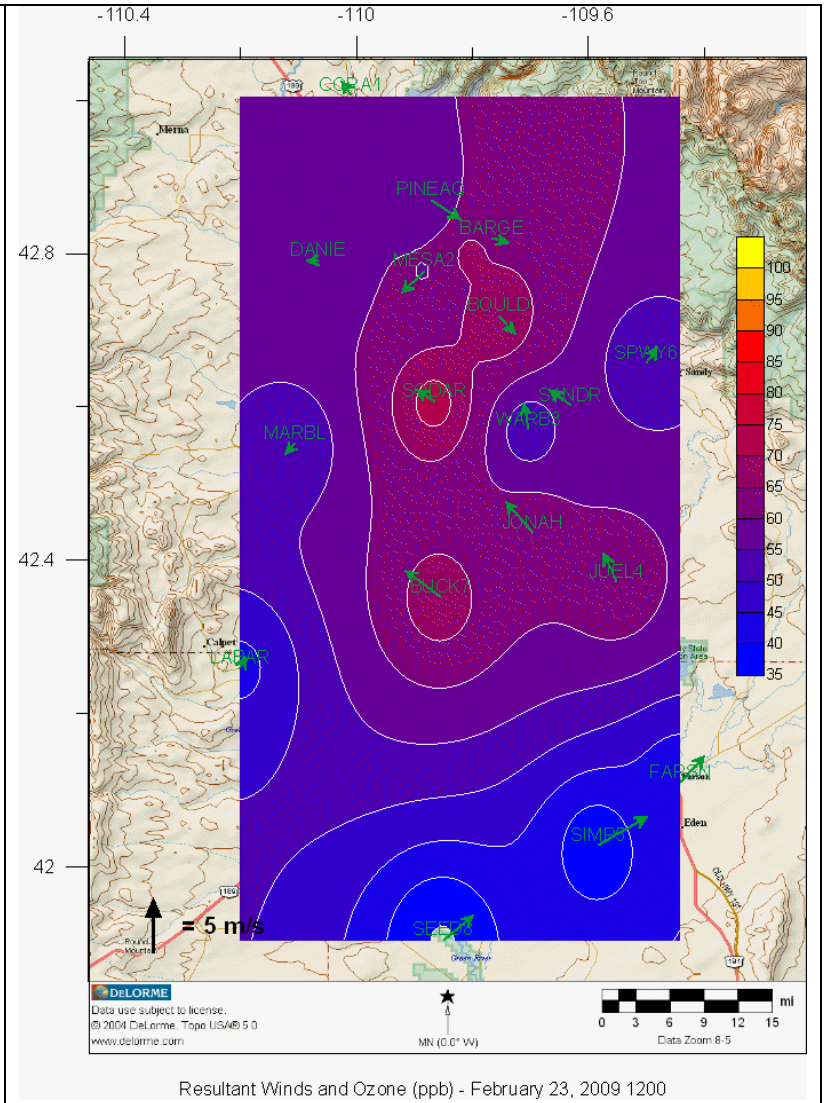


**Figure 4-19.** IOP 2.

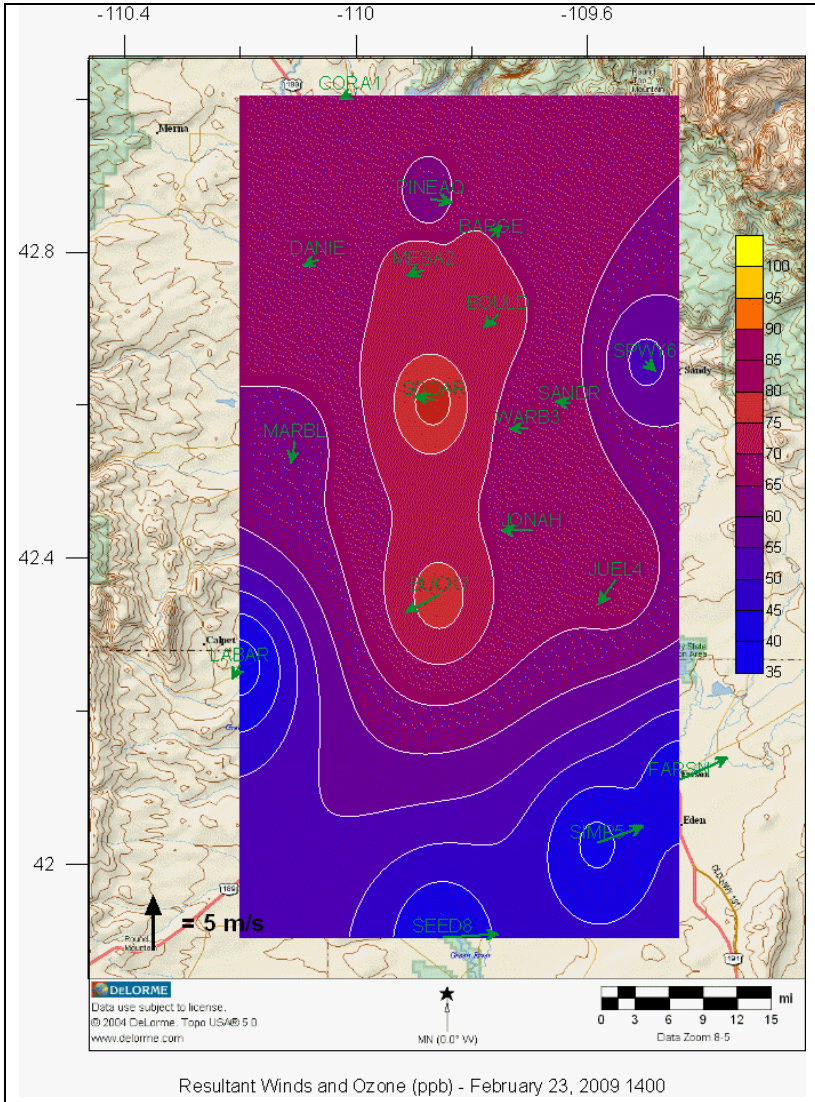


Resultant Winds and Ozone (ppb) - February 23, 2009 1400

**Figure 4-20**. IOP 2.

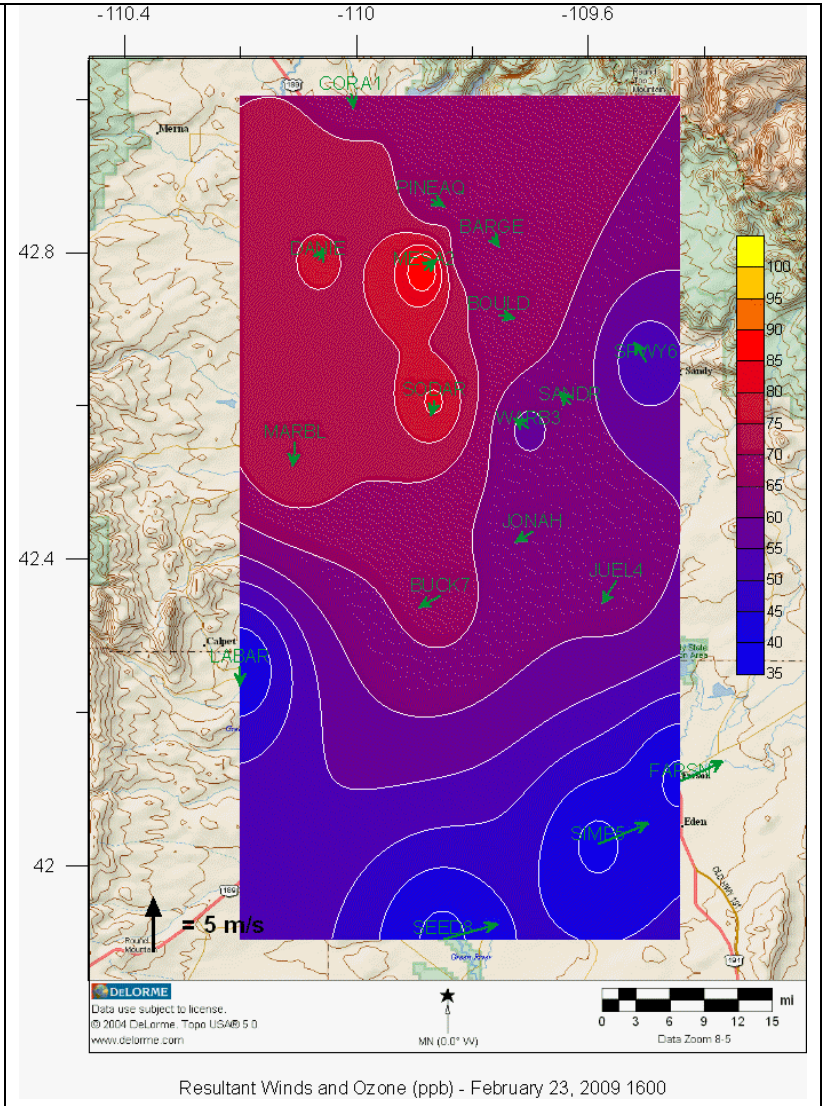


Resultant Winds and Ozone (ppb) - February 23, 2009 1600

**Figure 4-21**. IOP 2.

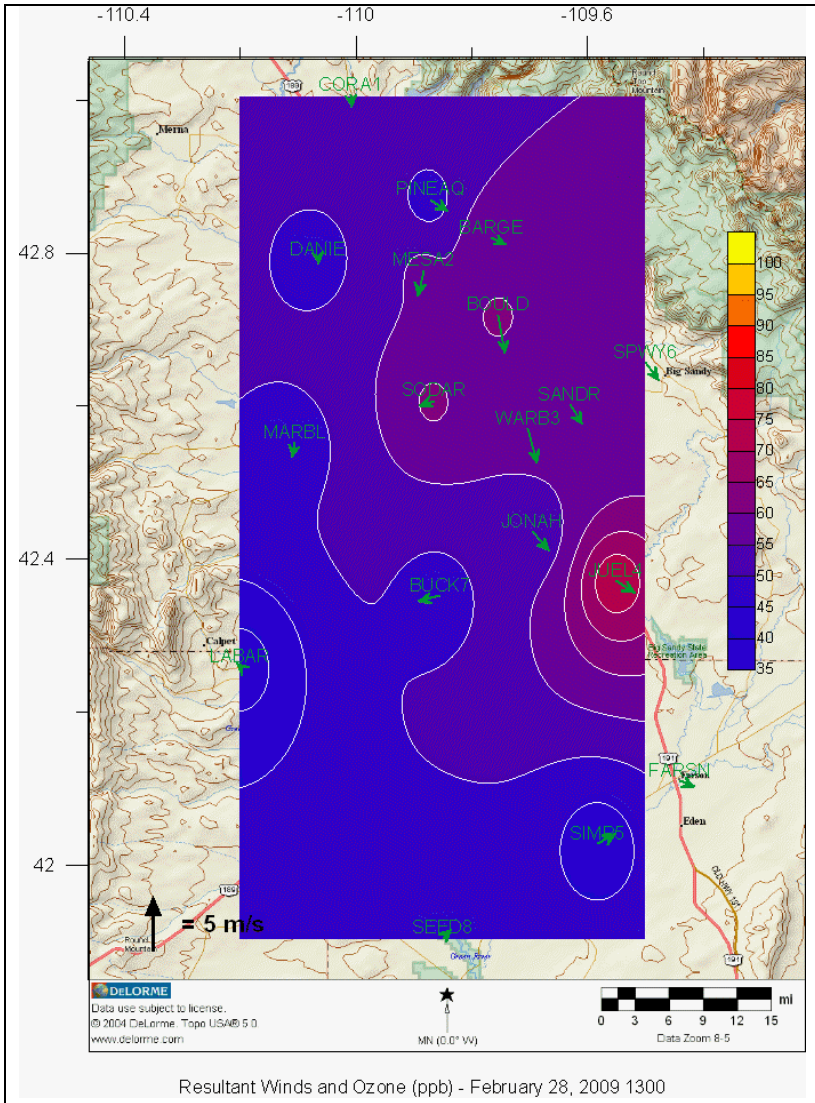


**Figure 4-22.** IOP 3.

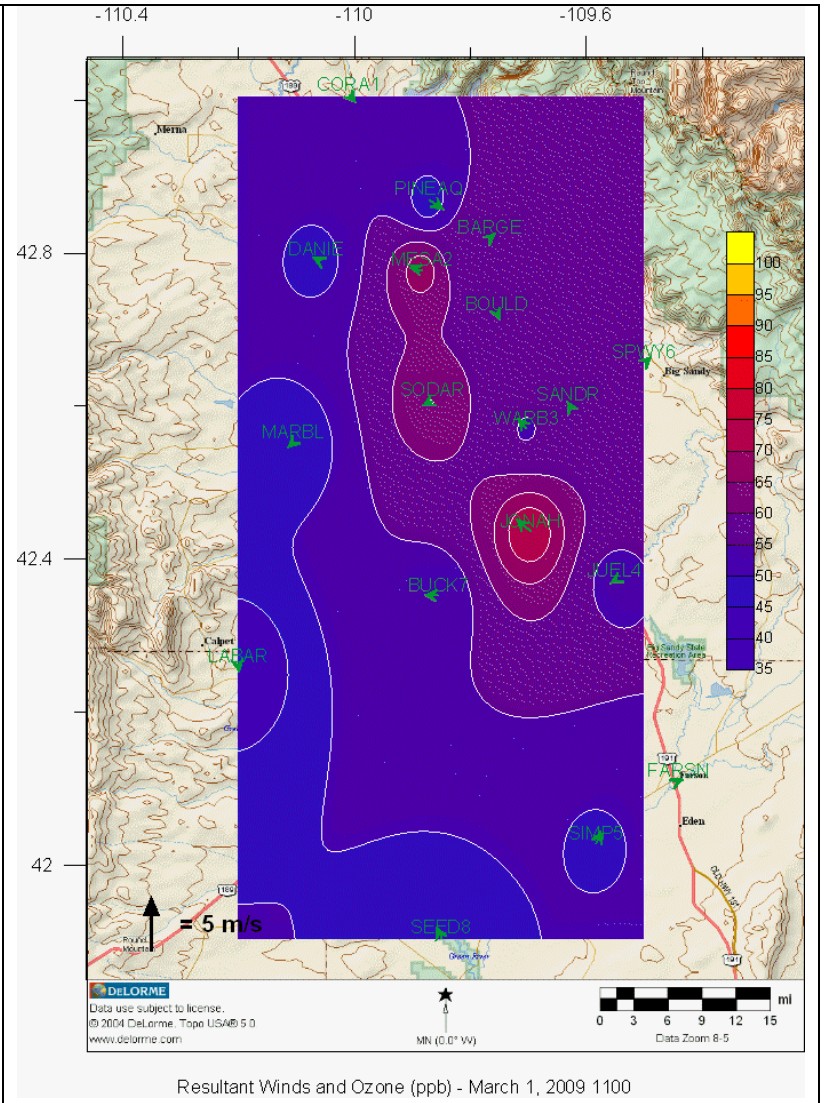


**Figure 4-23.** IOP 3.

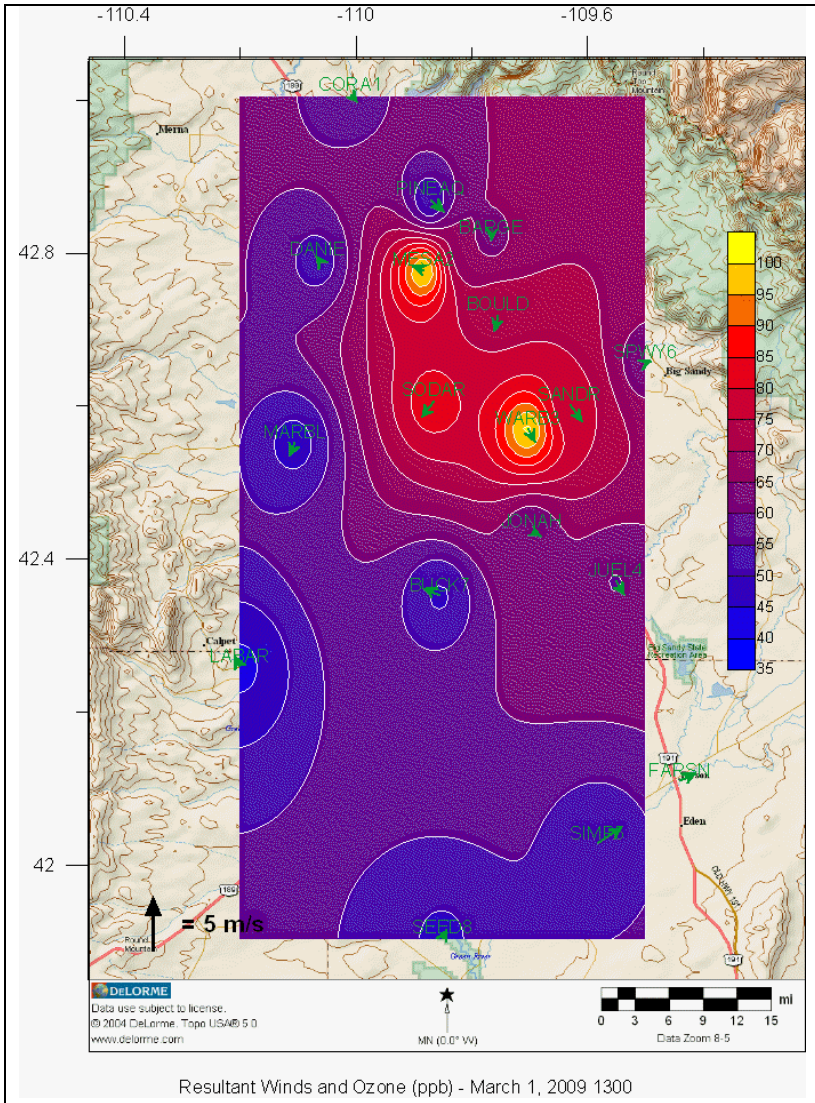


**Figure 4-24.** IOP 3.

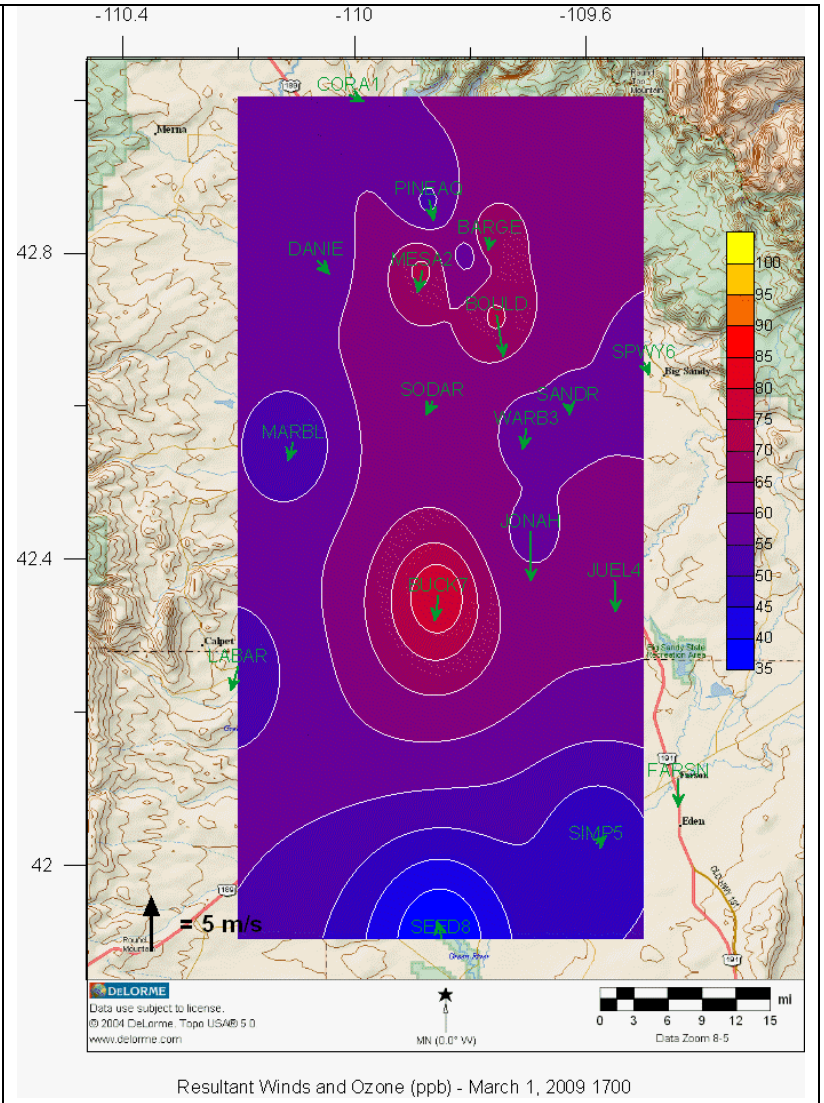


**Figure 4-25.** IOP 3.

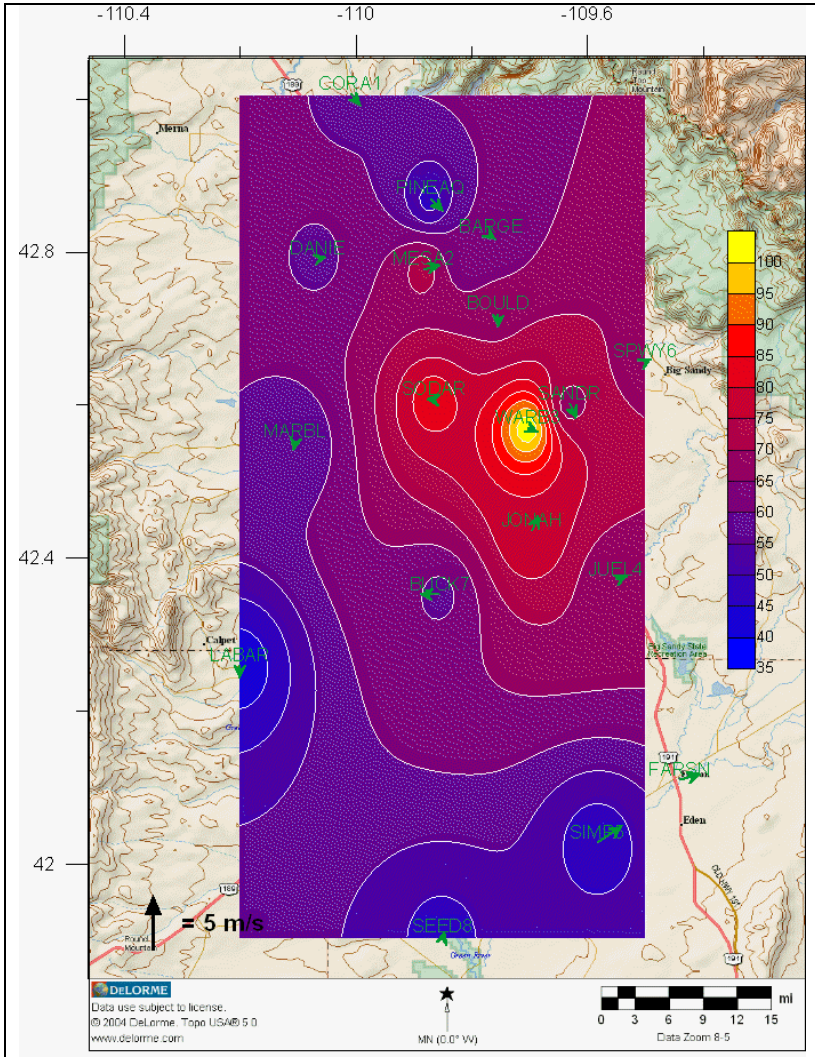


**Figure 4-26**. IOP 3.

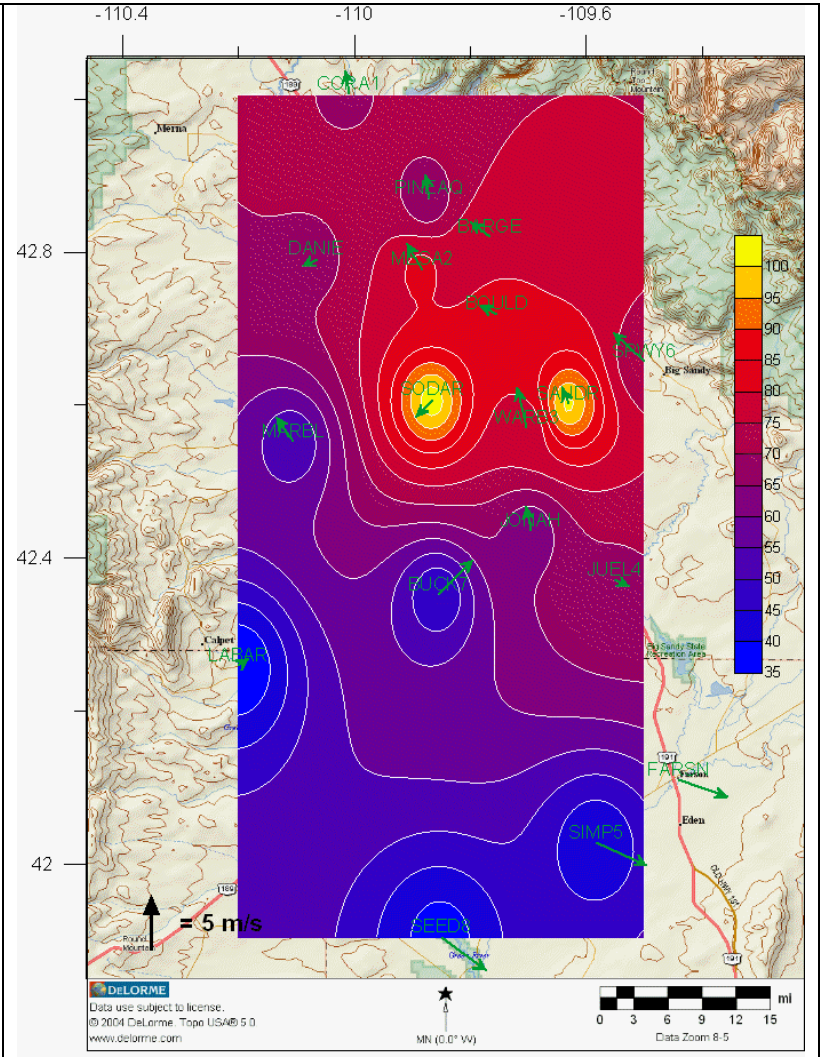


**Figure 4-27**. IOP 3.

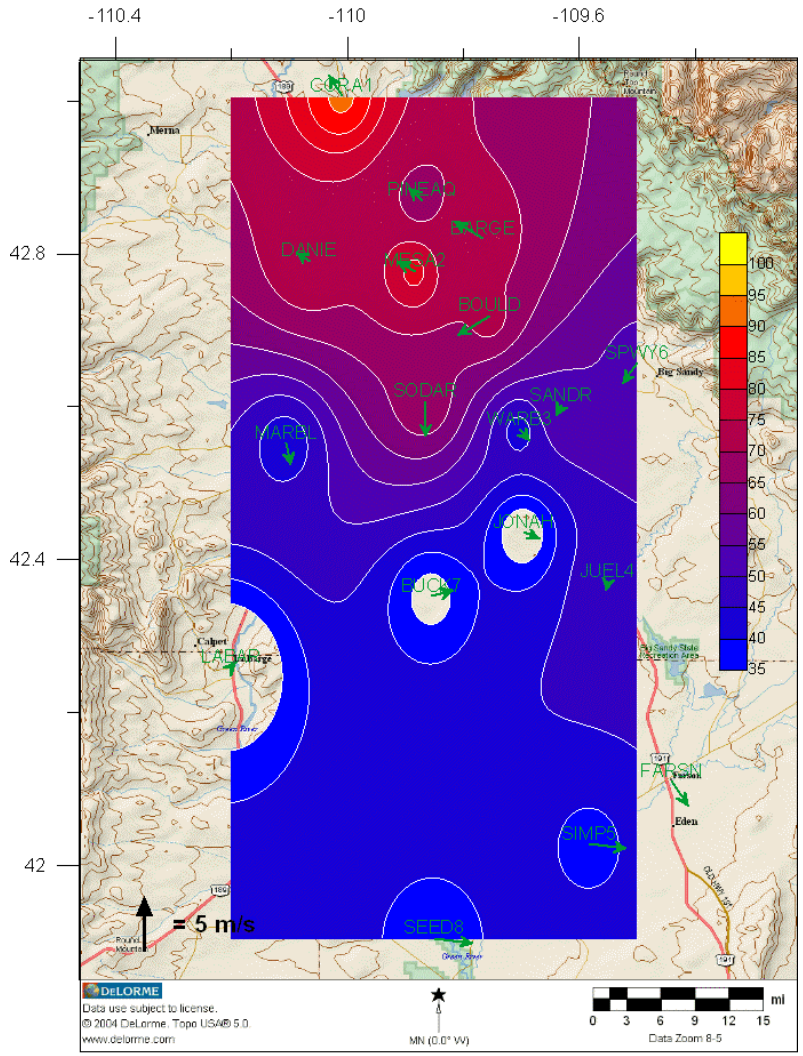


Resultant Winds and Ozone (ppb) - March 2, 2009 1600

**Figure 4-28**. IOP 3.

## 4.4 Conditions Aloft

### 4.4.1 Rawinsonde and Ozonesonde Data

Balloon-borne upper air soundings were launched from the Airport monitoring site (Wenz Field) during the two full-scale IOP field monitoring episodes of the UGWOS 2009 project (IOP 1 and IOP 3). A total of 27 soundings (16 rawinsondes, 11 ozonesondes) were launched during a total of seven operational days. Data recovery for all 27 upper air flights culminated at 6 km asl (approximately 18,700 feet asl).

Table 4-6 provides a summary of the dates and times of the upper air launches and also indicates the sky conditions existent during each flight. In addition, the comments section of the table indicates levels at which there were missing (msg.) data due to instrument malfunction (mostly loss of radio signal) and an estimation of the percent of the maximum sunshine observed at the time of the respective launches. Sky condition is important in that it provides an initial indication of solar insolation within the region. UV radiation from the sun is a critical factor for the formation of ozone, and cloud cover will therefore influence the potential for ozone generation.[2] In addition, sky cover observed in the field is a helpful indicator of the amount of solar energy at all wavelengths reaching the surface and thus the likely stability and mixing potential affecting the study area. In the Sky Condition column: "Few" indicates less than 10% cloud cover; "Sctrd". (scattered) is 10% to 50% cloud cover; "Brkn". (broken) stands for 51% to 99% coverage; and "Ovcst". (overcast) indicates 100% cloud cover. Only high and mid-level clouds affected the launch area during all of the upper air flights. Some lower cumulus (Cu) clouds were observed over the mountains to the east and west of the Green River Valley during March 3rd, but they did not affect insolation in the project area.

Only one flight experienced significant data loss due to instrument malfunction (radio signal loss), and that was the wen20413 flight launched at 1411 MST on Feb 4, 2009. The loss of the lower 359 meters of that flight made it difficult to determine the inversion base, but the loss was low enough to allow the determination of the top of the inversion. Virtually no reduction in IR solar radiation took place during the first IOP in early February. The same can be said for the first two days (February 28 and March 1) of the third IOP in early March. Some broken middle clouds may have reduced insolation a small amount during the morning of day three of the third IOP (March 2). The altostratus cloud deck continued to increase during the afternoon of that day resulting in totally obscuring the sun by the last sounding of the day. This loss of sunshine probably reduced surface heating during that afternoon, but may have prevented the trapping inversion from "burning" off. Sunshine was not obscured during the final IOP on March 3rd, but the sustained snow shower activity over all of the surrounding mountain ranges throughout the day indicated that the atmosphere had become much less stable.

[2] It should be noted that cloud configurations, such as scattered cumulus clouds, can result in enhancement of the amount of UV flux near the surface due to reflections from the sides of clouds.

**Table 4-6. R**awinsonde/ozonesonde Sky Conditions Summary (note: msg = missing value).

| Launch Date | Flight ID | Launch Time (mst) | Sky Conditions | Comments |
|---|---|---|---|---|
| 2/3/09 | wen20307 | 0754 | Few Ci/Cs | |
| 2/3/09 | wen20311 | 1110 | Few Ci/Cs | Lower 83 meters msg. |
| 2/3/09 | wen20314 | 1419 | Few -Cs | |
| 2/3/09 | wen20316 | 1717 | Few -Cs | Ozonesonde |
| 2/4/09 | wen20407 | 0722 | Sctrd. -Ci/Cs | Lower 50 meters msg. |
| 2/4/09 | wen20410 | 1028 | Sctrd. -Ci/Cs | |
| 2/4/09 | wen20413 | 1411 | Sctrd. -Ci/Cs | Ozonesonde; Lower 359 meters msg. |
| 2/4/09 | wen20416 | 1656 | Sctrd. -Ci/Cs | Ozonesonde |
| 2/5/09 | wen20507 | 0730 | Few Ac; Sctrd. -Ci; few lent. east | |
| 2/5/09 | wen20511 | 1124 | Sctrd. Ci/Cs | |
| 2/5/09 | wen20514 | 1430 | Sctrd. to Brkn. As; Brkn. -Ci/Cs | Ozonesonde; Sunshine ? 90% |
| 2/5/09 | wen20516 | 1654 | Sctrd. to Brkn. As; Brkn. Ci/Cs | Ozonesonde; Sunshine ? 70% |
| 2/28/09 | wen22811 | 1107 | Sctrd. Ci/Cs | |
| 2/28/09 | wen22814 | 1418 | Sctrd. high As; Sctrd. Ci/Cs | |
| 2/28/09 | wen22816 | 1629 | Sctrd. As; Sctrd. Ci/Cs; Brkn -Cs | Ozonesonde |
| 3/1/09 | wen30107 | 0736 | Sctrd. to Brkn. As; Brkn. -CS | Sunshine ? 90% |
| 3/1/09 | wen30111 | 1058 | Few As; Sctrd Ci/Cs; Brkn. -Cs | |
| 3/1/09 | wen30113 | 1329 | Few As; Sctrd Ci/Cs; Brkn. -Cs | Ozonesonde; Lower 67 meters msg. |
| 3/1/09 | wen30116 | 1634 | Sctrd. As; Sctrd Ci/Cs; Brkn. -Cs | Ozonesonde; Sunshine ? 90% |
| 3/2/09 | wen30207 | 0728 | Few AC/As; Brkn. As; Brkn. Cs | Sunshine ? 80% |
| 3/2/09 | wen30211 | 1036 | Sctrd. AC/As; Sctrd. Cs; Brkn. -Cs | Sunshine ? 90% |
| 3/2/09 | wen30213 | 1336 | Sctrd. to Brkn. As; Brkn. to Ovcst Cs | Ozonesonde; Sunshine ? 50% |
| 3/2/09 | wen30216 | 1623 | Brkn. As; Ovcst Cs | Ozonesonde; Sun obscurred |
| 3/3/09 | wen30307 | 0732 | Sctrd. Cu; Sctrd. Ac/As; Sctrd. Ci/Cs | Snowshowers obscuring only mtns. |
| 3/3/09 | wen30311 | 1037 | Sctrd. Cu; Sctrd. As; Sctrd. Ci | Snowshowers obscuring only peaks |
| 3/3/09 | wen30314 | 1404 | Sctrd. Cu over mountains: Sctrd. -Ci | No showers |
| 3/3/09 | wen30316 | 1600 | Sctrd. Cu over mountains: Sctrd. -Ci | Ozonesonde; Few showers over mtns. |

Table 4-7 presents a summary of the strength, depth and vertical location of temperature inversions measured by upper air balloon soundings run during UGWOS 2009 IOP field monitoring operations. The objective of this summary is to provide an all inclusive matrix overview of the stability characteristics of the boundary layer environment at and over the UGWOS Airport site during the two main IOP monitoring operations of 2009. Figure 4-29 presents a generalized diagram of key structural elements of a typical sounding. The inversion base temperature ("Inv. Base Temp") is the lowest temperature in the vertical temperature profile in the lower boundary layer. The peak inversion temperature ("Peak Inver. Temp") is the highest temperature recorded above the inversion base before temperatures begin to decrease with height. The inversion layer lapse rate ("Inv. Layer LR") is the rate of decrease with height based on the peak inversion temperature and the base inversion temperature and the difference in heights between the two, expressed as °C/100 meters. Note that for an inversion where temperatures are increasing with height, the value is negative. The more negative the value, the stronger the inversion. The inversion base height ("Inver. Base Hgt.") is the height, in meters above the ground level (mAGL), where the inversion base is located. The lower the base, the shallower the mixing layer (or stable layer) underneath. The inversion top height ("Inver. Top Hgt.") is the height of the highest temperature in the inversion. This level is also indicative of the thickness or depth of the stable layer. "WD/WS" are the wind direction (degrees) and wind speed (m/s) measured at the top of the inversion. "Peak Sonde O3" is the maximum ozone concentration detected by the ozonesonde during the sounding. "Peak O3 Hgt." is the height where the highest ozone concentration was measured.

**Table 4-7.** Rawinsonde/ozonesonde Data Summary.

| Launch Date | Launch Time (mst) | Inver. Base Temp (C°) | Peak Inver. Temp (C°) | Inv. Layer LR (C°/100m) | Inver. Base Hgt. (mAGL) | Inver. Top Hgt. (mAGL) | WD/WS (mps) | Peak Sonde O 3 (ppb) | Peak O3 Hgt. (mAGL) | Sodar Mixing Hgt. (m) |
|---|---|---|---|---|---|---|---|---|---|---|
| 2/3/09 | 0754 | -7.3 | -0.6 | -1.7 | 0 | 386 | 316/09 | NA | NA | >250 |
| 2/3/09 | 1110 | -2.5 | 1.8 | -2.1 | 0 | 202 | 310/09 | NA | NA | >250 |
| 2/3/09 | 1419 | -2.3 | -0.9 | -1.3 | 1200 | 1306 | 319/11 | NA | NA | >250 |
| 2/3/09 | 1717 | 0.5 | 2.1 | -0.8 | 319 | 509 | 314/09 | 46 | 124 | - |
| 2/4/09 | 0722 | -17.4 | 0.9 | -5.1 | 0 | 362 | 070/01 | NA | NA | 35 |
| 2/4/09 | 1028 | -12.5 | 1.4 | -1.7 | 29 | 833 | 209/02 | NA | NA | 75 |
| 2/4/09 | 1411 | -1.3 | 2.6 | -1.9 | 383 | 587 | 192/02 | 51 | 359 * | 90 |
| 2/4/09 | 1656 | -3.9 | 1.9 | -1.4 | 346 | 775 | 100/01 | 79 | 293 | 80 |
| 2/5/09 | 0730 | -18.9 | 0.4 | -3.8 | 0 | 511 | 180/04 | NA | NA | - |
| 2/5/09 | 1124 | -9.5 | 0.4 | -2.4 | 35 | 453 | 138/06 | NA | NA | 80 |
| 2/5/09 | 1430 | -3.8 | 0.4 | -1.2 | 66 | 410 | 132/06 | 66 | 271 | >250 |
| 2/5/09 | 1654 | -2.9 | 1.8 | -1.6 | 0 | 299 | 141/07 | 56 | 136 | 70 |
| 2/28/09 | 1107 | -14.9 | -6.1 | -2.4 | 110 | 478 | 308/04 | NA | NA | 120 |
| 2/28/09 | 1418 | -8.3 | -4.7 | -1.0 | 53 | 427 | 304/03 | NA | NA | 100 |
| 2/28/09 | 1629 | -7.0 | -2.9 | -2.3 | 190 | 368 | 333/04 | 52 & 71 | 103 & 1044 | 100 |
| 3/1/09 | 0736 | -11.7 | 1.1 | -2.6 | 19 | 519 | 048/02 | NA | NA | 35 |
| 3/1/09 | 1058 | -6.5 | 0.9 | -1.3 | 32 | 604 | 124/04 | NA | NA | 100 |
| 3/1/09 | 1329 | -2.1 | 2.0 | -0.9 | 111 | 567 | 151/03 | 67 | 130 | 110 |
| 3/1/09 | 1634 | -0.6 | 3.6 | -1.1 | 153 | 533 | 131/02 | 99 | 168 | >250 |
| 3/2/09 | 0728 | -9.3 | 3.7 | -2.4 | 0 | 534 | 220/05 | NA | NA | 50 |
| 3/2/09 | 1036 | -3.1 | 4.2 | -2.2 | 56 | 381 | 120/04 | NA | NA | 100 |
| 3/2/09 | 1336 | 1.6 | 4.8 | -1.1 | 179 | 476 | 201/03 | 83 | 233 | 90 |
| 3/2/09 | 1623 | 2.8 | 3.6 | -0.6 | 297 | 437 | 259/06 | 82 | 26 | >250 |
| 3/3/09 | 0732 | -1.8 | 3.8 | -2.7 | 0 | 204 | 220/09 | NA | NA | 40 |
| 3/3/09 | 1037 | 1.9 | 3.1 | -0.5 | 125 | 355 | 235/06 | NA | NA | >250 |
| 3/3/09 | 1404 | 7.1 | NA | NA | None | NA | 228/02 | NA | NA | >250 |
| 3/3/09 | 1600 | 7.0 | NA | NA | None | NA | 248/02 | 56 | 981 | >250 |

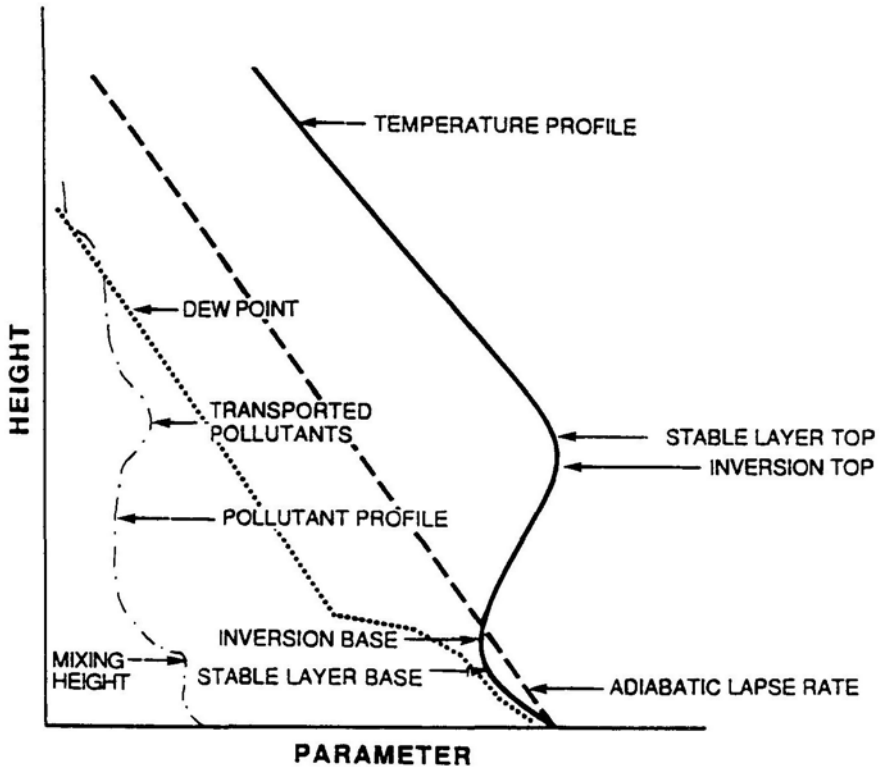


**Figure 4-29.** Key structural elements of a typical rawinsonde/ozonesonde sounding.

Consistent with the upper air data obtained during the 2008 study, mornings associated with episodic periods of increased ozone are characterized by strong surface-based inversions, and afternoons are characterized by moderate to strong elevated inversions with bases 150 to 400 meters above the ground. It is noteworthy that the rawinsonde measurements are consistent with the mixing height data obtained from the Sodar, presented in the final column of Table 4-7 and discussed in more detail in the following section. As shown in Figure 4-29, the mixing height should be similar to the base of the inversion. This is generally the case, with weaker inversions (lower lapse rates, typically between 0 and -2°C/100m) allowing some additional mixing above the inversion base.

Initial analysis of the upper air sounding results in Table 4-7 indicate that a mutual characteristic of the non-ozone days is low inversion lapse rates. Day one of both the first and third IOP showed this tendency. The main cause of this weak inversion characteristic is the lack of warmer air aloft. By the second and third days of both IOP's, the peak inversion temperature had increased by 2 to 3 C° in the first IOP and 6 to 8 C° during the second IOP. With warmer temperatures aloft, the nocturnal low-level inversions were stronger, as seen by the high lapse rates in the early morning soundings. Stronger inversions are more efficient in trapping overnight precursor emissions near the surface, and can be more persistent during the afternoon hours when surface heating is maximized. The influx of warmer air aloft is a characteristic of a post-anticyclonic synoptic weather pattern where the axis of a high pressure ridge is either over or slightly east of southwest Wyoming and subsidence associated with the ridge still persists in the area.

Comparing the height of the inversion bases between the two IOP's indicates that the bases were lower in the afternoon hours during the high ozone days of the second IOP as compared to the first IOP. This, along with the somewhat greater strength of the inversions during the second IOP, may account for the apparent greater ozone production measured during the second IOP.

Stability conditions characterized by the persistent strong low level inversions evident during the high ozone days of both IOP's, deteriorated rapidly during the last day of the second IOP, and to a lesser degree in the first IOP. However, mechanical mixing due to increased wind speeds was also a factor in reducing ozone production on Feb 5$^{th}$. Clearly, the end of the ozone episode during the last IOP would have occurred regardless of wind speeds as the thermodynamic characteristics of the boundary layer became definitively well mixed. By the afternoon of March 3$^{rd}$, there were no inversions detected by the balloon soundings and previously trapped emissions were free to dilute in an unlimited mixing layer. This was the result of the arrival of an approaching weather system.

Measured winds at the surface, in the lower boundary layer and at the synoptic scale level just above the lower layer, have been important indicators of the likely ozone impacts in the Upper Green River Basin in the past. With this in mind, a summary of the winds at those critical levels measured by the UGWOS 2009 ozonesonde and rawinsonde soundings are provided in Table 4-8. The table presents the wind directions ("WD") and wind speeds ("WS") recorded at the UGWOS Airport Meteorological Site (Surface) and by the balloon soundings in the lower boundary layer ("Lower Bound. Layer") and at the 700 mb constant pressure level (approximately 3 km above ground level). The winds that are presented as representative of the lower boundary layer were computed from the sonde-measured values recorded from the first reading above the ground to the top of the temperature inversion. Ozone and inversion top information were extracted from previous tables in this report and are included here to provide

reference values so that the winds at the critical levels can be compared under the various stability and ozone impact regimes.

Ozonesonde vertical profiles for the two IOPs are shown in Figures 4-30 and 4-31. The dominant feature during both IOPs is the presence of an elevated layer(s) of higher ozone concentrations typically at 100 to 300 meters AGL. These are plumes decoupled from the surface boundary layer. Processes that can lead to this layering include ozone generated aloft rather than at the surface due to the buoyant nature of many of the precursor sources, strong mechanical turbulence either locally or owing to the complex terrain that encompasses the Pinedale anticline, or transport of ozone from upwind areas that has been depleted in the lowest layers due to titration by fresh NO emissions.

To further provide points of comparison, Figures 4-32 and 4-33 presents plots from two late afternoon ozonesondes that were run during the third IOP on February 28, 2009 and March 1, 2009 respectively. The first sounding was launched at 1629 MST on the first day of first IOP, when only background level ozone concentrations were detected both at the ground and aloft. The second ozonesonde was run at 1634 MST during the middle two-day period of the IOP when higher concentrations of ozone were measured both at the ground and aloft within the mixing layer. Note that winds in the mixing layer and above tended to be northwesterly at speeds around 3 m/s in the mixing layer and greater than 9 m/s at the synoptic flow level during February 28$^{th}$. On March 1$^{st}$, winds near the surface were very light northwesterly, but averaged southwesterly at around 2.5 m/s within most of the mixing layer. In addition, winds above the mixing layer were southwesterly.

The presence of elevated ozone layers is for the most part consistent with findings from the 2008 study, though during 2008 there were cases where the ozone “plume” impacted the surface. This is due to differences in meteorology, affecting both the general location of the plume and the mixing conditions near the surface. In 2008, plumes were frequently located in the Boulder area, easily impacting Wenz Field and the ozonesonde measurements. In contrast, the plumes identified during 2009 were positioned more to the west, closer to the Sodar site. Thus, the ozonesondes at Wenz Field were only seeing the very edge of the plume. In addition, the temperature and humidity profiles during 2009 are consistent with an elevated layer, whereas profiles in 2008 associated with high surface concentrations allowed for better mixing immediately above the surface. This is shown in a comparison of ozonesonde data from two early March high ozone days, one in 2008 and one in 2009 (Figure 4-34). Both days had an elevated ozone layer near the surface but a key difference as evidenced by the temperature profile and wind shear is the higher mixing height in 2009 which resulted in ozone mixing through a deeper layer and consequently lower surface ozone concentration.

**Table 4-8.** Significant Wind Layers.

| Launch Date | Launch Time (mst) | Surface O3 (ppb) | Peak O3 (ppb) | Peak O3 Hgt. (mAGL) | Inver. Top Hgt. (mAGL) | Surface | | Lower Bound. Layer | | 700 mb | |
|---|---|---|---|---|---|---|---|---|---|---|---|
| | | | | | | WD (deg) | WS (m/s) | WD (deg) | WS (m/s) | WD (deg) | WS (m/s) |
| 2/3/09 | 0754 | 39 | NA | NA | 386 | 298 | 4.9 | 311 | 11.1 | 331 | 13.8 |
| 2/3/09 | 1110 | 46 | NA | NA | 202 | 305 | 6.5 | 314 | 9.8 | 325 | 12.2 |
| 2/3/09 | 1419 | 46 | NA | NA | 1306 | 300 | 2.5 | 320 | 9.4 | 331 | 8.8 |
| 2/3/09 | 1717 | 37 | 46 | 124 | 509 | 120 | 1.2 | 254 | 3.8 | 331 | 5.5 |
| 2/4/09 | 0722 | 29 | NA | NA | 362 | 316 | 2.7 | 057 | 3.7 | 267 | 6.4 |
| 2/4/09 | 1028 | 43 | NA | NA | 833 | 274 | 1.4 | 172 | 1.9 | 242 | 4.6 |
| 2/4/09 | 1411 | 59 | 51 | 359 | 587 | 025 | 0.8 | 142 | 2.6 | 263 | 4.0 |
| 2/4/09 | 1656 | 58 | 79 | 293 | 775 | 315 | 1.0 | 174 | 2.2 | 006 | 1.3 |
| 2/5/09 | 0730 | 28 | NA | NA | 511 | 302 | 1.6 | 178 | 3.2 | 220 | 3.1 |
| 2/5/09 | 1124 | 49 | NA | NA | 453 | 285 | 0.9 | 171 | 4.1 | 213 | 6.1 |
| 2/5/09 | 1430 | 61 | 66 | 271 | 410 | 132 | 0.7 | 134 | 3.5 | 228 | 5.2 |
| 2/5/09 | 1654 | 54 | 56 | 136 | 299 | 025 | 0.5 | 139 | 4.5 | 215 | 8.4 |
| 2/28/09 | 1107 | 54 | NA | NA | 478 | 295 | 0.9 | 272 | 2.4 | 295 | 7.9 |
| 2/28/09 | 1418 | 60 | NA | NA | 427 | 269 | 1.8 | 311 | 2.6 | 287 | 9.6 |
| 2/28/09 | 1629 | 59 | 52 & 71 | 103 &1044 | 368 | 325 | 1.1 | 310 | 2.8 | 298 | 9.3 |
| 3/1/09 | 0736 | 41 | NA | NA | 519 | 286 | 1.0 | 201 | 2.5 | 257 | 7.9 |
| 3/1/09 | 1058 | 59 | NA | NA | 604 | 072 | 0.7 | 156 | 3.0 | 273 | 5.4 |
| 3/1/09 | 1329 | 76 | 67 | 130 | 567 | 330 | 1.2 | 189 | 2.2 | 241 | 4.5 |
| 3/1/09 | 1634 | 77 | 99 | 168 | 533 | 335 | 1.5 | 243 | 2.5 | 262 | 3.3 |
| 3/2/09 | 0728 | 41 | NA | NA | 534 | 309 | 3.1 | 215 | 3.1 | 221 | 1.9 |
| 3/2/09 | 1036 | 53 | NA | NA | 381 | 095 | 0.4 | 164 | 3.1 | 290 | 0.2 |
| 3/2/09 | 1336 | 70 | 83 | 233 | 476 | 355 | 0.5 | 233 | 2.2 | 226 | 3.4 |
| 3/2/09 | 1623 | 84 | 82 | 26 | 437 | 241 | 0.6 | 179 | 3.7 | 244 | 2.8 |
| 3/3/09 | 0732 | 22 | NA | NA | 204 | 150 | 1.8 | 177 | 4.9 | 249 | 15.7 |
| 3/3/09 | 1037 | 46 | NA | NA | 355 | 119 | 2.5 | 167 | 3.1 | 241 | 9.2 |
| 3/3/09 | 1404 | 49 | NA | NA | NA | 209 | 3.0 | 224 | 8.0 | 225 | 9.7 |
| 3/3/09 | 1600 | 60 | 56 | 981 | NA | 239 | 2.5 | 233 | 12.7 | 235 | 15.6 |

Examination of the results depicted in Table 4-8 indicate that winds at the surface, in the mixing layer and in the synoptic flow aloft, tended to be moderate to strong northwesterly during the initial days of both UGWOS 2009 IOP's. Ozone concentrations remained at background levels during those days, as was the case during most of the other non-IOP days during the three-month field monitoring phase of UGWOS 2009. During the days of higher detected ozone concentrations, wind speeds at all levels were lighter, and directions tended to be southwesterly above the mixing layer and somewhat variable with a tendency to be southerly within the mixing layer. Winds at and near the surface tended to be northwesterly during most mornings with light speeds during the higher ozone days and stronger velocities on non-ozone days. Mixing layer wind directions during the afternoons of the ozone days of the first IOP tended to be southeasterly while afternoon mixing layer winds during the last IOP had a somewhat more southwesterly component. Without comprehensive mapping of the ozone plumes during the primary ozone days during both IOP's, it is difficult to determine whether the differences in ozone concentrations at and above the Airport Site were due to transport patterns or dilution. Since the highest ozone concentrations detected by the ozonesondes were above the ground in all cases except one, it is possible that higher concentrations of ozone were not well detected at the UGWOS 2009 surface sites because the ozone plumes were elevated and passed above the surface sites. The table also indicates that wind speeds aloft were on the increase during the final day of each IOP. In addition, wind directions tended to be southwesterly at the synoptic flow heights indicating the approach of broad scale troughing and a well-mixed air mass.

Particularly noteworthy is that, as in the 2008 study, there is no evidence of direct stratospheric intrusion of ozone contributing to the episodic boundary layer ozone. Graphical depictions of all of the upper air balloon soundings showing the vertical temperature, humidity, winds and ozone profiles are available as plots in Appendix C of this report.

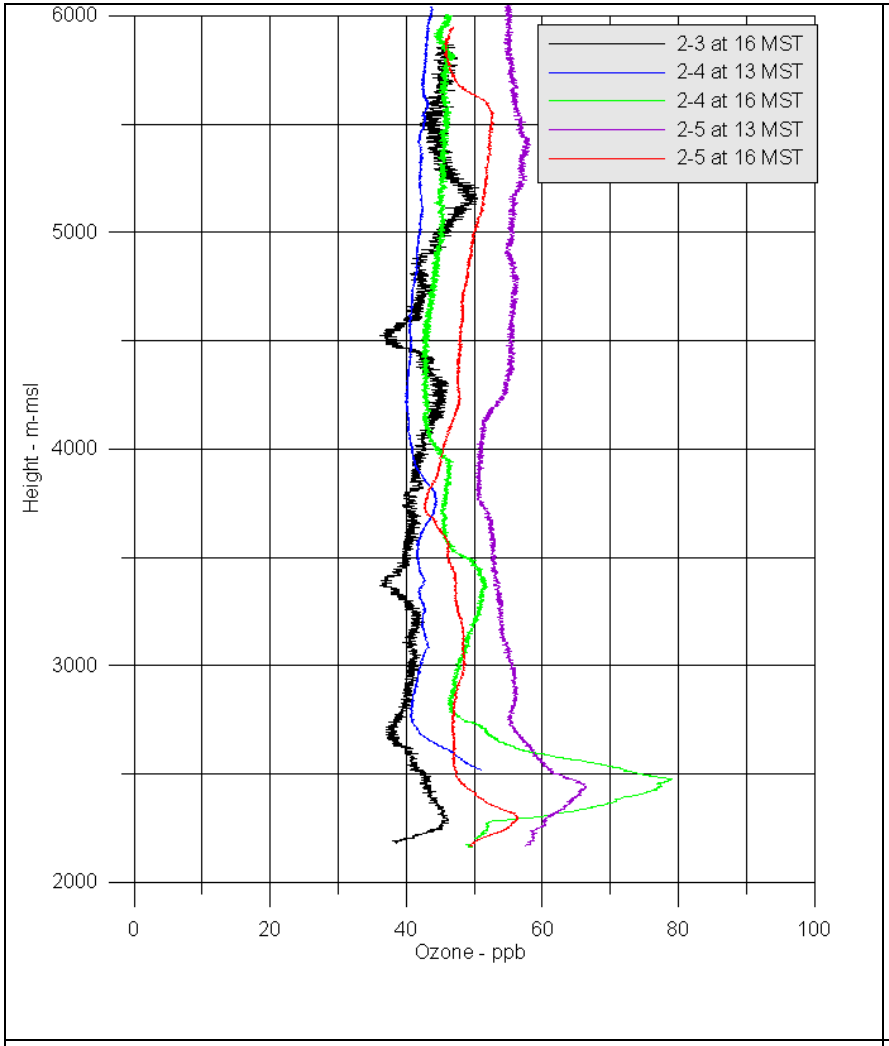


**Figure 4-30.** Ozonesonde profiles – IOP 1.

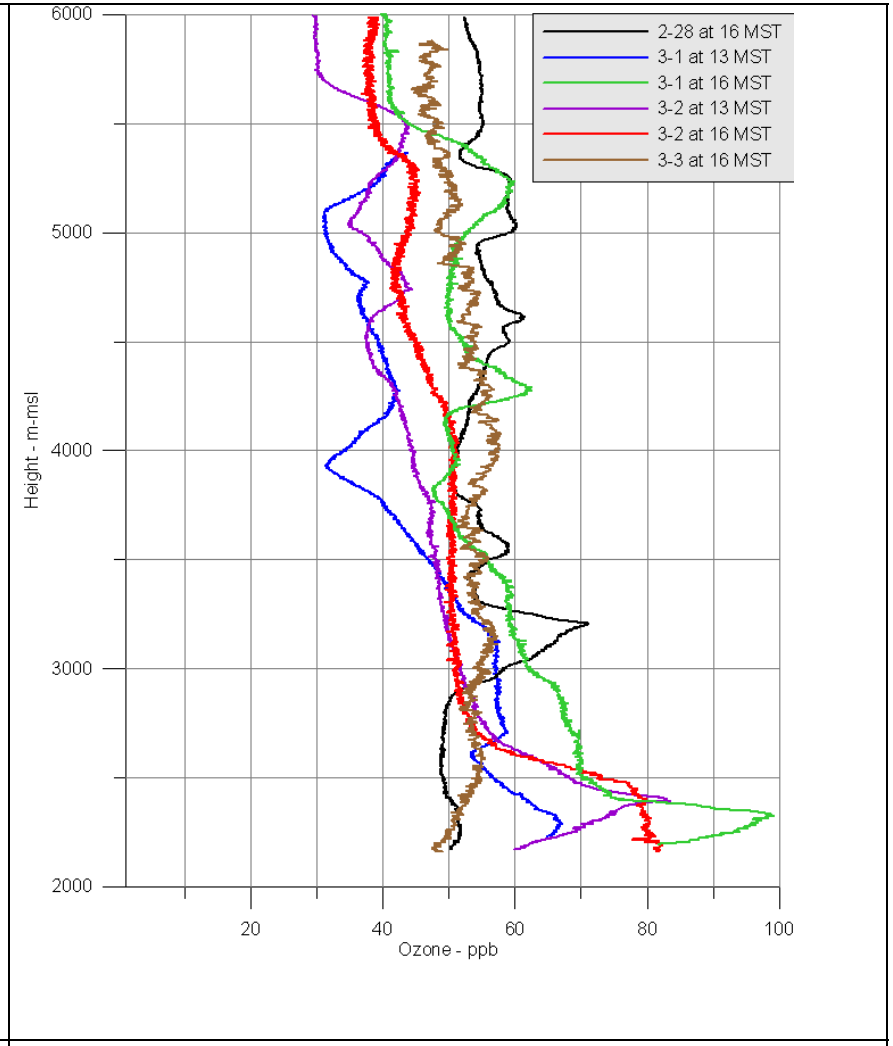


**Figure 4-31**. Ozonesonde profiles – IOP 3.

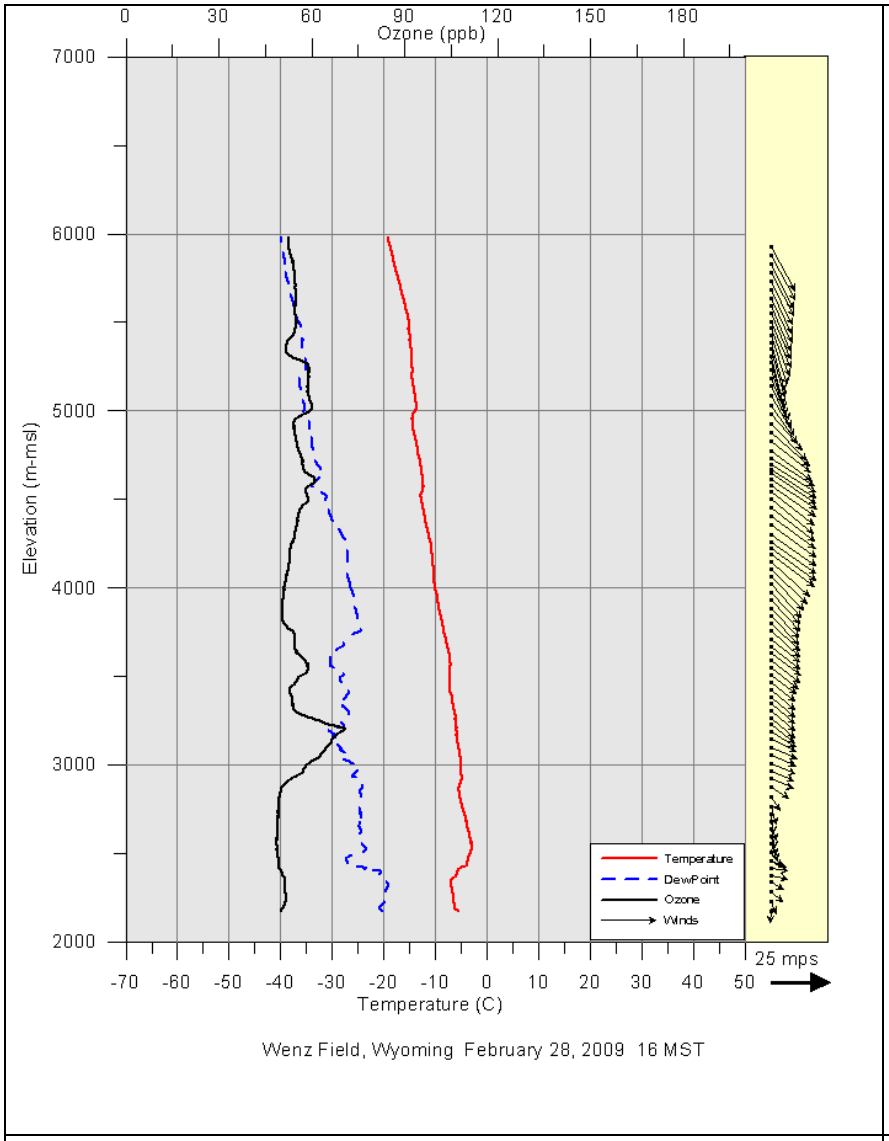


**Figure 4-32.** February 28 sounding – 16 MST.

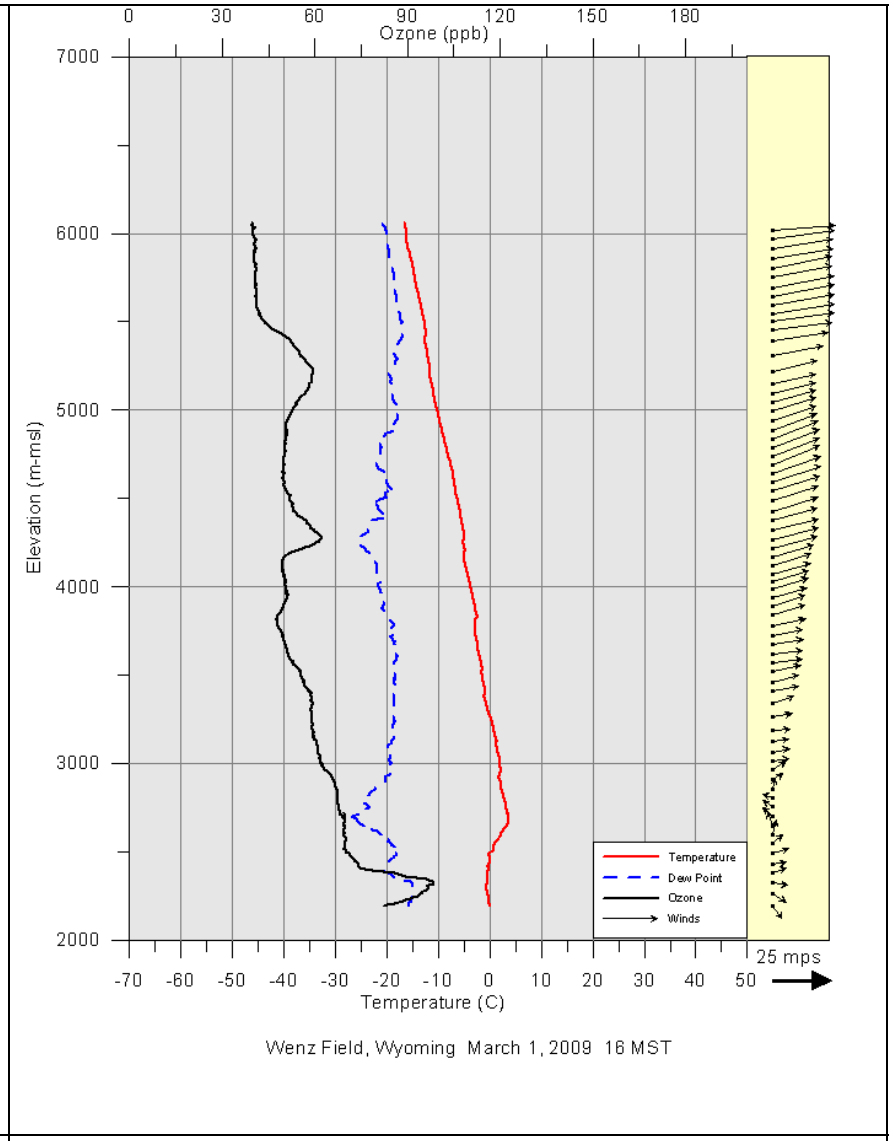


**Figure 4-33.** March 1 sounding – 16 MST.

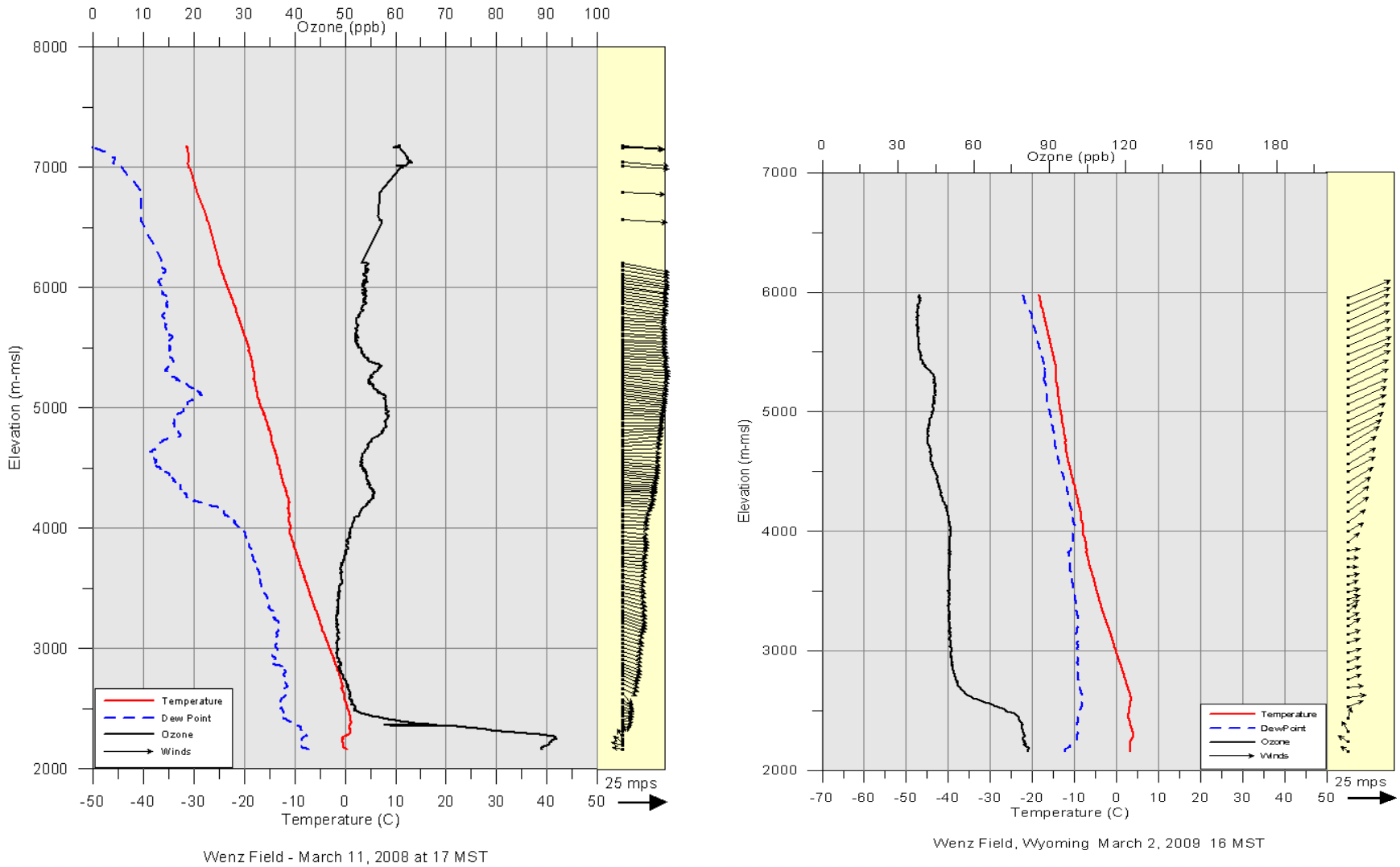


**Figure 4-34.** Comparison of late afternoon ozonesondes from 11 March 2008 (left) with 2 March 2009 (right). Note the different horizontal ozone scales

### 4.4.2 Analysis of miniSODAR™ Data

The miniSODAR™ (Sodar) produces a number of metrics that are potentially useful for identifying conditions leading to high surface ozone concentrations. As with the 2008 study, the most relevant data obtained from the Sodar were the mixing heights estimated from the Sodar's facsimile data. Figure 4-35 is the facsimile chart for March 2, 2009, the day that 8-hr ozone concentrations greater than 75 ppb were recorded at the Sodar site.

Table 4-9 summarizes key metrics obtained from the Sodar data relevant to conditions leading to high ozone - in this case specifically ozone measured at the Sodar site. These metrics include the following:

- Median mixing height – The median mixing height is reported for four periods: "AM" referring to midnight to noon, "PM" referring to noon to midnight, "Morning", referring to hours 0600 through 1100, and "Afternoon", referring to hours 1200 through 1700. Each of these periods can potentially play a role in determining the occurrence and duration of an ozone event. Because reported mixing heights of 250m actually mean greater than 250m, it is more appropriate to look at the median rather than the mean when summarizing the mixing heights.
- 30-meter winds – Winds measured by the Sodar at 30 meters are presented as being representative conditions within the mixed layer, while still being largely unaffected by the surface terrain. Winds are presented for two periods: 0600 – 1200 (morning) during which ozone precursors are likely accumulating, and 1200 – 1800 (afternoon), the period when higher concentrations were typically observed.
- UV radiation – While not measured specifically at the Sodar site, UV radiation reported from the Boulder site is presented due to its role in creating ozone and its indirect relationship with the reported mixing height. Observations during both the 2007 and 2008 studies showed that a lack of snow cover resulted in daytime heating of the surface due to absorbed solar radiation, causing thermal mixing and increased mixing heights. Outgoing UV radiation provided the only direct measurement of reflected radiation. While there were likely periods with differences between the actual snow cover at the Boulder and Sodar sites, the measurements are sufficiently representative of regional conditions during periods of extensive snow cover and very little snow cover to allow a comparison. Total Watt-hours per meter squared are presented for both incoming and outgoing (reflected) radiation.

Within the table, days of higher ozone concentration have been highlighted, with hourly averages greater than 60 ppb highlighted in yellow, and 8-hour averages greater than 60 ppb highlights in orange. Review of these data show that higher concentrations typically occur when the following conditions are met:

- AM mixing heights are less than or equal to 60 meters. This is indicative of very stable conditions that trap surface emissions during the morning. As shown in Figure 4-35, these low reported mixing heights are frequently just one layer of a multi-layered stratification of the air within the first 250 meters of the surface.
- Surface wind directions are from the northeast, the direction of significant local sources associated with drilling and production on the Mesa.

- Surface wind speeds are less than 2 m/s, typically both in the morning and the afternoon. This is further indication of the stable, stagnant conditions necessary for keeping precursor emissions within the area. Mixing heights inevitably rise to greater than 250 meters whenever average winds exceed 2.5 m/s.
- Median afternoon mixing heights are typically greater than 100 m. The ozonesonde data discussed above showed the highest ozone concentrations located significantly above the surface, typically at an altitude of 100 meters AGL. Since NOx is emitted in the heated exhaust of combustion sources, plume rise may result in the NOx accumulating to some extent at the top of the stable layer. These higher mixing heights may be a necessary mechanism for entraining higher concentrations from these layers aloft to the surface although a causal relationship between elevated ozone and afternoon mixing heights exceeding 100 m is not a given.
- Reflected UV radiation is at least 50% of the incoming UV radiation. This value is a direct result of the amount of snow on the surface. As mentioned in the 2008 report, this is important for two reasons. First, the UV data provide an indication of the overall radiation albedo. With more solar radiation reflected than absorbed, surface heating remains minimal, allowing strong stable conditions to persist in the mornings and precursor concentrations to accumulate. Reflected radiation rapidly decreases in mid March, and by March 17 values indicate a basically snowless surface. Nevertheless, low mixing heights are observed on March 19 and 20. These low mixing heights again correspond to low wind speeds, which are unique to this snowless period, implying that low wind speeds are the dominant condition needed for low mixing heights. Second, since UV radiation is a necessary requirement for ozone production, the reflected UV radiation effectively increases the amount of radiation available for ozone forming reactions. Data on March 19 and 20 appear to support this second reason. Conditions on these days meet those outlined above, with the exception of very little reflected radiation, apparently resulting in little ozone production. We note, however, that the UV albedo data are only representative of snow cover over a small area directly under the instrument at Boulder.

With the conditions outlined above in mind, it is useful to look at the IOP periods in detail. IOP 3 resulted in the highest ozone concentrations of the study, with an 8-hr ozone concentration greater than 75 ppb reported at the Sodar site on March 2 and just under 75 ppb on March 1. The average afternoon wind speed on March 2 is notably higher than 2 m/s, but this is due to a rapid increase in wind speed near the end of the period that ultimately flushed out the region and ended the ozone episode. Conditions during IOP 2 in late February were very similar to those during IOP 3, with an 8-hr ozone concentration of 73 ppb reported at the Sodar site. Both IOPs had favorable conditions over a 3-day period, with gradually increasing ozone concentration over the course of their respective periods. In contrast, ozone concentrations during the first IOP in early February, while showing increases above background, never developed to the higher 8-hour averages observed during IOP 2 and IOP 3.

As mentioned above in previous sections, one possible reason for the lack of elevated ozone concentrations during IOP 1 is a reduction in potential emissions of precursors that could have resulted from the voluntary reduction in exploration and production activities implemented by the energy companies during this period. Meteorology may also have contributed to the lower than expected concentrations, and the Sodar provides valuable data for investigating this

possibility. Figure 4-36 presents a side-by-side comparison of Sodar wind data from the surface to 100 meters AGL for IOP 1 and IOP 3. Data recovery for levels greater than 100 meters drops significantly below 75%, and the data in the first 100 meters is in any case the most important, as evidenced by the low mixing heights common to the IOPs. Wind roses are plotted for February 4 through 5 and March 1 through 2 for IOPs 1 and 3, respectively.

Review of the two periods shows many similarities. Wind speeds are predominantly less than 2 m/s and frequently from the northeast. Note again the existence of higher wind speeds during IOP 3, which again occurred at the end of the period. However, there are some notable differences that may explain the higher ozone concentrations during IOP 3. First, there is a high percentage of winds from the NNE during IOP 3 – a direct path from the sources on the Mesa. In contrast, winds during IOP 1 have a more predominant easterly component, and thus ozone precursors may not have been as available during IOP 1. In addition, IOP 1 has a greater percentage of wind speeds less than 1 m/s, particularly for the three levels closest to the surface. This again brings up the possibility introduced above that the air during IOP 1 may have been too stable to allow the entrainment of pollutants collected aloft. This is further supported by the low mixing heights that prevailed into the afternoon on February 4 and 5, whereas afternoon mixing heights on March 1 and 2, as well as February 23, were much higher.

Review of the early January data provides further hints that sufficient afternoon mixing (at least at the Sodar site) may be an important mechanism for high surface ozone. The period of January 16 through 22 is dominated by low surface winds from the northeast and low AM mixing heights. However, similar to IOP 1, the afternoon mixing heights remain low. While the lack of significant ozone production during this period may be due to low UV radiation, a noticeable increase in ozone is noted on the day when the median afternoon mixing height increases to greater than 250 meters.

The Sodar data has other data that have a potential of providing information regarding mixing, specifically the vertical wind speed (w) and the standard deviation of the vertical wind speed (sigma w). The use of these data was explored for this report, but no noticeable differences between ozone episodic and non-episodic days were readily noted. Further review of these data and a more in-depth analysis may provide useful information.

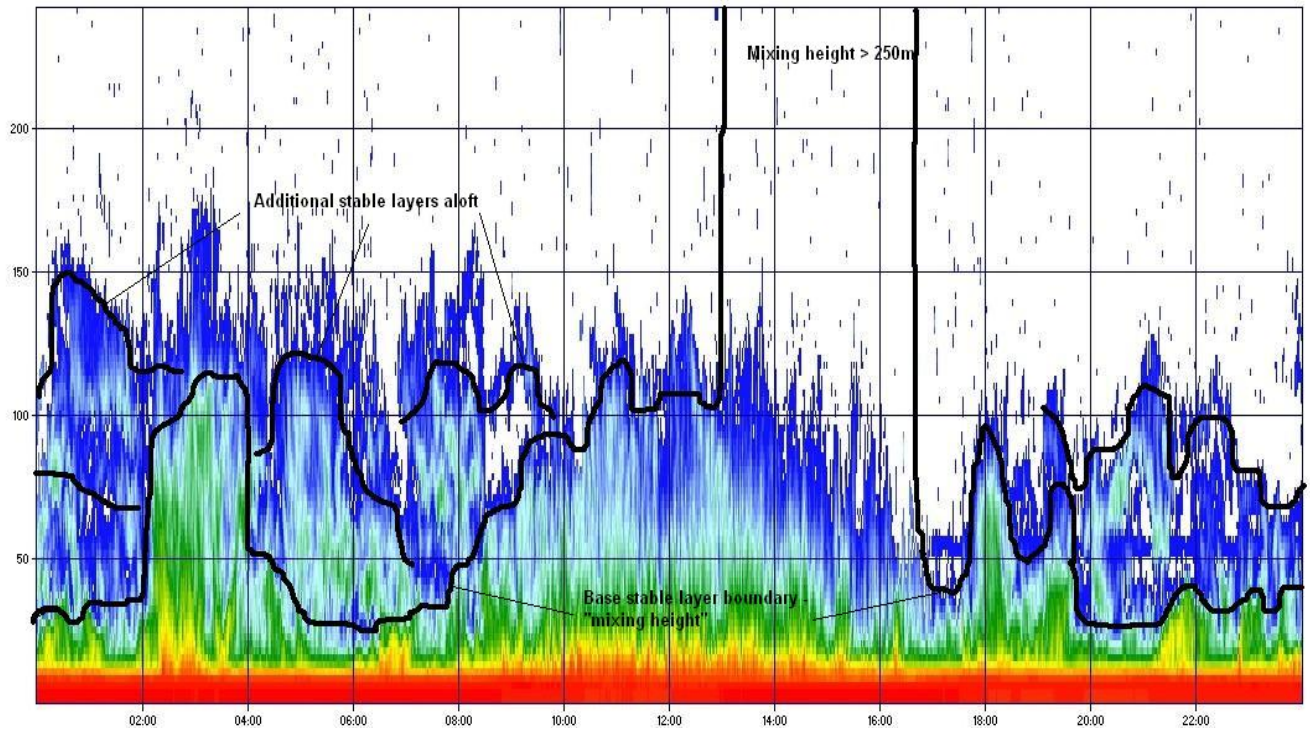


**Figure 4-35**. March 1, 2009 facsimile display.

**Table 4-9.** Summary of miniSodar data, Boulder UV measurements and maximum ozone concentrations at the Sodar site.

| | Median Mixing Height (m) | | | | 30-m Vector Winds (m/s) | | | | UV (W-hr/m$^2$) | | Peak Ozone (ppb) | |
|---|---|---|---|---|---|---|---|---|---|---|---|---|
| Date | AM | Mornng | PM | Afternoon | Morning WS | Morning WD | After. WS | After. WD | Incoming | Outgoing | 1-hr avg | 8-hr avg |
| 1/15/2009 | 250 | 250 | 250 | 250 | 7.34 | 319 | 8.62 | 309 | 176 | 144 | 39 | 37 |
| 1/16/2009 | 105 | 95 | 250 | 88 | 1.96 | 35 | 1.34 | 41 | 174 | 145 | 63 | 44 |
| 1/17/2009 | 100 | 100 | 75 | 115 | 1.28 | 33 | 1.24 | 83 | 178 | 144 | 60 | 45 |
| 1/18/2009 | 53 | 100 | 90 | 100 | 1.23 | 336 | 1.8 | 32 | 156 | 129 | 57 | 41 |
| 1/19/2009 | 65 | 63 | 43 | 250 | 1.37 | 23 | 1.26 | 72 | 184 | 151 | 64 | 51 |
| 1/20/2009 | 60 | 45 | 50 | 85 | 1.16 | 41 | 0.98 | 87 | 182 | 150 | 55 | 43 |
| 1/21/2009 | 40 | 48 | 70 | 95 | 1.06 | 45 | 1.01 | 103 | 185 | 150 | 53 | 43 |
| 1/22/2009 | 40 | 43 | 90 | 90 | 1.35 | 37 | 0.81 | 97 | 156 | 126 | 38 | 32 |
| 1/23/2009 | 143 | 250 | 250 | 250 | 2.01 | 288 | 4.97 | 329 | 171 | 142 | 37 | 36 |
| 1/24/2009 | 40 | 50 | 163 | 250 | 1.18 | 12 | 1.23 | 74 | 121 | 98 | 35 | 29 |
| 1/25/2009 | 50 | 63 | 250 | 250 | 1.02 | 354 | 2.47 | 163 | 111 | 107 | 30 | 29 |
| 1/26/2009 | 250 | 250 | 50 | 250 | 3.02 | 199 | 1.67 | 210 | 194 | 189 | 36 | 33 |
| 1/27/2009 | 250 | 250 | 250 | 250 | 12.39 | 310 | 8.21 | 327 | 202 | 204 | 44 | 42 |
| 1/28/2009 | 50 | 58 | 250 | 250 | 2.21 | 278 | 8.29 | 295 | 214 | 202 | 44 | 43 |
| 1/29/2009 | 250 | 250 | 250 | 250 | 1.98 | 327 | 7.57 | 325 | 226 | 208 | 44 | 42 |
| 1/30/2009 | 250 | 250 | 250 | 250 | 6.1 | 312 | 6.14 | 304 | 236 | 192 | 45 | 43 |
| 1/31/2009 | 75 | 75 | 175 | 90 | 1.33 | 38 | 1.25 | 59 | 218 | 182 | 65 | 53 |
| 2/1/2009 | 60 | 60 | 250 | 88 | 1.78 | 273 | 2.07 | 312 | 222 | 185 | 45 | 42 |
| 2/2/2009 | 250 | 250 | 250 | 250 | 2.55 | 254 | 3.78 | 332 | 225 | 180 | 45 | 43 |
| 2/3/2009 | 250 | 250 | 88 | 250 | 6.46 | 320 | 2.87 | 250 | 229 | 177 | 44 | 42 |
| 2/4/2009 | 55 | 58 | 78 | 95 | 1.41 | 41 | 1.03 | 90 | 236 | 180 | 81 | 61 |
| 2/5/2009 | 60 | 60 | 70 | 75 | 1.08 | 44 | 1.03 | 84 | 218 | 168 | 76 | 57 |
| 2/6/2009 | 75 | 80 | 250 | 250 | 1.58 | 19 | 3.79 | 315 | 206 | 148 | 56 | 49 |
| 2/7/2009 | 95 | 100 | 70 | 75 | 1.62 | 38 | 1.32 | 79 | 229 | 184 | 66 | 57 |
| 2/8/2009 | 60 | 73 | 78 | 68 | 1.51 | 1 | 1.38 | 46 | 173 | 126 | 50 | 44 |
| 2/9/2009 | 165 | 70 | 250 | 75 | 1.29 | 298 | 1.65 | 27 | 181 | 176 | 54 | 43 |
| 2/10/2009 | 250 | 250 | 250 | 250 | 2.81 | 331 | 9.59 | 314 | 254 | 205 | 44 | 41 |
| 2/11/2009 | 68 | 68 | 50 | 50 | 1.07 | 39 | 1.35 | 74 | 237 | 180 | 46 | 42 |
| 2/12/2009 | 68 | 70 | 45 | 250 | 1.14 | 35 | 1.29 | 78 | 260 | 207 | 54 | 46 |
| 2/13/2009 | 40 | 68 | 43 | 250 | 1.57 | 37 | 1.94 | 47 | 267 | 210 | 69 | 50 |
| 2/14/2009 | 70 | 70 | 250 | 160 | 1.48 | 325 | 1.59 | 352 | 231 | 196 | 57 | 51 |
| 2/15/2009 | 65 | 65 | 58 | 250 | 1.25 | 49 | 2.16 | 123 | 274 | 218 | 65 | 49 |
| 2/16/2009 | 48 | 68 | 250 | 250 | 1.34 | 52 | 1.49 | 72 | 241 | 184 | 61 | 54 |
| 2/17/2009 | 250 | 250 | 250 | 250 | 4.25 | 291 | 1.59 | 316 | 138 | 192 | 51 | 48 |
| 2/18/2009 | 90 | 83 | 250 | 250 | 1.25 | 25 | 7.31 | 304 | 222 | 259 | 49 | 45 |
| 2/19/2009 | 250 | 250 | 250 | 250 | 2.35 | 267 | 7.02 | 318 | 272 | 260 | 46 | 44 |
| 2/20/2009 | 50 | 90 | 250 | 250 | 0.91 | 47 | 9.65 | 310 | 289 | 255 | 49 | 45 |
| 2/21/2009 | 95 | 190 | 88 | 250 | 2.09 | 18 | 2.05 | 76 | 301 | 256 | 67 | 57 |
| 2/22/2009 | 53 | 53 | 50 | 163 | 1.67 | 35 | 1.68 | 101 | 239 | 197 | 71 | 57 |
| 2/23/2009 | 40 | 75 | 250 | 250 | 1.32 | 303 | 1.87 | 71 | 254 | 198 | 83 | 73 |
| 2/24/2009 | 250 | 250 | 250 | 250 | 4.8 | 247 | 4.99 | 278 | 215 | 175 | 53 | 40 |
| 2/25/2009 | 68 | 73 | 250 | 250 | 1.54 | 25 | 3.25 | 348 | 272 | 203 | 41 | 24 |
| 2/26/2009 | 250 | 250 | 250 | 250 | 2.42 | 62 | 8.35 | 238 | 260 | 219 | 45 | 44 |
| 2/27/2009 | 250 | 250 | 250 | 250 | 8.34 | 320 | 9.03 | 304 | 346 | 302 | 46 | 44 |
| 2/28/2009 | 188 | 123 | 78 | 125 | 1.63 | 34 | 1.64 | 75 | 344 | 297 | 68 | 61 |
| 3/1/2009 | 60 | 73 | 68 | 250 | 1.29 | 46 | 2 | 44 | 335 | 278 | 85 | 73 |
| 3/2/2009 | 60 | 88 | 250 | 135 | 1.4 | 34 | 3.51 | 15 | 270 | 216 | 103 | 76 |
| 3/3/2009 | 250 | 70 | 250 | 250 | 3 | 259 | 9.05 | 230 | 331 | 239 | 51 | 47 |
| 3/4/2009 | 250 | 250 | 250 | 250 | 4.34 | 258 | 7.33 | 253 | 272 | 153 | 51 | 49 |
| 3/5/2009 | 250 | 250 | 250 | 250 | 11.4 | 262 | 9.86 | 261 | 306 | 173 | 49 | 49 |
| 3/6/2009 | 100 | 175 | 250 | 250 | 2.94 | 109 | 5.61 | 265 | 276 | 153 | 48 | 47 |
| 3/7/2009 | 95 | 205 | 250 | 250 | 3.86 | 337 | 9.53 | 330 | 352 | 196 | 53 | 50 |
| 3/8/2009 | 250 | 250 | 250 | 250 | 5.16 | 189 | 8.53 | 265 | 311 | 158 | 53 | 50 |
| 3/9/2009 | 250 | 250 | 250 | 250 | 2.37 | 6 | 1.55 | 109 | 279 | 201 | 55 | 52 |
| 3/10/2009 | 250 | 250 | 250 | 250 | 4.68 | 267 | 5.25 | 297 | 338 | 241 | 50 | 48 |
| 3/11/2009 | 95 | 103 | 250 | 250 | 1.3 | 67 | 1.41 | 108 | 366 | 256 | 60 | 55 |
| 3/12/2009 | 105 | 138 | 250 | 250 | 1.05 | 44 | 4.21 | 345 | 379 | 246 | 64 | 54 |
| 3/13/2009 | 105 | 105 | 158 | 250 | 1.24 | 88 | 1.69 | 90 | 380 | 221 | 64 | 60 |
| 3/14/2009 | 55 | 115 | 163 | 250 | 1.41 | 56 | 2.45 | 53 | 377 | 193 | 82 | 63 |
| 3/15/2009 | 60 | 90 | 250 | 250 | 2.32 | 282 | 7.21 | 271 | 303 | 125 | 53 | 50 |
| 3/16/2009 | 250 | 250 | 250 | 250 | 5.2 | 184 | 9.86 | 246 | 232 | 63 | 40 | 38 |
| 3/17/2009 | 250 | 128 | 250 | 250 | 3 | 7 | 8.07 | 320 | 336 | 49 | 47 | 45 |
| 3/18/2009 | 138 | 138 | 250 | 250 | 1.06 | 76 | 4.08 | 6 | 339 | 26 | 51 | 47 |
| 3/19/2009 | 55 | 120 | 80 | 250 | 1.07 | 59 | 2.83 | 54 | 346 | 21 | 45 | 42 |
| 3/20/2009 | 78 | 105 | 160 | 250 | 1.91 | 53 | 3.44 | 62 | 317 | 15 | 47 | 44 |
| 3/21/2009 | 85 | 125 | 250 | 250 | 1.57 | 203 | 7.13 | 201 | 290 | 13 | 55 | 51 |
| 3/22/2009 | 250 | 250 | 250 | 250 | 4.68 | 126 | 5.69 | 202 | 212 | 15 | 47 | 45 |
| 3/23/2009 | 250 | 250 | 250 | 250 | 11 | 305 | 99.99 | 9999 | 221 | 35 | 47 | 44 |
| 3/24/2009 | 250 | 250 | 250 | 250 | 7.44 | 309 | 10.75 | 306 | 344 | 17 | 48 | 45 |
| 3/25/2009 | 78 | 170 | 250 | 250 | 3.49 | 308 | 9.96 | 281 | 273 | 14 | 49 | 47 |
| 3/26/2009 | 250 | 250 | 250 | 250 | 5.11 | 30 | 3 | 221 | 242 | 98 | 49 | 46 |
| 3/27/2009 | 250 | 250 | 250 | 250 | 3.12 | 289 | 9.51 | 303 | 342 | 40 | 51 | 49 |

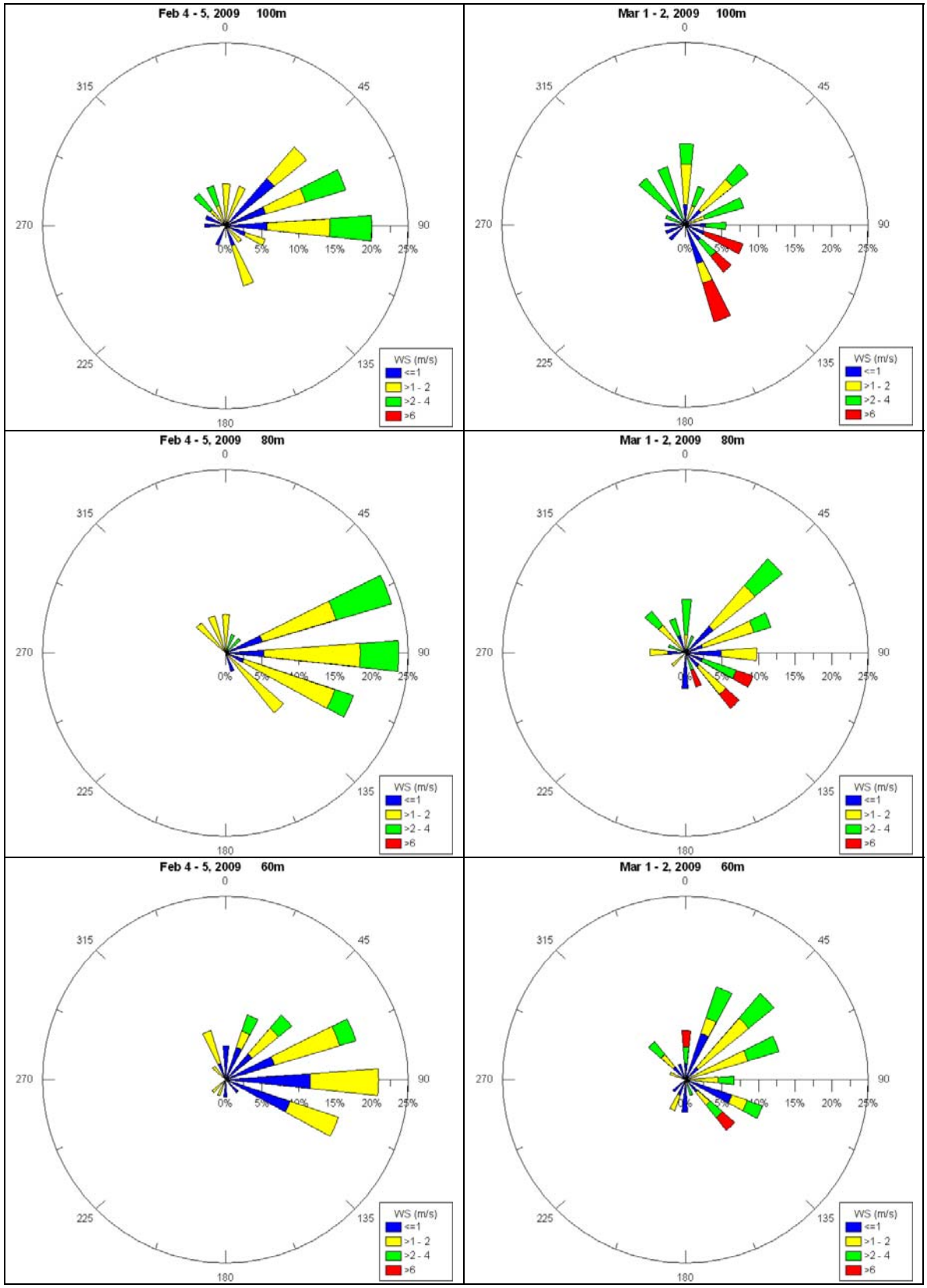


**Figure 4-36.** Comparison of IOP 1 and IOP 3 upper level winds.

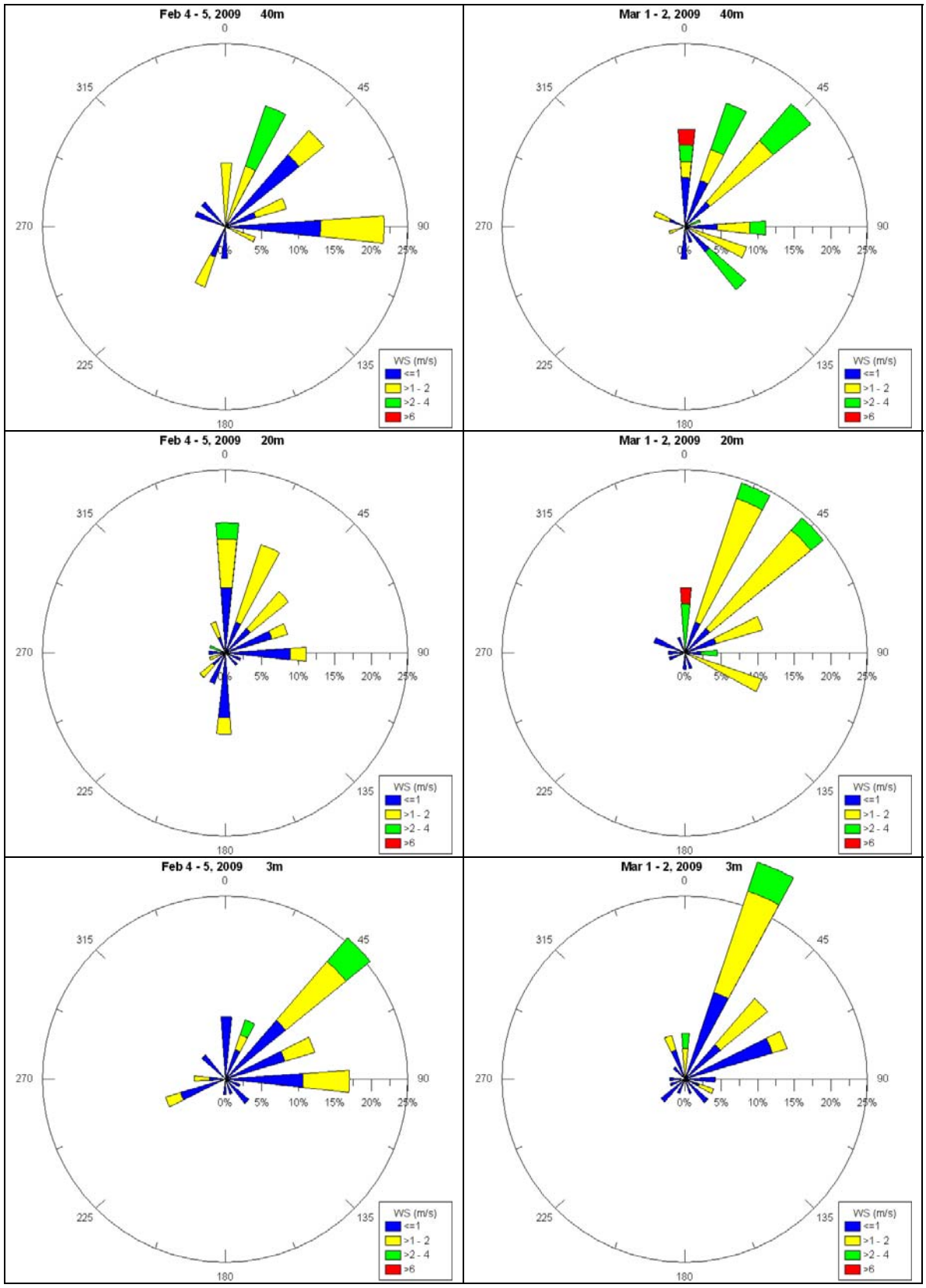


**Figure 4-36.**(continued). Comparison of IOP 1 and IOP 3 upper level winds.

## 4.5 Analysis of Precursor Data

### 4.5.1 Analysis of NMOC Data

Canister samples for analysis of VOCs via EPA method TO-14 and DNPH cartridge samples for analysis of carbonyls via EPA method TO-11 were collected twice daily at Jonah and Boulder II on IOP days. Sampling was set to start at 0600 and 1300 MST during each IOP day and end four hours later. Samples were not collected at Jonah during IOP#2 in order to conserve resources. During IOP#3, VOC canisters were collected at the SODAR site in addition to Jonah and Boulder II on the same schedule. A total of 39 VOC canister samples and 33 carbonyl cartridge samples were collected. These totals do not include blanks and duplicates collected for quality assurance (QA) purposes; a discussion of the QA results for the NMOC sampling program is provided in Section 3. Sample times and locations are listed in Table 4-10.

**Table 4-10.** VOC/carbonyl samples (times in MST) collected during each IOP.

| Date | Jonah Site | Boulder II Site | Sodar Site |
|---|---|---|---|
| **IOP #1** | | | |
| 2-3-09 | 0600 (VOC/Carb) | 0600 (VOC/Carb) | |
| | 1300 (VOC/Carb) | 1300 (VOC/Carb) | |
| 2-4-09 | 0600 (VOC/Carb) | 0600 (VOC/Carb) | |
| | 1300 (VOC/Carb) | 1300 (VOC/Carb) | |
| 2-5-09 | 0600 (VOC/Carb) | 0600 (VOC/Carb) | |
| | 1300 (VOC/Carb) | 1300 (VOC/Carb) | |
| **IOP #2** | | | |
| 2-21-09 | | 0600(VOC/Carb) | |
| | | 1300(VOC/Carb) | |
| 2-22-09 | | 0600(VOC/Carb) | |
| | | 1300(VOC/Carb) | |
| **IOP #3** | | | |
| 2-28-09 | 0600 (VOC/Carb) | 0600 (VOC/Carb) | 0600 (VOC) |
| | 1300 (VOC/Carb) | 1300 (VOC/Carb) | 1300 (VOC) |
| 3-1-09 | 0600 (VOC/Carb) | 0600 (VOC/Carb) | 0600 (VOC) |
| | 1300 (VOC/Carb) | 1300 (VOC/Carb) | 1300 (VOC) |
| 3-2-09 | 0600 (VOC/Carb) | 0600 (Carb) | 0600 (VOC) |
| | 1300 (VOC/Carb) | 1300 (Carb) | 1300 (VOC) |
| 3-3-09 | 0600 (VOC/Carb) | 0600 (VOC/Carb) | 0600 (VOC) |
| | 1300 (VOC/Carb) | 1300 (VOC/Carb) | 1300 (VOC) |
| 3-4-09 | | 0600 (VOC/Carb) | |

In addition to the analysis of the canister data for VOCs, several canisters from IOP#2 and IOP#3 were analyzed for methane (CH4) and carbon monoxide (CO) as listed in Table 4-11.

**Table 4-11**. Canister samples analyzed for CO and $CH_4$ (times in MST).

| IOP #2 | | | |
|---|---|---|---|
| **Date** | **Jonah** | **Boulder** | **Sodar** |
| 2/21/2009 | - | - | - |
| | - | 1300 | - |
| | | | |
| 2/22/2009 | - | 0600 | - |
| | - | 1300 | - |
| **IOP #3** | | | |
| **Date** | **Jonah** | **Boulder** | **Sodar** |
| 2/28/2009 | 0600 | 0600 | 0600 |
| | 1300 | 1300 | 1300 |
| | | | |
| 3/1/2009 | 0600 | 0600 | 0600 |
| | 1300 | 1300 | 1300 |
| | | | |
| 3/2/2009 | 0600 | - | 0600 |
| | 1300 | - | 1300 |
| | | | |
| 3/3/2009 | - | 0600 | 0600 |
| | 1300 | 1300 | 1300 |
| | | | |
| 3/4/2009 | - | 0600 | - |

Table 4-12 shows which compounds on the analytical target list were detected at each monitoring location. Shaded rows indicate compounds that were detected in one or more samples at all sites. Based on the relatively small samples sizes, differences in detection frequencies of less than about 10% are not very meaningful. Similar results for carbonyl compounds are listed in Table 4-13. Some compounds (methanol, 1-nonene, i-propylbenzene, etc.) were detected at Jonah that were not observed above the MDL at the Boulder or Sodar sites, most likely due to the higher total NMOC concentrations at Jonah as described below. Carbonyl sampling identified four aldehydes (acetaldehyde, butyraldehyde, crotonaldehyde, formaldehyde) and acetone present in most samples. This is similar to results from 2008 except that butyraldehyde was not detected in 2008 sampling but was detected in over half of the 2009 samples with concentrations at Boulder roughly double those observed at Jonah. Carbonyl sampling was not performed at the SODAR site.

As noted in the 2008 UGWOS report, unidentified NMHC was found to be a significant percentage of total NMHC in a number of samples collected during the 2008 field study, especially at Boulder where the total alkane loading is significantly lower than at Jonah. Further analysis of the 2008 data performed by EAS after completion of the 2008 study report revealed that the bulk of the unidentified mass in these samples was associated with one or two large peaks in the chromatograph (one at 35 minutes and one at 46 minutes) in addition to a large number of smaller peaks above about C8. MSI performed a special sampling program at Jonah and at Boulder during 11 – 13 January 2009 focused on confirming the presence of these peaks and identifying them. Results of the MSI/EAS study showed that:

- The same peaks found to comprise the bulk of the “unidentified” mass in the 2008 samples were present in the samples collected during the special study,

- The peak at 35 minutes, which was previously unidentified was in fact a very large toluene peak and,
- The peak at 46 minutes is isobutylene trimer (as determined via EPA method TO-15 GC/MS).

Isobutylene trimer is a product of pyrolysis of plastic materials and is not a compound one would normally expect to encounter in an ambient air sample. The January 2009 special study included collection of ambient samples on the roof of MSI's facility in Salt Lake City using the same sampling equipment that was used at Jonah and Boulder as a control. Analysis of these Salt Lake City samples also revealed the presence of isobutylene trimer. EAS noted that this peak was only present in samples collected via actuation of an automated valve. MSI/EAS concluded that this compound may have come from intermittent out gassing of an "O" ring seal in one of the solenoid valves and is therefore a sampling artifact. The complete MSI/EAS report is provided in Appendix D. With regard to the large toluene peaks, MSI/EAS noted that the high toluene samples are associated with a series of straight chain alkanes. The origin of material contributing the large number of fine-scale peaks above C8 on the chromatographs examined by EAS is not entirely clear. Some of this material may be associated with diesel exhaust .

Based on results of the MSI/EAS special study, speciation of NMOC samples collected during UGWOS '09 included identification of isobutylene trimer which is listed in Table 4-12 as 2-methyl-1-propene, trimer. This compound showed up in a few samples at each monitoring site. In addition, the C8+ fine scale peaks identified above were lumped into a "C8-C12 Organics" group which was common at Jonah and Boulder but not at the Sodar site.

**Table 4-12**. Summary of VOC compound detections (ND indicates compounds was not detected in *any* of the samples analyzed; percentage values indicate fraction of samples above the method detection limit; shaded rows indicate compounds detected in at least one sample at all sites).

| Compound | Jonah (14 Samples) | Boulder (19 Samples) | Sodar (8 Samples) |
|---|---|---|---|
| 1,2,3,5-Tetramethylbenzene | ND | ND | ND |
| 1,2,3-Trimethylbenzene | 16% | 29% | 12% |
| 1,2,4,5-Tetramethylbenzene | ND | ND | ND |
| 1,2,4-Trimethylbenzene | 74% | 57% | 12% |
| 1,2-Dimethyl-4-ethylbenzene | 5% | ND | ND |
| 1,3,5-Trimethylbenzene | 37% | 36% | 12% |
| 1,3-Butadiene | ND | ND | ND |
| 1,3-Diethylbenzene | 11% | 14% | ND |
| 1,3-Dimethyl-4-ethylbenzene | 21% | 21% | ND |
| 1,4-Diethylbenzene | 5% | 7% | ND |
| 1,4-Dimethyl-2-ethylbenzene | ND | ND | ND |
| 1-Butene | ND | ND | 25% |
| 1-Hexene | ND | 7% | 12% |
| 1-Nonene | ND | 21% | ND |
| 1-Pentene | ND | ND | ND |
| 2,2,4-Trimethylpentane | 11% | 79% | 12% |
| 2,2-Dimethylbutane | 16% | 71% | ND |
| 2,3,4-Trimethylpentane | ND | ND | 12% |
| 2,3-Dimethylbutane | 5% | 7% | ND |
| 2,3-Dimethylhexane | ND | 14% | ND |
| 2,3-Dimethylpentane | 11% | 71% | ND |
| 2,4-Dimethylhexane | ND | 14% | ND |
| 2,4-Dimethylpentane | 68% | 93% | 75% |
| 2,5-Dimethylhexane | ND | 36% | ND |

| Compound | Jonah (14 Samples) | Boulder (19 Samples) | Sodar (8 Samples) |
|---|---|---|---|
| 2-Ethyltoluene | 21% | 14% | ND |
| 2-Methyl-1-butene | ND | ND | 12% |
| 2-Methyl-1-heptene | ND | 29% | 12% |
| 2-Methyl-1hexene | 16% | 79% | 12% |
| 2-Methyl-1-propene, trimer | 37% | 14% | 12% |
| 2-Methyl-2-butene | ND | ND | ND |
| 2-Methylheptane | 16% | 71% | 12% |
| 2-Methylhexane | 37% | 100% | 50% |
| 2-Methylpentane | 53% | 93% | 88% |
| 3-Ethyl-3-methylpentane | ND | ND | 12% |
| 3-Ethyltoluene | 42% | 29% | 12% |
| 3-Methyl-1-butene | 11% | 7% | ND |
| 3-Methylcyclopentene | 16% | 36% | 12% |
| 3-Methylheptane | 21% | 64% | 12% |
| 3-Methylhexane | 37% | 93% | 50% |
| 3-Methylpentane | 74% | 100% | 75% |
| 4-Ethyltoluene | 53% | 29% | ND |
| 4-Methylheptane | 11% | 50% | ND |
| Acetone | 42% | 43% | 12% |
| Acetylene | 37% | 79% | 75% |
| a-Pinene | ND | ND | ND |
| Benzene | 79% | 93% | 88% |
| b-Pinene | ND | 7% | ND |
| c-2-Butene | ND | ND | ND |
| c-2-Pentene | ND | 7% | ND |
| C8-C12 Organics (6) | 74% | 93% | 12% |
| Cyclohexane | 74% | 93% | 100% |
| Cyclopentane | 42% | 93% | 62% |
| Cyclopentene | 5% | 7% | ND |
| Diisopropyl ether | ND | ND | ND |
| d-Limonene | ND | ND | ND |
| Dodecane | ND | ND | ND |
| Ethane | 89% | 100% | 88% |
| Ethanol | 84% | 57% | ND |
| Ethene | 53% | 100% | 75% |
| Ethyl tert butyl ether | ND | ND | ND |
| Ethylbenzene | 63% | 86% | 12% |
| i-Butane | 89% | 100% | 88% |
| Indan | 16% | 7% | ND |
| i-Pentane | 79% | 93% | 88% |
| i-Propylbenzene | ND | 14% | ND |
| Isoprene | 5% | ND | ND |
| Isopropanol | ND | ND | ND |
| m,p-xylene | 95% | 93% | 62% |
| Methanol | ND | 21% | ND |
| Methyl tert butyl ether | ND | ND | ND |
| Methylcyclohexane | 68% | 100% | 88% |
| Methylcyclopentane | 32% | ND | ND |
| Naphthalene | ND | ND | ND |
| n-Butane | 79% | 86% | 88% |
| n-Butylbenzene | 11% | 14% | ND |
| n-Decane | 68% | 71% | 12% |
| n-Heptane | 79% | 93% | 88% |
| n-Hexane | 74% | 93% | 88% |
| n-Nonane | 58% | 93% | 38% |
| n-Octane | 68% | 86% | 62% |
| n-Pentane | 74% | 86% | 100% |

| Compound | Jonah (14 Samples) | Boulder (19 Samples) | Sodar (8 Samples) |
|---|---|---|---|
| n-Propanol | ND | ND | ND |
| n-propylbenzene | 37% | 29% | ND |
| o-xylene | 74% | 93% | 38% |
| Propane | 95% | 100% | 88% |
| Propene | 74% | 93% | 25% |
| Styrene | ND | 7% | ND |
| t-2-Butene | ND | 7% | ND |
| t-2-Pentene | ND | ND | ND |
| Tert amyl methyl ether | ND | ND | ND |
| Tert butyl alcohol | ND | ND | ND |
| Toluene | 89% | 100% | 100% |
| Undecane | 16% | ND | ND |

**Table 4-13.** Summary of carbonyl compound detections (ND indicates compounds was not detected in *any* of the samples analyzed; percentage values indicate fraction of samples above the method detection limit; shaded rows indicate compounds detected in at least one sample at all sites).

| Compound | Boulder | Jonah |
|---|---|---|
| 2,5-Dimethylbenzaldehyde (ppbV) | ND | ND |
| Acetaldehyde (ppbV) | 84% | 92% |
| Acetone (ppbV) | 100% | 100% |
| Acrolein (ppbV) | ND | ND |
| Benzaldehyde (ppbV) | ND | ND |
| Butyraldehyde (ppbV) | 53% | 54% |
| Crotonaldehyde (ppbV) | 26% | 23% |
| Formaldehyde (ppbV) | 89% | 100% |
| Hexaldehyde (ppbV) | ND | ND |
| Isovaleraldehyde (ppbV) | ND | ND |
| m-Tolualdehyde (ppbV) | ND | ND |
| o-Tolualdehyde (ppbV) | ND | 8% |
| Propionaldehyde (ppbV) | ND | ND |
| p-Tolualdehyde (ppbV) | 5% | ND |
| Valeraldehyde (ppbV) | 11% | ND |

Average method detection limits for NMHC species for samples collected at Jonah and Boulder (Table 4-14) were similar to those from the 2008 study (ENVIRON, 2008b). Detection limits at the Sodar site are 1.6 times higher than those at Jonah and Boulder due to the lower sample mass that could be collected without a pump at the Sodar site. Carbonyl species detection limits (Table 4-15) are slightly better than those achieved in 2008.

**Table 4-14**. Average NMHC method detection limits (ppbV).

| Species | Boulder | Jonah | Sodar |
|---|---|---|---|
| 1,2,3,5-Tetramethylbenzene | 0.55 | 0.54 | 0.88 |
| 1,2,3-Trimethylbenzene | 0.55 | 0.54 | 0.88 |
| 1,2,4,5-Tetramethylbenzene | 0.55 | 0.54 | 0.88 |
| 1,2,4-Trimethylbenzene | 0.37 | 0.36 | 0.58 |
| 1,2-Dimethyl-4-ethylbenzene | 0.55 | 0.54 | 0.88 |
| 1,3,5-Trimethylbenzene | 0.37 | 0.36 | 0.58 |
| 1,3-Butadiene | 0.28 | 0.27 | 0.44 |
| 1,3-Diethylbenzene | 0.55 | 0.54 | 0.88 |
| 1,3-Dimethyl-4-ethylbenzene | 0.55 | 0.54 | 0.88 |
| 1,4-Diethylbenzene | 0.55 | 0.54 | 0.88 |
| 1,4-Dimethyl-2-ethylbenzene | 0.55 | 0.54 | 0.88 |
| 1-Butene | 0.37 | 0.36 | 0.58 |
| 1-Hexene | 0.37 | 0.36 | 0.58 |
| 1-Nonene | 0.55 | 0.54 | 0.88 |
| 1-Pentene | 0.37 | 0.36 | 0.58 |
| 2,2,4-Trimethylpentane | 0.37 | 0.36 | 0.58 |
| 2,2-Dimethylbutane | 0.37 | 0.36 | 0.58 |
| 2,3,4-Trimethylpentane | 0.55 | 0.54 | 0.88 |
| 2,3-Dimethylbutane | 0.37 | 0.36 | 0.58 |
| 2,3-Dimethylhexane | 0.55 | 0.54 | 0.88 |
| 2,3-Dimethylpentane | 0.37 | 0.36 | 0.58 |
| 2,4-Dimethylhexane | 0.55 | 0.54 | 0.88 |
| 2,4-Dimethylpentane | 0.37 | 0.36 | 0.58 |
| 2,5-Dimethylhexane | 0.55 | 0.54 | 0.88 |
| 2-Ethyltoluene | 0.55 | 0.54 | 0.88 |
| 2-Methyl-1-butene | 0.37 | 0.36 | 0.58 |
| 2-Methyl-1-heptene | 0.55 | 0.54 | 0.88 |
| 2-Methyl-1hexene | 0.37 | 0.36 | 0.58 |
| 2-Methyl-1-propene, trimer | 0.55 | 0.54 | 0.88 |
| 2-Methyl-2-butene | 0.37 | 0.36 | 0.58 |
| 2-Methylheptane | 0.55 | 0.54 | 0.88 |
| 2-Methylhexane | 0.37 | 0.36 | 0.58 |
| 2-Methylpentane | 0.37 | 0.36 | 0.58 |
| 3-Ethyl-3-methylpentane | 0.55 | 0.54 | 0.88 |
| 3-Ethyltoluene | 0.55 | 0.54 | 0.88 |
| 3-Methyl-1-butene | 0.37 | 0.36 | 0.58 |
| 3-Methylcyclopentene | 0.37 | 0.36 | 0.58 |
| 3-Methylheptane | 0.55 | 0.54 | 0.88 |
| 3-Methylhexane | 0.37 | 0.36 | 0.58 |
| 3-Methylpentane | 0.37 | 0.36 | 0.58 |
| 4-Ethyltoluene | 0.55 | 0.54 | 0.88 |
| 4-Methylheptane | 0.55 | 0.54 | 0.88 |
| Acetone | 0.55 | 0.54 | 0.88 |
| Acetylene | 0.55 | 0.54 | 0.88 |
| a-Pinene | 0.55 | 0.54 | 0.88 |
| Benzene | 0.28 | 0.27 | 0.44 |
| b-Pinene | 0.55 | 0.54 | 0.88 |
| c-2-Butene | 0.37 | 0.36 | 0.58 |
| c-2-Pentene | 0.37 | 0.36 | 0.58 |

| Species | Boulder | Jonah | Sodar |
|---|---|---|---|
| Cyclohexane | 0.28 | 0.27 | 0.44 |
| Cyclopentane | 0.28 | 0.27 | 0.44 |
| Cyclopentene | 0.28 | 0.27 | 0.44 |
| Diisopropyl ether | 0.55 | 0.54 | 0.88 |
| d-Limonene | 0.55 | 0.54 | 0.88 |
| Dodecane | 0.55 | 0.54 | 0.88 |
| Ethane | 0.28 | 0.27 | 0.44 |
| Ethanol | 0.55 | 0.54 | 0.88 |
| Ethene | 0.55 | 0.54 | 0.88 |
| Ethyl tert butyl ether | 0.55 | 0.54 | 0.88 |
| Ethylbenzene | 0.28 | 0.27 | 0.44 |
| i-Butane | 0.37 | 0.36 | 0.58 |
| Indan | 0.55 | 0.54 | 0.88 |
| i-Pentane | 0.28 | 0.27 | 0.44 |
| i-Propylbenzene | 0.55 | 0.54 | 0.88 |
| Isoprene | 0.37 | 0.36 | 0.58 |
| Isopropanol | 0.55 | 0.54 | 0.88 |
| m,p-xylene | 0.28 | 0.27 | 0.44 |
| Methanol | 0.55 | 0.54 | 0.88 |
| Methyl tert butyl ether | 0.55 | 0.54 | 0.88 |
| Methylcyclohexane | 0.55 | 0.54 | 0.88 |
| Methylcyclopentane | 0.37 | 0.36 | 0.58 |
| Naphthalene | 0.55 | 0.54 | 0.88 |
| n-Butane | 0.28 | 0.27 | 0.44 |
| n-Butylbenzene | 0.37 | 0.36 | 0.58 |
| n-Decane | 0.37 | 0.36 | 0.58 |
| n-Heptane | 0.28 | 0.27 | 0.44 |
| n-Hexane | 0.28 | 0.27 | 0.44 |
| n-Nonane | 0.37 | 0.36 | 0.58 |
| n-Octane | 0.28 | 0.27 | 0.44 |
| n-Pentane | 0.28 | 0.27 | 0.44 |
| n-Propanol | 0.55 | 0.54 | 0.88 |
| n-propylbenzene | 0.55 | 0.54 | 0.88 |
| o-xylene | 0.28 | 0.27 | 0.44 |
| Propane | 0.28 | 0.27 | 0.44 |
| Propene | 0.37 | 0.36 | 0.58 |
| Styrene | 0.55 | 0.54 | 0.88 |
| t-2-Butene | 0.37 | 0.36 | 0.58 |
| t-2-Pentene | 0.37 | 0.36 | 0.58 |
| Tert amyl methyl ether | 0.37 | 0.36 | 0.58 |
| Tert butyl alcohol | 0.55 | 0.54 | 0.88 |
| Toluene | 0.28 | 0.27 | 0.44 |
| Undecane | 0.55 | 0.54 | 0.88 |
| **Total Non-Methane Hydrocarbons** | **9.17** | **9.02** | **14.57** |

**Table 4-15**. Average method detection limits (ppbV) for carbonyl species.

| Parameter | Boulder | Jonah |
|---|---|---|
| 2,5-Dimethylbenzaldehyde | 0.08 | 0.07 |
| Acetaldehyde | 0.23 | 0.22 |
| Acetone | 0.18 | 0.17 |
| Acrolein | 0.18 | 0.17 |
| Benzaldehyde | 0.10 | 0.09 |
| Butyraldehyde | 0.14 | 0.14 |
| Crotonaldehyde | 0.15 | 0.14 |
| Formaldehyde | 0.34 | 0.32 |
| Hexaldehyde | 0.10 | 0.10 |
| Isovaleraldehyde | 0.12 | 0.12 |
| m-Tolualdehyde | 0.09 | 0.08 |
| o-Tolualdehyde | 0.09 | 0.08 |
| Propionaldehyde | 0.18 | 0.17 |
| p-Tolualdehyde | 0.09 | 0.08 |
| Valeraldehyde | 0.12 | 0.12 |

Statistical summaries of NMHC data are provided for the Jonah, Boulder and Sodar sites in Tables 4-16, 4-17 and 4-18, respectively. Statistical summaries of the carbonyl data are provided in Table 4-19. Acetaldehyde, acetone and formaldehyde concentrations are similar at Jonah and Boulder (carbonyl sampling was not performed at the Sodar site). Butyraldehyde was found at somewhat higher concentrations at Boulder and crotonaldehyde was detected at Boulder but not at Jonah but the significance of these differences is not obvious.

**Table 4-16.** VOC summary statistics based on values above MDL for samples collected at Jonah.

| Jonah – VOC Species | | | | | | | | | | |
|---|---|---|---|---|---|---|---|---|---|---|
| **Compound** | **Max** | **Min** | **Mean** | **Q1** | **Q2** | **Q3** | **N** | **ND** | **%ND** | **N+ND** |
| 1,2,3-Trimethylbenzene (ppbV) | 2.23 | 0.72 | 1.34 | 0.72 | 1.08 | 1.33 | 4 | 10 | 71% | 14 |
| 1,2,4-Trimethylbenzene (ppbV) | 4.21 | 0.46 | 1.34 | 0.49 | 0.57 | 1.60 | 8 | 6 | 43% | 14 |
| 1,3,5-Trimethylbenzene (ppbV) | 1.89 | 0.39 | 0.77 | 0.43 | 0.49 | 1.89 | 5 | 9 | 64% | 14 |
| 1,3-Diethylbenzene (ppbV) | 2.75 | 0.59 | 1.67 | | | | 2 | 12 | 86% | 14 |
| 1,3-Dimethyl-4-ethylbenzene (ppbV) | 2.44 | 0.93 | 1.58 | | | | 3 | 11 | 79% | 14 |
| 1,4-Diethylbenzene (ppbV) | 1.00 | 1.00 | 1.00 | | | | 1 | 13 | 93% | 14 |
| 1-Hexene (ppbV) | 0.62 | 0.62 | 0.62 | | | | 1 | 13 | 93% | 14 |
| 1-Nonene (ppbV) | 1.38 | 0.89 | 1.10 | | | | 3 | 11 | 79% | 14 |
| 2,2,4-Trimethylpentane (ppbV) | 5.00 | 0.39 | 1.69 | 0.53 | 0.85 | 2.51 | 11 | 3 | 21% | 14 |
| 2,2-Dimethylbutane (ppbV) | 3.82 | 0.36 | 1.41 | 0.56 | 0.81 | 1.63 | 10 | 4 | 29% | 14 |
| 2,3-Dimethylbutane (ppbV) | 0.61 | 0.61 | 0.61 | | | | 1 | 13 | 93% | 14 |
| 2,3-Dimethylhexane (ppbV) | 0.80 | 0.80 | 0.80 | | | | 2 | 12 | 86% | 14 |
| 2,3-Dimethylpentane (ppbV) | 2.54 | 0.38 | 1.04 | 0.48 | 0.54 | 1.38 | 10 | 4 | 29% | 14 |
| 2,4-Dimethylhexane (ppbV) | 1.04 | 1.02 | 1.03 | | | | 2 | 12 | 86% | 14 |
| 2,4-Dimethylpentane (ppbV) | 18.17 | 1.62 | 5.65 | 2.03 | 2.68 | 9.25 | 13 | 1 | 7% | 14 |
| 2,5-Dimethylhexane (ppbV) | 2.77 | 0.71 | 1.70 | 1.10 | 1.39 | 2.77 | 5 | 9 | 64% | 14 |
| 2-Ethyltoluene (ppbV) | 1.23 | 0.70 | 0.96 | | | | 2 | 12 | 86% | 14 |
| 2-Methyl-1-heptene (ppbV) | 1.50 | 0.52 | 1.06 | 0.52 | 0.73 | 1.49 | 4 | 10 | 71% | 14 |
| 2-Methyl-1hexene (ppbV) | 3.24 | 0.37 | 1.15 | 0.47 | 0.64 | 1.65 | 11 | 3 | 21% | 14 |
| 2-Methyl-1-propene, trimer (ppbV) | 4.59 | 0.74 | 2.66 | | | | 2 | 12 | 86% | 14 |
| 2-Methylheptane (ppbV) | 4.42 | 0.51 | 1.72 | 0.64 | 0.93 | 2.00 | 10 | 4 | 29% | 14 |
| 2-Methylhexane (ppbV) | 8.23 | 0.62 | 2.46 | 0.79 | 1.16 | 3.58 | 14 | 0 | 0% | 14 |
| 2-Methylpentane (ppbV) | 25.36 | 0.83 | 7.54 | 2.15 | 3.74 | 12.00 | 13 | 1 | 7% | 14 |
| 3-Ethyltoluene (ppbV) | 2.15 | 0.51 | 1.12 | 0.51 | 0.71 | 1.10 | 4 | 10 | 71% | 14 |
| 3-Methyl-1-butene (ppbV) | 6.30 | 6.30 | 6.30 | | | | 1 | 13 | 93% | 14 |
| 3-Methylcyclopentene (ppbV) | 11.03 | 1.36 | 7.36 | 5.24 | 8.40 | 11.03 | 5 | 9 | 64% | 14 |
| 3-Methylheptane (ppbV) | 8.35 | 0.61 | 3.07 | 1.12 | 1.45 | 8.01 | 9 | 5 | 36% | 14 |
| 3-Methylhexane (ppbV) | 7.79 | 0.55 | 2.47 | 0.83 | 1.43 | 4.18 | 13 | 1 | 7% | 14 |
| 3-Methylpentane (ppbV) | 14.82 | 0.77 | 4.33 | 1.41 | 2.23 | 6.53 | 14 | 0 | 0% | 14 |
| 4-Ethyltoluene (ppbV) | 3.14 | 0.64 | 1.85 | 0.64 | 1.42 | 2.19 | 4 | 10 | 71% | 14 |
| 4-Methylheptane (ppbV) | 3.71 | 0.55 | 1.71 | 0.88 | 0.91 | 3.40 | 7 | 7 | 50% | 14 |
| Acetone (ppbV) | 21.64 | 0.53 | 7.49 | 1.62 | 3.25 | 10.55 | 6 | 8 | 57% | 14 |
| Acetylene (ppbV) | 202.90 | 1.90 | 32.75 | 2.57 | 4.36 | 18.21 | 11 | 3 | 21% | 14 |
| Benzene (ppbV) | 41.15 | 3.26 | 12.02 | 4.72 | 5.15 | 18.35 | 13 | 1 | 7% | 14 |
| b-Pinene (ppbV) | 1.50 | 1.50 | 1.50 | | | | 1 | 13 | 93% | 14 |
| c-2-Pentene (ppbV) | 0.94 | 0.94 | 0.94 | | | | 1 | 13 | 93% | 14 |
| C8-C12 Organics (6) (ppbV) | 59.80 | 6.72 | 23.05 | 8.95 | 20.69 | 28.71 | 13 | 1 | 7% | 14 |
| Cyclohexane (ppbV) | 29.62 | 2.12 | 9.17 | 3.12 | 4.43 | 15.24 | 13 | 1 | 7% | 14 |
| Cyclopentane (ppbV) | 7.23 | 0.64 | 2.46 | 0.99 | 1.24 | 4.26 | 13 | 1 | 7% | 14 |
| Cyclopentene (ppbV) | 0.88 | 0.88 | 0.88 | | | | 1 | 13 | 93% | 14 |
| Ethane (ppbV) | 741.80 | 18.18 | 193.40 | 94.88 | 114.40 | 220.70 | 14 | 0 | 0% | 14 |
| Ethanol (ppbV) | 74.53 | 5.77 | 42.22 | 12.90 | 33.31 | 56.09 | 8 | 6 | 43% | 14 |
| Ethene (ppbV) | 544.90 | 1.08 | 46.26 | 4.65 | 7.27 | 11.05 | 14 | 0 | 0% | 14 |
| Ethylbenzene (ppbV) | 4.30 | 0.37 | 1.43 | 0.44 | 0.64 | 1.51 | 12 | 2 | 14% | 14 |
| i-Butane (ppbV) | 140.10 | 6.70 | 46.67 | 17.46 | 32.91 | 65.36 | 14 | 0 | 0% | 14 |
| Indan (ppbV) | 3.11 | 3.11 | 3.11 | | | | 1 | 13 | 93% | 14 |
| i-Pentane (ppbV) | 79.40 | 0.26 | 26.87 | 10.78 | 17.91 | 42.34 | 13 | 1 | 7% | 14 |
| i-Propylbenzene (ppbV) | 1.02 | 1.00 | 1.01 | | | | 2 | 12 | 86% | 14 |
| m,p-xylene (ppbV) | 24.18 | 1.11 | 8.98 | 3.41 | 4.88 | 21.79 | 13 | 1 | 7% | 14 |
| Methanol (ppbV) | 141.70 | 47.59 | 99.53 | | | | 3 | 11 | 79% | 14 |
| Methylcyclohexane (ppbV) | 54.52 | 1.77 | 15.76 | 5.19 | 7.68 | 22.57 | 14 | 0 | 0% | 14 |
| n-Butane (ppbV) | 172.30 | 16.09 | 56.53 | 18.87 | 34.67 | 80.12 | 12 | 2 | 14% | 14 |
| n-Butylbenzene (ppbV) | 0.62 | 0.61 | 0.62 | | | | 2 | 12 | 86% | 14 |
| n-Decane (ppbV) | 6.96 | 0.42 | 1.59 | 0.54 | 0.77 | 1.23 | 10 | 4 | 29% | 14 |
| n-Heptane (ppbV) | 18.46 | 0.85 | 5.73 | 2.06 | 3.08 | 9.54 | 13 | 1 | 7% | 14 |
| n-Hexane (ppbV) | 32.67 | 2.27 | 10.17 | 3.78 | 4.87 | 16.13 | 13 | 1 | 7% | 14 |
| n-Nonane (ppbV) | 6.90 | 0.48 | 2.06 | 0.70 | 1.36 | 3.22 | 13 | 1 | 7% | 14 |
| n-Octane (ppbV) | 12.24 | 1.07 | 4.10 | 1.62 | 2.34 | 4.55 | 12 | 2 | 14% | 14 |
| n-Pentane (ppbV) | 63.26 | 4.92 | 20.85 | 7.14 | 10.40 | 29.33 | 12 | 2 | 14% | 14 |
| n-propylbenzene (ppbV) | 4.83 | 0.59 | 1.80 | 0.59 | 0.72 | 1.08 | 4 | 10 | 71% | 14 |
| o-xylene (ppbV) | 6.76 | 0.45 | 2.13 | 0.88 | 1.13 | 4.37 | 13 | 1 | 7% | 14 |
| Propane (ppbV) | 464.70 | 10.23 | 136.30 | 50.03 | 63.67 | 211.30 | 14 | 0 | 0% | 14 |
| Propene (ppbV) | 14.29 | 0.58 | 2.95 | 0.76 | 1.09 | 5.43 | 13 | 1 | 7% | 14 |
| Styrene (ppbV) | 0.77 | 0.77 | 0.77 | | | | 1 | 13 | 93% | 14 |
| t-2-Butene (ppbV) | 1.63 | 1.63 | 1.63 | | | | 1 | 13 | 93% | 14 |
| Toluene (ppbV) | 78.69 | 2.32 | 22.08 | 8.97 | 12.13 | 24.14 | 14 | 0 | 0% | 14 |

| Jonah – VOC Lumped Species | | | | | | | | | | |
|---|---|---|---|---|---|---|---|---|---|---|
| **Compound** | **Max** | **Min** | **Mean** | **Q1** | **Q2** | **Q3** | **N** | **ND** | **%ND** | **N+ND** |
| Aromatics (ppbV) | 1097.00 | 56.58 | 363.80 | 149.00 | 208.50 | 551.20 | 14 | 0 | 0% | 14 |
| Isoparaffins (ppbV) | 1686.00 | 59.33 | 518.30 | 168.90 | 352.70 | 746.50 | 14 | 0 | 0% | 14 |
| Napthlenes (ppbV) | 661.70 | 19.80 | 189.00 | 56.96 | 92.87 | 259.20 | 14 | 0 | 0% | 14 |
| Olefins (ppbV) | 1554.00 | 12.80 | 171.40 | 24.54 | 48.02 | 78.04 | 14 | 0 | 0% | 14 |
| Oxygenates (ppbV) | 287.20 | 11.54 | 123.20 | 35.56 | 117.00 | 239.50 | 9 | 5 | 36% | 14 |
| Paraffins (ppbV) | 3692.00 | 76.84 | 1231.00 | 517.40 | 750.20 | 2034.00 | 14 | 0 | 0% | 14 |
| Total Identified (ppbC) | 8301.00 | 447.10 | 2748.00 | 1374.00 | 1641.00 | 3803.00 | 14 | 0 | 0% | 14 |

**Table 4-17.** VOC summary statistics based on values above MDL for samples collected at Boulder.

| Boulder – VOC Species | | | | | | | | | | |
|---|---|---|---|---|---|---|---|---|---|---|
| **Compound** | **Max** | **Min** | **Mean** | **Q1** | **Q2** | **Q3** | **N** | **ND** | **%ND** | **N+ND** |
| 1,2,3-Trimethylbenzene (ppbV) | 0.94 | 0.67 | 0.83 | | | | 3 | 16 | 84% | 19 |
| 1,2,4-Trimethylbenzene (ppbV) | 5.41 | 0.41 | 1.99 | 0.64 | 1.15 | 2.96 | 14 | 5 | 26% | 19 |
| 1,2-Dimethyl-4-ethylbenzene (ppbV) | 0.90 | 0.90 | 0.90 | | | | 1 | 18 | 95% | 19 |
| 1,3,5-Trimethylbenzene (ppbV) | 1.17 | 0.41 | 0.79 | 0.45 | 0.73 | 1.17 | 7 | 12 | 63% | 19 |
| 1,3-Diethylbenzene (ppbV) | 0.72 | 0.72 | 0.72 | | | | 2 | 17 | 89% | 19 |
| 1,3-Dimethyl-4-ethylbenzene (ppbV) | 1.71 | 0.59 | 1.01 | 0.59 | 0.69 | 1.05 | 4 | 15 | 79% | 19 |
| 1,4-Diethylbenzene (ppbV) | 0.87 | 0.87 | 0.87 | | | | 1 | 18 | 95% | 19 |
| 2,2,4-Trimethylpentane (ppbV) | 0.43 | 0.42 | 0.42 | | | | 2 | 17 | 89% | 19 |
| 2,2-Dimethylbutane (ppbV) | 0.59 | 0.52 | 0.56 | | | | 3 | 16 | 84% | 19 |
| 2,3-Dimethylbutane (ppbV) | 0.71 | 0.71 | 0.71 | | | | 1 | 18 | 95% | 19 |
| 2,3-Dimethylpentane (ppbV) | 0.46 | 0.39 | 0.43 | | | | 2 | 17 | 89% | 19 |
| 2,4-Dimethylpentane (ppbV) | 2.48 | 0.35 | 1.10 | 0.49 | 0.87 | 1.88 | 13 | 6 | 32% | 19 |
| 2-Ethyltoluene (ppbV) | 1.05 | 0.73 | 0.96 | 0.73 | 1.00 | 1.04 | 4 | 15 | 79% | 19 |
| 2-Methyl-1hexene (ppbV) | 0.73 | 0.49 | 0.59 | | | | 3 | 16 | 84% | 19 |
| 2-Methyl-1-propene, trimer (ppbV) | 7.42 | 0.61 | 2.56 | 0.71 | 1.33 | 5.23 | 7 | 12 | 63% | 19 |
| 2-Methylheptane (ppbV) | 0.92 | 0.52 | 0.69 | | | | 3 | 16 | 84% | 19 |
| 2-Methylhexane (ppbV) | 1.25 | 0.51 | 0.83 | 0.59 | 0.90 | 0.95 | 7 | 12 | 63% | 19 |
| 2-Methylpentane (ppbV) | 3.29 | 0.40 | 1.57 | 0.52 | 1.21 | 2.47 | 10 | 9 | 47% | 19 |
| 3-Ethyltoluene (ppbV) | 1.15 | 0.53 | 0.84 | 0.60 | 0.85 | 0.95 | 8 | 11 | 58% | 19 |
| 3-Methyl-1-butene (ppbV) | 2.52 | 0.35 | 1.44 | | | | 2 | 17 | 89% | 19 |
| 3-Methylcyclopentene (ppbV) | 5.37 | 0.87 | 3.52 | | | | 3 | 16 | 84% | 19 |
| 3-Methylheptane (ppbV) | 1.11 | 0.60 | 0.78 | 0.60 | 0.69 | 0.72 | 4 | 15 | 79% | 19 |
| 3-Methylhexane (ppbV) | 1.20 | 0.43 | 0.80 | 0.51 | 0.83 | 1.15 | 7 | 12 | 63% | 19 |
| 3-Methylpentane (ppbV) | 10.23 | 0.39 | 3.27 | 1.09 | 1.92 | 4.43 | 14 | 5 | 26% | 19 |
| 4-Ethyltoluene (ppbV) | 1.82 | 0.70 | 1.25 | 1.00 | 1.11 | 1.76 | 10 | 9 | 47% | 19 |
| 4-Methylheptane (ppbV) | 0.75 | 0.57 | 0.66 | | | | 2 | 17 | 89% | 19 |
| Acetone (ppbV) | 25.33 | 0.66 | 6.63 | 0.71 | 2.50 | 8.95 | 8 | 11 | 58% | 19 |
| Acetylene (ppbV) | 23.24 | 0.55 | 5.20 | 1.73 | 2.64 | 3.43 | 7 | 12 | 63% | 19 |
| Benzene (ppbV) | 5.18 | 0.69 | 2.39 | 1.32 | 2.10 | 3.52 | 15 | 4 | 21% | 19 |
| C8-C12 Organics (6) (ppbV) | 40.96 | 10.95 | 24.53 | 16.54 | 23.61 | 31.77 | 14 | 5 | 26% | 19 |
| Cyclohexane (ppbV) | 3.80 | 0.33 | 1.43 | 0.52 | 0.75 | 1.94 | 14 | 5 | 26% | 19 |
| Cyclopentane (ppbV) | 1.16 | 0.19 | 0.66 | 0.30 | 0.49 | 0.89 | 8 | 11 | 58% | 19 |
| Cyclopentene (ppbV) | 0.52 | 0.52 | 0.52 | | | | 1 | 18 | 95% | 19 |
| Ethane (ppbV) | 169.00 | 0.66 | 55.25 | 12.18 | 23.58 | 80.68 | 17 | 2 | 11% | 19 |
| Ethanol (ppbV) | 204.70 | 3.31 | 65.36 | 22.77 | 38.77 | 98.78 | 16 | 3 | 16% | 19 |
| Ethene (ppbV) | 9.67 | 1.35 | 5.87 | 4.85 | 5.48 | 7.50 | 10 | 9 | 47% | 19 |
| Ethylbenzene (ppbV) | 1.64 | 0.38 | 0.97 | 0.49 | 0.94 | 1.14 | 12 | 7 | 37% | 19 |
| i-Butane (ppbV) | 24.26 | 2.54 | 8.71 | 3.58 | 6.82 | 13.90 | 17 | 2 | 11% | 19 |
| Indan (ppbV) | 1.96 | 0.56 | 1.04 | | | | 3 | 16 | 84% | 19 |
| i-Pentane (ppbV) | 59.51 | 0.31 | 13.57 | 3.86 | 9.25 | 20.06 | 15 | 4 | 21% | 19 |
| Isoprene (ppbV) | 0.39 | 0.39 | 0.39 | | | | 1 | 18 | 95% | 19 |
| m,p-xylene (ppbV) | 5.56 | 0.20 | 2.59 | 0.66 | 2.20 | 4.43 | 18 | 1 | 5% | 19 |
| Methylcyclohexane (ppbV) | 6.76 | 0.69 | 2.68 | 1.10 | 1.72 | 4.74 | 13 | 6 | 32% | 19 |
| Methylcyclopentane (ppbV) | 7.05 | 0.85 | 2.36 | 0.94 | 1.45 | 2.27 | 6 | 13 | 68% | 19 |
| n-Butane (ppbV) | 25.98 | 0.74 | 7.88 | 2.43 | 3.47 | 12.42 | 15 | 4 | 21% | 19 |
| n-Butylbenzene (ppbV) | 0.69 | 0.43 | 0.56 | | | | 2 | 17 | 89% | 19 |
| n-Decane (ppbV) | 2.67 | 0.38 | 1.22 | 0.81 | 1.04 | 1.76 | 13 | 6 | 32% | 19 |
| n-Heptane (ppbV) | 2.54 | 0.14 | 0.87 | 0.33 | 0.45 | 1.41 | 15 | 4 | 21% | 19 |
| n-Hexane (ppbV) | 4.02 | 0.42 | 1.58 | 0.56 | 1.12 | 2.03 | 14 | 5 | 26% | 19 |
| n-Nonane (ppbV) | 2.31 | 0.35 | 0.96 | 0.53 | 0.86 | 1.34 | 11 | 8 | 42% | 19 |
| n-Octane (ppbV) | 2.37 | 0.28 | 0.92 | 0.40 | 0.67 | 1.49 | 13 | 6 | 32% | 19 |
| n-Pentane (ppbV) | 8.33 | 0.33 | 3.42 | 1.26 | 2.30 | 6.28 | 14 | 5 | 26% | 19 |
| n-propylbenzene (ppbV) | 1.53 | 0.64 | 1.03 | 0.84 | 0.94 | 1.21 | 7 | 12 | 63% | 19 |
| o-xylene (ppbV) | 2.17 | 0.42 | 1.27 | 0.75 | 1.13 | 1.82 | 14 | 5 | 26% | 19 |
| Propane (ppbV) | 77.66 | 0.32 | 23.38 | 5.88 | 10.83 | 34.15 | 18 | 1 | 5% | 19 |
| Propene (ppbV) | 15.11 | 0.41 | 4.16 | 0.63 | 1.07 | 9.15 | 14 | 5 | 26% | 19 |
| Toluene (ppbV) | 10.93 | 0.37 | 4.96 | 3.33 | 5.03 | 6.68 | 17 | 2 | 11% | 19 |
| Undecane (ppbV) | 5.09 | 1.59 | 3.16 | | | | 3 | 16 | 84% | 19 |

| Boulder - VOC Lumped Species | | | | | | | | | | |
|---|---|---|---|---|---|---|---|---|---|---|
| **Compound** | **Max** | **Min** | **Mean** | **Q1** | **Q2** | **Q3** | **N** | **ND** | **%ND** | **N+ND** |
| Aromatics (ppbV) | 258.80 | 2.87 | 124.70 | 48.49 | 118.70 | 201.20 | 19 | 0 | 0% | 19 |
| Isoparaffins (ppbV) | 468.90 | 1.22 | 132.10 | 37.23 | 75.23 | 215.40 | 18 | 1 | 5% | 19 |
| Napthlenes (ppbV) | 87.24 | 2.85 | 32.76 | 8.94 | 13.67 | 71.24 | 17 | 2 | 11% | 19 |
| Olefins (ppbV) | 77.76 | 0.91 | 24.71 | 8.25 | 14.62 | 42.03 | 18 | 1 | 5% | 19 |
| Oxygenates (ppbV) | 409.30 | 1.97 | 132.50 | 45.55 | 77.53 | 237.70 | 17 | 2 | 11% | 19 |
| Paraffins (ppbV) | 810.80 | 0.79 | 241.40 | 61.01 | 112.60 | 378.20 | 19 | 0 | 0% | 19 |
| Total Identified (ppbC) | 1913.00 | 9.17 | 829.40 | 272.60 | 795.10 | 1230.00 | 19 | 0 | 0% | 19 |

**Table 4-18**. VOC summary statistics based on values above MDL for samples collected at the Sodar site.

| Sodar – VOC Species | | | | | | | | | | |
|---|---|---|---|---|---|---|---|---|---|---|
| **Compound** | **Max** | **Min** | **Mean** | **Q1** | **Q2** | **Q3** | **N** | **ND** | **%ND** | **N+ND** |
| 1,2,3-Trimethylbenzene (ppbV) | 1.09 | 1.09 | 1.09 | | | | 1 | 7 | 88% | 8 |
| 1,2,4-Trimethylbenzene (ppbV) | 1.63 | 1.63 | 1.63 | | | | 1 | 7 | 88% | 8 |
| 1,3,5-Trimethylbenzene (ppbV) | 0.86 | 0.86 | 0.86 | | | | 1 | 7 | 88% | 8 |
| 1-Butene (ppbV) | 1.36 | 0.97 | 1.16 | | | | 2 | 6 | 75% | 8 |
| 1-Hexene (ppbV) | 1.64 | 1.64 | 1.64 | | | | 1 | 7 | 88% | 8 |
| 2,2,4-Trimethylpentane (ppbV) | 0.67 | 0.67 | 0.67 | | | | 1 | 7 | 88% | 8 |
| 2,3,4-Trimethylpentane (ppbV) | 2.38 | 2.38 | 2.38 | | | | 1 | 7 | 88% | 8 |
| 2,4-Dimethylpentane (ppbV) | 2.24 | 0.76 | 1.45 | 0.97 | 1.49 | 1.70 | 6 | 2 | 25% | 8 |
| 2-Methyl-1-butene (ppbV) | 0.72 | 0.72 | 0.72 | | | | 1 | 7 | 88% | 8 |
| 2-Methyl-1-heptene (ppbV) | 0.95 | 0.95 | 0.95 | | | | 1 | 7 | 88% | 8 |
| 2-Methyl-1hexene (ppbV) | 1.70 | 1.70 | 1.70 | | | | 1 | 7 | 88% | 8 |
| 2-Methyl-1-propene, trimer (ppbV) | 1.07 | 1.07 | 1.07 | | | | 1 | 7 | 88% | 8 |
| 2-Methylheptane (ppbV) | 1.18 | 1.18 | 1.18 | | | | 1 | 7 | 88% | 8 |
| 2-Methylhexane (ppbV) | 1.04 | 0.63 | 0.83 | 0.63 | 0.72 | 0.92 | 4 | 4 | 50% | 8 |
| 2-Methylpentane (ppbV) | 4.25 | 0.80 | 2.09 | 1.22 | 2.09 | 2.48 | 7 | 1 | 12% | 8 |
| 3-Ethyl-3-methylpentane (ppbV) | 0.94 | 0.94 | 0.94 | | | | 1 | 7 | 88% | 8 |
| 3-Ethyltoluene (ppbV) | 0.92 | 0.92 | 0.92 | | | | 1 | 7 | 88% | 8 |
| 3-Methylcyclopentene (ppbV) | 1.62 | 1.62 | 1.62 | | | | 1 | 7 | 88% | 8 |
| 3-Methylheptane (ppbV) | 2.73 | 2.73 | 2.73 | | | | 1 | 7 | 88% | 8 |
| 3-Methylhexane (ppbV) | 1.32 | 0.76 | 0.98 | 0.76 | 0.77 | 1.07 | 4 | 4 | 50% | 8 |
| 3-Methylpentane (ppbV) | 9.45 | 0.74 | 2.53 | 0.83 | 1.19 | 1.63 | 6 | 2 | 25% | 8 |
| Acetone (ppbV) | 8.43 | 8.43 | 8.43 | | | | 1 | 7 | 88% | 8 |
| Acetylene (ppbV) | 96.81 | 2.65 | 21.08 | 4.66 | 6.26 | 8.50 | 6 | 2 | 25% | 8 |
| Benzene (ppbV) | 4.65 | 1.80 | 3.07 | 1.88 | 3.29 | 3.78 | 7 | 1 | 12% | 8 |
| C8-C12 Organics (6) (ppbV) | 11.34 | 11.34 | 11.34 | | | | 1 | 7 | 88% | 8 |
| Cyclohexane (ppbV) | 4.02 | 0.90 | 2.03 | 0.91 | 1.64 | 2.56 | 8 | 0 | 0% | 8 |
| Cyclopentane (ppbV) | 0.98 | 0.52 | 0.75 | 0.70 | 0.72 | 0.98 | 5 | 3 | 38% | 8 |
| Ethane (ppbV) | 105.90 | 30.57 | 62.16 | 46.32 | 59.42 | 80.45 | 7 | 1 | 12% | 8 |
| Ethene (ppbV) | 9.98 | 1.71 | 4.69 | 1.81 | 2.69 | 6.04 | 6 | 2 | 25% | 8 |
| Ethylbenzene (ppbV) | 0.50 | 0.50 | 0.50 | | | | 1 | 7 | 88% | 8 |
| i-Butane (ppbV) | 18.01 | 5.02 | 12.06 | 7.52 | 12.85 | 15.22 | 7 | 1 | 12% | 8 |
| i-Pentane (ppbV) | 11.42 | 3.07 | 7.04 | 4.99 | 6.81 | 9.47 | 7 | 1 | 12% | 8 |
| m,p-xylene (ppbV) | 4.79 | 1.04 | 2.51 | 2.14 | 2.27 | 4.79 | 5 | 3 | 38% | 8 |
| Methylcyclohexane (ppbV) | 7.33 | 1.54 | 3.79 | 1.57 | 4.04 | 4.94 | 7 | 1 | 12% | 8 |
| n-Butane (ppbV) | 19.24 | 5.89 | 12.99 | 8.76 | 13.86 | 17.02 | 7 | 1 | 12% | 8 |
| n-Decane (ppbV) | 1.10 | 1.10 | 1.10 | | | | 1 | 7 | 88% | 8 |
| n-Heptane (ppbV) | 2.26 | 0.54 | 1.24 | 0.65 | 1.30 | 1.78 | 7 | 1 | 12% | 8 |
| n-Hexane (ppbV) | 3.76 | 0.93 | 2.25 | 1.30 | 2.57 | 2.85 | 7 | 1 | 12% | 8 |
| n-Nonane (ppbV) | 1.36 | 0.67 | 0.94 | | | | 3 | 5 | 62% | 8 |
| n-Octane (ppbV) | 1.97 | 0.40 | 1.14 | 0.83 | 1.10 | 1.97 | 5 | 3 | 38% | 8 |
| n-Pentane (ppbV) | 6.59 | 1.10 | 4.23 | 1.97 | 3.94 | 5.35 | 8 | 0 | 0% | 8 |
| o-xylene (ppbV) | 1.06 | 0.44 | 0.71 | | | | 3 | 5 | 62% | 8 |
| Propane (ppbV) | 81.00 | 16.30 | 50.19 | 23.82 | 49.13 | 79.28 | 7 | 1 | 12% | 8 |
| Propene (ppbV) | 10.49 | 1.62 | 6.06 | | | | 2 | 6 | 75% | 8 |
| Toluene (ppbV) | 7.36 | 0.80 | 4.34 | 2.08 | 4.76 | 5.82 | 8 | 0 | 0% | 8 |

| Sodar – VOC Lumped Species | | | | | | | | | | |
|---|---|---|---|---|---|---|---|---|---|---|
| **Compound** | **Max** | **Min** | **Mean** | **Q1** | **Q2** | **Q3** | **N** | **ND** | **%ND** | **N+ND** |
| Aromatics (ppbV) | 193.30 | 20.97 | 76.24 | 28.38 | 56.92 | 91.50 | 8 | 0 | 0% | 8 |
| Isoparaffins (ppbV) | 316.90 | 10.31 | 131.40 | 51.27 | 102.20 | 155.40 | 8 | 0 | 0% | 8 |
| Napthlenes (ppbV) | 80.35 | 16.18 | 39.39 | 17.10 | 30.11 | 52.33 | 8 | 0 | 0% | 8 |
| Olefins (ppbV) | 217.10 | 14.74 | 52.35 | 17.01 | 29.82 | 35.84 | 8 | 0 | 0% | 8 |
| Oxygenates (ppbV) | 25.30 | 25.30 | 25.30 | | | | 1 | | 0% | 1 |
| Paraffins (ppbV) | 542.10 | 7.62 | 341.50 | 190.00 | 395.60 | 455.20 | 8 | 0 | 0% | 8 |
| Total Identified (ppbC) | 1295.00 | 115.00 | 668.00 | 312.40 | 648.40 | 840.60 | 8 | 0 | 0% | 8 |

**Table 4-19**. Summary of carbonyl data.

| Jonah - Carbonyls | | | | | | | | | | |
|---|---|---|---|---|---|---|---|---|---|---|
| **Compound** | **Max** | **Min** | **Mean** | **Q1** | **Q2** | **Q3** | **N** | **ND** | **%ND** | **N+ND** |
| Acetaldehyde (ppbV) | 2.30 | 0.78 | 1.33 | 0.83 | 1.14 | 1.64 | 12 | 1 | 8% | 13 |
| Acetone (ppbV) | 7.55 | 1.17 | 3.61 | 2.66 | 3.19 | 4.79 | 13 | 0 | 0% | 13 |
| Butyraldehyde (ppbV) | 2.31 | 0.39 | 1.32 | 0.55 | 1.03 | 2.24 | 7 | 6 | 46% | 13 |
| Crotonaldehyde (ppbV) | 2.91 | 1.04 | 1.91 | | | | 3 | 10 | 77% | 13 |
| Formaldehyde (ppbV) | 5.79 | 1.29 | 2.74 | 1.79 | 2.33 | 3.39 | 13 | 0 | 0% | 13 |
| o-Tolualdehyde (ppbV) | 0.81 | 0.81 | 0.81 | | | | 1 | 12 | 92% | 13 |
| **Boulder - Carbonyls** | | | | | | | | | | |
| **Compound** | **Max** | **Min** | **Mean** | **Q1** | **Q2** | **Q3** | **N** | **ND** | **%ND** | **N+ND** |
| Acetaldehyde (ppbV) | 2.65 | 0.61 | 1.31 | 0.76 | 1.33 | 1.42 | 16 | 3 | 16% | 19 |
| Acetone (ppbV) | 9.38 | 0.23 | 3.76 | 2.59 | 3.25 | 5.24 | 19 | 0 | 0% | 19 |
| Butyraldehyde (ppbV) | 7.17 | 0.58 | 3.13 | 1.31 | 2.16 | 4.63 | 10 | 9 | 47% | 19 |
| Crotonaldehyde (ppbV) | 2.66 | 1.14 | 1.81 | 1.29 | 1.30 | 2.66 | 5 | 14 | 74% | 19 |
| Formaldehyde (ppbV) | 8.08 | 0.49 | 3.01 | 1.94 | 2.37 | 4.84 | 17 | 2 | 11% | 19 |
| p-Tolualdehyde (ppbV) | 2.85 | 2.85 | 2.85 | | | | 1 | 18 | 95% | 19 |
| Valeraldehyde (ppbV) | 0.78 | 0.69 | 0.74 | | | | 2 | 17 | 89% | 19 |

Average NMOC sample composition by site is summarized in Figure 4-37. As in previous years, the TNMHC concentrations are highest at Jonah with concentrations at Boulder just one third of the Jonah average and Sodar slightly lower than Boulder. Paraffins and isoparaffins dominate the sample composition at each site, consistent with the strong influence of natural gas sources. Olefin content is low at all sites but the Sodar site has more than double the fraction observed at Jonah and Boulder. Aromatics (with napthlenes) sample fractions are nearly identical at all three sites at just under 20%. C8 – C12 organics average over 20% of TNMHC at Boulder but are approximately 10% or less at Jonah and Sodar. This, together with the higher oxygenate content, accounts for most of the lower paraffin percentage at Boulder. Unidentified TNMHC is minimal in these samples, averaging approximately 10% at Boulder and Jonah and just over 5% at the Sodar site.

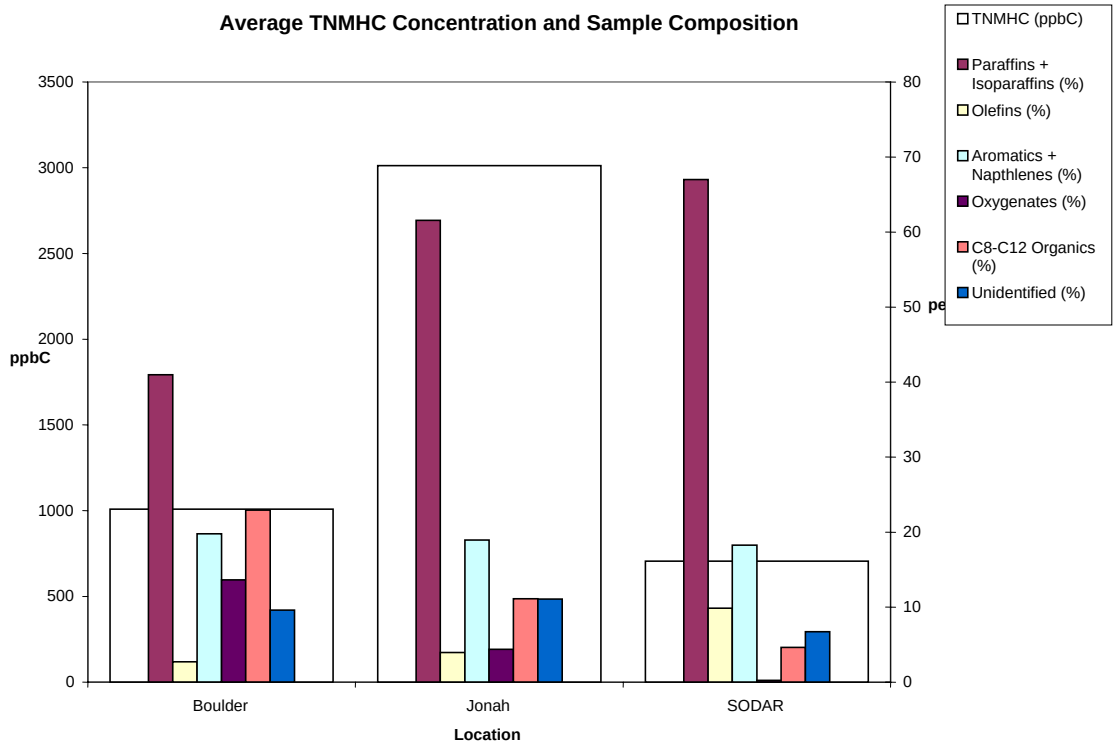


**Figure 4-37**. TNMHC concentrations (wide light blue bars) and average NMHC sample compositions by sampling location.

Figure 4-38 summarizes NMHC sample composition as a function of time of day: samples collected during the morning (06:00 – 11:00 MST) are compared with samples collected during the afternoon (13:00 – 18:00 MST). Afternoon TNMHC concentrations are lower reflecting enhance ventilation during the afternoon hours. Morning and afternoon sample compositions are similar with the exception that C8-C12 organics fractions are higher in the afternoon samples Unidentified NMHC is also higher in the afternoon, consistent with the lower TNMHC concentrations.

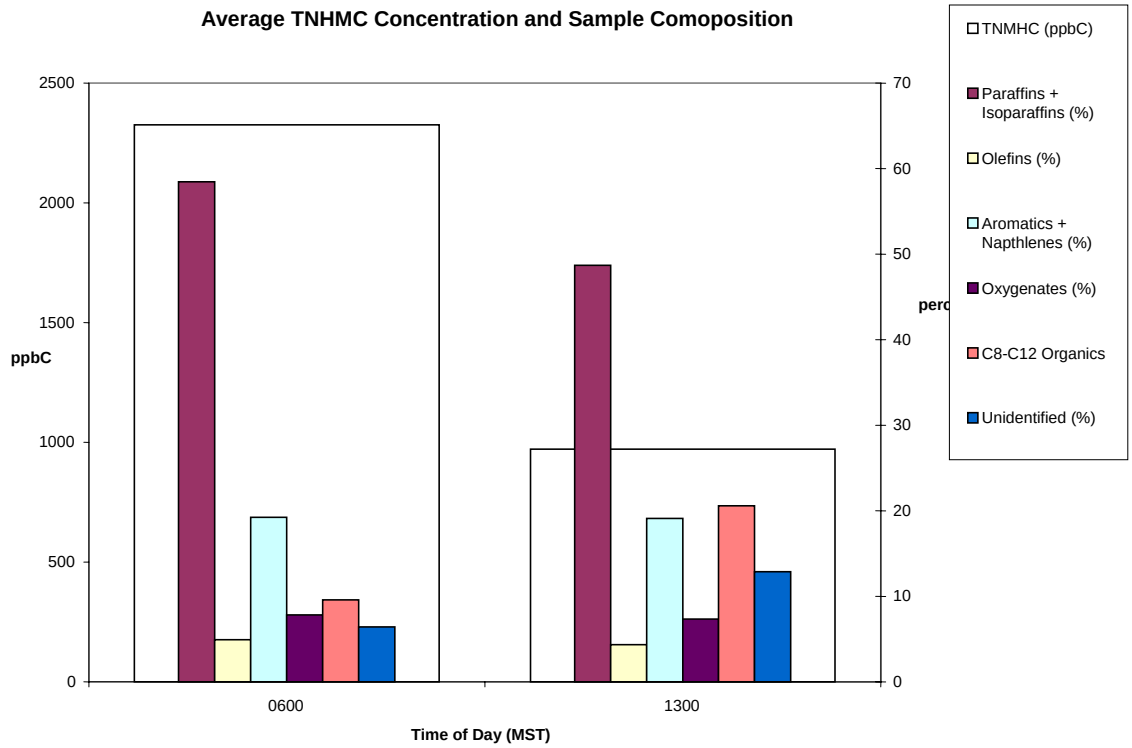


**Figure 4-38.** TNMHC concentrations (wide light blue bars) and average NMHC sample composition by sampling time (6:00 – 11:00 and 13:00 – 18:00 MST) based on data from all sampling locations.

Average contributions of individual species to paraffins, olefins, aromatics and oxygenates at each monitoring site are summarized in Figure 4-39; only species averaging greater than 0.5% contribution to each lumped species group are listed in this figure. Paraffin contents are generally consistent across all three locations with propane and ethane being the biggest species. Olefins consist primarily of propene, ethene and acetylene with much higher acetylene content at the Sodar site suggesting the presence of a nearby source. Aromatics consist mostly of toluene, m,p-xylene and benzene. Major oxygenate species vary from site to site; oxygenate content at the Sodar site was negligible (Figure 4-37). The higher oxygenate content of the Boulder samples appears to be due in part to ethanol but ethanol was not observed at Jonah. Given problems with ethanol contamination noted in Section 3, these results appear unlikely to be representative of actual ethanol levels at Boulder.

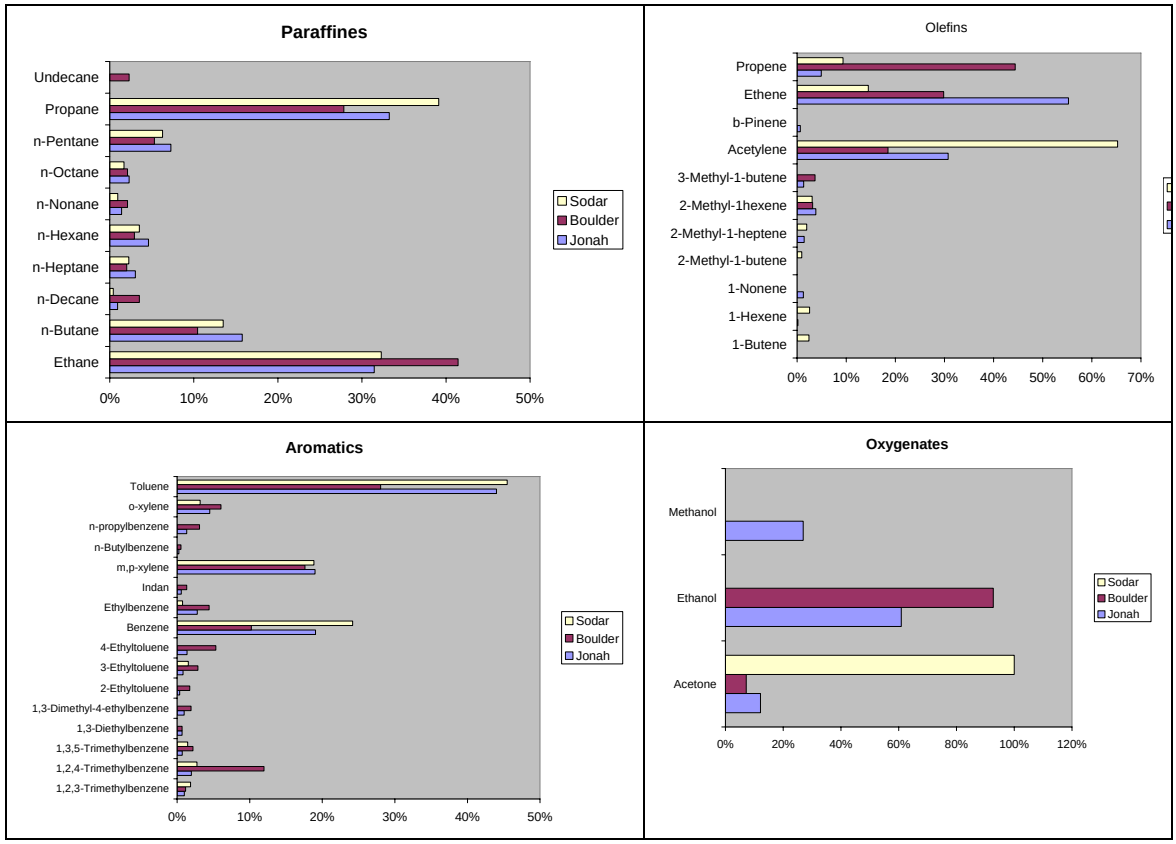


**Figure 4-39**. Average contributions of individual NMHC species to species groups (only species contributing more than 0.5% to each lumped species group are listed).

Average concentrations of the most commonly observed NMOC species are compared in Figure 4-40. Only species observed above the MDL in at least 75% of samples collected at Jonah are included in this figure. As in 2008, light alkanes are most common but in 2009, with proper identification of the toluene peak, it is clear that toluene is a notable exception to the preponderance of alkanes in these data. Acetylene concentrations are noticeably higher than would otherwise be expected at the Sodar site whereas other motor fuel combustion byproducts are not, suggesting a possible local source such as welding.

A comparison of median NMHC composition from the 2009 data collected at Jonah and Boulder is presented in Figure 4-41 (values from data collected at the SODAR site are not included here due to the limited number of samples collected at this site). Alkanes at Boulder are more heavily skewed towards i-pentane as compared to Jonah.

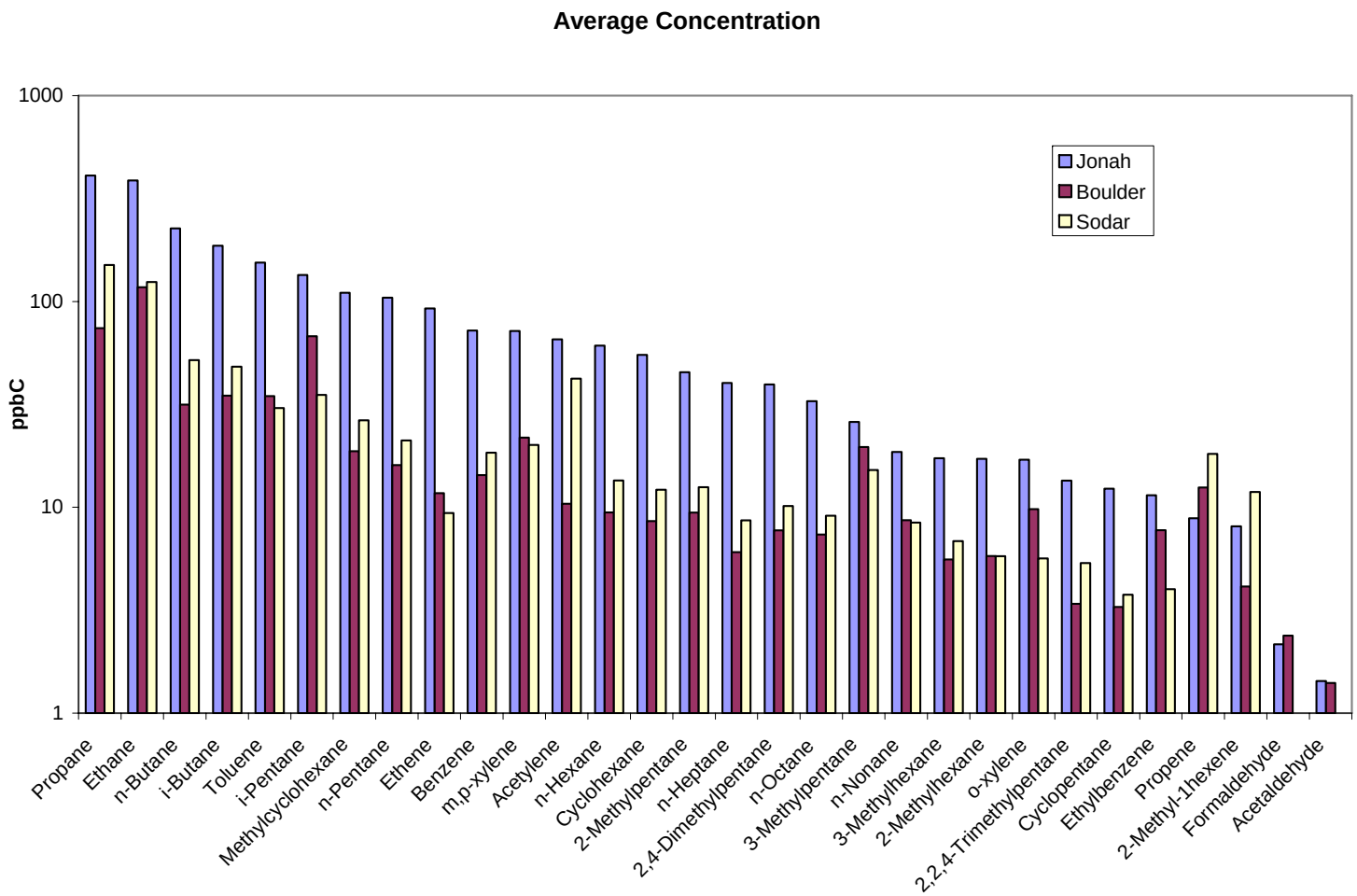


**Figure 4-40.** Average concentrations of most common NMOC species at each monitoring location (species listed are those detected in at least 75% of all samples collected at Jonah).

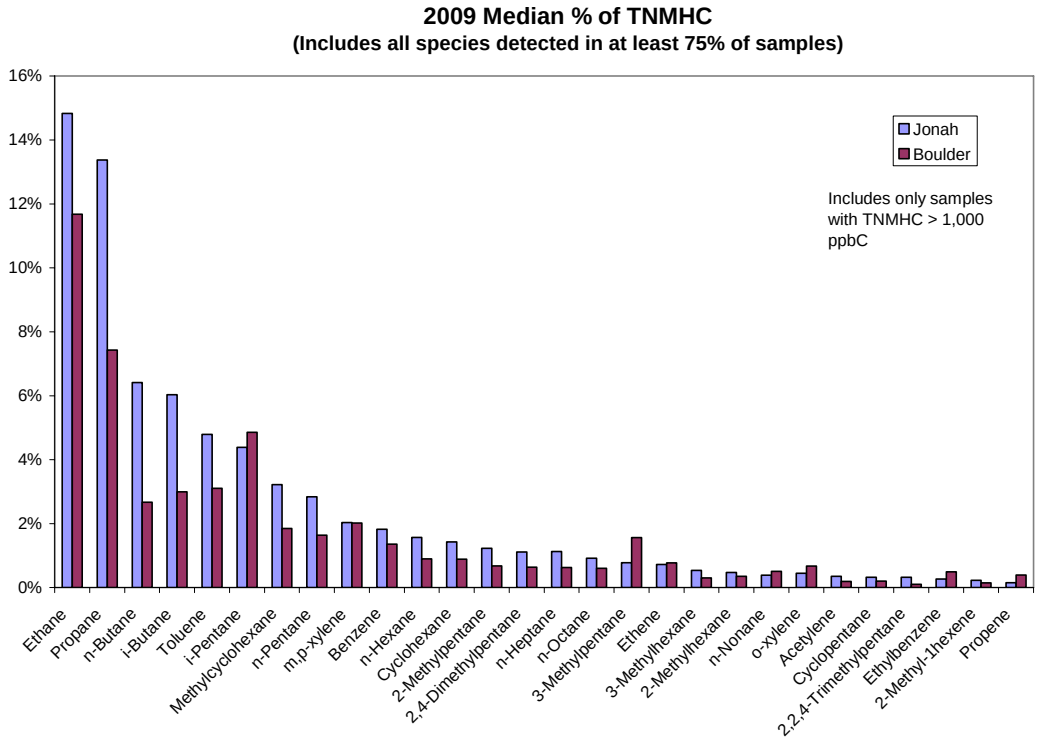


**Figure 4-41.** Comparison of median NMHC percent composition at Jonah and Boulder from 2009 data (values from the SODAR site not shown due to limited sample size).

## Comparison of NMOC between 2008 and 2009

A comparison of TNMHC concentrations at Jonah and Boulder measured during the 2008 and 2009 field studies in presented in the form of box plots in Figure 4-42 Box plots provide a concise summary of the key features of the statistical distribution of these data: a key to the box plot symbols is provided in Figure 4-43. Average and median TNMHC concentrations were similar in both years although the upper extreme concentrations were higher in 2008, consistent with the stronger inversions and lower mixing heights during some of the 2008 IOP days.

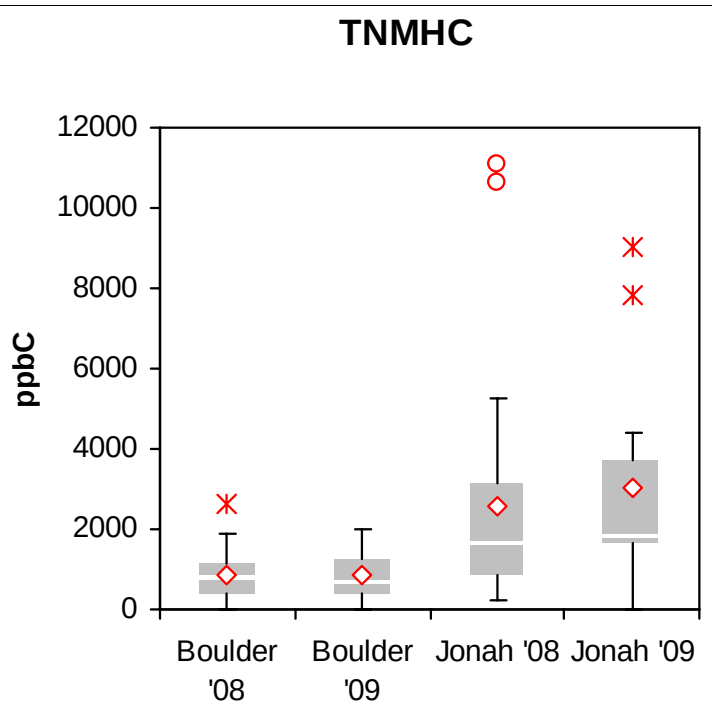


**Figure 4-42.** Box plot comparison of TNMHC concentrations in 2008 and 2009 at Boulder and Jonah.

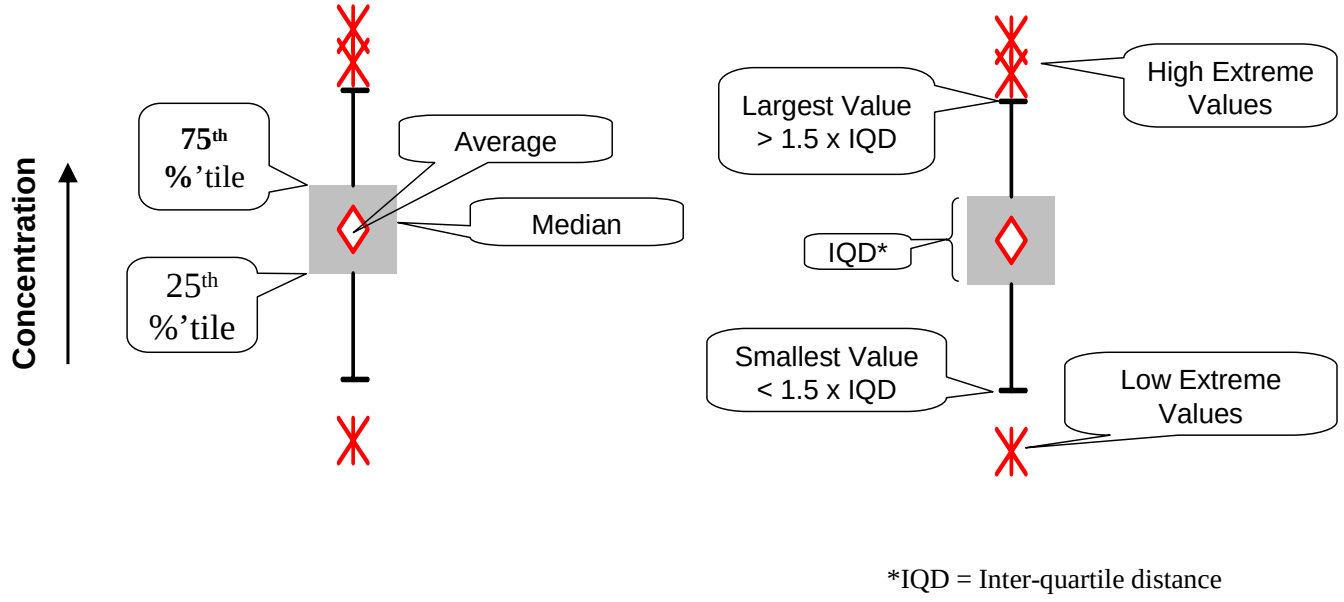


**Figure 4-43.** Key to box plot symbols used in Figure 4- 42.

Average composition of NMOC at Jonah and Boulder during 2008 and 2009 is presented in Figure 4-44. Compositions are roughly similar between the two years with the exception of greater fractions of ethene, m,p-xylene and toluene in 2009 at both locations and considerably more i-pentane (and 3-methylpentane) present at Boulder in 2009 as compared to 2008, consistent with the comparison of NMHC compositions from the 2009 data at Jonah and Boulder shown in Figure 4-41

As NMOC species vary greatly in the degree to which they participate in photochemical reactions, a comparison of average concentrations with reactivity weighted concentrations is instructive. Figures 4-45 and 4-46 present such a comparison using maximum incremental reactivity (MIR) weighted concentrations for the most common NMOC species observed at Jonah and Boulder, respectively. Ethene is the most abundant species on a reactivity weighted basis at Jonah although concentrations are low relative to the less reactive light alkanes. Toluene and xylenes are relatively abundant and more reactive than the light alkanes at both sites resulting in higher reactivity weighted concentrations.

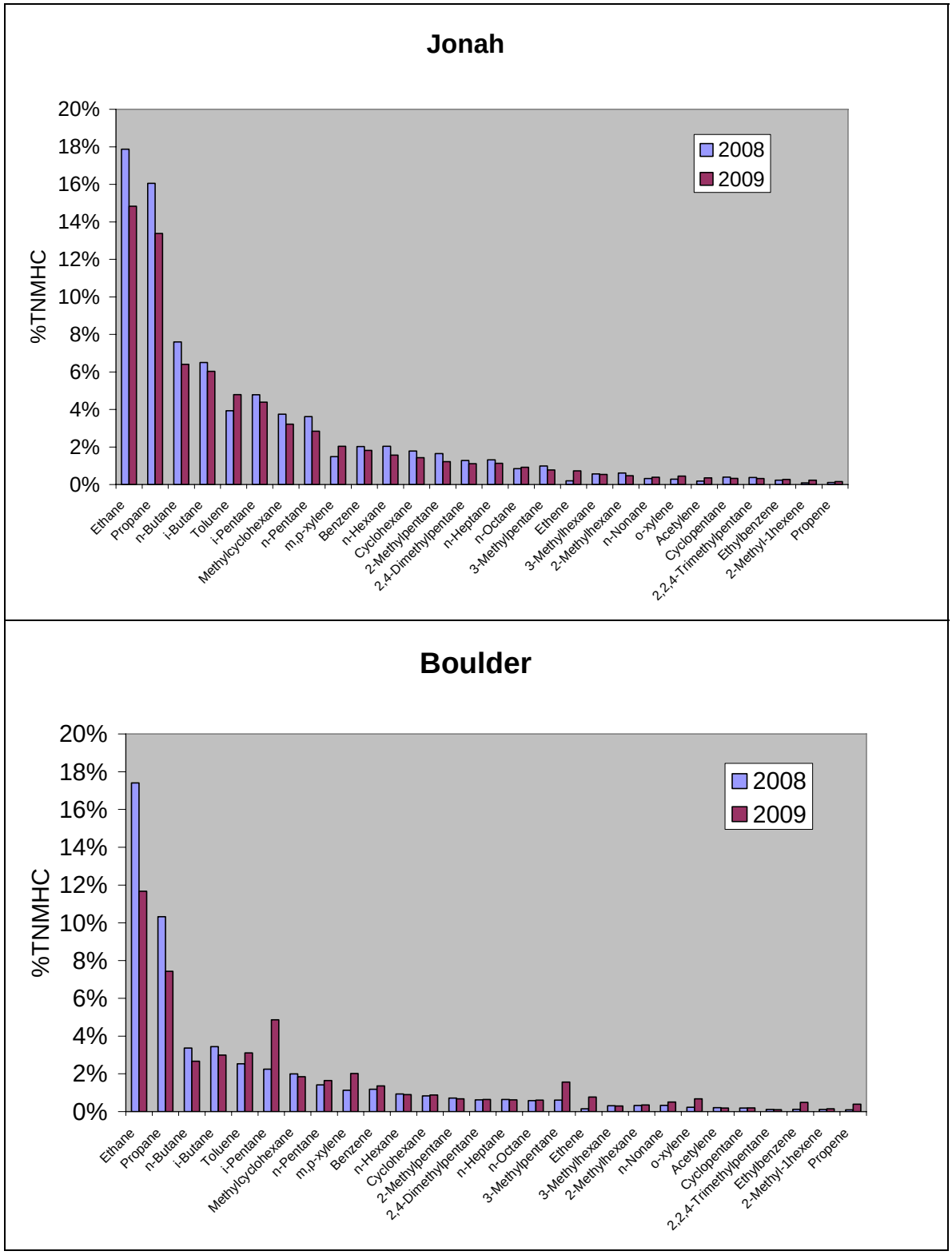


**Figure 4-44.** Average NMHC composition of most abundant species at Jonah (top) and Boulder (bottom) in 2008 as compared to 2009.

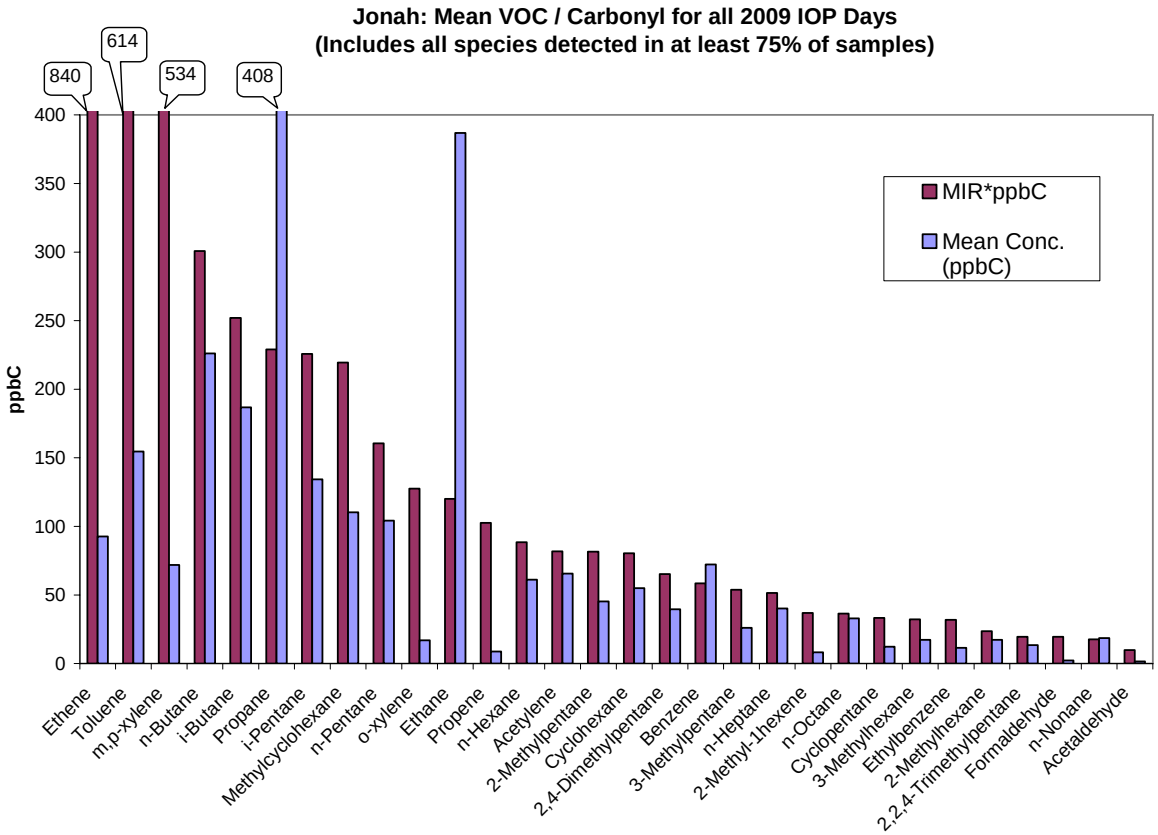


**Figure 4-45.** Comparison of average maximum incremental reactivity (MIR) weighted concentrations average concentrations and of most common NMOC species at Jonah (species listed are those detected in at least 75% of all samples collected at Jonah).

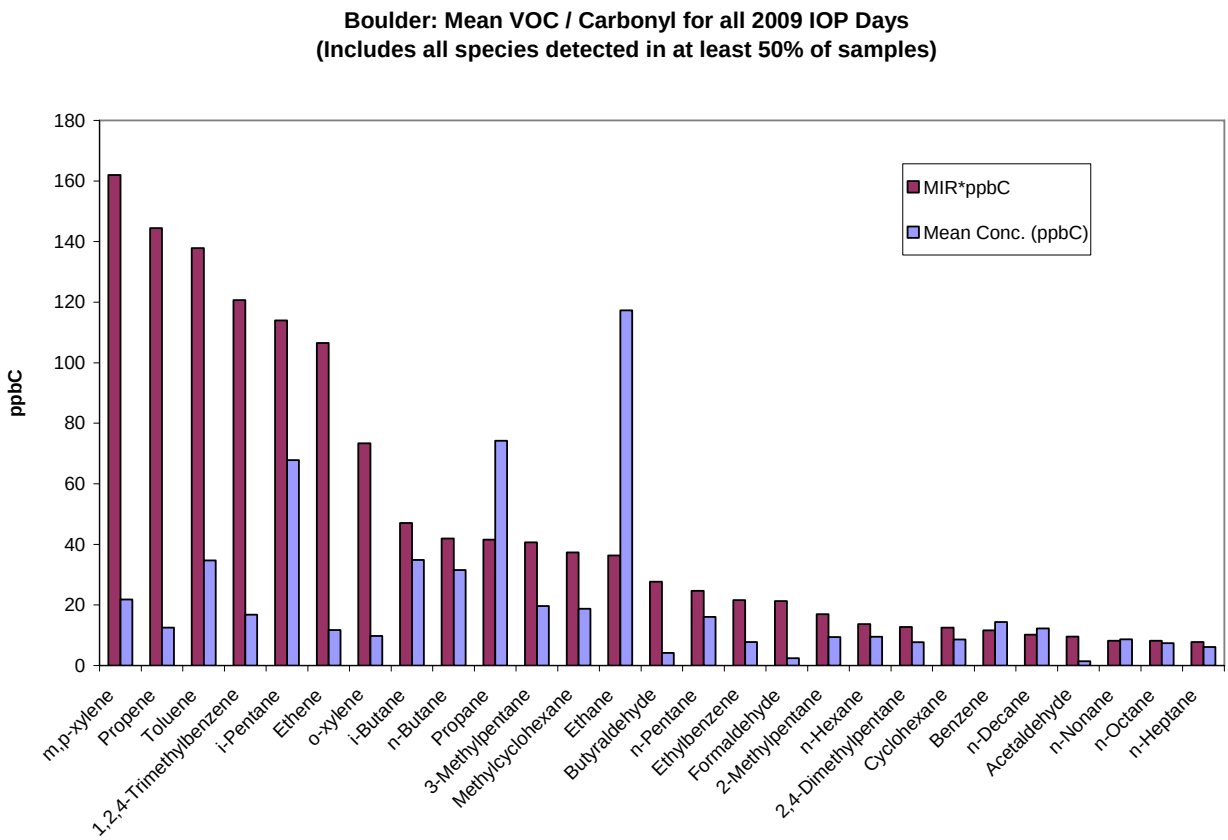


**Figure 4-46.** Comparison of average concentrations and average maximum incremental reactivity (MIR) weighted concentrations of most common NMOC species at Boulder (species listed are those detected in at least 50% of all samples collected at Boulder).

### 4.5.2 Analysis of Methane Data

As indicated in Table 4-11, a total of 24 canister samples collected during IOP #2 and #3 were analyzed for methane ($CH_4$) via EPA Method TO-11 in addition to the usual NMHC analysis. Examination of the $CH_4$ portion of the TOG (Figure 4-47) reveals a $CH_4$ background level of just over 1,500 ppb, roughly consistent with expected global background levels (Warneck, 2000). Apart from this background concentration, local organic compound emission sources average roughly 50% $CH_4$ as a percent of TOG in ppbC.

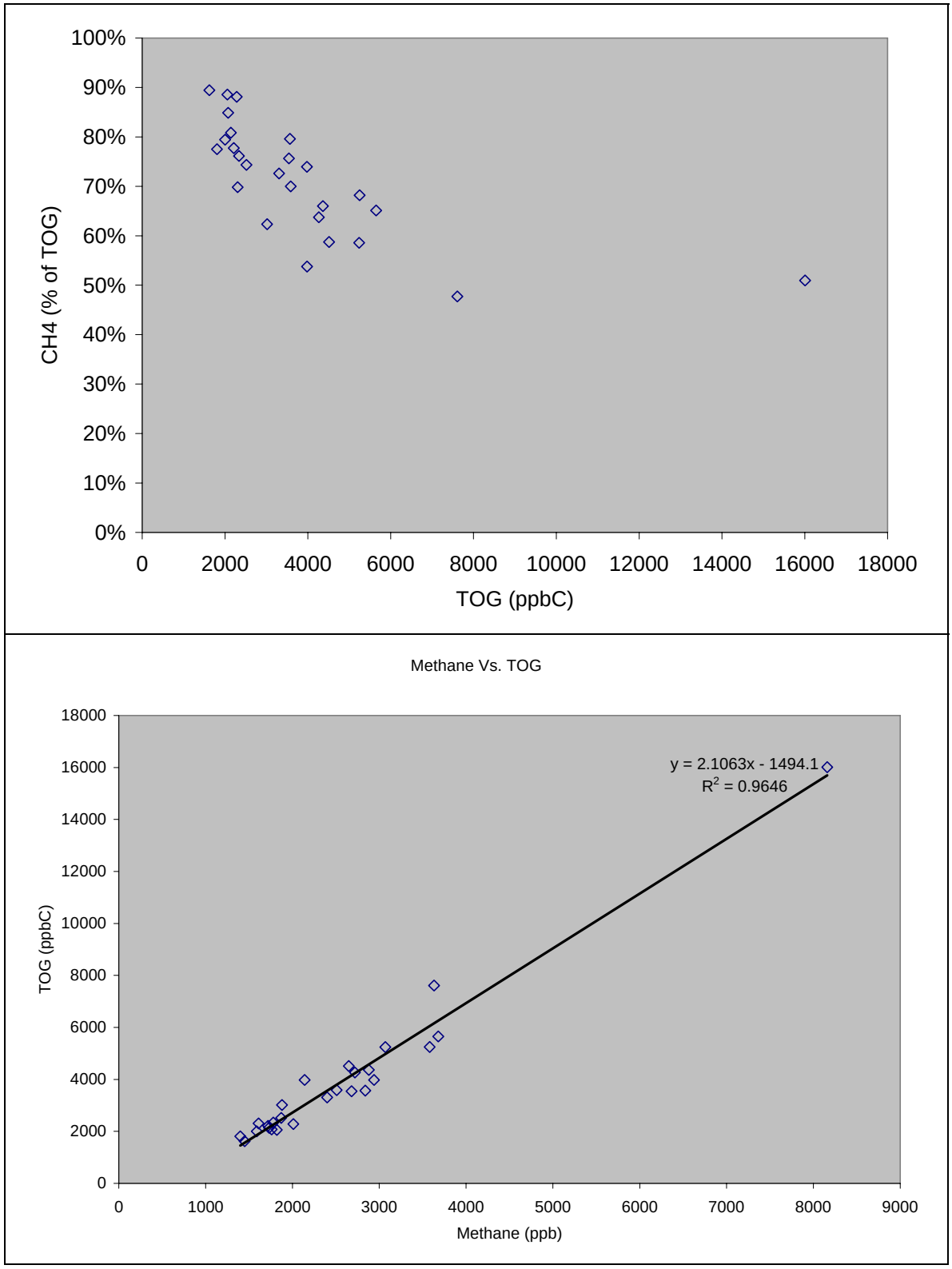


**Figure 4-47.** Methane as a percent of TOG (top panel) and regressed against TOG (bottom panel).

### 4.5.3 Analysis of NOy and NO2 and PAN Measurements

While a detailed analysis of the comparison of $NO_2$ measured by $NO_x$ chemiluminescence and gas chromatography is beyond the scope of this measurement project, the comparison is of interest, particularly during elevated ozone episodes. As an example, Figure 48 plots the concentrations of $NO_2$ from the chemiluminescent analyzer vs that from the gas chromatograph on the IOP day of March 1, 2009. The slope is 1.35, indicating that the gas chromatograph concentrations are significantly lower than those from the chemiluminescent analyzer. The linearity of this plot suggests that this bias is similar for the entire day which indicates that the higher chemiluminescent values are not due to positive interference biases from other reactive nitrogen species. Almost identical results were obtained on M arch 2, 2009. The source of this bias would need to be explored via additional field studies in which the uncertainty of the gas chromatographic measurements is reduced by use of a more effective ozone scrubber.

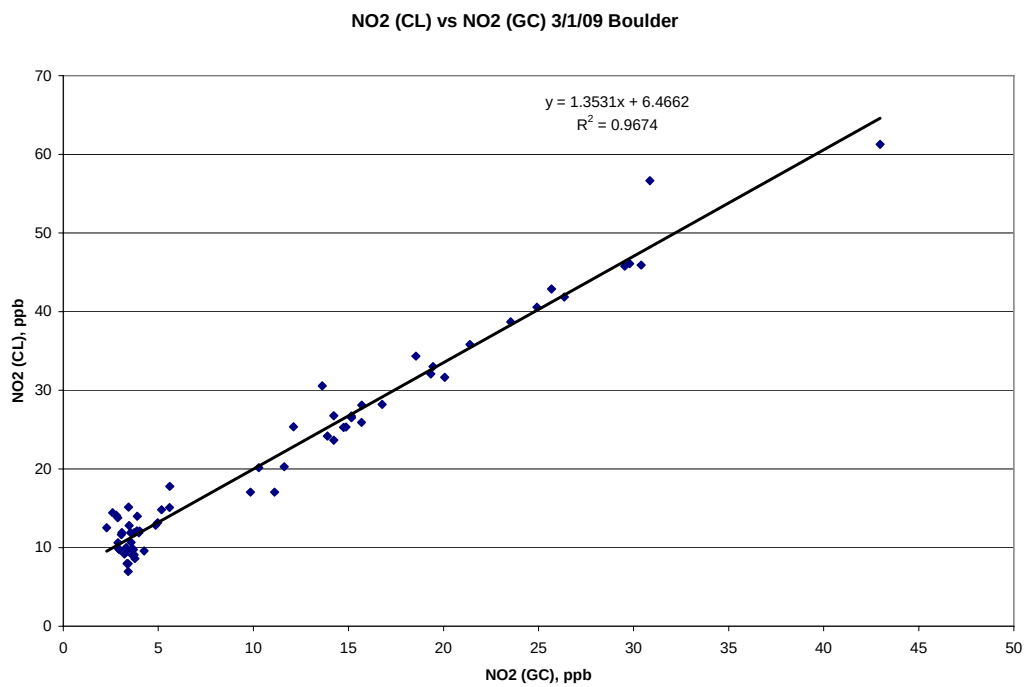


**Figure 4-48**. Comparison of NO2 measured by chemiluminescent NOx analyzer and NO2 gas chromatograph.

The gas chromatographic traces generally showed considerable noise at the time PAN was expected to elute and therefore PAN was near or below the detection limit for much of the measurement period. As a result, data for these measurements were not reported to the data base. However, chromatograms during the three IOP days of February 23 and March 1 and 2 were evaluated manually. Figure 49 shows a chromatogram of a sample during a high ozone period at 16:00 hours on March 1, 2009 in which the PAN concentration was approximately 0.6ppb. A distinct and measureable PAN peak is evident. Similar results were obtained on February 23rd and March 2nd. Figures 4-50 through 4-52 show the time series of PAN measurements during the three IOP days. Note that the PAN concentrations peak in the afternoon and that the concentration reached nearly 1ppb. While this is not a significant amount of the total NOy concentration, these data may be useful in validating photochemical models used to predict ozone formation.

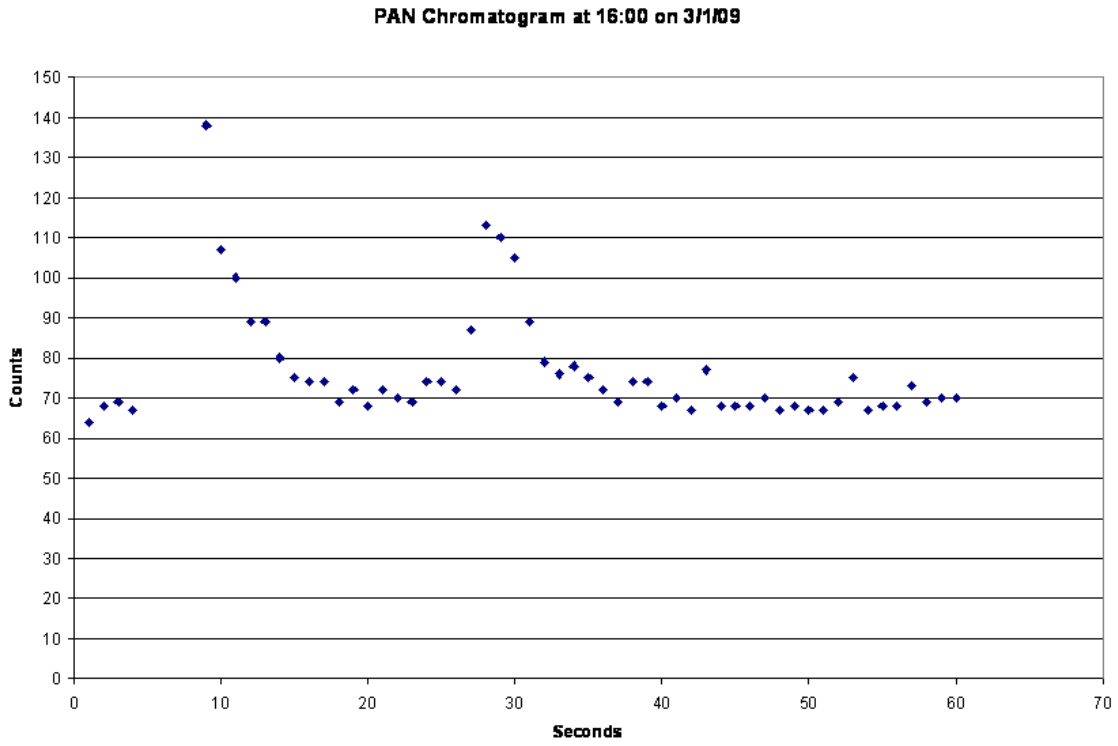


**Figure 4-49**. Chromatogram from sample analyzed at 16:00 hours on 3/1/09 showing distinct PAN peak at 19 seconds.

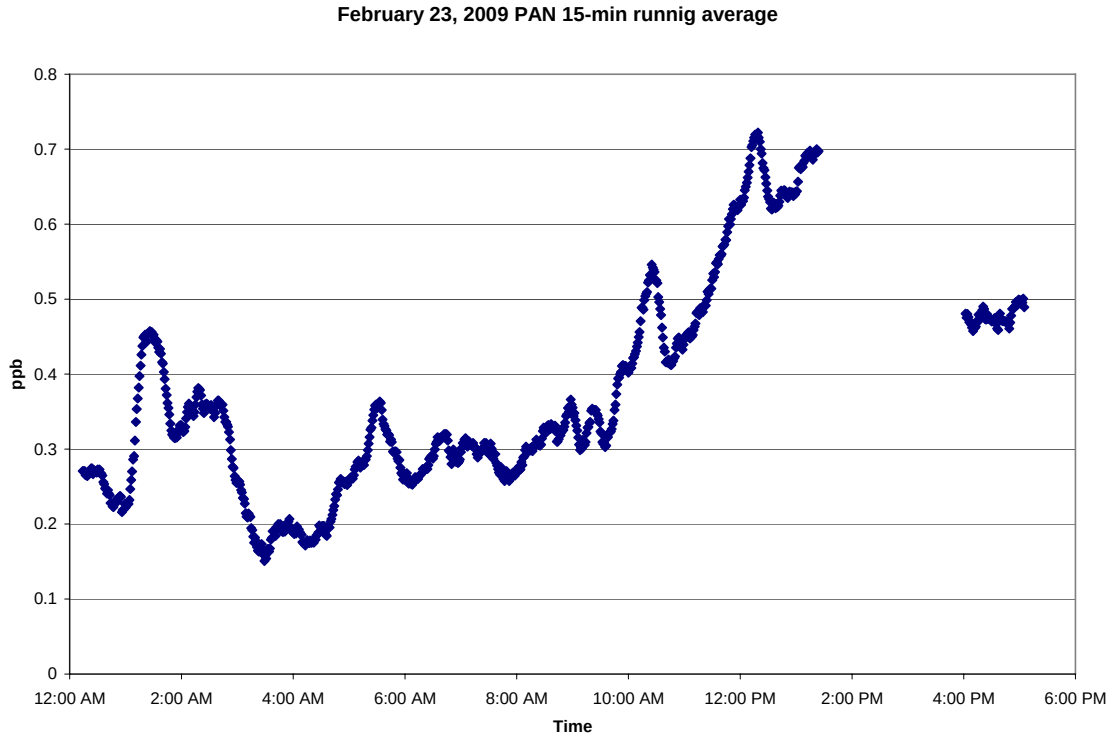


**Figure 54-0.** Time series plot of PAN concentrations on February 23, 2009.

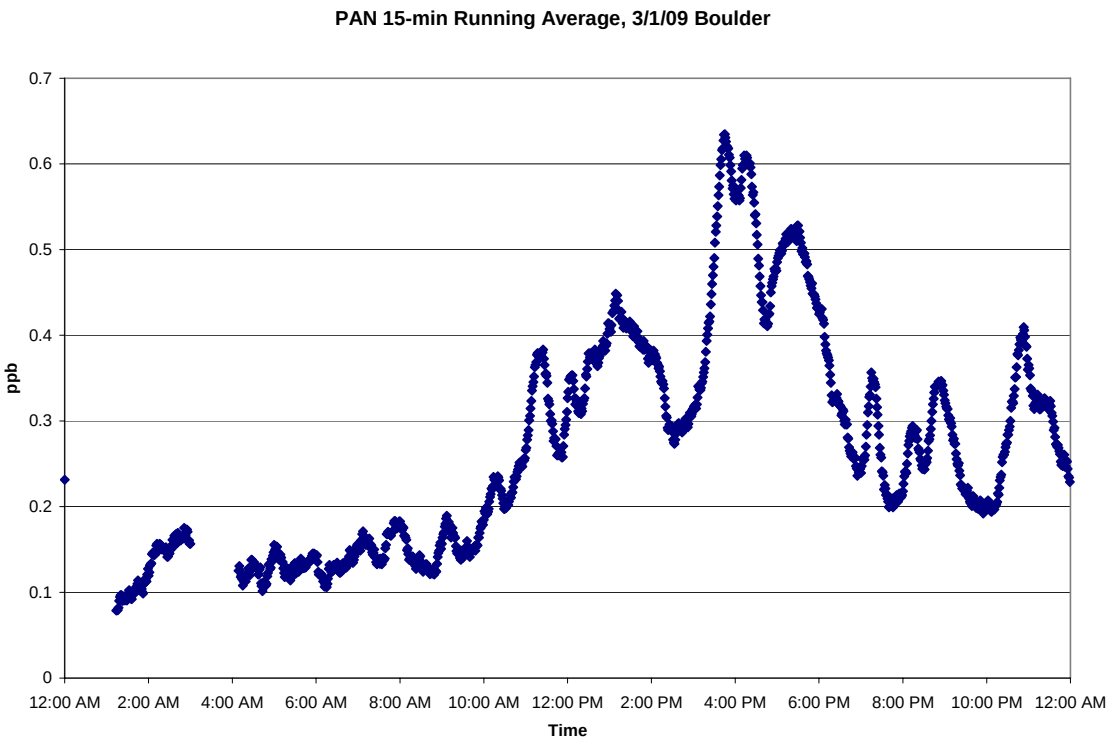


**Figure 4-51.** Time series plot of PAN concentrations on March 1, 2009.

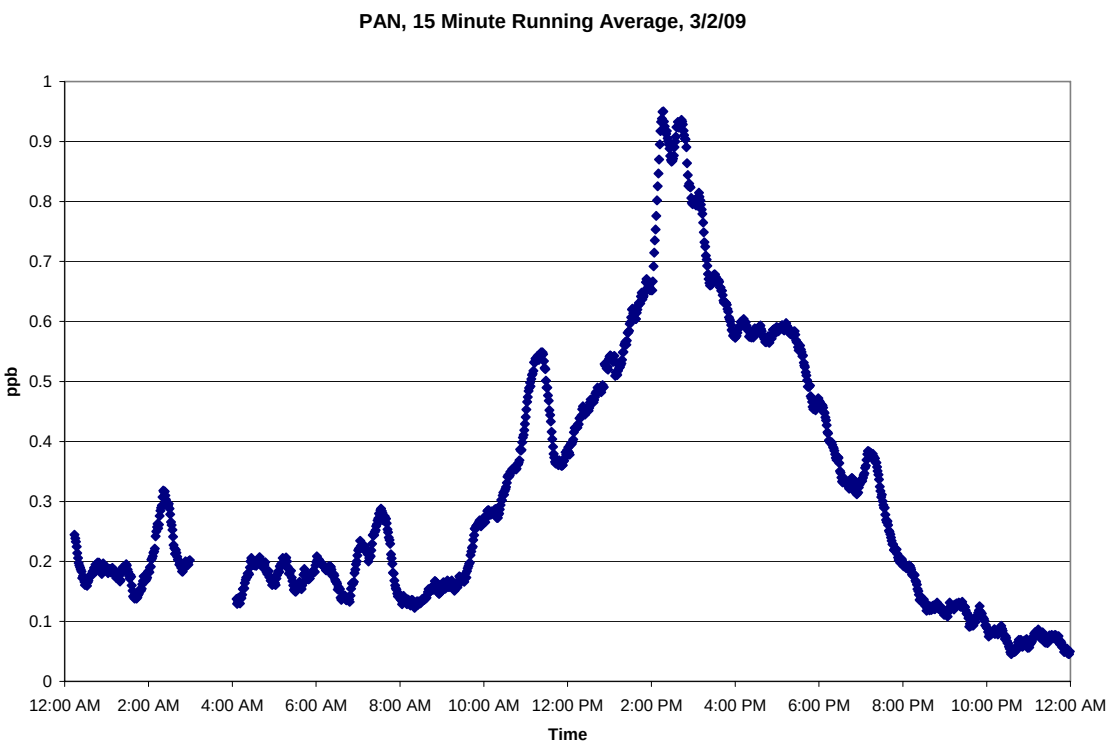


**Figure 4-52.** Time series plot of PAN concentrations on March 2, 2009.

Comparisons of $NO_x$ and $NO_y$ for the entire study period were not made since the $NO_y$ would be expected to be significantly different from $NO_x$ only during periods containing aged photochemical smog. An example comparison for the 1 March IOP day was presented in Section 3.3.5.

#### 4.5.4 Analysis of $NO_2$ Photolysis Measurements

Direct measurements of the $NO_2$ photolysis rate ($k_1$) were made at the Boulder II site as described in Section 2. The $k_1$ apparatus was operated during the following eight days:

February: 21, 22, 28

March: 1, 4, 19, 27, 28

During these periods all of the data were valid. For comparison purposes the data were compared with both modeled $k_1$ based on zenith angle and with the total solar radiometer operated at the site.

Three different models were used for comparison. The first was from Peterson (1976) and the second and third were from Jeffries (1991) at both ground and 640 m above the ground. To do the comparison, the zenith angles were calculated hourly at the site using a web-based calculator: (http://solardat.uoregon.edu/SolarPositionCalculator.html) and entering the time and coordinates of the site. Since we report $k_1$ as 15-minute averages, the $k_1$ values immediately before and after the hour were averaged.

Figure 4-53 compares the measured $k_1$ with that from three different models. In February the agreement between measured and modeled was quite good, while in March the measured values were lower, especially at lower zenith angles.

To determine if these values were lower because of less snow cover or greater cloud cover, the measured $k_1$ values were compared with total solar radiation. Figure 4-54 shows the same four days as Figure 4-53 comparing the $k_1$ measured with the total solar measured at the site. Note that the scales are the same except that $k_1$ is 1000 times lower. In February the two value track each other closely are nearly the same on this scale. In March the $k_1$ values are lower than the total solar on the relative scale and lower than the $k_1$ values in February. This is especially noticeable at the lower zenith angle during mid-day.

Compared to both the modeled $k_1$ and measured total solar the measured $k_1$ values were significantly lower in March. This is most likely due to a change in albedo. It is not likely than the $k_1$ values are in error because:

- Similar $k_1$ values were measured at the CE-CERT environmental chamber before and after the field study.
- The $k_1$ measurement is not dependent on instrument calibration.
- The difference in $k_1$ values was lower at mid-day when compared to both modeled $k_1$ and measured total solar radiation.

We conclude that UV available for photochemical reactions is enhanced by the snow covering the ground, which was much greater in February than in March as evidenced by a significant drop off in reflected UV radiation at Boulder after mid-March (see Figure 4-55).

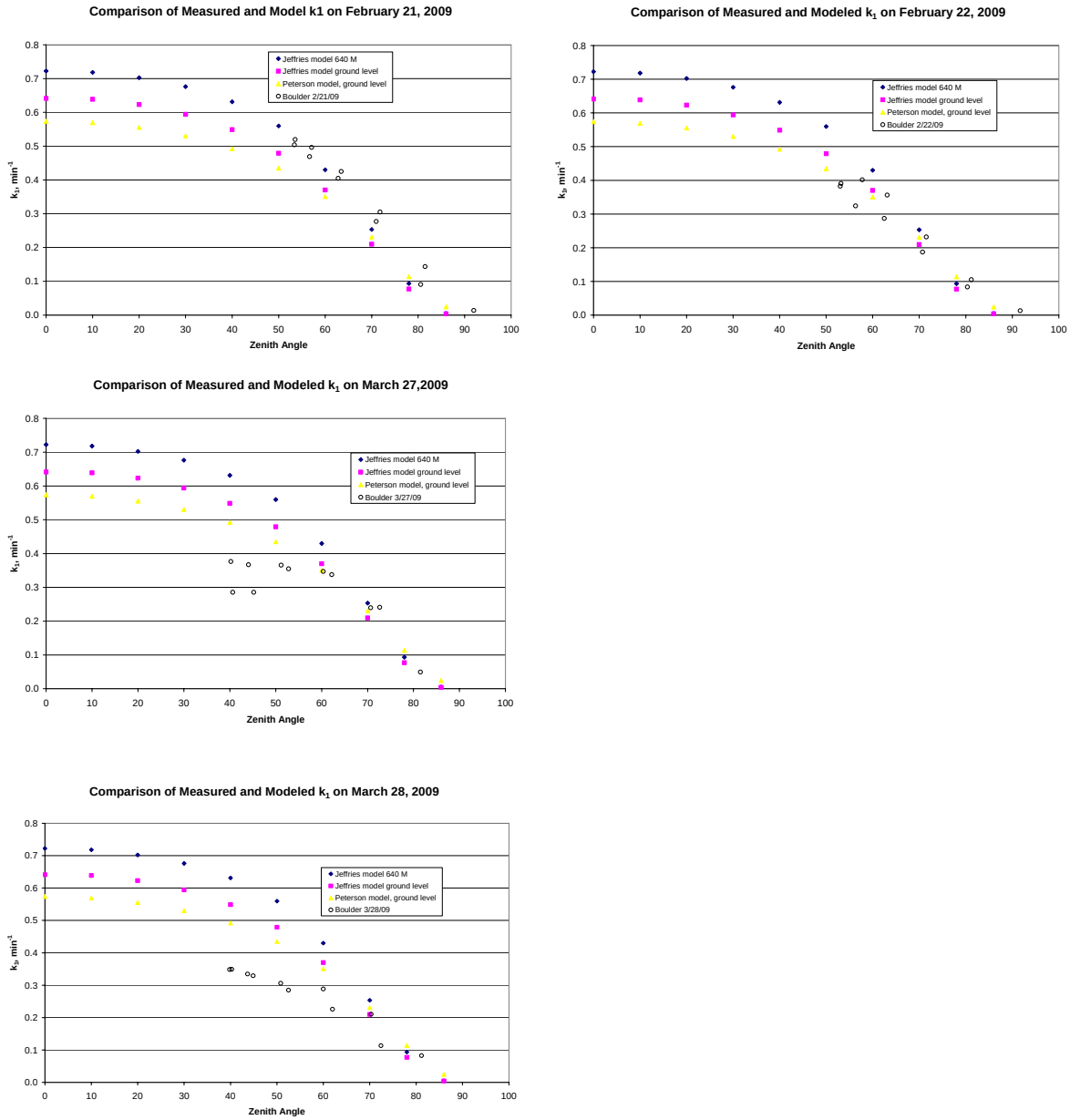


**Figure 4-53.** Comparison of measured and modeled $k_1$.

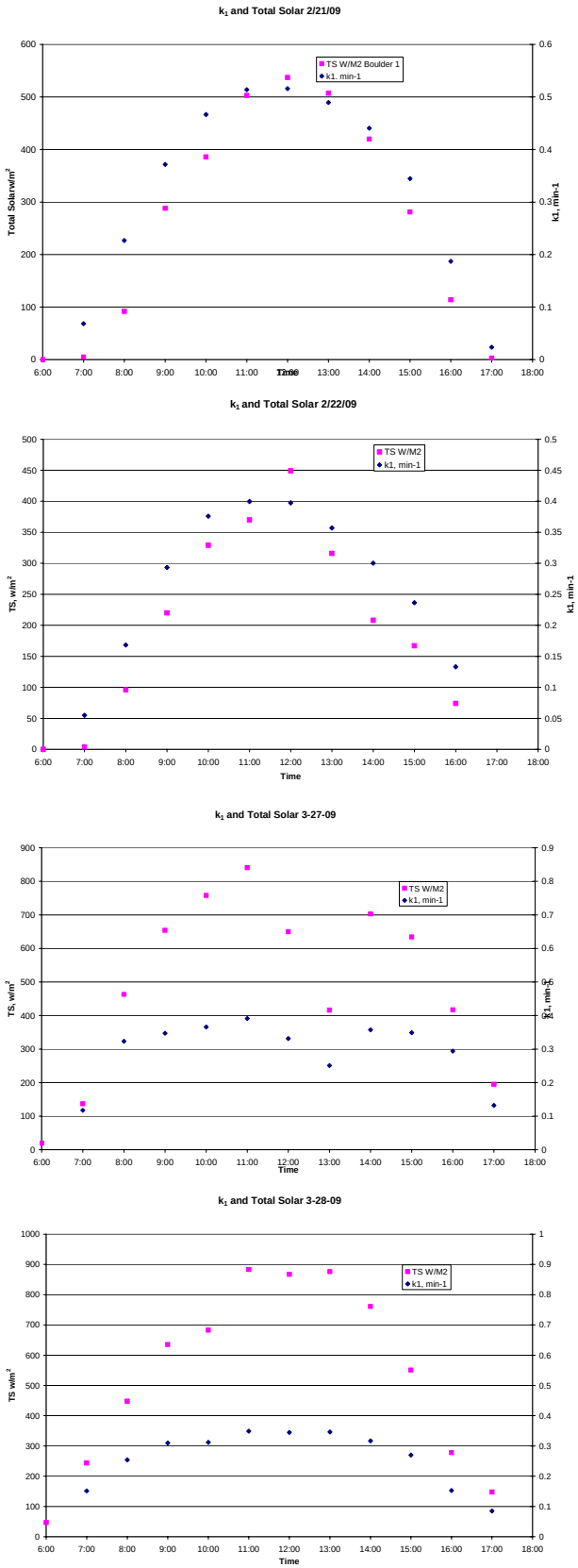


**Figure 4-54.** Comparison of measured $k_1$ with total solar radiation.

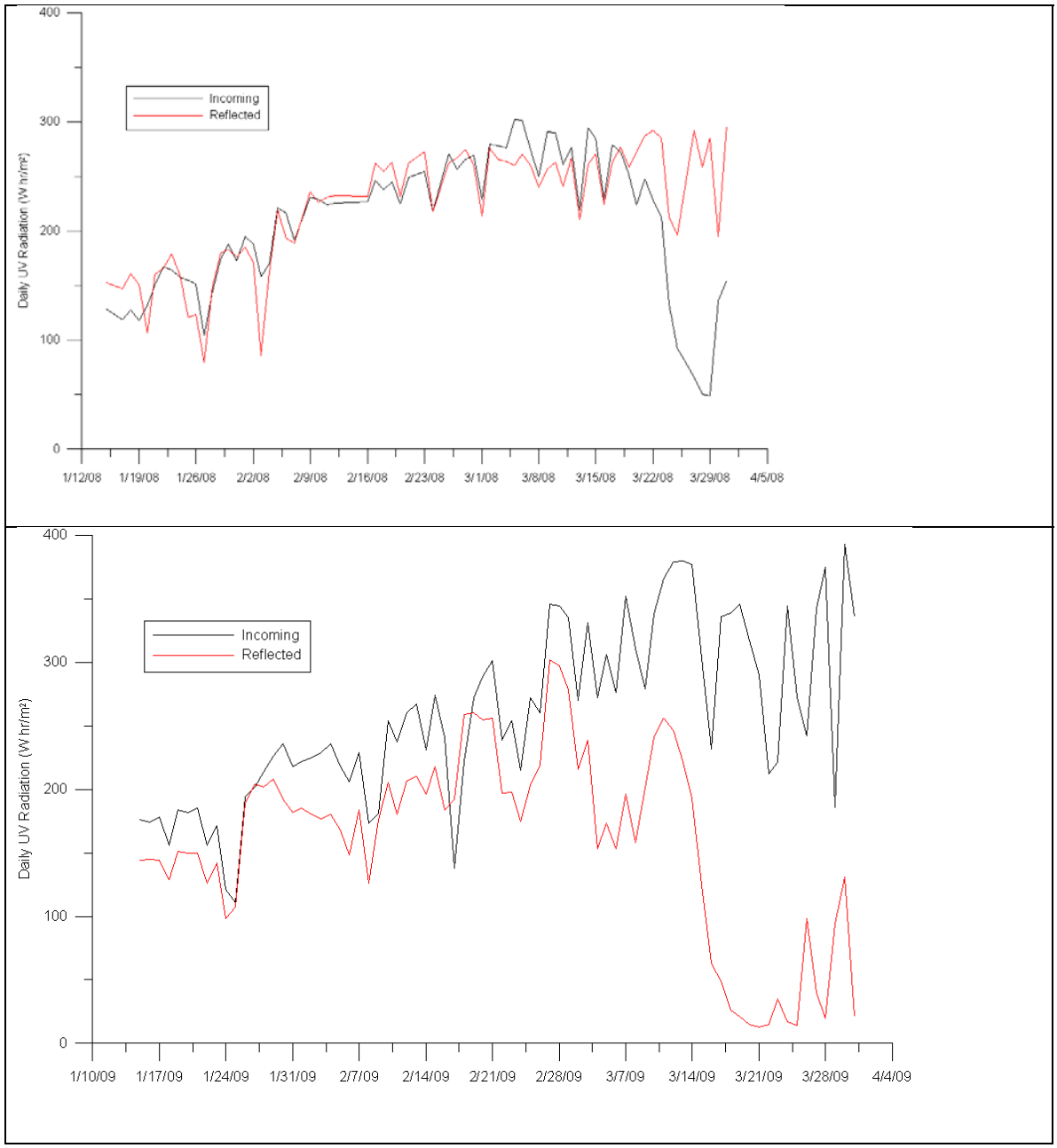


**Figure 4-55.** Comparisons of incoming and reflected UV measured at Boulder during January – March 2008 (top) and 2009 (bottom). Measurements during much of 2008 and, to a lesser extent during certain periods in 2009 were impacted by an apparent negative bias in the incoming UV measurement, possibly associated with dirt or frost buildup on the instrument (see ENVIRON, 2008b). These results should therefore only be interpreted in a qualitative sense.

# 5. SUMMARY, CONCLUSIONS AND RECOMMENDATIONS

## 5.1 Summary and Conclusions

As a follow-up to studies conducted during 2007 and 2008, a third Upper Green Winter Ozone Study (UGWOS) field measurement campaign was undertaken between mid-January and 31 March 2009 to study ozone episode development in the Upper Green River Basin (UGRB). Meteorological and aerometric measurement activities in 2009 consisted of an expanded network of temporary, tripod mounted monitoring stations for continuous recording of wind, temperature and ozone concentrations (mesonet); continuous monitoring of CO, $SO_2$ and nitrogen species (NO, $NO_2$, NOy, PAN) at the location of the permanent Boulder monitoring site, and boundary layer wind profiling via acoustic sounding (sodar). During intensive operating periods when elevated ozone conditions were forecast, these routine measurements were supplemented with upper-level measurements of winds and ozone via rawinsondes and ozonesondes released at regular intervals from the Pinedale airport and non-methane organic compound sampling at three locations: Boulder, Jonah and the sodar site.

The frequency and severity of ozone levels during 2009 was not as extensive as was the case in 2008. Ozone concentrations above 75 ppb (8-hour average) were observed on just three days with the highest levels recorded at the Mesa and Sodar monitoring sites which were not deployed in 2008. Eight-hour average ozone levels did not exceed 75 ppb at any of the three permanent monitoring sites located in the study area (Boulder, Daniel and the new Pinedale site) during the 2009 study period. Strong, persistent upper-level high pressure ridges which affected the UGRB in 2008 occurred only briefly in 2009. Snow cover, which has been determined from an analysis of UGWOS data collected in previous years to be a key necessary ingredient in the occurrence of ozone episodes in the UGRB, was not as extensive or long-lived in 2009 as was the case in 2008. Measurements of mixing heights showed that the persistent, extremely shallow mixing depths observed in 2008 did not occur to the same extent in 2009 and it appears likely that this limited the magnitude of ozone concentrations in 2009.

Another difference between the 2008 and 2009 study periods was the introduction of a voluntary emission reductions program during 2009. Under this program, operators in Sublette County took steps to reduce emissions on days when the WDEQ issued an Health Advisory. Health Advisories were called based on an ozone forecasts made by the WDEQ using criteria similar to those used in UGWOS for forecasting IOP days. During the 2009 study, the WDEQ issued a Health Advisory for 2 February and again for 3 February. During this two day period, operators responded by instituting various temporary measures to reduce activities that generate emissions of air pollutants. A summary of operator responses to the February 2-3 Health Advisory is presented in Table 5-1. While it is not possible to quantify the impact of these operator responses on emissions, it is noteworthy that approximately half of the operators responded by postponing initiation of fraccing and completion operations and blowdowns and deferring hauling of liquids. These responses have the potential to eliminate a fairly substantial amount of VOC emissions during this period. As it turned out, however, weather conditions during 2-3 February were not particularly favorable to ozone formation and no elevated ozone was observed in the UGWOS study area.

**Table 5-1.** Summary of operator responses to WDEQ Health Advisories during 2-3 February 2009.

| Response | No. Operators Responding (out of 22) |
|---|---|
| Defer truck and equipment Refueling (evening hours only) | 15 |
| Do not overfill gas tanks, tighten fuel caps | 4 |
| Minimize Vehicle Idling | 17 |
| Minimize vehicle miles traveled (consolidate trips, car-pool, postpone) | 14 |
| Reduce speed limit by 5mph | 4 |
| Keep vehicles tuned up and tires properly inflated | 4 |
| Fuel Additives in company vehicles | 2 |
| Use environmentally safe paints, cleaning products & chemicals | 4 |
| Postpone nonessential construction | 15 |
| Postpone nonessential maintenance | 18 |
| Postpone initiation of fraccing/ completion | 11 |
| Share completion BMPs with other operators | 4 |
| Postpone initiation of blowdowns | 10 |
| Minimize Use of Ancillary Equipment (light plants, portable generators, pumps, etc.) | 13 |
| Turn down heat trace pumps | 2 |
| Defer liquid hauling from tanks (to evening) | 13 |
| Leak Detection | 6 |
| Production Operations Surveillance: PM and during advisory | 3 |
| Shut-in uncontrolled facilities | 3 |
| Limit Drilling Operations | 3 |
| Delay Well Connect Activities (pipeline companies) | 1 |
| Delay Line Pigging (pipeline companies) | 1 |
| Delay charging of desiccant dehydration units | 1 |

The expanded network of mesonet sites deployed in 2009, together with meteorological and aerometric monitoring sites established during the study period as part of the Sublette County Human Health Risk Assessment study, allowed for a somewhat more detailed mapping of wind patterns and ozone levels than was possible in previous years. Wind patterns under ozone episode conditions were found to be consistent with patterns observed in 2008, including the characteristic afternoon wind direction reversals from northwest to southeast. There was significant spatial variability in ozone, with isolated peak concentrations occurring at locations determined by the predominant wind directions on each day. No significant periods of elevated ozone were observed at the new Pinedale monitoring site and the only high readings at Daniel and Cora occurred during brief periods on 23 February and 2 March. Ozone concentrations remained low at monitoring sites south of an east-west line defined by the Buckhorn and Juell monitoring sites, including La Barge, Farson, Simpson, Seedskadie and other sites in southwestern Wyoming (OCI-Trona, Murphy Ridge and Warmsutter).

Results of the UV and chemiluminescent ozone monitoring method inter-comparison analysis show good agreement between the two methods after some initial problems with the chemiluminescent monitor were resolved. There is no evidence of any significant positive interference biases in the UV method data from aromatics or other contaminants.

Results of non-methane organic compound sampling were generally consistent with results from 2008 after taking into account the likely disposition of material originally included as “unidentified” in the 2008 samples, including correct identification of toluene, the isobutylene

trimer artifact, and the group of interrelated C8+ species. Results from the 2009 samples confirm the importance of toluene as well as m,p-xylene and benzene, especially on a reactivity weighted basis. Carbonyl species concentrations were similar to those observed in 2008. NMHC samples collected at the sodar site had an overall composition similar to that at Jonah and Boulder and TNMHC concentrations at this site were on par with those observed at Boulder. TNMHC concentrations in 2009 were similar to those observed in 2008 although the upper extreme concentrations were higher in 2008, consistent with the stronger inversions and lower mixing heights during some of the 2008 IOP days. NMHC composition at Boulder is distinguished by a higher proportion of these C8+ species.

## 5.2 Recommendations

Although UGWOS study results obtained from the 2007 – 2009 field studies have allowed us to identify the major features of elevated winter ozone events in the Upper Green River Basin, the full potential spatial extent of these events has not been definitively determined because the weaker episodes observed using the more extensive monitoring network deployed in 2009 may have had a more limited spatial extent than the major episodes which occurred in 2008. We therefore recommend continued monitoring during the 2010 winter ozone season using a network of fixed and mesonet sites similar to what was used in 2009. These data would be greatly enhanced by continued operation of the sodar used in this year's study to provide information on low level wind shears and mixing heights.

While NMOC monitoring to date has provided a good characterization of the organic compound characteristics in the vicinity of the Jonah and Pinedale Anticline well fields, questions remain regarding the composition and potential sources of the C8+ heavy hydrocarbon compounds which make up 20% on average of the TNMHC at Boulder. If a significant fraction of this material is determined to have a high reactivity, it could have important implications for ozone formation. Sample collection and analysis techniques used thus far in the UGWOS program are not designed to identify the composition of this material. Alternative sampling and analysis methods are available, however, and should be considered for inclusion in a future field study. WDEQ may also wish to consider the deployment of a continuous or semi-continuous NMHC analyzer to provide greater temporal resolution. While auto-GCs have been used for this purpose in many urban areas, they are relatively expensive to operate. A more cost-effective arrangement may be to deploy a continuous TNMHC monitor and collect collocated canister samples for laboratory analysis during periods of high TNMHC concentrations using an automated technique.

A strong correlation between ozone and particulate matter (PM) concentrations has been noted in the UGWOS data. However, little is currently known about the composition of the PM. Although this may not have a direct bearing on ozone formation, the elevated PM contributes to haze in the region and information about the sources of primary and secondary PM components could shed light on the relative importance of ozone precursor sources. We therefore recommend WDEQ consider a conducting a speciated PM sampling program during the next winter season.

# REFERENCES

Carter, W.P.L. 1998. Updated maximum incremental reactivity scale for regulatory applications. CE-CERT, University of California, Riverside CA.

ENVIRON, T&B Systems and MSI. 2008b. "2008 Upper Green River Winter Ozone Study". ENVIRON International Corp., Novato, CA, October.

ENVIRON, T&B Systems and MSI. 2008a. "2007 Upper Green River Winter Ozone Study". ENVIRON International Corp., Novato, CA, April.

Fitz, D.; K. Bumiller, A. Lashgari. 2003. Measurement of $NO_y$ during SCOS97-NARSTO Atmos. Environ. 37, Supplement #2:S119-S134

Fitz, D.R., D.V. Pankratz, K. Bumiller and M.R. Smith. 2002. Measurement of $NO_2$ and PAN by gas chromatography with luminol detection. Air and Waste Management Association Symposium on Air Quality Measurement Methods and Technology – 2002. San Francisco, CA November 13-15.

Jeffries, H. E. 1991. "UNC Solar Radiation Models," unpublished draft report for EPA Cooperative Agreements CR813107, CR813964 and CR815779".

Peterson, J. T. 1976: "Calculated Actinic Fluxes (290 - 700 nm) for Air Pollution Photochemistry Applications", EPA-600/4-76-025, June.

Warneck, P. 2000. Chemistry of the Natural Atmosphere, Second Ed., Academic Press.

Yurganov, L. 2000. Carbon monoxide inter-annual variations and trends in the Northern Hemisphere: Role of OH. *International Global Atmospheric Chemistry (IGAC) Newsletter*, Issue 21, September. http://www.igac.noaa.gov/newsletter/21/trends.php

Zafonte, L.; P.L. Rieger and J.R. Holmes. (1977) Nitrogen dioxide photolysis in the Los Angeles Atmosphere. *Environ. Sci. Technol.* **11**:483-487.